Terms and Conditions of Use of Digitised Theses from Trinity College Library Dublin

Copyright statement

All material supplied by Trinity College Library is protected by copyright (under the Copyright and Related Rights Act, 2000 as amended) and other relevant Intellectual Property Rights. By accessing and using a Digitised Thesis from Trinity College Library you acknowledge that all Intellectual Property Rights in any Works supplied are the sole and exclusive property of the copyright and/or other IPR holder. Specific copyright holders may not be explicitly identified. Use of materials from other sources within a thesis should not be construed as a claim over them.

A non-exclusive, non-transferable licence is hereby granted to those using or reproducing, in whole or in part, the material for valid purposes, providing the copyright owners are acknowledged using the normal conventions. Where specific permission to use material is required, this is identified and such permission must be sought from the copyright holder or agency cited.

Liability statement

By using a Digitised Thesis, I accept that Trinity College Dublin bears no legal responsibility for the accuracy, legality or comprehensiveness of materials contained within the thesis, and that Trinity College Dublin accepts no liability for indirect, consequential, or incidental, damages or losses arising from use of the thesis for whatever reason. Information located in a thesis may be subject to specific use constraints, details of which may not be explicitly described. It is the responsibility of potential and actual users to be aware of such constraints and to abide by them. By making use of material from a digitised thesis, you accept these copyright and disclaimer provisions. Where it is brought to the attention of Trinity College Library that there may be a breach of copyright or other restraint, it is the policy to withdraw or take down access to a thesis while the issue is being resolved.

Access Agreement

By using a Digitised Thesis from Trinity College Library you are bound by the following Terms & Conditions. Please read them carefully.

I have read and I understand the following statement: All material supplied via a Digitised Thesis from Trinity College Library is protected by copyright and other intellectual property rights, and duplication or sale of all or part of any of a thesis is not permitted, except that material may be duplicated by you for your research use or for educational purposes in electronic or print form providing the copyright owners are acknowledged using the normal conventions. You must obtain permission for any other use. Electronic or print copies may not be offered, whether for sale or otherwise to anyone. This copy has been supplied on the understanding that it is copyright material and that no quotation from the thesis may be published without proper acknowledgement.

Biogenesis of histone mRNAs in the yeast *Saccharomyces cerevisiae*

A thesis submitted to the University of Dublin
for the Degree of Doctor of Philosophy
by

Ruth Alice Canavan

February 2007

Department of Microbiology
Moyne Institute of Preventive Medicine
Trinity College, Dublin

DECLARATION

This thesis has not been submitted as an exercise for a degree at any other university. Except where stated, the work described therein was carried out by me alone.

I give permission for the Library to lend or copy this thesis upon request.

Signed: 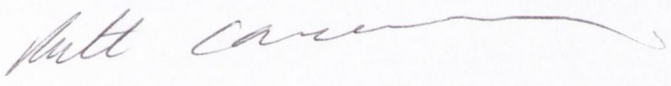

Declaration

I certify that the experimentation recorded herein represents my own work, unless otherwise stated in the text, and has not been previously presented for a higher degree at this or any other University. This thesis may be lent at the discretion of the Librarian.

Name

Ruth Alice Canavan

Acknowledgements

My special thanks to my supervisor, Dr. Ursula Bond, for training, advice and supervision in the yeast histone research field. It has been a remarkable four years of further learning in the research field. I am also grateful to Tharappel C. James for constant experimental advice. I also want to thank Blanca, Paul, Gerry and Gwen for assistance in the lab. I thank Jane for her assistance and patience in looking for the disappearing hot-labelled DIG. How can I forget David, Henry, Margaret, Myriam, Paddy, Joe, Ronan and Fionnuala from the prep room, thank you all for supplying the basic things we need for research. Thanks to past and present members in CJD for sharing equipments. Thanks to everyone in the Moyne Institute who were helpful to me over the last four years. I wish to say good luck to the new postgraduates in the Bond lab.

I also want to give special thanks to Dr. Domenico Libri, Dr. Nick Proudfoot and Dr. David Tollervey for providing yeast strains. This research project was supported by the Trinity College Postgraduate Award and Enterprise Ireland. Thank you for making this research project possible.

Many thanks to Declan Treanor and Orlaith O'Brien from the disability services in Trinity College, Dublin, for your encouragement, consideration and practical support. I am also grateful to your colleagues in the disability services. Each and everyone of you showed me great kindness.

I especially want to thank Blanca and Judy for being so friendly when I first arrived at the Moyne Institute, entering the unknown. Thank you also to Judith, Sara and Eoin for being supportive and good friends. A special thank you to Kieran, a friend and note-taker for my lab meetings, for being there for me as well. A thank you note to the friends I have had over the last few years for supporting me and giving me their friendship.

Finally, I wish to give my utmost special thanks to my Mum and Dad, and to my brothers, James and David, for their constant love, encouragement and support.

Conferences

Canavan, R. and Bond, U. Interaction of CFIA and the nuclear exosome with the Distal Downstream Element of the yeast *HTB1* mRNA defines the fate of the mRNA during the cell-cycle. Poster presentation at 9th Annual Meeting of the RNA Society, Wisconsin, USA, June 2003.

Bond U, Beglan, P. and Canavan, R. Poster presentation at the EMBO workshop on RNA 3'-end processing, Brasenose College, Oxford University, 2005.

Index of Figures

Index of Tables

Abbreviations

A_{260}	absorption at 260 nm
A_{660}	absorption at 660 nm
AE buffer	Acetic EDTA buffer
°C	degrees Celsius
CTD	C-terminal domain
DEPC	Diethyl pyrocarbonate
dNTP	Deoxy nucleotide triphosphate
DIG	Digoxigenin
DNA	Deoxyribonucleic acid
DNase	DNA hydrolysing enzyme
DDE	Distal downstream element
EDTA	Ethylenediaminetetraacetic acid
hr	hour
hrs	hours
kDa	kilodalton
KCl	Potassium chloride
LB	Luri-Bertani media
MAB	Maleic acid buffer
mRNA	Messenger ribonucleic acid
$MgCl_2$	Magnesium chloride
min	minute
mins	minutes
mM	millimolar
ml	millilitre

M	molar
MOPS	3-Morpholinopropanesulfonic acid
Mg^{2+}	Magnesium (2+) cation
$MgSO_4$	Magnesium(+2) cation sulphate
Mutant DDE	pSAC15, pSAC20 and pSAC21 plasmids
NaCl	Sodium chloride
ng	nanograms
nt	nucleotides
nm	nanometers
OD	optical density
%	grams per 100ml
PCR	Polymerase chain reaction
PEG	Polyethylene glycol
pH	-log10[H+] ions (measure of acidity or alkalinity)
RNase	RNA hydrolyzing enzyme
RT-PCR	Reverse transcriptase polymerase chain reaction
RNA	Ribonucleic acid
rpm	revolutions per minute
SOC	super optimal broth
SSC	Di-sodium citrate
SDS	Sodium dodecyl sulphate
SLBP	Stem-loop binding protein
sec	second
secs	seconds
SDW	standard water
Taq DNA polymerase	DNA polymerase from *Thermus aquaticus*

TBE	Tris Borate EDTA
Tris	Tris(hydroxymethyl)aminomethane
T_m	melting temperature
Tween 20	Polyoxyethylenesorbitab monolaurate
U	units (of Enzyme)
µl	microlitre
µM	micromolar
Vol	Volume
YEPD	Yeast extract peptone dextrose
YEPGal	Yeast extract peptone galactose
v/v	volume per volume
w/v	weight per volume
WT	Wild type
WT DDE	PLJ31 plasmid

Contents

Chapter 1

Introduction

1.1 Overview

The typical eukaryotic human diploid cell contains $3.2x10^9$ base pairs of deoxyribonucleic acid (DNA) which, if presented in an extended form, would measure 1.2m in length. The large amount of DNA is tightly wrapped and compacted through its interaction with a set of small basic proteins called histones (Alberts *et al*, 2002). Histones are positively charged proteins that facilitate the folding of DNA. Four types of histones have been described: H2A, H2B, H3 and H4 (Baxevanis and Landsman, 1997). A 147 base pair segment of eukaryotic DNA associates with histones, forming an octameric protein complex known as the nucleosome (Baxevanis and Landsman, 1998; Grunstein and Mann, 1992). The quaternary structure of the nucleosome is stabilised through an interaction with an additional histone, H1. This structure is highly conserved. The level of compaction of DNA varies during the life cycle of the cell. During interphase, chromatin is relatively decondensed and distributed throughout the nucleus. As cells enter mitosis, chromatin condenses into chromosome structures, which are relatively transcriptionally silent. As the cells undergo DNA replication, the newly formed DNA must be repackaged into chromatin. Therefore the production of histones is tightly controlled to ensure that maximum production occurs in the S-phase of the cell cycle (Xu *et al*, 1990).

Two types of histones are recognised: replication-dependent and replication-independent. Replication-dependent histones are tightly co-ordinated with DNA synthesis. Histone mRNAs are maximally expressed in the S-phase of the cell-cycle, coinciding with DNA synthesis. Histone gene expression is regulated through transcriptional and post-transcriptional mechanisms, resulting in a 35-fold increase in cellular histone mRNA levels during the S-phase phase of Chinese hamster ovary cells (Whitfield *et al*, 2000). Degradation of histone mRNA occurs as the cells progress into the G_2-phase. In HeLa cells, there is a 3- to 5-fold increase in the transcription rate of histone synthesis (Harris and Marzluff, 1991). Furthermore, post-transcriptional regulation adds to the accumulation

of histone mRNAs in the S-phase, causing a further increase of 6- to 8-fold (Harris *et al*, 1991). Post-transcriptional regulation includes 3'-end processing, transport and stability of the mRNAs. The replication-independent histone variants operate independently of replication. These variants are repressed in the S-phase, but are elevated in the G_2-, M- and G_1-phases. Replication independent histone variants play a housekeeping role to prevent inappropriate transcription of genes until the next S-phase (Altheim and Schultz, 1999). Cell-cycle regulation of histone mRNAs, leading to maximum expression in the S-phase, is highly conserved between lower and higher eukaryotes. Despite the conservation of function, the mechanisms of histone mRNA biogenesis vary between the lower and higher eukaryotes. Histone mRNAs in yeast, fungi and protozoa possess poly (A) tails (Fahrner *et al*, 1980). In contrast to lower eukaryotes, higher eukaryotes such as mammalian histone mRNAs, are non-polyadenylated and contain a conserved stem-loop structure immediately upstream of the 3'-end of the mRNA (Marzluff, 2005; Williams, 2005).

This thesis aims to extend our knowledge of histone mRNA biogenesis in *Saccharomyces cerevisiae* by examining the roles of various 3'-end processing, transcription termination, RNA degradation and export factors in this process. The introduction presents the background research into the general 3'-end mRNA processing and histone 3'-end processing mechanisms in yeast and mammals. The interconnected mechanisms of transcription, termination, degradation and export are also discussed in detail.

1.2 3'-end processing of eukaryotic mRNAs

Eukaryotic messenger RNA precursors (pre-mRNA) contain sequences to direct 3'-end processing reactions. The 3'-end processing events, which include endonucleolytic cleavage followed by polyadenylation of the upstream cleavage site. Endonucleolytic cleavage leaves the upstream fragment of the pre-mRNA to become polyadenylated into mature mRNA while the downstream fragment of the pre-mRNA is degraded. Poly (A) tails are involved in the regulation of mRNA stability, initiation of translation, translational efficiency and transporting mature mRNA from the nucleus to the cytoplasm (Colgan and Manley, 2005). All eukaryotic cells are polyadenylated with the exception for replication-dependent histone mRNAs. Somehow throughout evolution, poly (A) tails were lost from replication-dependent histone mRNAs. Any defects in 3'-end processing would lead to diseases like thalassemias and lysozomal storage disorders (Scorilas, 2002). In mammalian cells, the sequences for 3'-end processing are conserved, whereas yeast cells utilise degenerate signals to facilitate 3'-end processing. Despite these differences, the cleavage and polyadenylation factors required for the 3'-end processing reactions are conserved and similar between mammalian and yeast cells. Cis-acting sequences function in directing the trans-acting factors to the pre-mRNA for efficient 3'-end processing. In the next section, the trans-acting factors required for efficient 3'-end processing in mammals and yeasts are discussed.

1.2.1 Cleavage and polyadenylation factors in mammalian cells

In mammals, a number of trans-acting factors are necessary for 3'-end mRNA formation *in vitro*. The two steps, cleavage and polyadenylation, required for mRNA 3'-end formation can be analysed separately. Cleavage of mammalian pre-mRNA substrates requires cleavage and polyadenylation specificity factor (CPSF), cleavage stimulation factor (CstF),

cleavage factors (CFI_m and $CFII_m$) and poly (A) polymerase (PAP). The polyadenylation step involves CPSF, PAP and poly (A) binding protein (PABP) (*Table 1.1*).

Cleavage and polyadenylation specificity factor (CPSF) is a complex consisting of CPSF-160, CPSF-100, CPSF-73, CPSF-30 and hFip1. The CPSF complex is the central player for cleavage and polyadenylation of pre-mRNA. Manley *et al* (1995) purified the CPSF-160 protein and showed that this protein is bound to AAUAAA-containing RNAs. The AAUAAA sequence is a 3'-end processing signal required for 3'-end processing of pre-mRNAs. CPSF-160 also interacts with CstF-77 and PAP (Colgan and Manley, 1997; Murthy and Manley, 1995) (*Figure 1.1*). CPSF-73 is the putative endonuclease responsible for 3'-end cleavage reaction (Jenny and Keller, 1996; Ryan *et al*, 2004). Knowing that *Drosophilia* clipper protein (CLP) is involved in endonucleolytic activity, Zarudnaya *et al* (2002) showed that its homologue, CPSF-30, is also an endonuclease (Zarudnaya *et al*, 2002). Kaufmann *et al* (2004) identified the new human Fip1 (hFip1), which is a subunit of the CPSF complex and has been shown to stimulate PAP activity in poly (A) synthesis. The hFip1 protein interacts with PAP, CPSF-30, CPSF-160 and CstF-77 (Kaufmann *et al*, 2004).

Cleavage stimulation factor (CstF) is a heterotrimer with three subunits, CstF-77, CstF-64 and CstF-50. CstF-50 facilitates protein-protein interactions and CstF-77 subunit does not bind directly to the RNA sequences, but is important for polyadenylation (Benoit *et al*, 2002). The CstF-64 complex binds to RNA via its N-terminal RNP-type binding domain giving rise to the assembly of the CstF complex onto the RNA.

CFI_m complex consists of 70, 59 and 25 kDa subunits. Vries *et al* (2000) purified and fractionated the human $CFII_m$ from HeLa cells and separated the complex into two components in relation to their activity, namely $CFIIA_m$ and $CFIIB_m$ (Vries *et al*, 2000). The mouse CFI-25 subunit interacts with CFI-70 and PAP. CFI-25 may also play a role in the recruitment of PAP enzyme or assembly of proteins in the 3'-end processing complex

(Hana and Lee, 2001). $CFIIA_m$ complex is important in cleavage and consists of hClp1 and hPcf11, which are homologous to the yeast CFIA subunits, Clp1p and Pcf11p (Vries *et al*, 2000). $CFIIB_m$ complex is not involved in 3'-end processing, but may play a stimulatory role and the factors involved remain to be uncovered (Uetz *et al*, 2000).

The poly (A) polymerase (PAP, 82 kDa) catalyses poly (A) synthesis. The C-terminal domain of PAP is rich in serine and threonine residues, which are phosphorylated and facilitate its activity (Zhao *et al*, 1999). Poly (A) binding protein (PABP) interacts with the newly formed Poly (A) tail. Both nuclear and cytoplasmic forms of PABP have been identified. PABPs contain RNA-recognition motifs (RRM), which facilitate RNA binding (Mangus *et al*, 2003). Nuclear poly (A) binding protein (PABPN1) interacts with 11-14 adenylate residues and also binds to CPSF. PAP enzyme is stimulated by the PABPN1 until the full-length poly (A) tail is formed.

1.2.2 Assembly of mammalian cleavage and polyadenylation machinery

The model of mRNA 3'-end processing in mammalian cells has been elucidated from many research studies (Canadillas *et al*, 2003; Darnell, 2000; Manley and Takagaki, 1996; Ryan *et al*, 2004). The complex consists of many interactions between CPSF, CstF, CFI_m, $CFII_m$, PAP and PABPN1. The cleavage reaction requires CPSF, CstF, CFI_m and $CFII_m$ for efficient cleavage. The cleavage reaction is followed by polyadenylation, which recruits PAP and PABPN1 to the complex. CstF, CFI_m and $CFII_m$ factors leave the assembly before polyadenylation takes place. The cleavage and polyadenylation model in mammalian cells is shown in Figure 1.1.

Figure 1.1 also shows the 3'-end processing signals, which include a highly conserved AAUAAA motif, downstream elements and the poly (A) site, all of which are essential in 3'-end processing of pre-mRNAs. The AAUAAA motif is essential for cleavage and poly (A) addition (Zhao *et al*, 1999). The downstream elements include loosely conserved

U-rich and GU-rich elements, which lay 30 nucleotides 3' to the cleavage site. The preferred site of cleavage usually contains the CA dinucleotide, which is the Poly (A) site (Zhao *et al*, 1999).

The transcription factor, TFIID, consists of a TATA-binding protein that binds to the TATA promoter. This binding plays a key role in RNA polymerase II activation at the transcription initiation stage and recruits the CPSF complex at. The CPSF complex is transferred to the RNA Polymerase II (Pol II) complex, where it interacts with the C-terminal domain (CTD) of Pol II. (Dantonel and Laszlo, 1997; Hirose and Manley, 1998). The CTD is the largest subunit of RNA polymerase II which functions transcription and provides a platform for 3'-end processing factors. The CstF-77 and CstF-50 also interact with the carboxyl-terminal domain of RNA Polymerase II, indicating that transcription and 3'-end processing of the emerging transcript are linked and co-ordinated (McCracken *et al*, 1997). CPSF remains associated with the Polymerase complex as it transverses the gene until it reaches the end of the gene. The CstF-77 protein facilitates the bridging of CstF-64 and CstF-50. The CstF-64 protein has an RNP-type binding domain that binds to the GU/G-rich downstream element of the pre-mRNA and has recently been shown to associate with a newly identified heat-labile factor, symplekin, *in vitro* (Takagaki and Manley, 2000).

Further interaction studies reveal that hClp1 interacts with CFI_m and CPSF complexes, but not with CstF and PAP (Ohnacker *et al*, 2000). Subsequently, PAP assembles with PABPN1, allowing the rapid process of polyadenylation to occur to form the mature mRNA.

Table 1.1: Mammalian pre-mRNA 3'-end processing factors

Factor	Reaction step involved in	Polypeptide composition (kDa)	Properties of processing factor	Reference
CFI_m	Cleavage	70	Binds to RNA with preference for polyadenylation precursor	(Hana and Lee, 2001)
		59	Binds RNA	(Hana and Lee, 2001)
		25	Binds RNA	(Hana and Lee, 2001)
$CFII_m$	Cleavage	47	hClp1	(Vries *et al*, 2000)
		Unknown	hPcf11	(Vries *et al*, 2000)
CstF	Cleavage	77	Connects CstF-64 and CstF-50. Interacts CPSF-160	(Salinas *et al*, 1998)
		64	Binds GU- and U-rich downstream signals	(Canadillas *et al*, 2003)
		50	Interacts with carboxyl-terminal domain of Polymerase II and CstF-77	(McCracken *et al*, 1997)
CPSF	Cleavage and polyadenylation	160	Binds to PAP and CstF-77. Binds to AAUAAA sequence	(Murthy and Manley, 1995)
		100	23% identical and 49% similarity to CPSF-73	(Jenny *et al*, 1994)
		73	23% identical and 49% similarity to CPSF-100	(Rüegsegger *et al*, 1996)
		30	Binds to CPSF-160 and poly (U)	(Barabino *et al*, 1997)
		66	hFip1	(Kaufmann *et al*, 2004)
PAP	Cleavage and polyadenylation	77/82	Catalyses AMP polymerisation and interacts with CPSF	(Zhao *et al*, 1999)
PABPN1	Poly (A) elongation	33	Stimulates poly (A) polymerase and essential for poly (A) length control. Binds to CPSF-30	(Kerwitz *et al*, 2003)
RNA Pol II	Cleavage	200	Binds CPSF and CstF	(Zhao *et al*, 1999)

Figure 1.1: Schematic representation of the mammalian cleavage complex and mammalian polyadenylation complex. (A) The mammalian cleavage complex assembly consists of CFI_m, $CFII_m$, CstF and CPSF. The arrow shown represents the poly (A) site and the red figure represents the CTD of RNA Polymerase II. PAP interacts with CPSF-160, CstF-77 and hFip1. **(B)** As the 3'-end processing machinery progresses from cleavage to polyadenylation, CFI_m,$CFII_m$ and CstF leave the complex and the downstream sequences are degraded. The nuclear poly (A) binding protein (PABPN1) and PAP assemble to form the polyadenylation complex. **(C)** The mammalian polyadenylation complex consists of CPSF, PABPN1 and PAP. The CPSF complex assembles around the AAUAAA sequence. The PAP adds poly (A) tails of adenine residues to the 3'-end with the assistance of PABPN1.

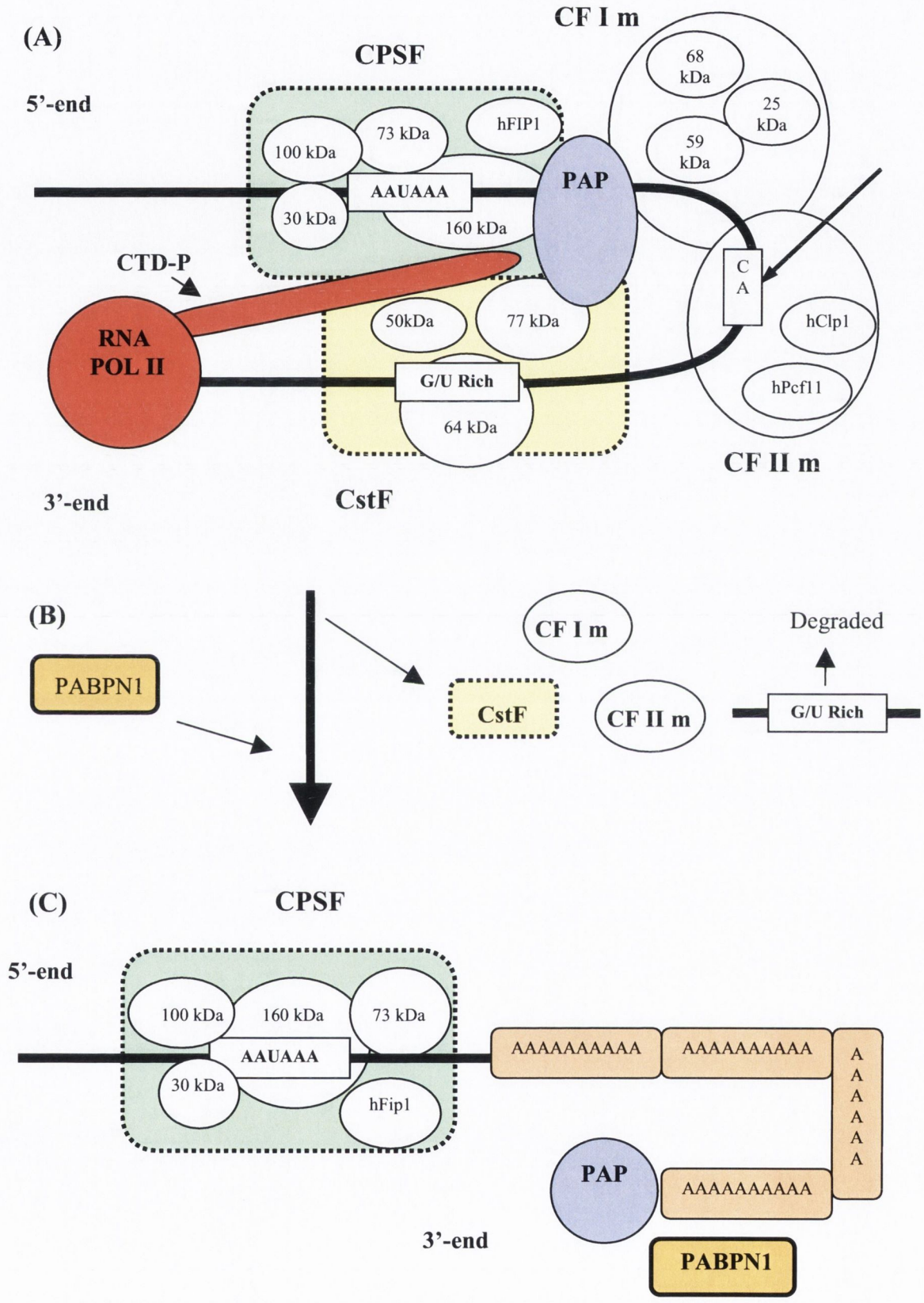
(A)
CF I m
CPSF
5'-end
68 kDa
25 kDa
59 kDa
hFIP1
73 kDa
100 kDa
AAUAAA
30 kDa
160 kDa
PAP
CTD-P
C
A
RNA POL II
50kDa
77 kDa
hClp1
G/U Rich
hPcf11
64 kDa
CF II m
3'-end
CstF
(B)
PABPN1
CF I m
Degraded
CstF
CF II m
G/U Rich
(C)
CPSF
5'-end
100 kDa
160 kDa
73 kDa
AAUAAA
30 kDa
hFip1
AAAAAAAAAA
AAAAAAAAAA
A
A
A
A
A
A
PAP
AAAAAAAAAA
3'-end
PABPN1

1.3 Cleavage and polyadenylation factors in yeast cells

In the yeast, *Saccharomyces cerevisiae,* a number of trans-acting factors have been identified which are required for cleavage and polyadenylation. The cleavage/polyadenylation factor I (CFI), which has two subunits (CFIA and CFIB), and cleavage factor II (CFII) are necessary for cleavage to occur. The polyadenylation step requires CFIA, polyadenylation factor I (PFI), poly (A) polymerase (PAP) and poly (A) binding protein (Pab1p) (*Table 1.2*) (Zhao *et al*, 1999).

CFIA is a tetrameric factor consisting of Rna14p, Rna15p, Pcf11p and Clp1p (cleavage and polyadenylation protein 1), with molecular weights of 76 kDa, 38 kDa, 70 kDa and 50 kDa polypeptides respectively. Temperature-sensitive alleles of RNA14, RNA15 and PCF11 have been shown to be deficient in 3'-end processing and transcription termination (Amrani *et al*, 1997; Barilla *et al*, 2001). Rna14p and Rna15p are homologous to the mammalian cleavage stimulation factors, CstF-77 and CstF-64. Poly (A) binding protein, Pab1p, was co-purified with CFIA and CFIB. Further research is required to elucidate Clp1 protein involvement in 3'-end processing (Gross and Moore, 2001a).

CFIB factor consists of one 73 kDa polypeptide, Hrp1, which is required for correct cleavage and polyadenylation *in vivo* (Guisbert *et al*, 2006). Hrp1p has RNA recognition motifs (RRMs) and interacts with the two CFIA components, Rna14p and Rna15p. Hrp1p was discovered as a suppressor of a temperature-sensitive *npl3* allele, which is required for mRNA export. Hrp1p possibly has an additional role of linking 3'-end processing and mRNA export from the nucleus (Kessler *et al*, 1997).

CFII is a heterotetramer consisting of Yhh1/Cft1 (150 kDa), Ydh1/Cft2 (105 kDa), Ysh1/Brr5 (100 kDa) and Pta1 (90k kDa). The first three proteins are homologues of the mammalian 160 kDa CPSF, 30 kDa CPSF, 100 kDa CPSF, respectively. Pta1 has no mammalian homologies (*Tables 1.2 and 1.3*). These factors are required for both cleavage and polyadenylation (Zhao *et al*, 1997).

PFI is a large complex consisting of nine polypeptides, ranging in size from 150 to 20 kDa. The complex contains Fip1 (50 kDa), Yth1 (26 kDa), Pfs2 (53 kDa), Pfs1 (58 kDa) and CFII subunits. The PFI complex can be isolated with CFII through affinity purification. The combination of PFI and CFII has been termed as cleavage and polyadenylation factor (CPF) (Ohnacker *et al*, 2000). Seven new components (Ref2, Pti1, Ssu72, Glc7, YOR179C, YKL018W and YKL059C) have been discovered along with the CPF complex (Gavin *et al*, 2002).

Ref2 (RNA end formation) and Pti1 were not found to be important for mRNA 3'-end processing. Instead, they were found to be important for the 3'-end formation of small nucleolar RNAs (snoRNAs) (Nadea *et al*, 2003). Ssu72 has been shown to associate with CPF and is required for anti-termination activity of CPF during RNAP II elongation (Dichtl *et al*, 2002a). The phosphatase, Glc7, was found to interact with Pta1 and plays a role in 3'-end processing (He and Moore, 2005). Further research is necessary to understand the role of the uncharacterised proteins YOR179C, YKL018W and YKL059C in 3'-end processing.

The first 3'-end processing factor from yeast to be purified was poly (A) polymerase (PAP). PAP interacts directly with Fip1p and this interaction provides regulation of the PAP activity during polyadenylation (Preker *et al*, 1995). The poly (A) binding protein (Pab1p) is involved in poly (A) tail synthesis and mRNA stability. The temperature-sensitive *pab1* alleles have been shown to have normal pre-mRNA cleavage, but abnormally long poly (A) tails. Two-hybrid screening was carried out to identify factors interacting with Pab1. A new factor, Pab1p-binding protein 1 (Pbp1p), was found to interact with the C-terminus of Pab1 and this protein promotes proper polyadenylation (Mangus *et al*, 2004b).

PAN, a Pab1p-dependent 3'-5' poly (A) exoribonuclease, is required to trim back the length of the newly synthesised poly (A) tails to the appropriate length (Dheur *et al*, 2005).

PAN consists of two proteins, Pan2p (127 kDa) and Pan3p (76 kDa), and is recruited by Pab1. Recent studies have shown that Pab1 and PAN also play an important role in releasing mRNAs from the nucleus to the cytoplasm (Mangus *et al*, 2004a).

1.3.1 Assembly of yeast cleavage and polyadenylation machinery

Many of the yeast 3'-end processing factors share homology with some of the 3'-end processing factors in mammals. The cleavage and polyadenylation model for yeast is shown in Figure 1.2. The model is based on recent research from a number of sources (Ohnacker *et al*, 2000; Proudfoot and O'Sullivan, 2002; Zhao *et al*, 1999).

Three cis-elements, the efficiency element, the positioning element and the poly (A) site are required for 3'-end signalling (*Figure 1.2*). The sequences in yeast are more complex since they are less conserved and vary in their arrangement. The efficiency element (EE) is situated upstream of the cleavage site. The distance from the cleavage site can vary. Usually, the sequences consist of UA dinucleotides or U-rich stretches (Zhao *et al*, 1999). The second element is the positioning element, which contains a loosely conserved AAUAAA sequence and is located 13-27 nucleotides upstream of the cleavage site. The distances between the efficiency and positioning elements are sensitive to spacing between them (Helden *et al*, 2000). The poly (A) site consists of a consensus sequence $Py(A)_N$, where Py stands for pyrimidine. The poly (A) site recognition is poorly researched. An A-rich sequence is not discussed (but is mentioned below) and is shown in Figure 1.2.

The CFIA, CFIB, CFII and PFI complexes are recruited to the genes during transcription initiation (Licatalosi *et al*, 2002). CFIA, CFIB and CFII are required for cleavage. The CFIA complex, Rna14 subunit, was found to interact directly with Rna15 *in vivo* and *in vitro* (Noble *et al*, 2004). The Rna15 protein specifically binds to the A-rich sequence (not discussed above) with Rna14p and Hrp1p. Mutation in either Rna15p or the A-rich element

abolishes the binding and eliminates the functions of CFI. The poly (A) binding protein, Pab1p, was found to co-purify with CFIA and CFIB, and interacts with Rna15p. The CFIB complex, consisting of Hrp1p, binds to the efficiency element. The Rna14 protein bridges Rna15 and Hrp1 (Gross and Moore, 2001b). The Clp1 protein (CFIA complex) binds to the Pcf11 and Ysh1 protein subunits (Noble *et al*, 2007)

The C-terminal domain (CTD) of the largest subunit of RNA Polymerase II functions by recruiting the RNA processing machinery to the transcription unit and is required for 3'-end cleavage *in vivo*. The CTD-binding domain of Pcf11p binds directly to the CTD of RNA Polymerase II (Licatalosi *et al*, 2002). Pcf11p interacts with CPF components, Ydh1p, Yhh1p and Ysh1p, and also weakly with Pta1p. The poly (A) site is the binding site for Yhh1/Cft1 of the CPF complex. Yhh1 has also been shown to interact with the CTD of RNA Polymerase II. Thus, Yhh1 is involved in direct interactions with the RNA substrate and the CTD of RNA Polymerase II (Dichtl *et al*, 2002b). The Yhh1/Cft1 and Ysh1/Brr5 subunits of CFII have been shown to interact with Rna14 and Clp1. Ydh1/Cft2p interacts with many CPF subunits, including Yhh1p/Cft1p, Ysh1p/Brr5p, Pta1p, Pfs2p and Ssu72p, indicating a possibility that there is more than one Ydh1p molecule present in the 3'-end processing event (Kyburz *et al*, 2003). The interaction of the Yth1p subunit with Fip1p and RNA is important for correct cleavage and poly (A) addition (Tacahashi *et al*, 2003).

The Pfs2 protein of the PFI complex interacts with Rna14, Ysh1 and Fip1 proteins (Ohnacker *et al*, 2000). Fip1p interacts physically with Pap1p, Yth1p and Rna14p. This association suggests that there is an important interaction between CFI, PFI and PAP (Helmling *et al*, 2001). One of the new components of CPF, Pti1, has been found to interact with Pta1 and Ref2 through two-hybrid analysis (Dheur and Minivielle-Sebastia, 2003). Ssu72 physically and genetically interacts with the Pta1 and is only required for cleavage (He *et al*, 2003).

The CPF complex consists of 16 polypeptides and its mechanism of assembly onto the RNA substrate is not clear including cleavage site selection. The role of some new uncharacterised factors from CPF has not been investigated. For some of the yeast factors, mammalian homologues have not been identified. Therefore, further research is necessary to completely characterise the RNA-protein and protein-protein interactions of the factors required for 3'-end processing.

Table 1.2: Yeast pre-mRNA 3'-end processing factors

Factor	Reaction step involved in	Polypeptide composition (kDa)	Gene	Properties of processing factor	Reference
CFIA	Cleavage and polyadenylation	76	RNA14	Interacts with RNA15	(Noble *et al*, 2004)
		70	PCF11	Interacts with RNA14 and RNA15	(Gross and Moore, 2001b)
		50	CLP1	Binds to Pcf11 and Ysh1	(Gross and Moore, 2001a)
		38	RNA15	Interacts with RNA14. Binds A-rich	(Mandart and Parker, 1995)
	Polyadenylation	70	PABI	Interacts with RNA15. Poly (A) tail length control	(Amrani *et al*, 1997)
CFIB	Cleavage	73	HRP1/Nab4	Interacts with RNA14 and RNA15	(Kessler *et al*, 1997)
CFII	Cleavage and polyadenylation	150	YHH1/CFT1	Interacts with CTD of POL II	
		105	YDH1/CFT2	RNA binding depends on ATP	
		100	YSH1/BRR5		
		90	PTA1	Interacts with phosphatase, Glc7	
PFI	Polyadenylation	150	YHH1/CFT1	Interacts with CTD of POL II	(Dichtl *et al*, 2002b)
		105	YDH1/CFT2	RNA binding depends on ATP	(Kyburz *et al*, 2003)
		100	YSH1/BRR5		(Kessler *et al*, 1997)
		90	PTA1	Interacts with phosphatase, Glc7	(He and Moore, 2005)
		64	PAP1	Catalyses poly (A) extension. Interacts with FIP1	(Helmling *et al*, 2001)
		58	PFS1	Interacts with YDH1	(Zhao and Moore, 1999)
		50	FIP1	Interacts with RNA14, YTH1, CFII and PAP1	(Helmling *et al*, 2001)
		53	PFS2	Interacts with YSH1, FIP1 and RNA14	(Ohnacker *et al*, 2000)
		26	YTH1	Interacts with FIP1 and RNA	(Tacahashi *et al*, 2003)

Table 1.3: Mammalian and yeast pre-mRNA 3'-end processing factors

Factor	Polypeptide composition (kDa)	Gene	Mammalian homologues
CFIA	76	RNA14	CstF-77
	72	PCF11	hPcf11
	50	CLP1	hClp1
	38	RNA15	CstF-64
CFIB	73	HRP1	–
CFII	150	YHH1/CFT1	CPSF-160
	105	YDH1	CPSF-100
	100	YSH1/BRR5	CPSF-73
	90	PTA1	–
PFI	150	YHH1/CFT1	CPSF-160
	105	YDH1	CPSF-100
	100	YSH1/BRR5	CPSF-73
	85	PTA1	–
	64	PAP1	Poly (A) polymerase
	58	PFS1	–
	55	FIP1	hFip1
	53	PFS2	–
	26	YTH1	CPSF-30

Figure 1.2: Schematic representation of the yeast cleavage complex and yeast polyadenylation complex. (A) The yeast cleavage complex assembly consists of CFIB binding to the efficiency element. CFII assembles around the A/U-rich element and CFIA assembles around the A-rich element. The arrow shown represents the poly (A) site and the red figure represents the CTD of Polymerase II. PAP interacts with Rna15. **(B)** As the 3'-end processing machinery progresses from cleavage to polyadenylation, CFIB leaves the complex and the G/U-rich sequence is degraded. The PFI, PAN and PABI assemble to form the polyadenylation complex. **(C)** The yeast polyadenylation complex consists of CFIA, PFI/CFII (CPF), PAP, PABI and PAN. The PFI/CFII complex assembles around the A/U-rich sequence. The underlined factors of CPF are the new components, whose interactions have not yet been characterised. The CFIA remains at the A-rich sequence. The PABI adds poly (A) tails of adenine residues to the 3'-end with the assistance of Pan2, Pan3 and poly (A) binding protein to perform proper polyadenylation.

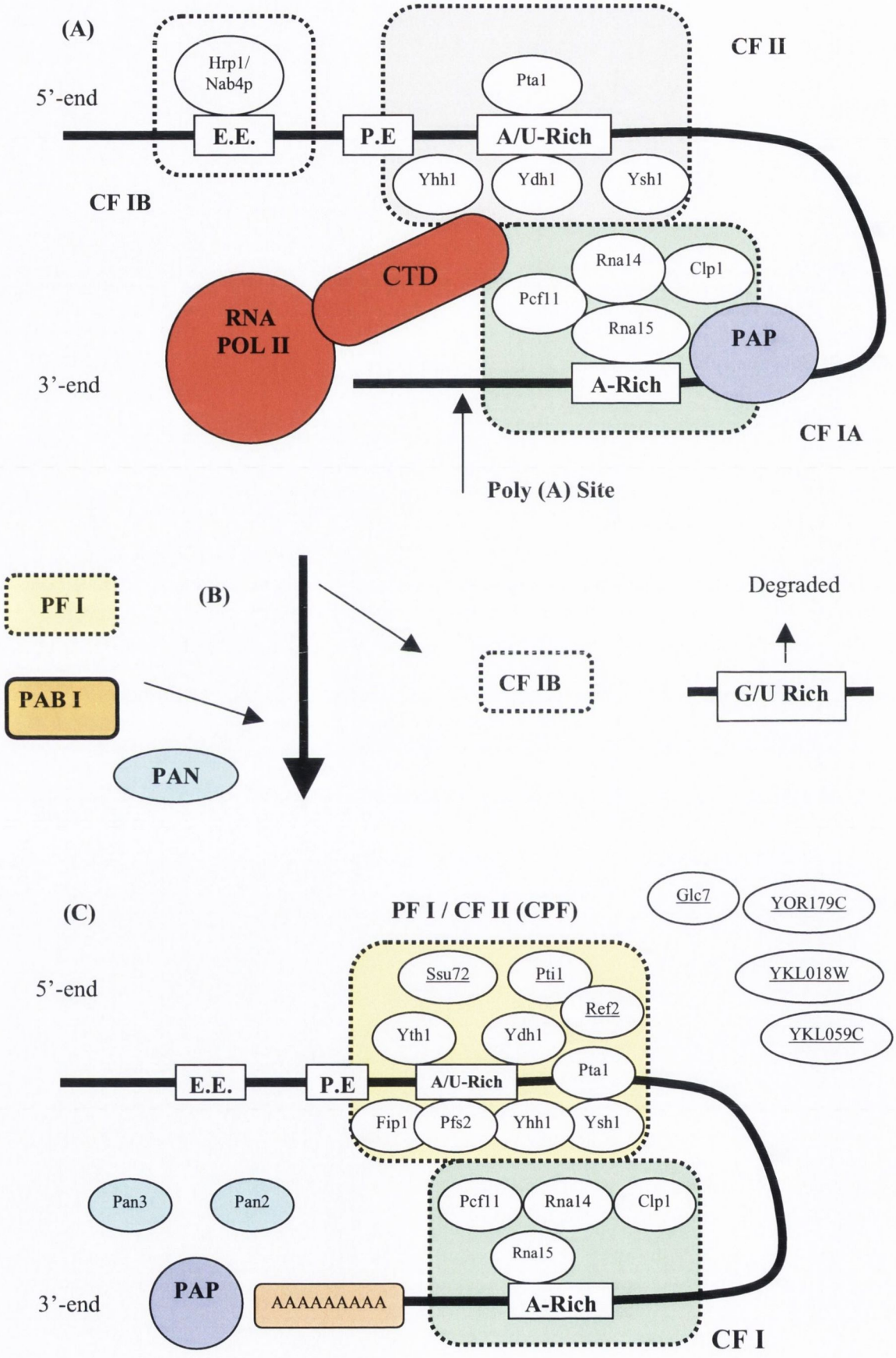
(A)
5'-end
Hrp1/
Nab4p
E.E.
P.E
A/U-Rich
Pta1
CF II
Yhh1
Ydh1
Ysh1
CF IB
CTD
RNA
POL II
Rna14
Clp1
Pcf11
Rna15
PAP
3'-end
A-Rich
CF IA
Poly (A) Site
PF I
(B)
PAB I
PAN
CF IB
Degraded
G/U Rich
(C)
PF I / CF II (CPF)
Glc7
YOR179C
5'-end
Ssu72
Pti1
Ref2
YKL018W
Yth1
Ydh1
YKL059C
E.E.
P.E
A/U-Rich
Pta1
Fip1
Pfs2
Yhh1
Ysh1
Pan3
Pan2
Pcf11
Rna14
Clp1
Rna15
3'-end
PAP
AAAAAAAAA
A-Rich
CF I

1.4 Interrelationships between mRNA 3'-end formation and other processes

RNA Polymerase II plays a key role in gene expression. It mediates the recruitment of many factors involved in transcription: 5'-capping, 3'-end formation, degradation and export of the pre-mRNA (Hagiwara and Nojima, 2007). The transcription machinery is highly conserved from yeast to mammals. In prokaryotes, all genes are transcribed by the same RNA polymerase. The RNA polymerase consists of 2α, 1β, 1β', ω and σ subunits which functions in transcription initiation and elongation. In contrast, eukaryotic transcription is performed by three RNA polymerases which have different functions. Unlike eukaryotes, single-celled prokaryotes have neither nucleus nor histones. The function of poly (A) tails in prokaryotes also seems to be different to eukaryotes. The poly (A) tracts are 14-60 nucleotides long in bacterial and 80-200 nucleotides long in eukaryotes (Sarkar, 1997). Once the RNA molecules are polyadenylated at their 3'-ends in *E.Coli*, the RNA goes through a polyadenylation RNA degradation mechanism. The polyadenylation RNA degradation mechanism causes the mRNAs to be destabilised and degraded by the 3'-5' exonucleases instead of stabilised, as occurs in eukaryotes (Dreyfus and Regnier, 2002).

Eukaryotic cells contain three types of RNA polymerases: I, II and III, which transcribe different genes. The first RNA polymerase, polymerase I, functions in transcribing the 28S, 18S and 5.8S ribosomal RNA (rRNA) genes. The rRNAs are clustered together with ribosomal proteins to form the rRNA bodies known as ribosomes. The ribosomes provide the connection between the mRNAs and tRNAs with their attached amino acids to catalyse polypeptide synthesis. RNA polymerase II transcribes mRNAs which encodes for proteins. It also transcribes small nuclear RNAs (snRNAs) and small nucleolar RNAs which are non-polyadenylated and require 3'-end processing to mature snRNA. snRNA functions in splicing pre-mRNA to mature mRNA. The small nucleolar RNAs are involved in

maturation of rRNAs, snRNAs and mRNAs (Morlando *et al*, 2002). Polymerase III functions in transcribing tRNAs which assemble the amino acids together for protein synthesis. The 3' and 5' ends of pre-tRNAs are processed by exo- and endo-ribonucleases. tRNA recognises the mRNA sequences and attach to the correct amino acid sequences which initiates protein synthesis and elongation (Turner *et al*, 2005).

For many years, researchers focused on deciphering the mechanisms of the individual mRNA transcription and processing reactions, instead of linking the mRNA events together. New insights into the links between pre-mRNA processing events and the mRNA associated factors required to ultimately promote the final export as mature mRNAs, known as messenger ribonucleoprotein complexes (mRNP), revealed that these processes are tightly co-ordinated. In the following sections, the communications between transcription, 3'-end processing, termination, degradation and export are discussed.

1.4.1 Coupling of 3'-end formation and transcription

The C-terminal domain (CTD) is the largest subunit of RNA Polymerase II consisting of 26 heptad repeats with the sequence Tyr-Ser-Pro-Thr-Ser-Pro-Ser in *Saccharomyces cerevisiae* (Proudfoot, 2004). There are 52 heptad repeats in mammals. The CTD acts as a recruitment platform for transcription and mRNA processing factors and is important for coupling 3'-end formation and transcription (Noble *et al*, 2005). As a result, efficient splicing, capping and 3'-end formation depends on the CTD in yeast and mammals (Rosonina and Blencowe, 2004). Studies using deletions in the CTD (RNA pol II Δ CTD) in the *rpb1-1* mutant background, showed that the CTD was required for efficient 3'-end cleavage of pre-mRNAs. Additionally, the poly (A) tails were shown to be shorter in CTD deletion strains which also lacked poly (A) nuclease (PAN) (Licatalosi *et al*, 2002).

Initially, RNA Polymerase II is phosphorylated at serine 5 at the promoter by a number of kinases. The Cdk7 subunit phosphorylates the CTD on serine 5 and recruits the mRNA

capping enzyme, guanylyltransferase. The second kinase, Cdk8, is thought to negatively regulate initiation. As serine 5 becomes dephosphorylated, the serine 2 becomes phosphorylated by CTDK-1 (CTD kinase 1) and Bur1 kinase, which promotes elongation in *Saccharomyces cerevisiae*. During the transcription cycle, binding of 3'-end processing factors to the CTD depends on the phosphorylation state of the CTD (Ahn *et al*, 2004; Komarnitsky *et al*, 2000). Several 3'-end processing factors have been proposed to bind to the phosphorylated CTD, these include CFIA, CFIB and PFI, subunits of Ydh1p/Cft2p and Fip1p (Licatalosi *et al*, 2002).

Pcf11 protein recruits the CFIA and CFIB complex (consisting of Rna14, Rna15, Clp1 and Hrp1 proteins) to the CTD domain via its N-terminal CTD-interaction domain (CID). The CID domain of Pcf11 protein recognises the serine 2 phosphorylated CTD of RNA Polymerase II during the elongation phase of the transcription cycle (Licatalosi *et al*, 2002).

In 2005, Rigo and Martinson demonstrated that interaction of the pre-mRNA downstream of the poly (A) site with RNA Polymerase II was essential for 3'-end processing *in vitro*. Using DNA oligonucleotides complementary to downstream sequences and RNase H assays, the tether between the pre-mRNA and the Polymerase was severed, leading to a drastic reduction in the efficiency of 3'-end processing (Rigo and Martinson, 2005). Interestingly, Ssu72 is a phosphatase that interacts with transcription initiation factor, TFIIB, and was found to interact with Pta1, a subunit of PFI, *in vitro* and *in vivo* (Ansari and Hampsey, 2005; He *et al*, 2003). Ssu72 protein also directly interacts with the Rpb2 subunit of RNA Polymerase II to initiate the transcription process (Pappas and Hampsey, 2000). The main role of Ssu72 protein is to connect 3'-end processing to transcription by providing a bridge for transcription initiation factor TFIIB, Pta1p, Ydh1p and Rpb2p (Dichtl *et al*, 2002b).

In mammalian cells, the PC4 (Sub1 in yeast) complex is a co-activator required to activate transcription *in vitro* and is analogous to Ssu72 (Calvo and Manley, 2005). The transcription factor, TFII, and PC4 make up the transcription initiation site which bind to the 3'-end mRNA processing factors, CstF64 (Rna15 in yeast) and mammalian Ssu72 (Ssu72 in yeast). The interaction between the PC4 co-activator and CstF64 is conserved from yeast to humans. The factors influence transcription initiation and 3'-end formation in metazoan cells (Bentley, 2005).

1.4.2 Coupling of 3'-end formation and termination

Termination is an important step in gene expression since it allows the release of transcripts from the transcription site and release of RNA Polymerase II from the DNA template (Howe, 2002). This recycling step allows the transcription process to continue as Polymerase II goes back to the promoters. The transcription termination elements also play a role in preventing transcriptional interference leading to proper transcription of genes. The mechanism of termination requires the recognition of pause sites and poly (A) sites. Transcription termination appears to be triggered by pausing of the Polymerase once it has traversed the poly (A) site. Transcription termination pause sites have been identified downstream of a number of mammalian genes. The best characterised pause site is the MAZ (G-rich sequences) site downstream of the human C2 complement gene. Multiple MAZ sites downstream of a synthetic poly (A) site promote efficient 3'-end cleavage and polyadenylation, while mutation of the MAZ site abolishes the process (Yonaha and Proudfoot, 1999).

Another sequence that can promote transcription termination is the CoTC (co-transcriptional cleavage) complex, lying downstream of the human β-globin gene. In addition to promoting transcription termination, this site appears to act as an additional cleavage site on the pre-mRNA downstream of the poly (A) site. The lack of consensus

sequences in the downstream region of pre-mRNAs for Polymerase pause sites, may indicate that multiple mechanisms may prevail (Gromak *et al*, 2006). The human 5'→3' exonuclease, Xrn2p, recognises the CoTC sequence. Xrn2p also degrades the RNA from the 5'-end and in doing so promotes transcription termination (Teixeira *et al*, 2004; West *et al,* 2004). Evidence has shown that cis-acting 3'-end processing signals are required to terminate transcription (proudfoot, 1989). This led to Birse *et al* (1998) to investigate whether the trans-acting 3'-end processing factors affect transcription termination. Transcription run on analysis in the temperature-sensitive 3'-end cleavage mutants, *rna14*, *rna15* and *pcf11*, revealed that inhibition of 3'-end cleavage led to a lack of transcription termination and an accumulation of read-through transcripts (Birse *et al*, 1998).

Recent studies by Park *et al* (2004) have uncovered a role for the CTD in transcription termination (Park *et al*, 2004). Using truncation mutants of the mammalian CTD, the authors demonstrated that the CTD was not required for RNA Polymerase II poly (A) dependent pausing, but did play a role in RNA Polymerase II release.

Several CTD binding proteins have been shown to play a role in transcription termination. Truncations created in the CTD domains in yeast have been shown to reduce 3'-end processing, capping and splicing (McCracken *et al*, 1997). Pcf11p and Yhh1p are components of CFI and PFI. Yhh1 mutant strains have been observed to be defective in transcription termination. It is known that Yhh1p binds to the poly (A) site, but it is also assumed to bind to the CTD, although no evidence has been provided as yet (Dichtl *et al*, 2002b). Pcf11 has been shown to act as a releasing factor capable of disrupting the interaction between RNA Polymerase II and the nascent transcripts. Transcription termination defects in the CTD or the CID domain in Pcf11 caused termination defects in yeast (Zhang *et al*, 2005). Therefore, both the CTD of Polymerase II and CID of Pcf11 play a role in transcription termination. Also, in metazoan cells, hPcf11 appears to act as a bridge between the CTD and the nascent RNA. hPcf11 can also inhibit transcription at low,

but not high, nucleotide concentrations, suggesting that hPcf11 dismantles paused RNA Polymerase complexes in metazoan cells (Zhang and Gilmour, 2006).

The question as to how termination occurs has been a source of confusion for decades for many scientists. Within the last two years, Kim *et al* (2004), Teixeira *et al* (2004) and West *et al* (2004) presented plausible models to explain the process. Two mechanisms have been put forward, namely the 'allosteric' (anti-terminator) model and the 'torpedo' model.

In the proposed anti-terminator model, RNA Polymerase II passes the poly (A) signal. The Polymerase then becomes modified, causing the release or recruitment of termination factors, leading to the release of DNA template, RNA template and other factors (*Figure 1.3(A)*, adapted from Luo and Bentley, 2004). The anti-terminator model has come from data indicating that termination can take place in the absence of cleavage. Electron microscopy images of RNA Polymerase II genes in *Drosophilia* demonstrated that the majority of full-length transcripts were released from the template prior to cleavage. This indicates that the assembly of cleavage and polyadenylation factors may be sufficient to trigger termination. In fact, prokaryotic *E. coli* termination factor, rho, has been shown to release the yeast RNA Polymerase II from pause sites downstream of the poly (A) site of a eukaryotic mRNA (Lang *et al*, 1998).

The alternative torpedo model involves the 5'→3' exonuclease, Rat1p. When the pre-mRNA is cleaved, the 5' phosphate on the released downstream RNA is exposed to the 5'→3' exonuclease, Rat1p. Rat1p then digests the unstable pre-mRNA transcript rapidly until it reaches the Polymerase, triggering termination by physically interacting with RNA Polymerase II (*Figure 1.3(B)*, adapted from Luo and Bentley, 2004).

A novel protein, Rtt103p, has been isolated by affinity chromatography of yeast whole-cell extracts and was found to bind to the carboxyl-terminal domain of RNA Polymerase II during transcription. Rtt103p was found to be associated with Rat1p and its partner, Rai1p. The temperature-sensitive strains, *rat1* and *rai1*, exhibited termination defects. Further

analysis revealed that 3'-end processing factors, CFIA and CPF, interact with Rtt103p, Rat1p and Rai1p, indicating that Rat1p may play a role in 3'-end processing or that 3'-end processing and termination are ultimately linked (Kim *et al*, 2004).

Recently, it has been demonstrated that Rat1p is not merely a termination factor, but is also essential for recruitment of 3'-end processing factors. Pcf11p has been shown to interact with Rat1p, indicating that Rat1p recruits the 3'-end termination factor, Pcf11p. Taken together, the data supports a model in which Pcf11p acts as a termination factor and Rat1p as the torpedo factor (*Figure 1.3(C)*, adapted from Luo *et al*, 2006).

Nrd1p (nuclear pre-mRNA down-regulation) is a 3'-end RNA-binding protein that promotes transcription termination of small nuclear RNAs (snRNA) and small nucleolar RNAs (snoRNA) (Steinmetz *et al*, 2001). Nrd1p has an N-terminal interacting domain that recognises the CTD of RNA Polymerase II. For recognition to the CTD of Pol II, Sen1p, a helicase and Nab1p, a RNA-binding protein must interact with Nrd1p. Mutant strains of NRD1 have also demonstrated termination defects. Interestingly, recent work has discovered that Nrd1 recruits the exosome component, Rrp6, to snRNA and snoRNA (Arigo *et al*, 2006; Vasiljeva and Buratowski, 2006). Recently, Kim *et al* performed CHIP analysis that indicated that rat1 mutant is normal in snoRNA termination. This data points to Nrd1, Nab3 and Sen1 being the strongest candidate for snoRNA termination (Kim *et al*, 2006). Again, further work is necessary to determine the mechanisms of how Nrd1 contributes to transcription termination and what role the nuclear exosome might play in this process.

The phosphatase and transcription initiator factor, Ssu72p, has also been shown to be involved in termination (Steinmetz and Brow, 2003). Deletion of the exosome component, Rrp6, in a *ssu72* background corrected the termination defect, suggesting that the 3'→5' exonuclease complex may play a role in transcription termination (Dichtl *et al*, 2002a). These results indicate that Ssu72p acts as an anti-termination factor when the protein is

with the CPF complex during elongation. When the yeast Ssu72p was deleted or when the transcriptional activator, Sub1p, was over-expressed, termination defects were observed. These results indicate that the Sub1 protein plays a role in anti-termination when it is bound to Rna15p during elongation (Calvo and Manley, 2001). The Ssu72p was also found to regulate other enzymes during elongation, such as the phosphatase, FCP1 (Calvo and Manley, 2005).

Figure 1.3: Models for termination by RNA Polymerase II. The proposed models for transcription termination by RNA Polymerase II demonstrate coupling between transcription, termination and 3'-end processing. **(A)** The anti-terminator model. Polymerase II is in its active conformation during elongation (green oval). The blue circle denotes the 5' cap and the black line (tail of Pol II) is the CTD of Polymerase II where phosphorylation occurs. The lighting bolt is the poly (A) cleavage site. When the Polymerase passes the poly (A) site (AAUAAA), it is modified to a non-processive form, causing termination and release of Polymerase II. The dotted line is the degraded downstream RNA. **(B)** The torpedo model. The orange star on top of Polymerase II is the 5'→3' exonuclease, Rat1p. After cleavage (lighting bolt), Rat1p is attracted to the 5' phosphate and begins digesting the remaining RNA to the Polymerase II complex, triggering termination. Eventually, Rat1p and Polymerase II dissociate from the DNA template. **(C)** A hybrid of the anti-terminator and torpedo models. The interaction of Rat1 and cleavage/polyadenylation factors to the Polymerase II complex is proposed to cause an allosteric change in Polymerase II, which will trigger termination. The blue triangle denotes the Pcf11 factor.

A) Anti-terminator model

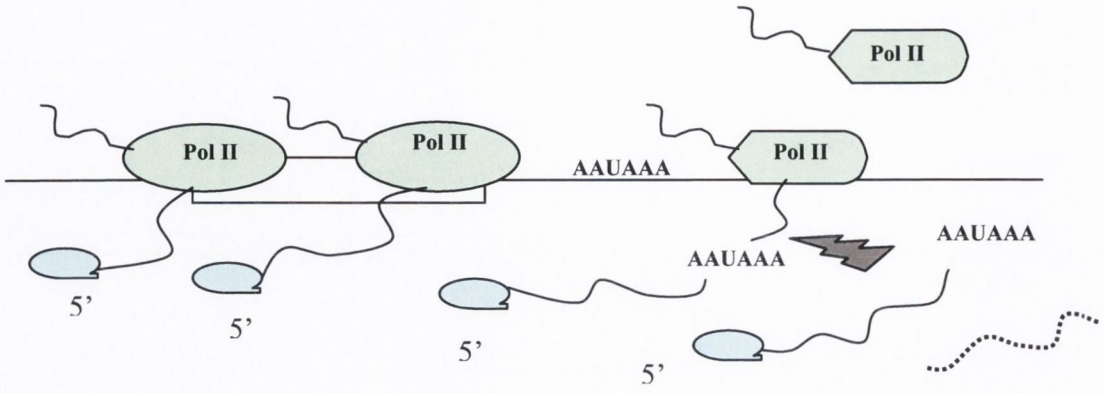

B) Torpedo model

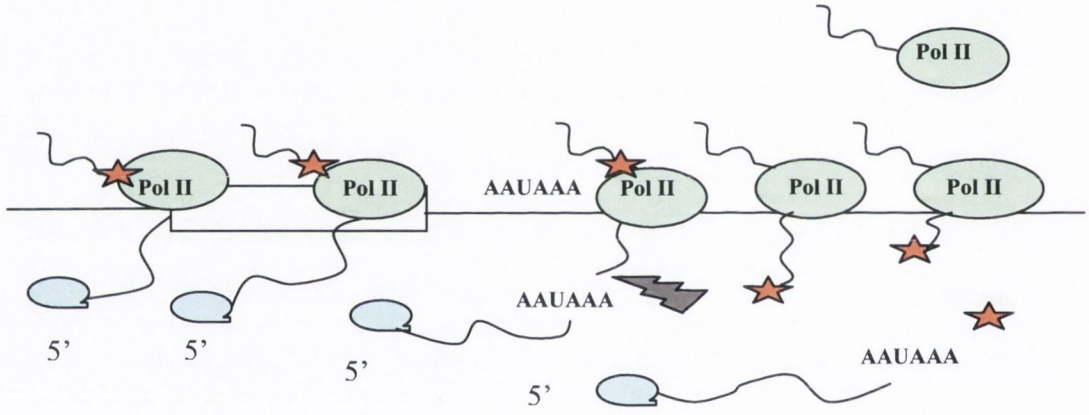

C) A hybrid of the anti-terminator and torpedo models

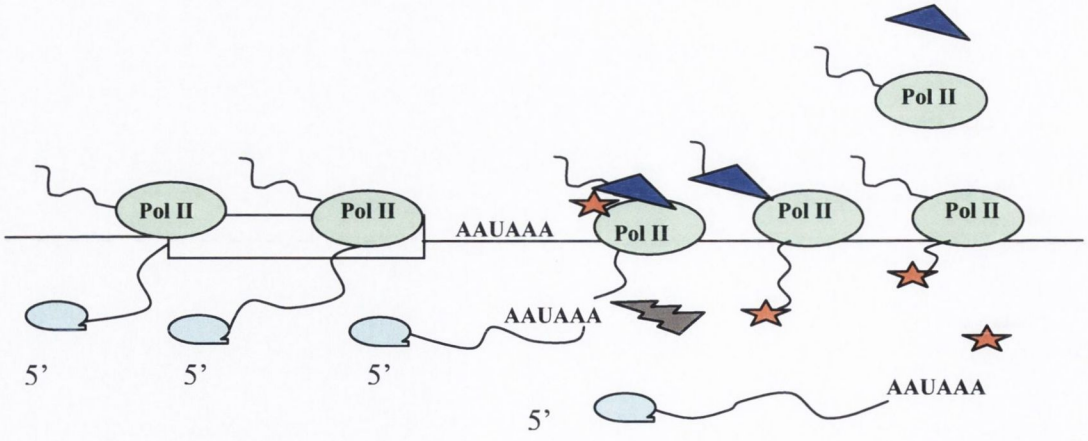

1.4.3 Coupling of 3'-end processing with the nuclear exosome: Nuclear surveillance of mRNA processing

Pre-mRNA must undergo mRNA processing by several processing factors in order to develop into mature mRNAs, known as messenger ribonucleoprotein complexes (mRNP). Only mature mRNP can be exported from the nucleus to the cytoplasm. The exosome is a 3'→5' exoribonuclease complex found in both the cytoplasm and the nucleus. The nuclear exosome contains 10 core proteins and an additional unique protein, Rrp6p (Butler, 2002; Jensen *et al*, 2003). The role of the nuclear exosome is to act as a surveillance system to prevent unprocessed mRNAs from being exported from the nucleus to the cytoplasm. Rrp6p was found to be homologous to the human nuclear-restricted component, PM-Scl protein (100 kDa), antibodies to which are associated with the human auto-immune connective tissue disease, Scleroderma (Allmang *et al*, 1999; Brouwer *et al*, 2001). In addition to a role in control of mRNA expression, Rrp6p is also involved in processing of the 7S pre-rRNA to 5.8S rRNA, which forms a component of the 60S complex, and in the processing of some snRNAs and snoRNAs (Hoof *et al*, 2000).

A number of studies within the nucleus in yeast have uncovered a link between the nuclear exosome and mRNA 3'-end processing. The first indication of this link came from an analysis of poly (A) polymerase (PAP) (Burkard and Butler, 2000). The temperature-sensitive mutant, *pap1-1*, caused a reduction in the poly $(A)^+$ mRNA levels at the restrictive temperature, whereas in the genetic background, *pap1-1/Δrrp6*, the levels of poly $(A)^+$ were similar to the WT levels. This provided the first evidence that the cleavage and polyadenylation machinery and the exosome appear to compete for the same substrate, the pre-mRNA. Subsequent studies, using a variety of *pap1* mutant strains, confirmed the role of Rrp6p in a RNA surveillance pathway that rapidly degraded aberrant polyadenylated RNAs (Milligan *et al*, 2005). The role of the nuclear exosome in nuclear surveillance of pre-mRNA processing was further established in studies by Libri *et al*

(2002). Using a series of mutant strains defective in mRNA elongation, *Δhpr1* and *Δmft1*, and 3'-end processing, *rna14-1* and *rna15-2*, the authors showed that the pre-mRNA was retained in the nucleus. However, the double mutants, *Δhpr1/Δrrp6*, *Δmft1/Δrrp6*, *rna14-1/Δrrp6* and *rna15-2/Δrrp6*, showed no retention, indicating the Rrp6p functions in nuclear retention. RNAs produced in the *Δhpr1* and *Δmft1* strains were truncated at their 3'-end, but the *Δhpr1/Δrrp6* and *Δmft1/Δrrp6* strains showed restoration of the 3'-end levels similar to the WT. This indicated that the transcripts resulting from aberrant transcription elongation were substrates for Rrp6p (Libri *et al*, 2002).

Mutations in RNA14 or RNA15 resulted in the inhibition of both 3'-end cleavage and transcription termination, leading to the promotion of long 3'-end extended pre-mRNAs. These transcripts have also been shown to be substrates for the nuclear exosome. Furthermore, functional short polyadenylated transcripts can be produced from the long 3'-end extended transcripts in a *rna14.1/Δrrp6* background, suggesting that the nuclear exosome component, Rrp6p may play a role in generating functional mRNAs via a mechanism independent of 3'-end cleavage and polyadenylation (Torchet *et al*, 2002). Alternatively, it could be argued that deletion of RRP6 stabilises unprocessed pre-mRNAs, which may be later cleaved and polyadenylated by a sub-optimal cleavage and polyadenylation complex lacking Rna14p or Rna15p.

1.4.4 Coupling of the exosome with nuclear mRNA export

Nuclear pore complexes (NPCs) are situated in the nuclear envelope and provide a channel for transport between the cytoplasm and the nucleus (*Figure 1.4*, adapted from Allen *et al*, 2000; Cole and Scarcelli, 2006; Jimeno *et al*, 2002; Reed, 2003). NPCs are composed of nucleoporin proteins which facilitate substrates going in and out of the nucleus, cytoplasmic filaments, nuclear basket, cytoplasmic coaxial ring and nucleoplasmic ring.

During transcription and processing, mRNAs associate with a number of proteins that facilitate their interaction with the NPC and their subsequent export from the nucleus. These messenger ribonucleoprotein complexes (mRNPs) first interact with the RNA helicase and splicing factor, Sub2p (UAP56 in metazoans). Sub2p promotes the interaction with Yra1p and the THO complex. The THO complex with Sub2p and Yra1p is known as the THO-TREX complex. The THO complex is a transcription complex that consists of Hpr1p, Tho2p, Mft1p and Thp2p (Vinciguerra and Stutz, 2004). Hpr1p functions in recruiting Sub2p and Yra1p to the mRNP (Zenklusen and Stutz, 2002). The mRNA export adapter, Yra1p (Aly in metazoans), recruits Mex67p-Mtr2p (TAP/p15 in metazoans), leading to Sub2p displacement, and promotes interaction of the mRNP with the nucleoporins in the NPC. The Mex67p-Mtr2p complex interacts with the shuttling protein, Npl3p (Gilbert and Guthrie, 2004). The mRNP complex binds to nucleoporins on the cytoplasmic filaments, including Ddp5/Rat8, Nup159/Rat7, Nup42/Rip1, Nup100, Nsp1, Nup82 and Gle1.

So far, fifty nucleoporins have been identified and placed into two groups. One group includes repeat-containing proteins, XFXFG, GLFG and XXFG repeats. Rat7p/Nup159p contains 22 XXFG repeats and Rip1/Nup42p is 75% similar to the repeat regions of Rat7p. Many interactions have been discovered between the nucleoporins, demonstrating that these factors are essential for nuclear export. The Rat7p forms a complex with Nup82p and Nsp1p, and also interacts with another nucleoporin, Nup116p. Any defects in these proteins lead to severe defects in mRNA export (Bailer *et al*, 2000). Further research has shown that the nucleoporin, Rat8p/Dbp5p, interacts with Rat7p, Gle1p, Rip1p and Nsp1p (Lund and Guthrie, 2005; Strahm *et al*, 1999). Also, the mRNA export receptor, Mex67p/Mtr2p, requires specific sequences within the nucleoporins (like Rat7p, Rip1p, Nsp1p and Nup116p) for docking, interactions with other nucleoporins and final export through the NPC (Straber *et al*, 2000).

In 2000, Burkard and Butler provided evidence linking the 3'→5' nuclear exonuclease, Rrp6 protein, to Pap1p and with the nucleo-cytoplasmic export shuttling protein, Npl3p (Burkard and Butler, 2000). These findings suggest that Rrp6p interacts with the 3'-end processing machinery and participates in nuclear mRNA degradation. Localisation assays performed by Thomsen *et al* (2003) provided further evidence demonstrating a link between nuclear export and the nuclear exosome, Rrp6p. It is known that Rrp6p is required for nuclear retention of aberrant mRNAs (Thomsen *et al*, 2003). From FISH analysis, the mRNAs in the *rat7*, *rip1*, *rat7-1/Δrrp6* and *rip1-1/Δrrp6* mutant strains were found to be retained in the nucleus and were not exported to the cytoplasm, indicating the link between nuclear export and the nuclear exosome (Hilleren *et al*, 2001; Thomsen *et al*, 2003).

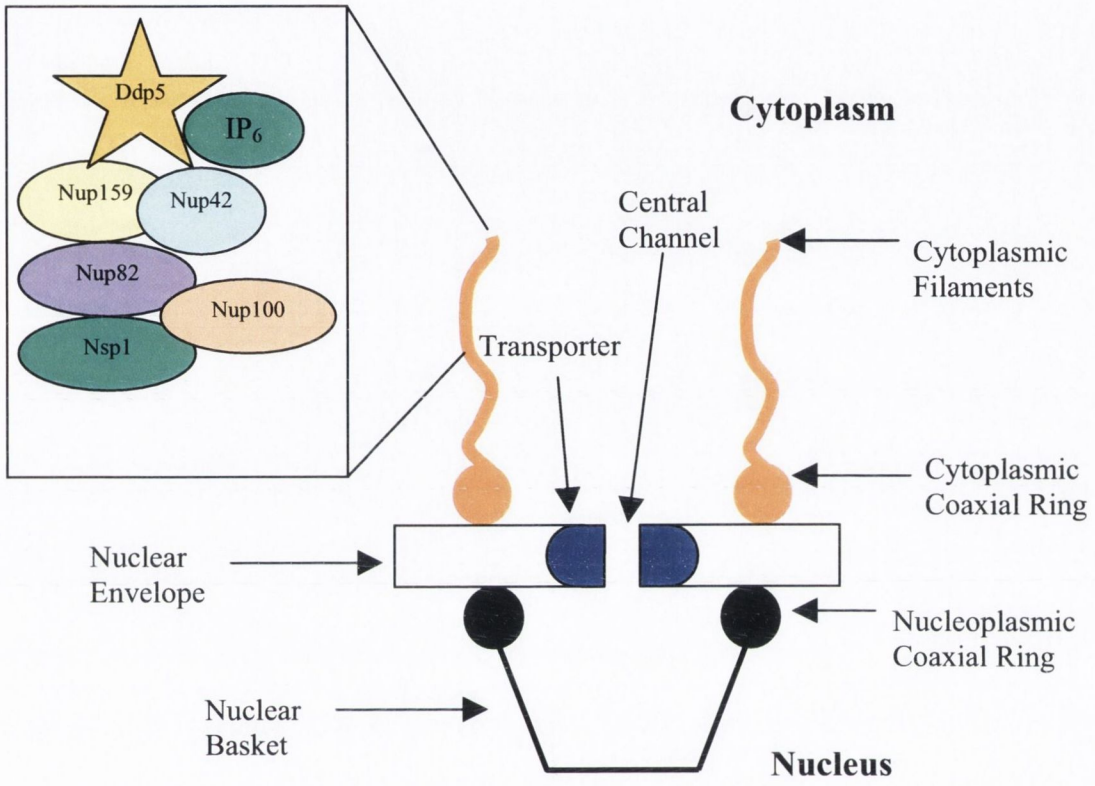

Figure 1.4: mRNA export machinery from the nucleus to the cytoplasm.

When the mRNP complex travels from the nucleus through the nuclear basket and central channel, it binds to the nucleoporins in the cytoplasmic filaments before being exported to the cytoplasm for translation. These nucleoporins include Ddp5/Rat8, Nup159/Rat7, Nup42/Rip1, Nup100, Nsp1, Nup82 and Gle1. IP_6 is one of the phosphoinositides found in cells along with the nucleoporin proteins.

1.4.5 Coupling of 3'-end processing with nuclear mRNA export

The 3'-end processing factors, Rna14p, Rna15p and Pcf11p, are essential for mRNA 3'-cleavage and transcription termination. *In situ* hybridisation revealed that mutations in RNA14, RNA15 or PAP lead to nuclear retention of RNA transcripts (Brodsky and Silver, 2000). Research carried out on Pab1p, PAN and Nab2p, provided further evidence of the connections between 3'-end processing and nuclear mRNA export. Pab1p is a poly (A) binding protein, which functions in proper poly (A) addition to the pre-mRNAs. Further research is required to understand the role of Pab1p in mRNA export. PAN (3'→5' poly (A) exoribonuclease) binds to the poly (A) sites to trim the Poly (A) tail to its correct size. Fluorescence imaging has shown that nuclear retention of the SSA4 mRNA occurs in PAN mutants (Dunn *et al*, 2005). This result demonstrates that PAN is a 3'-end processing nuclease which regulates the release of mRNAs from the nucleus to the cytoplasm. A second nuclear poly (A) binding protein, Nab2p, has a function in poly (A) tail length control *in vitro* and *in vivo*. The temperature-sensitive strain, *nab2,* exhibited hyper-adenylated transcripts, whereas the wild type processed normal poly (A) tail lengths. The RNA transcripts were localised in the nucleus in the *nab2* background (Hector *et al*, 2002). Interestingly, the nuclear export factors, Rat7p, Gle1p, Mex67p and Rat8p/Dbp5p, affect 3'-end processing, as well as export, by stalling mRNA biogenesis as the transcripts are hyperadenylated in the mutants (Hilleren and Parker, 2001).

1.5 Other RNA processing reactions

1.5.1. Processing of rRNA and tRNA

Like eukaryotic pre-mRNAs, other RNAs, such as rRNAs and tRNAs, also undergo post-transcriptional processing. The RNase MRP (mitochondrial RNA processing) is an enzymatic complex that cleaves a specific site (A3) in the internal transcribed spacer 1 region of precursor rRNA, leading to the release of the mature 5'-end of 5.8S rRNA (Li *et al*, 2004a). RNase MRP is only present in eukaryotes and is essential for cell viability. The yeast holoenzyme has an RNA subunit, NME1, and nine essential proteins, Pop1p, Pop3, Pop4, Pop5, Pop6, Pop7, Pop8, Rpp1p and Snm1p (*Table 1.4*). The complex resides mainly in the nucleolus (99%), whereas a small amount was found to reside in the mitochondria. As well as rRNA processing, the complex is involved in mRNA degradation and turnover of selected cell-cycle regulated messenger RNAs. Gill *et al* (2004) demonstrated that cleavage of the 5'-untranslated region of the CLB2 mRNA led to its degradation, leading to cell-cycle progression. The CLB2 mRNA encodes for a β-type cyclin (Cai *et al*, 2002; Gill *et al*, 2006; Gill *et al*, 2004). The human RNase MRP contains an RNA referred to as 7-2 and six proteins, Pop1p, Rpp29p, Pop5p, Pop6p, Rpp20p and Rpp30p.

Ribonuclease P (RNase P) is an enzyme that functions in endonucleolytic cleavage of the 5'-leader of precursor tRNAs to a mature 5' termini. The RNase P RNA is 369 nucleotides long in *Saccharomyces cerevisiae* and 286 nucleotides long in Schizo*saccharomyces pombe* (Lee and Engelke, 1989). The complex has been found in all living cells, including *Saccharomyces cerevisiae*, and many organelles, including mitochondria and chloroplasts. Within *Saccharomyces cerevisiae,* the complex has been detected in the nucleus and nucleoplasm. The holoenzyme in *Saccharomyces cerevisiae* consists of one RNA and nine proteins associated through protein interactions. The nine protein subunits are Pop1p, Pop3p, Pop4p, Pop5p, Pop6p, Pop7p, Pop8p, Rpp1p and Rpp2p (Houser-Scott *et al*, 2002;

Xiao and Engelke, 2005). The RNase P RNA is encoded by the RPR1 gene and consists of 84 nucleotides of 5' leader, a short 3'-trailing sequence and an internal promoter for Polymerase III. In the human RNase P, Pop1p, Rpp29p, Rpp20p, Rpp30p show homologies to the yeast Pop1p, Pop4p, Pop5p and Pop7p respectively. The human RNA sequence is referred to as the H1 RNA and the complex includes the REP38, RRP40, RRP25 and RRP14 proteins, which have no homologies to the yeast complex.

The RNase MRP and RNase P are evolutionary and structurally conserved. Eight proteins (Pop1p, Pop3p, Pop4p, Pop5, Pop6p, Pop7p, Pop8p and Rpp1p) in yeast RNase MRP are also present in RNase P. Both the RNAs within the complexes are folded into similar secondary structures, but have weak sequence homologies. Many protein-protein interactions take place between the protein subunits, particularly between Pop1p, Pop4p and Pop7p, with human homologies demonstrating the strongest interactions. This supports a theory that Pop1p, Pop4p and Pop7p may play a central role in the RNase MRP and RNase P complexes. Snm1 protein is unique to the RNase MRP, while Rpr2 protein is the only protein unique to RNase P. Recently, a new protein, designated RNase MRP protein 1, was purified from the *Saccharomyces cerevisiae* RNase MRP complex. Further work is required to establish the protein's association with the RNase MRP complex (Salinas *et al*, 2005). The RNase P and RNase MRP complexes are very similar and exist as separate complexes within the cell.

Table 1.4: Subunit composition of *S. cerevisiae* and human RNase P and RNase MRP complexes

Yeast Gene				Human Gene		
RNaseP	**RNase MRP**	**Subunit type**	**Molecular weight (kDa)**	**RNaseP**	**RNase MRP**	**Reference**
RPR1	–	RNA	120	H1	–	(Welting and Pruijn, 2004)
–	NME1	RNA	112	–	7-2	(Welting and Pruijn, 2004)
POP1	POP1	Protein	100.5	POP1	POP1	(Eenennaam *et al*, 2001a)
POP3	POP3	Protein	22.6	–	–	(Dichtl and Tollervey, 1997)
POP4	POP4	Protein	32.9	RPP29	RPP29	(Eenennaam *et al*, 2001b)
POP5	POP5	Protein	19.6	POP5	POP5	(Eenennaam *et al*, 2001b)
POP6	POP6	Protein	18.2	–	POP6	(Xiao *et al*, 2002)
POP7	POP7	Protein	15.8	RPP20	RPP20	(Salinas *et al*, 2005)
POP8	POP8	Protein	15.5	–	–	(Salinas *et al*, 2005)
RPP1	RPP1	Protein	32.2	RPP30	RPP30	(Salinas *et al*, 2005)
RPP2	–	Protein	16.3	–	–	(Lee and Engelke, 1989)
–	SNM1	Protein	22.5	–	–	(Xiao *et al*, 2002)
–	–	Protein	–	REP38	–	(Eenennaam *et al*, 2001a)
–	–	Protein	–	RRP40	–	(Welting and Pruijn, 2004)
–	–	Protein	–	RPP25	–	(Welting and Pruijn, 2004)
–	–	Protein	–	RPP14	–	(Welting and Pruijn, 2004)

1.6 Formation of 3'-ends of histone mRNAs and cell-cycle regulation of histone mRNAs

The next section deals with histone 3'-end processing in mammalian and yeast cells. In 1981, Wu and Bonner defined two forms of histone mRNAs, the replication-dependent variants and basal, replication-independent histone, variants. The replication-independent variants were found to account for 10% of total histone synthesis and have similar levels throughout the cell cycle. Replication-dependent variants account for 90% of histone synthesis, accumulate in the S-phase and are tightly coupled to DNA synthesis (Wu and Bonner, 1981). The mammalian replication-dependent histone mRNAs form a unique class of mRNAs in so far as they lack introns and are non-polyadenylated transcripts containing a conserved stem-loop structure at the 3'-end. Mammalian histone gene expression is regulated at both the transcriptional and post-transcriptional levels, resulting in a 35-fold increase in cellular histone mRNA levels during the S-phase of the cell cycle. Degradation of histone mRNA occurs as the cells progress into the G_2-phase. Unlike the mammalian replication-dependent histone RNAs, histone RNAs in lower eukaryotes, such as fungi, protozoa and yeast, are polyadenylated and lack the characteristic stem-loop structure at the 3'-end. Despite these apparent differences, yeast histone mRNAs are cell-cycle regulated. The divergence in the structure and mRNA 3'-end processing mechanism between the lower and higher eukaryotes present an interesting evolutionary paradox.

1.6.1 Mammalian histone mRNA 3'-end formation

Formation of the 3'-ends of replication-dependent mammalian histone mRNA requires an endonucleolytic cleavage of the primary transcripts (pre-mRNA). Efficient 3'-end formation requires two conserved cis-acting sequence elements, which include a stem-loop structure lying immediately upstream and a purine-rich element lying immediately downstream of the cleavage site (Kolev and Steitz, 2005; Marzluff, 2005). The stem-loop

structure consists of a 6 bp stem and a 4 bp loop, which is recognised by a stem-loop binding protein (SLBP1) (Dejong *et al*, 2002). The second cis-acting sequence is a loosely conserved purine-rich element, which is known as the histone downstream element (HDE), located 10-12 nucleotides downstream from the cleavage site. Two other trans-acting factors, the U7 snRNP and heat-labile factor, are required for efficient 3'-end processing. Mutations created in the stem-loop structure or the sequences flanking the stem loop of a mouse histone mRNA result in decreased histone mRNA levels (Battle and Doudna, 2001; Pandey *et al*, 1994). From foot-printing experiments, mutations in the stem-loop structure and/or sequences flanking the stem-loop structure caused a reduction in the binding affinity of SLBP, both *in vivo* and *in vitro* (Williams and Marzluff, 1995). This indicates that the SLBP recognises the RNA sequences in the stem-loop structure and plays an important role in histone processing. The SLBP (31 kDa) was identified by Martin *et al* (1997) and it has no known homologues in yeast.

The second mammalian cis-acting sequence is the histone downstream element (HDE), which is located approximately 10 nucleotides downstream of the 3'-end cleavage site. The HDE consensus sequence for humans is G/AAAGAGCUG (Cho *et al*, 1995). The GAAAGA sequence in the HDE for the sea urchin was found to be complementary to 3-8 nucleotides of the sea urchin U7 snRNA. Subsequent studies revealed a similar complementarity between the human H2B mRNA and the U7 snRNP. Disruption of base pairing leads to a reduction of 3'-end processing *in vitro* (Bond *et al*, 1991). A series of mutations were made in the mouse H2A-614 gene between the stem-loop structure and the HDE, which caused decreased processing *in vitro*. As each consecutive base pair was removed, the cleavage site is moved upstream by one base pair (Scharl and Steitz, 1996). The fixed site of 10 bases between the stem-loop structure and the HDE, known as the molecular ruler effect, is necessary for efficient cleavage. Further research demonstrated that separating the stem-loop structure from the HDE in the mouse H2A pre-mRNA altered

the cleavage site, but the U7 snRNP still recognised the substrates regardless of the HDE location. Immunoprecipitation experiments with the anti-SLBP antibody demonstrated that the SLBP formed a stable complex between the SLBP, U7 snRNP, HDE and pre-mRNA (Dominski and Marzluff, 1999). A novel factor was recently discovered by two-hybrid analysis to interact with the SLBP: this factor is the zinc finger protein (hZFP100) with a molecular mass of 100 kDa. hZFP100 interacts with SLBP, the stem-loop binding structure and even the U7 snRNP (Dominski *et al*, 2002; Zhao *et al*, 1999). The third trans-acting factor, heat-labile factor, has recently been identified as the protein symplekin by its sensitivity to heat treatment (Dominski and Marzluff, 1999).

The symplekin factor is 150 kDa and is a component of the 14.7S HLF complex (Kolev and Steitz, 2005). Through fractionation experiments, the subunits of cleavage and polyadenylation specificity factor (CPSF) and the subunits of cleavage and stimulatory factor (CstF) were shown to co-purify with the heat-labile factor and to play a role in 3'-end histone processing. The CPSF-73 factor was recently identified as an endonuclease, responsible for releasing the U7 snRNP (Dominski *et al*, 2005). The latter finding provides the first indication of a common molecular machinery required for the processing of both polyadenylated and non-polyadenylated mRNAs. A second exonuclease, 3'hExo, has been shown to interact with the stem-loop structure and the SLBP (Yang *et al*, 2006; Dominski *et al*, 2003). The theory was put forward that the 3'hExo component degrades the histone mRNA since it causes displacement of the SLBP and changes the stem-loop structure. Further interactions were uncovered between hZFP100 and U7 snRNP-specific Lsm11 protein (*Figure 1.5*). The Lsm11 protein contributes to binding the proteins to the Sm core region of the U7 snRNP and to assemble the U7 snRNP to the complex.

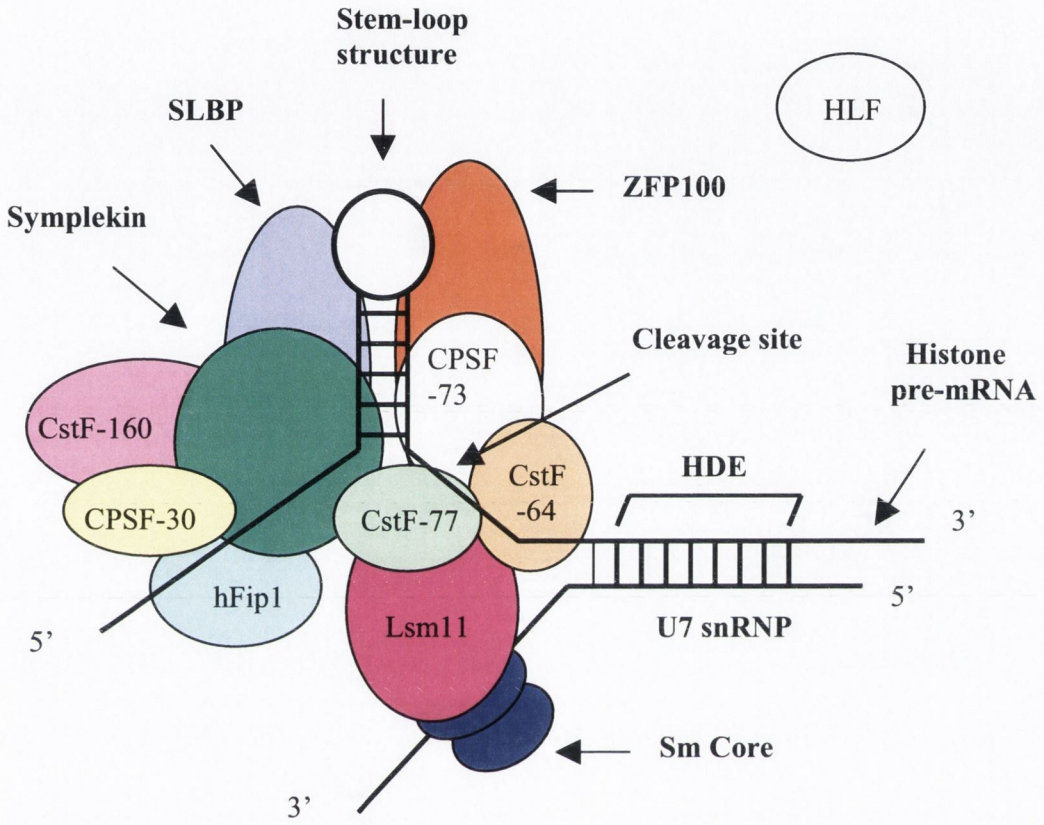

Figure 1.5: The 3'-end of the mammalian histone mRNA. The histone downstream element is base pairing with the U7 snRNP. The zinc finger binding protein 100 (ZFP100) and stem-loop binding protein (SLBP) bind to the stem-loop structure. The proteins shown are known or predicted interactions within the pre-mRNA complex. The proteins include CPSF-160, CPSF-73, CPSF-30, CstF-30, CstF-77, CstF-64, hFip1, Lsm11, ZFP100 and symplekin.

1.6.2 Mammalian histone mRNA levels during the cell cycle

1.6.2.1 Transcriptional regulation

Mammalian histone gene expression during the cell cycle is regulated through a number of individual elements. The histone gene promoter consists of the core promoter, subtype-specific consensus elements (SSCS) and distal activating domain. The core promoter (CP) consists of a TATA box and is important for transcription initiation. Mutations in the TATA box abolish transcription of histone genes (Grunstein and Mann, 1992). The SSCS has been shown to consist of a conserved CCAAT sequence and control the synthesis of histone genes into the S-phase (Sive *et al*, 1986). The SSCS have been shown to disturb the transcription efficiency of histone genes in the S-phase of the cell cycle when mutations were made. The third element involved in gene expression is the distal activating domain (DAD), which determines which histone gene will be the major determinant in each cell cycle (Heintz, 1991).

1.6.2.2. Post-transcriptional regulation

Post-transcriptional regulation was established to involve both mRNA degradation and 3'-end processing of histone pre-mRNAs (Harris *et al*, 1991). Maximum 3'-end processing occurs in the S-phase of the cell cycle. The U7 small nuclear ribonucleoprotein (snRNP) is an important component in histone cleavage reactions. The levels of the U7 snRNP were found to be constant throughout the cell cycle (Bond and Yario, 1994; Hoffman and Birnstiel, 1990). The heat-labile factor was found to decrease in the G_1-phase under mild heat treatment. These results show for the first time that the heat-labile factor, symplekin, is cell-cycle regulated (Kolev and Steitz, 2005; Luscher and Schumperli, 1987). Further work is required to investigate if there are more heat-labile factors or if symplekin is the only heat-labile factor in the histone machinery.

Furthermore, the stem-loop binding protein (SLBP) is also cell-cycle regulated. There are minute amounts of SLBP observed at the G_1-phase. From analysis of Chinese hamster ovary cells, the SLBP accumulated in the late G_1-phase and early S-phase is followed by degradation at the end of the S-phase (Whitfield *et al*, 2000). The phosphorylation on two threonines on the SLBP contributes to the degradation process as cells progress from the late S-phase to G_2-phase (Jaeger *et al*, 2005; Zheng *et al*, 2003).

1.6.3 Yeast histone mRNA 3'-end formation

In comparision to higher eukaryotes, little information exists on histone mRNAs regulation in lower eukaryotes. Fahrner *et al* (1980) purified yeast histone mRNA for the first time. From oligo (dT) and *in vitro* experiments, they demonstrated that H2A, H2B, H3 and H4 mRNAs in yeasts are polyadenylated (Fahrner *et al*, 1980). The cis-acting and trans-acting factors influencing yeast histone 3'-end processing remain unexplored.

1.6.4 Yeast histone mRNA levels during the cell cycle

1.6.4.1 Transcriptional regulation

There are four main loci encoding the major core histones that contain transcribed gene pairs: *HTA1-HTB1*, *HTA2-HTB2*, *HHT1-HHF1* and *HHT2-HHF2*. The HTA1-*HTB1* and *HTA2-HTB2* gene pairs carry genes for H2A and H2B, while the *HHT1-HHF1* and *HHT2-HHF2* loci carry genes for H3 and H4 (Ericksson *et al*, 2005). Upstream activating sequences (UASs), containing a consensus sequence of (G/A)TTCCN_6TTCNC, is present at the H2A, H2B, H3 and H4 histone promoters. These sequences are usually clustered in the centre of each promoter. The *HTA1* and *HHT1* genes have four conserved UAS sequences, whereas the *HTA2* and *HHT2* genes contain 6 possible UAS sequences. The trans-acting factor, Spt10p, binds to all four histone UAS sequences. This sequence-specific binding protein functions in correct chromatin assembly. The UAS sequence has a

positive and negative role. The positive role is controlling the activation of transcriptions and correct cell-cycle periodicity. Repression of transcription in the G_1- and G_2-phases of the cell cycle is also mediated by the UAS sequence (Ericksson *et al*, 2005; Osley and Lycan, 1987).

The mRNAs from the *HTA1-HTB1*, *HHT1-HHF1* and *HHT2-HHF2* genes accumulate through transcriptional activation between the G_1- to S-phase. As the cells enter early G_1-, G_2- and M-phases, RNA is repressed by several trans-acting factors (Sutton *et al*, 2001). The trans-acting factors include the HIR1, HIR2 and Asf1 proteins. The HIR (histone regulation) genes are negative regulators. Hir2p, together with Hir1p and Hir3p, cause transcription repression of a HTA1-*lac* reporter gene (Spector *et al*, 1997). Asf1p was discovered to bind to Hir1p in yeast. Asf1p also represses transcription and plays a role in the cell cycle (Sutton *et al*, 2001). However, the mechanism of repression is not clear.

1.6.4.2 Post-transcriptional regulation

In the early 1980s, experiments were carried out for the first time confirming that histone mRNA levels are tightly regulated at the transcriptional and post-transcriptional levels. The cells were synchronised with the α_1-factor, causing the cells to arrest in the G_1-phase. After the mating pheromone factor was removed, cells initiated cell-cycle progression. The H2A and H2B mRNA levels were shown to accumulate in the S-phase. When DNA levels increased, the histone mRNA levels increased; when DNA levels decreased, the histone mRNA levels, similarly, decreased (Hereford and Osley, 1981). Lycan *et al* (1987) investigated the post-transcriptional events in histone mRNA levels in *Saccharomyces cerevisiae* during the cell cycle. They demonstrated that the histone H2B-lacZ gene fusion, containing 80 amino acids of the H2B 5' coding region, showed no cell-cycle accumulation pattern compared to the normal H2B gene. This indicated that the 5'-end of

the histone gene was not responsible for the S-phase accumulation and that the 3'-end might play a role. Hence, Xu *et al* (1990) carried out a series of experiments to address Whether the 3'-end of histone genes contribute to post-transcriptional events during the cell cycle. They constructed a plasmid, consisting of the bacterial neomycin phosphotransferase II gene (neo), fused upstream of the last 17 amino acids of the *HTB1* coding sequence and 3' untranslated sequence under the control of the GAL1 promoter. This construct (*neo-HTB1*) was transformed into the YM259 Mata cells and was shown to be cell-cycle regulated. The *HTB1* mRNAs in the cell were found to accumulate similarly to the *neo-HTB1* construct. Deletions of 66 to 103 bp in the 3' untranslated portion of the *HTB1* resulted in the loss of cell-cycle regulation.

Using the same *neo-HTB1* construct, Campbell *et al* (2002) showed that a specific sequence, lying approximately 100nts downstream of the 3'-end cleavage sites of the *HTB1* mRNA, contributes to cell-cycle regulation (Campbell *et al*, 2002). This purine-rich sequence was termed the distal downstream element (DDE). The mutations in the DDE resulted in cell-cycle defects. This study also demonstrates that a protein factor binds to the DDE, which may play a possible role in stabilising the pre-mRNA during the cell cycle.

1.7 Objectives of study

The aim of this research was to examine the role of post-transcriptional processing in the overall regulation of histone levels during the cell cycle in yeast. The general mRNA 3'-end processing machinery is presumed to be involved in histone 3'-end processing. As yet, the individual trans-acting factors involved in histone 3'-end processing remain unexplored. The influence of various trans-acting factors involved in mRNA 3'-end processing, termination, degradation and export on the biogenesis of histone mRNAs in asynchronous and cell-cycle synchronised yeast cells was explored to extend our knowledge of histone processing in yeast. In Chapter 3, the cleavage factor, CFIA, and the

exosome protein factor, *Δrrp6,* were investigated to determine whether they play a role in *HTB1* mRNA processing. The resulting data supports the hypothesis that the CFIA and exosome compete with each other in histone mRNA processing. In addition, the results demonstrate that the 5'→3' exonuclease, Rat1, plays a role in histone processing in the *neo-HTB1* and *HTB1* transcripts. In Chapter 4, cell-cycle experiments were used to explore the link between transcription termination, 3'-end processing and cell-cycle regulation of histone genes. The results demonstrate that the exosome contributes to the turnover of *HTB1* mRNA in the G_2-phase of the cell cycle. In Chapter 5, the final stages of mRNA histone biogenesis, prior to being exported from the nucleus to the cytoplasm, were investigated. It was found that the nucleoporins, Nup159/Rat7, in the nuclear pore complex were required for *HTB1* export, while Nup42p/Rip1 were not required for *HTB1* export. In Chapter 6, the *pop1-1* mutant was investigated in histone biogenesis. The reduction in the rRNA levels was evident, indicating that the rRNA synthesis was defective. However, the mRNA levels for endogenous *HTB1*, *neo-HTB1* and *ACT1* were also reduced, like the *pop1-1* mutant, suggesting a role for Pop1 in the processing of general mRNAs.

Chapter 2

Materials and Methods

2.1 Culture conditions

2.1.1 Yeast strains and growth conditions

The *Saccharomyces cerevisiae* strains used in this study are listed in Table 2.1. Yeast strains were cultured at 30°C in YEPGal medium (1% (w/v) yeast extract, 2% (w/v) bacto peptone, 2% (w/v) galactose) or YEPD medium (1% (w/v) yeast extract, 2% (w/v) bacto peptone, 2% (w/v) dextrose) to an optical density at 660nm [OD_{660}] of between 0.4 and 2.0. The yeast strains containing plasmids were cultured in synthetic complete agar medium [2% (w/v) agar, 2% (w/v) glucose, 6.7% (w/v) yeast nitrogen base without amino acids and ammonium sulphate, 0.5% (w/v) ammonium sulphate, yeast synthetic drop-out medium (14mg/ml), adenine (10mg/ml), lysine (10mg/ml), tryptophan (10mg/ml), leucine (10mg/ml), histidine (10mg/ml) and uracil (2.5mg/ml)]. Uracil was omitted from the media for strains harbouring plasmids with a URA3 gene.

2.1.2 Bacterial strains and growth conditions

The *Escherichia coli* strain, XL1-blue supercompetent (*Stratagene, recA1 endA1 gyrA96 thi-1 hsdR17 supE44 relA1 lac[F' proAB lac^{q}ZΔM15 Tn10(Tet^r)]*) was used for plasmid propagation. *E. coli* cells transformed with plasmids were grown in Luri-Bertani media (LB; 1% (w/v) tryptone, 0.5% (w/v) yeast extract and 10mM NaCl) overnight at 37°C, with carbenicillin added to a final concentration of 50μg/ml. The antibiotic stock solution was filter-sterilised and diluted with SDW to a final stock concentration of 50mg/ml.

2.1.3 Monitoring the growth of yeast and bacterial cultures

A UV/vis spectrometer (*Biophotometer/Genesys 10uv ThermoSpectronic*) was used to monitor the growth of yeast and bacterial cultures by measuring the optical densities (OD) at 660nm (OD_{660}). Yeast and bacterial cultures (1ml) were placed into the semi-micro cuvettes (*Sarstedt*) prior to determining the OD readings.

2.1.4 Stocks of bacteria and yeast cells

Bacteria cultures were grown in Luri-Bertani media, LB, overnight at 37°C until the culture grew to an OD_{660} of 0.8 ($1.26x10^7$ cells/ml). The bacterial culture was diluted with 30% glycerol to a final concentration of 15% in the cryo-vial tubes. The tubes were stored in -70°C.

The yeast cells were cultured in either YEPGal or YEPD medium at 22°C or 30°C overnight until the cell density reached $2x10^7$ cells/ml. Sterile glycerol (30%) was added to the cells in sterile cryo-vial tubes to give a final concentration of 15%. Stocks were transferred to -70°C for long-term storage.

2.2 Transformation of bacteria with plasmid DNA

The XL1-blue supercompetent bacterial cells (*Stratagene*) were thawed on ice. β-mercaptoethanol was added to 100µl of supercompetent cells to give a final concentration of 25mM. The mixture was incubated on ice for 10 mins, with gentle swirling every 2 mins. Plasmid DNA (10ng) was added to the competent cell suspension and incubated on ice for 30 mins. The bacterial suspension was heat-shocked in a 42°C water bath for 45 secs and incubated on ice for a further 2 mins. SOC medium [2% (w/v) tryptone, 0.5% (w/v) yeast extract, 10mM NaCl, 2.5mM KCl, 20mM glucose, 10mM Mg^{2+} stock (10mM $MgCl_2$, 10mM $MgSO_4$)] was pre-warmed to 42°C and added (900µl) to the bacterial suspension. The mixture was incubated in a water bath at 37°C for 45 mins. A second 100µl of bacterial cells was treated in the same manner, but without plasmid DNA, as a control for contamination. Following incubation, 200µl of the transformation mix was plated on LB agar plates (LB and 1% agar) containing 50µg/ml of carbenicillin antibiotic. The transformation was incubated overnight at 37°C and transformants were selected the following day.

2.3 Isolation of plasmid DNA from bacteria

Genelute^{TM} plasmid miniprep kit (*Sigma*) was used to extract plasmid DNA from 1ml of *E. coli* cultures. The cells were harvested by pelleting 1ml of the cell culture for 1 min at 13,200 rpm in an Eppendorf Microcentrifuge (*5415D model*). The bacterial pellets were resuspended with 200µl of resuspension solution and then 200µl of lysis solution. The microfuge tubes were inverted gently 6-7 times until the mixture became viscous. The cell debris was precipitated by adding 350µl of neutralisation/binding buffer. The tubes were inverted 6-7 times and centrifuged at 13,200 rpm for 10 mins (*5415D model*). The cleared lysate was added to the GeneEluate miniprep binding column and spun for 1 min at 13,200 rpm (*5415D model*). After the centrifugation step, 750µl of diluted wash solution was added to the column and the centrifugation step was repeated. A further spin of 13,200 rpm for 2 mins was performed. The column was moved to a fresh tube. Elution solution (30µl) was added to the column and centrifuged at 13,200 rpm for 1 min (*5415D model*). This step was carried out twice more to make a final volume of 90µl. The solutions were provided by *Sigma*.

2.4 Transformation of yeast with plasmid DNA

DNA plasmids were introduced into the yeast strains using the lithium acetate procedure (Ito *et al*, 1983). The yeast cells were grown in YEPD overnight at 30°C. The culture was diluted to a density of approximately $5x10^6$ cells/ml and incubated at 30°C for 3 to 5 hrs until growth reached $2x10^7$ cells/ml. The harvested culture was centrifuged in a 50ml sterile tube at 4,000 rpm in a Sorval SS-34 rotor for 5 mins. The pellets were resuspended in 25ml of SDW and the centrifugation step was repeated. The cells were resuspended in 1.0ml of 0.1M lithium acetate and incubated at 30°C for 1 hr. Cells were pelleted at 13,200 rpm for 15 secs in an Eppendorf Microfuge (*5415D model*) after the incubation period. Finally, the cells were resuspended in 500µl with 0.1M lithium acetate, resulting in a cell

density of $2x10^9$ cells/ml. Salmon sperm DNA (1mg/ml) was boiled for 5 mins and quickly chilled in ice while harvesting the cells. The suspension was pipetted into 50µl aliquots. Each aliquot was centrifuged briefly and the lithium acetate was discarded.

The following solutions were added to the cell pellets in the following order: 34.48% polyethylene glycol (PEG) (w/v), 0.1M lithium acetate, 140µg salmon sperm DNA and 1µg of plasmid DNA. This volume was made up to 350µl with SDW. The mixture was vortexed vigorously to resuspend the cells. Tubes were incubated at 30°C for 30 mins and heat-shocked at 42°C for 30 mins. The cells were collected by centrifugation at 4,000 rpm for 15 secs in an Eppendorf Microfuge (*5415D model*). The pellets were resuspended in SDW (1ml) and 400µl of the suspension was plated on synthetic complete agar medium minus uracil. The transformants were selected within 2-4 days.

2.5 Transformation of temperature-sensitive mutants with plasmid DNA

The lithium acetate procedure was carried out as described in Section 2.4, with some modifications to cater for the temperature-sensitive mutant strains. The temperature-sensitive yeast cells were grown in YEPD for 2 days at 22°C. The culture was diluted to a cell density of $5x10^6$ cells/ml and incubated at 22°C overnight until cells reached a final concentration of $2x10^7$ cells/ml. The harvested culture was centrifuged in a 50ml sterile tube at 4,000 rpm in a Sorval SS-34 rotor for 5 mins. The pellets were resuspended in 25ml of SDW and the centrifugation step was repeated. Cells were resuspended in 1.0ml of 0.1M lithium acetate and incubated at 22°C for 2 hrs. The cells were pelleted at 13,200 rpm (*5415D model*) for 15 secs after the incubation period and resuspended in a final volume of 500µl of 0.1M lithium acetate, resulting in a cell density of $2x10^9$ cells/ml. The transformation mix was added as described in Section 2.4 and was vortexed vigorously to resuspend the cells. The tubes were incubated at 22°C for 40 mins and heat-shocked at

30°C for 30 mins. The cells were collected by centrifugation at 4,000 rpm in an Eppendorf Microcentrifuge (*5415D model*) for 15 secs and the pellets were resuspended in SDW (1ml). The suspension (400µl) was plated on synthetic complete agar medium minus uracil. Transformants were selected within 7-10 days at 22°C.

2.6 Isolation of plasmid DNA from yeast cells

Yeast strains harbouring plasmids containing a URA marker were grown in synthetic complete media without uracil overnight at 30°C. Yeast culture (1.5ml) was centrifuged at 13,200 rpm for 15 secs in an Eppendorf Microcentrifuge (*5415D model*). The supernatant was decanted and the pellets were resuspended in 200µl of Breaking Buffer (2% (v/v) Triton X-100, 1% (w/v) SDS, 0.1M NaCl, 0.01M Tris HCl, pH8, 0.001M EDTA). A spatula tip-sized amount of acid-washed glass beads and 200µl of phenol:chloroform was added. The mixture was vigorously vortexed for 3 mins and centrifuged at 13,200 rpm for 10 mins in an Eppendorf Microcentrifuge (*5415D model*). One-tenth volume of sodium acetate (3M, pH5.3) and 2.5 volumes of ethanol (100%) were added to the supernatant fraction and the samples were incubated at -70°C for 45 mins. Following centrifugation, the pellets were dried and resuspended in 50µl of SDW. The plasmid DNA was transformed into *E. coli* cells, as described in Section 2.2.

2.7 Synchronisation of yeast cells by the α_1- pheromone mating factor

The yeast cells were grown in YEPGal or YEPD medium to early log phase and were diluted in YEPGal or YEPD medium overnight. The α_1-mating factor (TRP-HIS-TRP-LEU-GLN-LEU-LYS-PRO-GLY-GLN-PRO-MET-TYR) was added to give a final concentration of 2µg/ml and the culture was incubated for 3 hrs at 30°C. When 90% of the cells demonstrated a peanut-shaped (shmooed) appearance under microscopic examination, cells were centrifuged at 7,000 rpm in a Sorvall SS-34 rotor for 15 mins at 4°C. The cells

were washed twice with SDW at 7,000 rpm for 15 mins to remove the α_1-factor. Pellets were resuspended in 200ml of pre-warmed YEPGal or YEPD medium. Samples (10ml) were collected at 5 or 10 mins intervals and centrifuged at 7,000 rpm for 7 mins (*Sorvall SS-34 rotor*). The pelleted cells were frozen at -70°C.

2.8 Nucleic acid analysis

2.8.1 Phenol/chloroform extraction

An equal volume of phenol/chloroform (1:1(v/v) buffered with Tris HCl, pH8.0) was added to the DNA mix and vortexed. The mixture was centrifuged at 13,200 rpm for 5 mins to separate the aqueous and organic phases (Eppendorf Microfuge, *5415D model*). The top layer was removed and the step above was repeated once more. After the second centrifugation step, the aqueous layer was removed and nucleic acids were precipitated by adding 0.1 Vol of 3M sodium acetate (pH5.3) and 2.5 Vol of 100% (v/v) ethanol at -70°C for 45 mins. The sample was centrifuged and resuspended with DEPC-treated water.

2.8.2 Calculation of nucleic acid concentrations

A UV/vis spectrometer (*Biophotometer/Genesys 10uv ThermoSpectronic*) was used to determine the concentration of RNA and DNA samples at an absorbance of 260nm (A_{260}). A quartz curvette was used to measure the concentrations of the samples, which were diluted 1:500 in SDW. An absorbance of one unit at 260nm corresponds to 50 µg/ml *double* stranded DNA and 40 µg/ml *single* stranded RNA.

The ratio of the readings at 260nm and 280nm (A_{260}/A_{280}) estimates the purity of the RNA and DNA. The A_{260}/A_{280} should be 1.8-2 for high quality nucleic acid.

2.9 RNA analysis

2.9.1 RNA isolation by the hot-phenol method

The hot-phenol method, developed by Krieg, was used to isolate total RNA with some modifications (Krieg, 1996). Cells were harvested (10ml, OD_{660}=1.6) by centrifugation at 7,000 rpm for 7 mins at 4°C in a Sorvall SS-34 rotor. Pellets were washed with 10ml of ice-cold SDW and centrifuged again. The pellets were resuspended in 500µl of ice-cold AE buffer (10mM EDTA and 50mM Sodium Acetate, pH5.3) and 50µl of 10% SDS (w/v). The resuspended extract was transferred to a 1.5ml tube and 550µl of pre-warmed phenol buffered with AE solution was added (pH5.3, 65°C). The extract was vortexed at maximum speed for 30 secs. Tubes were incubated for 30 mins at 65°C, with vigorous vortexing for 10 secs every 5 mins. The debris and organic phase was separated from the upper aqueous phase by centrifugation at 13,200 rpm for 5 mins at 4°C in an Eppendorf Microfuge (*5415D model*). The upper aqueous phase was recovered and re-extracted twice more: firstly, with 500µl ice-cold AE buffered-phenol, pH5.3, and, secondly, 450µl chloroform. The RNA was precipitated by adding 0.1 Vol of 3M sodium acetate (pH5.3) and 2.5 Vol of 100% (v/v) Ethanol at -70°C for 45 mins. Samples were centrifuged at 13,200 rpm for 5 mins at 4°C and, following a short drying period, the pellets were resuspended in 50µl DEPC-treated SDW.

2.9.2 Formaldehyde-agarose gel electrophoresis

RNA samples were separated on 1% formaldehyde containing agarose gels with 1x MOPS running buffer (20mM MOPS, 5mM sodium acetate, 1mM EDTA, pH7.0). RNA samples, 30-60µg, were precipitated with 0.1 Vol of 3M sodium acetate (pH5.3) and 2.5 Vol of 100% (v/v) ethanol at -70°C for 45 mins. RNA pellets were dissolved in 20µl of RNA denaturing buffer [1µl DEPC-treated SDW, 3.5µl formaldehyde, 10µl formamide, 2µl 10x MOPS buffer (200mM MOPS, 50mM sodium acetate, 10mM EDTA, pH7.0),

3.5µl formaldehyde gel loading buffer (0.1% bromophenol Blue, 0.1% xylene cyanol, 50% (w/v) glycerol and 10mM EDTA, pH8.0)]. Samples were incubated at 68°C for 15 mins and chilled on ice prior to loading onto the gel. Gels were run at 25V, using a POWER/PAC 300 (*BIO-RAD*), for 14-16 hrs in the fume-hood.

2.9.3 Northern analysis

RNA was transferred from the agarose gel to a nylon filter membrane (*Biodyne® B 0.45µ, Pall Corporation*), with a minimum of 6 hrs transfer time by capillary transfer using 20x SSC (3M NaCl, 0.3M sodium citrate, pH7.0). Nucleic acids were cross-linked to the membrane using a UV light (program, C3, setting, 150mJoule, Gene linker, *Bio-Rad*). Membranes were pre-hybridised with hybridisation solution [7% SDS, 5x SSC, 2% blocking buffer, 0.1% N-lauroylsarcosine and 50mM sodium-phosphate (pH7.0)] for 90 mins at 68°C. A fresh batch of hybridisation buffer containing 2ng of digoxigenin-UTP DNA probe was added and membranes were incubated overnight at 68°C in the hybridisation oven. Following hybridisation, the membranes were washed twice for 15 mins in 2x washing solution at room temperature (2x SSC, 0.1% SDS), followed by two more washes in 0.5x washing solution (0.5x SSC, 0.1% SDS) for 15 mins at 50°C. Membranes were finally washed twice in washing buffer [1x MAB (0.1M maleic acid, 0.15M NaCl, pH7.5), 0.3% (v/v) tween®20] for 5 mins at room temperature. The membrane was immersed in blocking buffer (1x MAB with 1% (w/v) casein) for 40 mins, followed by incubation with antibody solution (Anti-DIG-alkaline phosphate (*Roche*), diluted 1:10,000 in blocking buffer) for 30 mins. Two more stringent washes for 15 mins with washing buffer were performed, followed by chemiluminescent detection with CDP-star (0.25mM, *Sigma*) in detection buffer (100mM NaCl, 100mM Tris-HCl, pH9.5). The membranes were exposed to X-ray film (Hyperfilm, *Amersham Biosciences*).

2.9.4 Northern stripping

Membranes were washed in water twice for 10 mins and then incubated in stripping solution [DEPC-treated SDW and 0.1% SDS (w/v)] for 60 mins at 68°C in an oven. The solution was changed after 30 mins. Following stripping, the membranes were rinsed in water and then in 2x SSC. After the washes, membranes were hybridised in solution [7% SDS, 5x SSC, 2% blocking buffer, 0.1% N-lauroylsarcosine and 50mM sodium-phosphate (pH7.0)] for 90 mins and the probe was later added overnight at 68°C in hybridisation solution.

2.9.5 Quantification of mRNA via blots

Levels of mRNA were quantified using the densitometric program, Quantity One, Version 4.2.1 (GS-800 calibrated densitometry, *Bio-Rad*). X-ray films were scanned using the GS-800 calibrated densitometry machine. An optical density value for each RNA band was obtained following subtraction of the background using the Quantity One programme. For the cell-cycle experiments, the 30 mins time point was used as a reference. The optical density value for each time point was divided by the optical density value for the 30 mins time point. The normalised optical density for the endogenous *HTB1* or *neo-HTB1* mRNA levels at each time point was divided by the normalised optical density for each of the actin mRNA bands (*ACT1*). The graphs were then plotted, using either Microsoft Office Excel (2003) or Graph Prism, 4.0.

2.10 Polymerase chain reaction, amplification of RNA

2.10.1 Purification of RNA

RNA samples were treated with DNase I to eliminate any contaminating DNA before proceeding to RT-PCR. RNA (30µg) was incubated with 0.02U RNasin® ribonuclease inhibitor, 1x DNase I buffer (40mM Tris-HCl (pH8.0), 10mM $MgSO_4$ and 1mM $CaCl_2$)

and 10U DNase I (*Promega*) in a final volume of 50µl at 30°C for 1 hr. This was followed by further purification of RNA by using the RNaesy mini kit (*Qiagen*). The volume was adjusted to 100µl with DEPC-treated SDW. The lysate buffer (350µl) was added to the RNA sample, followed by 250µl of 100% ethanol. The mixture was added to an RNeasy column and centrifuged at 13,200 rpm for 15 secs. The flow-through was discarded and 500µl of RPE buffer (wash) was added to the column and the centrifugation step was repeated. The column was washed once more with RPE buffer by centrifugation at 7,000 rpm for 2 mins. Finally, the column was spun at 13,200 rpm for 1 min to eliminate any excess wash solution. The column was transferred to a fresh eppendorf tube. DEPC-treated SDW (30µl) was added to the column and centrifuged for 1 min at 13,200 rpm. This step was repeated twice, to give a final volume of 90µl.

2.10.2 Reverse transcription of RNA

RNA samples (2µg) were reversed transcribed in a reaction mixture containing 1x ImProm-II™ buffer (*Promega*), 6mM $MgCl_2$, 0.5mM dNTP mix, 1mM reverse primer, 0.01U RNasin® ribonuclease inhibitor (*Promega*) and 0.5µl of ImProm-II™ reverse transcriptase (*Promega*). The final volume was 20µl. Samples were incubated at 25°C for 5 mins and 42°C for 60 mins, followed by inactivation at 70°C for 15 mins. The cDNA product was amplified, as described in Section 2.10.3.

2.10.3 Amplification of DNA and cDNA by polymerase chain reaction (PCR)

PCR reactions were carried out in final volume of 25µl containing 0.2mM dNTPs, 1x thermophilic DNA buffer (10mM Tris-HCl (pH9.0)), 50mM KCl and 0.1% Triton X-100 (*Promega*), 1.5mM $MgCl_2$, 0.04U Taq polymerase (*NEB/Bioline*), 400nM forward primer, 400nM reverse primer and 2-10ng of the desired DNA template or 2µl of the cDNA (prepared as outlined in Section 2.10.2) using a GeneAmp® PCR System 2700 machine.

The primers used are listed in Table 2.2. The reaction was performed using the following amplification parameters which consisted of initial denaturation of 95°C for 5 mins, 25 cycles of denaturation at 94°C for 30 secs, annealing at 55°C for 1 min, extension at 72°C for 0.45 secs and one round of final extension at 72°C for 7 mins. Loading dye buffer, 3µl (0.25% bromophenol blue, 0.25% xylene cyanol FF and 50% glycerol), was added to the PCR samples, which were subsequently electrophoresed on a 1% TBE agarose gel with 1x TBE running buffer (89mM Tris-base, 88mM Boric Acid, 0.02mM EDTA).

The *Wallace rule* (i) was used to calculate the melting temperature (T_m) for short oligonucleotides (<20 nucleotides). A, T, G and C refer to the base composition of the oligonucleotides (Wallace *et al.*, 1979).

$$(i) \quad T_m = 2(A+T) + 4(G+C)$$

The annealing temperature was 5-10°C below the T_m value.

2.10.4 Real-time polymerase chain reaction (Real-time PCR)

Real-time quantitative PCR was performed using a Rotor-gene RG-3000 machine (*Corbett Research*) with SYBR Green I dye. The 15µl reaction mixture contained 7.5µl of 2x SYBR Green Jumpstart Ready mix (containing 20mM Tris-HCl (pH8.3), 100mM KCl, 7mM $MgCl_2$, 0.4mM each dNTP, 0.05U/µl Taq DNA polymerase, Jumpstart Taq antibody and SYBR Green I, *Sigma*), together with 2µl of template (reverse transcription reaction product as prepared in Section 2.10.2), 400nM forward primer and 400nM reverse primer. The primers used for amplification of *HTB1* (HTB1_Endo_F and HTB1_Endo_R) and *ACT1* (Actin_F(2) and Actin_R(2)) cDNAs are listed in Table 2.2. The amplification protocol consisted of an initial denaturation step of 94°C for 2 mins, followed by 40 amplification cycles at 94°C for 15 secs, 55°C for 60 secs and 72°C for 60 secs.

2.10.5 Quantification of cDNA using real-time PCR

cDNA levels were quantified from the fluorescence readings obtained from the real-time program, Rotor-Gene 6. Fluorescence values represent the SYBR Green I dye incorporated into the amplified DNA during the amplification reaction and is directly proportional to the concentration of the cDNA. The threshold value, C_T, was set to record the fluorescence signal against the background and represents the exponential phase of the amplification cycle. The 30 mins time point was used as a reference. The C_T values for each time point was divided by the 30 mins time point. The normalised C_T values for the endogenous *HTB1* mRNA levels was divided by the normalised C_T values for the corresponding actin mRNA levels (*ACT1*). The graphs were then plotted using Graph Prism 4.0.

2.10.6 Colony polymerase chain reaction

Colonies were picked up on eppendorf tips and resuspended in 100µl of DEPC-treated SDW. The colony PCR reaction was carried out in a volume of 40µl, containing 62.5µM dNTPs, 1x thermophilic DNA buffer [10mM Tris-HCl (pH9.0), 50mM KCl and 0.1% Triton X-100 (*Promega*)], 2.5mM $MgCl_2$, 2U Taq polymerase (*NEB/Bioline*), 400nM forward primer, 400nM reverse primer and 5 µl of the colony suspension. The amplification conditions consisted of initial denaturation of 96°C for 2 mins, 30 cycles of denaturation at 94°C for 40 secs, annealing at 55°C for 40 secs, extension at 72°C for 1 min and one round of final extension at 72°C for 10 mins.

2.10.7 Amplification of digoxygenin-UTP labeled DNA probes

A standard PCR amplification procedure, described in Section 2.10.3, was used to prepare digoxygenin-UTP labeled DNA probes, with the exception that the dNTP mix was replaced by digoxigenin-UTP probe mix (1.86mM dATP, 1.86mM dCTP, 1.86mM dGTP, 1.3mM dTTP and 0.65mM alkali-labile DIG-11-UTP, pH7).

2.10.8 Dot blotting of digoxygenin-UTP labeled DNA probes

Serial dilution of the digoxigenin-UTP labelled probe was spotted onto a piece of nylon membrane. Once the probe dried, the membrane was washed briefly in washing buffer (1x MAB, 0.3% (v/v) tween®20) at room temperature and then incubated in blocking buffer (1x MAB with 1% (w/v) casein) for 30 mins. Blocking buffer was removed and the membrane was incubated with antibody solution (Anti-DIG-alkaline phosphate, diluted 1:10,000 in blocking buffer) for 30 mins. Following this incubation, membranes were washed twice in washing buffer (1x MAB, 0.3% (v/v) tween®20) for 15 mins. Chemiluminescence was detected with CDP-star (0.25mM, *Sigma*) in detection buffer (100mM NaCl, 100mM Tris-HCl, pH9.5) by exposure to X-ray film (Hyperfilm, *Amersham Biosciences*).

Table 2.1: Yeast strains used in this study

Strains	Genotype or description	Source
S150	MAT**a**, *leu*2-3_112, *ura*3-52, *trp*1-289, *his*3Δ	Bond, U., TCD (Campbell *et al*, 2002)
W303A	MAT**a**, *leu*2-3_112, *ura*3-52, *trp*1Δ2, *his*3-11, *ade*2-1, *can*1-100	Euroscarf
W303B	MAT**a**, *leu*2-3_112, *ura*3-1, *trp*1-1, *his*3-11, *ade*2-1, *can*1-100	Libri, D., CNRS
rna14-1	MAT**α**, *leu*2-3_112, *ura3-1, trp1-1*, *his*3-11_15, *ade*2-1, *rna*14-1	Proudfoot, N., Oxford U
rna15-1	MAT**α**, *leu*2-3_112, *ura3-1, trp1-1*, *his*3-11_15, *ade*2-1, *rna*15-2	Proudfoot, N., Oxford U
pcf11-2	MAT**a**, *leu*2-3_112, *ura3-1, trp*1Δ2, *his*3-11_15, *ade*2-1, *pcf*11-2	Proudfoot, N., Oxford U
rna14-3	MAT**α**, *leu*2-3_112, *ura3-1*, *trp*1-1, *his*3-11_15, *ade*2-1, *can*1-100, *rna*14-3	Libri, D., CNRS
rna15-2	MAT**a**, *leu*2-3_112, *ura3-1*, *trp*1-1, *his*3-11_15, *ade*2-1, *can*1-100, *rna*15-2	Libri, D., CNRS
rrp6KO	MAT**α**, *leu*2-3_112, *ura*3, *trp*1, *his*3, *ade*2, rrp6::KAN	Libri, D., CNRS
W303.rrp6KO	MAT**a**, *leu*2, *ura*3, *trp*1, *his*3, *ade*2, , rrp6::KANr	Libri, D., CNRS
rna14-3/Δrrp6	MAT**a**, *leu*2-3_112, *ura*3-1, *trp*1-1, *his*3-11_15, *ade*2-1, *can*1-100, *rna*14-3, rrp6::KAN	Libri, D., CNRS
rna15-2/Δrrp6	MAT**a**, *leu*2-3_112, *ura*3-1, *trp*1-1, *his*3-11_15, *ade*2-1, *can*1-100, *rna*15-2, rrp6::KAN	Libri, D., CNRS
RAT7	MAT**α**, *leu*2-3 _112, *ura*3-52, *trp*1-1, *his*4-539, cup1::LEU2PM	Libri, D., CNRS (Hilleren *et al*, 2001)
rat7	MAT**a**, *leu*2-3_112 or *leu*2Δ1, *ura*3-52, *his3Δ*200, *his*4-539, rat7-1, cup1::LEU2PM, (yRP1579)	Libri, D., CNRS (Hilleren *et al*, 2001)
rat7/Δrrp6	MAT**a**, *leu*2-3_112 or *leu*2Δ1, *ura*3-52, *trp*1-1, *his3Δ*200 and/or –539, rat7-1 rrp6::URA3, cup1::LEU2PM, (yRP1585)	Libri, D., CNRS (Hilleren *et al*, 2001)
rip1	MAT**a**, *leu*2-3_112, *ura*3-1, *trp*1-1, *his*3-11_15, *ade*2-1, rip1::KAN (yRP1586)	Libri, D., CNRS (Hilleren *et al*, 2001)
RAT1	MAT**a**, *leu*2Δ1, *ura*3-52, *trp*1Δ63 (FY8)	Libri, D., CNRS
rat1	MAT**a**, *leu*2Δ1, *ura*3-52, *trp*1Δ63, *rat1-1* (FY433)	Libri, D., CNRS
pop1-1	MAT**a**, *leu*2-3, *ura*2-3, *trp*1-289, *ade*2_112, ARG4∆EcoR5, GAL:U4 TRP1 pop1-1 ts	Tollervey, D., Edinburgh U

Table 2.2: Oligonucleotides used in this study

Oligonucleotides	Sequence 5' – 3'	Nucleotide position	Source
*HTB1*_F	GAAAAGAAACCAGCCTCC	15-33 nts relative to the ATG site in the endogenous *HTB1* sequence	Campbell *et al*, 2002
*HTB1*_R	GAGTAGAGGAAGAGTACTTGG	367-388 nts relative to the ATG site in the endogenous *HTB1* sequence	Campbell *et al*, 2002
Actin_F(1)	TAGATTTTTCACGCTTACTGC	Northern blot	Bond U, TCD
Actin_R(1)	GGCTGCAGGTCGACTCTAGA	Northern blot	Bond U, TCD
Neo_F	TACCTGCCCATTCGACCACCAAGCG	367-388 nts relative to the ATG site in the *Neo-HTB1* sequence	Campbell *et al*, 2002
Neo_R	GTCATTTCGAACCCCAGAGTCCCGCTC	736-760 nts relative the ATG site in the *Neo-HTB1* sequence	Campbell *et al*, 2002
*HTB1*1_Endo_F	GGCGCATGTCTGCTAAAGCCGAAAAG	1-22 nts nts relative to the ATG site in the endogenous *HTB1* sequence	This work
*HTB1*_Endo_R	GCGCTTCTTGTTATACGCAGCC	251-270 nts relative to the ATG site in the endogenous *HTB1* sequence	This work
Actin_F(2)	CCGCCTGAATTAACAATGGATT	(-11)-7 nts relative to the ATG site in the *ACT1* sequence	This work
Actin_R(2)	CTCTCAATTCGTTGTAGAAGGT	572-594 nts relative to the ATG site in the *ACT1* sequence	This work
*HTB1*For1	GTCTCTGAAGGTACTAGAGCTG	342-265 nts relative to the ATG site in the endogenous *HTB1* sequence	This work
*HTB1*Rev1	GGCCGCGGATTAAACTATTATACAA	472-488 nts relative to the ATG site in the endogenous *HTB1* sequence	This work
*HTB1*Rev2	TAAGCGCATTCCCTCTATGAGAC	551-572 nts relative to the ATG site in the endogenous *HTB1* sequence	This work
*HTB1*Rev3	TTTCTGAGTCATTAATAAGCAACACTA	619-645 nts relative to the ATG site in the endogenous *HTB1* sequence	This work
*HTB1*Rev4	GAAGTTAATCACAACAGAGGGTT	787-815 nts relative to the ATG site in the endogenous *HTB1* sequence	This work
*HTB1*Rev5	TTTTATACGTGCGTATTCTATTGTTCA	869-895 nts relative to the ATG site in the endogenous *HTB1* sequence	This work
*HTB1*Rev6	TGAAGTGCAGCTGACGATC	978-996 nts relative to the ATG site in the endogenous *HTB1* sequence	This work

Chapter 3

3'-end cleavage and exosome factors play a role in *HTB1* mRNA processing

3.1 Introduction

Eukaryotic precursor messenger RNAs (pre-mRNA) are processed at their 3'-ends. In yeast, five trans-acting factors, cleavage/polyadenylation factor I (CFI), cleavage factor II (CFII), polyadenylation factor I (PFI), poly (A) polymerase (Pap1p) and poly (A) binding protein (Pab1p) are required for 3'-end mRNA formation. The trans-acting factors responsible for histone 3'-end cleavage in *Saccharomyces cerevisiae* have remained unexplored, but there is evidence that the general mRNA 3'-end processing machinery is involved. Butler *et al* (1990) used crude cell extracts to show that efficient endonucleolytic cleavage and polyadenylation of a precursor H2B2 mRNA occur *in vitro* (Butler *et al*, 1990). Individual components have been identified for mammalian histone processing, but similar analysis has not been carried out for yeast histones.

CFIA is composed of four subunits: Rna14p, Rna15p, Pcf11p and Clp1p. Rna14p, Rna15p and Pcf11p are necessary for cleavage activity with CFII *in vitro* (Gross and Moore, 2001a). A considerable amount of research has focused on mutations in RNA14, RNA15 and PCF11. Transcription run-on analysis have shown that mutations in any of the three subunits impair transcription termination, indicating a link between 3'-end processing and transcription termination (Birse *et al*, 1998).

Pre-mRNA must undergo mRNA processing by several processing factors to promote the final export as mature mRNA. The nuclear exosome retains any hypo- and hyper-adenylated mRNA near the transcription sites and destroys aberrant mRNA (Hilleren *et al*, 2001). The exosome is a complex of 3'→5' exoribonucleases, consisting of 11 components including the unique nuclear protein, Rrp6p. The complex prevents unprocessed mRNAs from being exported from the nucleus.

Recently, the 5'→3' exoribonuclease, Rat1p, has shed light on the possible mechanisms in which transcription termination occurs by RNA Polymerase II. Two proposed mechanisms have been put forward to explain this process, namely the

'allosteric' (anti-terminator) model and the 'torpedo' model (*Figure 1.3*). In the proposed torpedo model, following mRNA 3'-end cleavage, a newly generated 5'-end of the cleaved precursor RNA is exposed to the 5'→3' exonuclease, Rat1p. Rat1p digests the unstable pre-mRNA transcript rapidly until it reaches RNA Polymerase II, thus triggering termination. Supporting the torpedo model, Kim *et al* (2004) have demonstrated termination defects in *rat1-1* cells using CHIP assays (chromatin immunoprecipitation). Recent evidence indicates that Rat1p may play a role in 3'-end processing (Kim *et al*, 2004).

Many questions surround the mechanisms of histone mRNA 3'-end processing in *Saccharomyces cerevisiae*. The apparent dichotomy in the mechanisms used to generate the 3'-ends of histone mRNA in the lower eukaryotes (fungi, protozoa and yeast) and the higher eukaryotes (mammals) raises some interesting evolutionary questions. The absence of the unique histone mRNA components in fungi, such as the U7 snRNP and the stem-loop binding protein, suggest that genes encoding these components have been lost at some stage in evolutionary history and that an alternative mechanism has evolved in fungi to regulate the formation of the 3'-ends of histone mRNAs. Furthermore, the structural differences in the histone mRNAs in higher and lower eukaryotes points to a divergence in mechanisms for the formation of the 3'-ends of histone mRNAs. The experiments performed in this chapter were undertaken to increase our understanding of the molecular basis of histone mRNA 3'-end processing. To define the factors required for histone mRNA 3'-end processing, we first examined the role of known components of the general 3'-end processing machinery. The cleavage factors, Rna14, Rna15 and Pcf11, were investigated in this study. Another investigation was carried out to understand the impact of the exonucleases, Rrp6 and Rat1, in histone 3'-end processing.

3.2 Results

3.2.1 The 3'-end processing factor CFIA is required for 3'-end processing of *neo-HTB1* transcripts

In this study, we utilised a yeast model plasmid, PLJ31 (WT *neo-HTB1*), to investigate 3'-end processing of yeast histones. The yeast shuttle vector contains the neomycin phosphotransferase II gene (Neo) under the control of the galactose 4 promoter (GAL4) (*Figure 3.1*). The neomycin gene encodes neomycin phosphotransferase II, which confers resistance to G418 antibiotic. Downstream of the Neo gene is part of the histone gene (*HTB1*), which encodes the last 17 coded amino acids, the 3' untranslated region and approximately 600 nucleotides of downstream sequences, including the purine-rich distal downstream element (DDE). The DDE lies approximately 110nt downstream of the cleavage sites of the *Saccharomyces cerevisiae HTB1* gene. This consists of a putative stem-loop structure. Previous studies have shown that the DDE was found to lie in the region of transcription termination (Campbell *et al*, 2002).

The known trans-acting factors of CFIA required for cleavage/polyadenylation and transcription termination were investigated to determine whether they play a role in 3'-end processing of the *neo-HTB1* mRNAs. Mutants of the three gene products of CFIA, *rna14*, *rna15* and *pcf11*, were used in this study (*Table 2.1*).

Thermosensitive mutants, *rna14-1*, *rna15-1* and *pcf11-2*, were transformed with the plasmid, PLJ31. When the cells reached a desirable OD_{660}, the cells were placed at 22°C and 37°C for 1 hr. Total RNA from the samples was extracted and electrophoresed on formaldehyde-containing agarose gels. The RNA was then transferred to nylon membranes. The membranes were subsequently hybridised with a DIG-labelled DNA probe, complementary to the neo section of the *neo-HTB1* gene (*Table 2.2*). After a series of stringent washes, chemiluminescent detection was carried out and the X-ray film exposed, as described in Chapter 2 (Section 2.9).

At the permissive temperature (22°C), correctly processed WT *neo-HTB1* mRNA was observed in the *rna14-1* and *rna15-1* backgrounds (*Figure 3.2(iii)*, Lane 1 compared to lanes 2 and 3). Correctly cleaved 3'-end transcripts were also observed in the wild type *neo-HTB1* mRNA in the *pcf11-2* background at 22°C (*Figure 3.2(iii)*, Lane 1 compared to lane 4). However, in addition to mature mRNA, elongated read-through transcripts were also observed (*Figure 3.2(iii)*, See arrow, Lane 4). Examination of the rRNA and *ACT1* mRNA levels indicate that RNA was overloaded in the *pcf11-2* background at 22°C (*Figure 3.2(i), (ii)*, Lane 4). This result confirms that termination is more strongly impaired in the *pcf11-2* background than in the *rna14-1* and *rna15-1* backgrounds. PCF11 is also important for binding to the CTD of RNA Polymerase II and RNA transcripts. The CTD-binding domain of Pcf11 is essential for termination (Zhang *et al*, 2005). Therefore, termination defects may be caused by the loss of the CTD-domain in *pcf11-2* at 22°C. RNA14 and RNA15 do not directly bind to the CTD-domain of RNA Polymerase II.

At the non-permissive temperature (37°C), full cleavage of the neo-*HTB1* transcript was observed in the WT background, although the overall levels of the transcript were reduced at this temperature (*Figure 3.2(iii)*, Lane 5). The steady state levels of the n*eo-HTB1* mRNAs were extensively reduced in the CFIA mutant backgrounds (*Figure 3.2(iii)*, Lanes 6-8). This data correlates with previous findings demonstrating defects in 3'-end cleavage and termination at the non-permissive temperature in the *rna14* and *rna15* mutant strains (Libri *et al*, 2002). A low level of read-through transcripts were observed at 37°C in the *rna14-1*, *rna15-1* and *pcf11-2* backgrounds, compared to no read-though in the WT (*Figure 3.2(iii)*, See arrows, Lanes 6-8 compared to lane 5). The *ACT1* probe was used as a control. Similar *ACT1* mRNA levels were detected in the WT and mutant strains at 22°C, whereas the *ACT1* mRNA levels were reduced at 37°C

(*Figure 3.2(ii)*, Lanes 1-4 compared to lanes 5-8). *ACT1* mRNA and rRNA levels for the WT strain at 37°C is slightly overloaded on the gel (*Figure 3.2(i)*, Lane 5).

Taken together, this data suggests that the *neo-HTB1* mRNAs are rapidly degraded under conditions when 3'-end processing is inhibited. Some read-through transcripts were observed when 3'-end processing was inhibited, suggesting that other processing mechanisms are required to generate the mature mRNA. Furthermore, the differences of the *ACT1* and *neo-HTB1* mRNAs in the mutant backgrounds suggested that the *neo-HTB1* mRNAs has a much shorter half-life than the *ACT1* mRNAs.

Figure 3.1: Systematic representation of the PLJ31 plasmid. The red box is the Neo gene, the white box is the *HTB1* gene and the green box is the DDE. The arrows represent the cleavage sites. Below the DDE sequence are the characteristics of the mutants used to investigate histone 3'-end processing and cell-cycle regulation in this study. The location of the *HTB1* sequences, cleavage sites and DDE are shown relative to the start of translation for the Neo gene (+1).

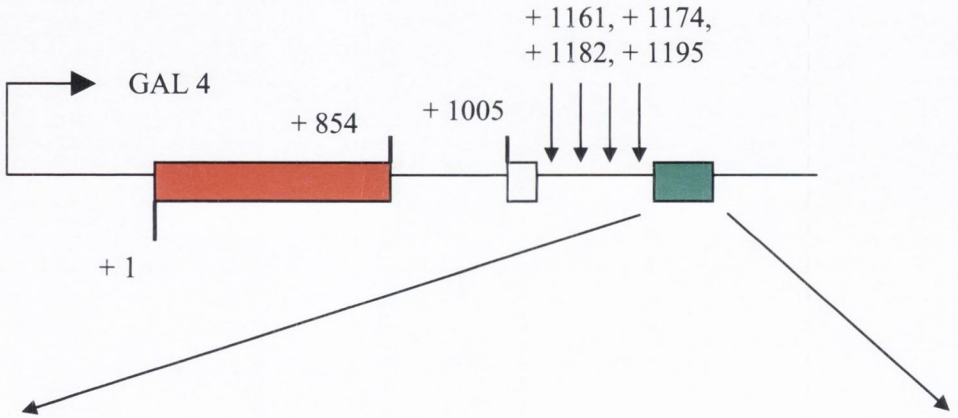

WT	GAATAAATAGTGTTGCTTATTAATGACTCAGAAAAAGTTTCCACATGATA
pSAC15	GAG
pSAC20	GGC CAA
pSAC21	GGC CAA TAC

Name	Phenotype
WT	WT
pSAC15	WT
pSAC20	Decreased mRNA stability
pSAC21	Altered cell-cycle regulation

Figure 3.2: Northern blot analysis of *neo-HTB1* mRNA in CFIA mutants. Total RNA, 30µg, was isolated from the following yeast strains, Lanes 1 and 5; WT (S150-2B, *Table 2.1*) containing the PLJ31 plasmid, Lanes 2 and 6; *rna14-1* containing the PLJ31 plasmid, Lanes 3 and 7; *rna15-1* containing the PLJ31 plasmid, Lanes 4 and 8; *pcf11-2* containing the PLJ31 plasmid, at the permissive temperature, 22°C (Lanes 1-4), or following incubation of the mutants for 1 hr at the non-permissive temperature, 37°C (Lanes 5-8). **(i)** Ethidium bromide stained gel showing the ribosomal RNAs. rRNA was used as a control of equal loadings on the gel. **(ii)** The blot was hybridised with the ACT1 probe. **(iii)** The blot was hybridised with the neo-specific probe. The arrows show read-through transcripts in Lanes 4, 6, 7 and 8. The northern blot autoradiograph was spliced together from the same gel in order to clarify the results.

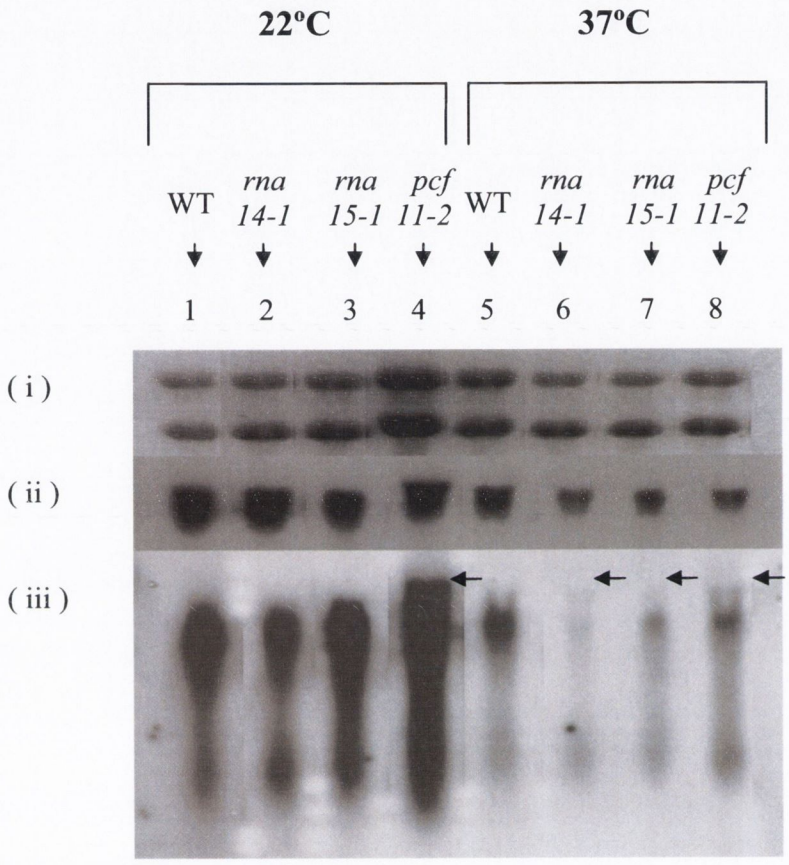
22°C
37°C
WT
rna 14-1
rna 15-1
pcf 11-2
WT
rna 14-1
rna 15-1
pcf 11-2
1
2
3
4
5
6
7
8
(i)
(ii)
(iii)

3.2.2 The nuclear exosome contributes to *neo-HTB1* mRNA biogenesis with 3'-end processing

Data shown in Figure 3.2 indicates that the *neo-HTB1* mRNA is rapidly degraded following inhibition of 3'-end processing. Previous studies have shown that the read-through transcripts generated as a result of inhibition of 3'-end processing are substrates for the nuclear exosome complex, which includes the unique nuclear protein, Rrp6p (Libri *et al*, 2002).

To investigate whether the exosome plays a role in 3'-end processing of histone mRNAs, the PLJ31 plasmid (WT) was transformed into a deletion strain, *Δrrp6*. Northern blotting was carried out with the thermosensitive mutants, *rna14-1*, *rna14-3*, *rna15-2* and *Δrrp6* alone, or with the double mutants, *rna14-3/Δrrp6* and *rna15-2/Δrrp6*. Cell culture and Northern blotting procedures were performed, as described in Chapter 2 (Section 2.9). The RNA was probed with the *neo-HTB1* probe (*Table 2.2*).

Mature mRNAs were observed in the WT strain (S150-2B) transformed with the PLJ31 plasmid at the permissive temperature (*Figure 3.3(ii)*, 22°C, Lane 1). The *neo-HTB1* mRNA levels in the *Δrrp6* background were similar to the WT mRNA levels (*Figure 3.3(ii)*, 22°C, Compare Lane 1 to Lane 7). In *rna14* and *rna15-2* strains, the WT-neo-*HTB1* mRNA is cleaved correctly and mature transcripts are evident (*Figure 3.3(ii)*, 22°C, compare Lanes 2 and 3 with Lane 1). There was some stabilisation of the mature mRNA within the *rna14* backgrounds (*Figure 3.3(ii)*, 22°C, Lanes 2 and 3). Increased levels of the *neo-HTB1*-WT were observed at the permissive temperature within the *rna14-3/Δrrp6* and *rna15-2/Δrrp6* double mutants, although these lanes are slightly overloaded (*Figure 3.3(i), (ii)*, 22°C, Lanes 5 and 6).

The WT neo-*HTB1* mRNA is highly unstable and reduced mRNA levels were observed at 37°C (*Figure 3.3(ii)*, 37°C, Lane 1). Similar *neo-HTB1* mRNAs was observed in the *Δrrp6* background and in the WT background (*Figure 3.3(ii)*, 37°C, Lane 7 compared to Lane 1).

As previously observed under most conditions where 3'-end cleavage is inhibited, the neo-*HTB1* mRNA is rapidly degraded (*Figure 3.3(ii)*, 37°C, Lanes 2 and 3). The *ACT1* mRNA levels were higher in the *rna15-2* background compared to the *rna14* backgrounds, indicating that the RNA sample was overloaded in this lane (*Figure 3.3(ii)*, 37°C, Lane 4). However, when the nuclear exosome is also inhibited, *rna14-3/Δrrp6* and *rna15-2/Δrrp6*, the neo-*HTB1* transcripts are stabilised, similar to that observed in the WT background, and stable read-through transcripts are apparent (*Figure 3.3(ii)*, 37°C, Lanes 5 and 6). This is most apparent in the *rna14-3/Δrrp6* sample (*Figure 3.3(ii)*, 37°C, See arrows, Lanes 5 and 6). Thus, it appears that inhibition of 3'-end processing in the absence of the nuclear exosome function leads to the accumulation of read-through transcripts, which can subsequently be restored to transcripts of similar size to the mature mRNA.

Figure 3.3: Northern blot analysis of *neo-HTB1* mRNA in CFIA and exosome mutants. Total RNA, 30μg, was isolated from the following yeast strains, Lane 1; WT (S150-2B, *Table 2.1*) containing the PLJ31 plasmid, Lane 2; *rna14-1* containing the PLJ31, Lane 3; *rna14-3* containing the PLJ31 plasmid, Lane 4; *rna15-2* containing the PLJ31 plasmid, Lane 5; *rna14-3/Δrrp6* containing the PLJ31 plasmid, Lane 6; *rna15-2/Δrrp6* containing the PLJ31 plasmid, Lane 7; *Δrrp6* containing the PLJ31 plasmid, at the permissive temperature, 22°C, or following incubation of the mutants for 1 hr at the non-permissive temperature, 37°C. **(i)** Ethidium bromide stained gel showing the ribosomal RNAs. rRNA was used as a control of equal loadings on the gel. **(ii)** The blot was hybridised with the neo-specific probe. The northern blot autoradiograph was spliced together from the same gel in order to clarify the results.

22°C

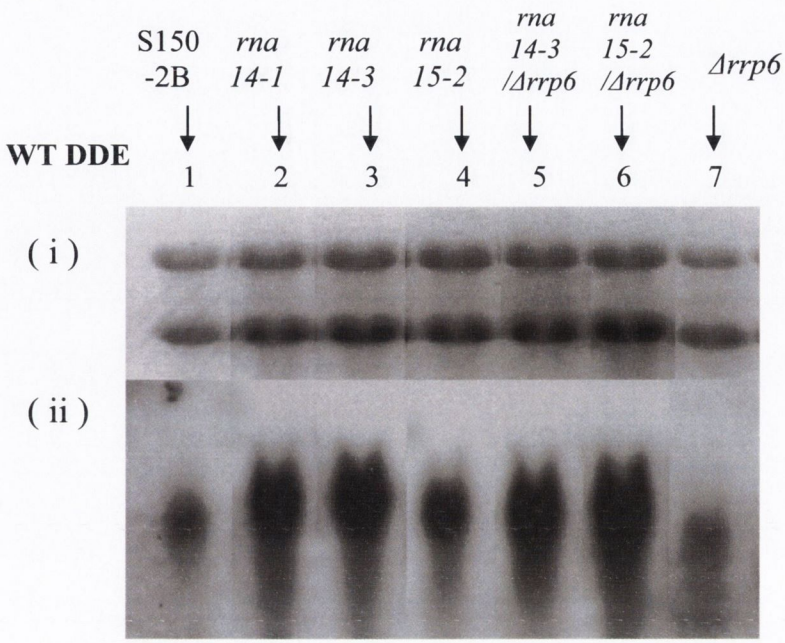
S150 -2B
rna 14-1
rna 14-3
rna 15-2
rna 14-3 /Δrrp6
rna 15-2 /Δrrp6
Δrrp6
WT DDE
1
2
3
4
5
6
7
(i)
(ii)

37°C

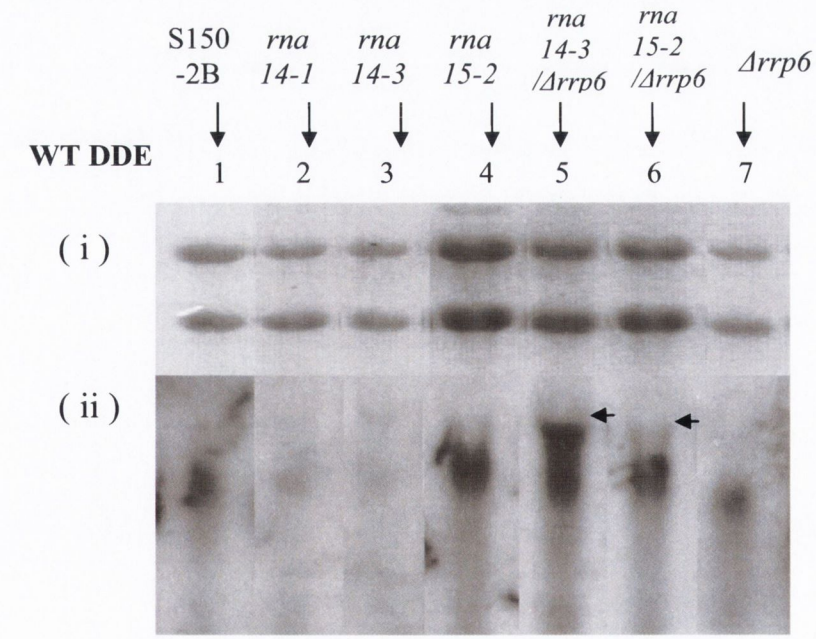
S150 -2B
rna 14-1
rna 14-3
rna 15-2
rna 14-3 /Δrrp6
rna 15-2 /Δrrp6
Δrrp6
WT DDE
1
2
3
4
5
6
7
(i)
(ii)

3.2.3 Investigating the role of the DDE in *neo-HTB1* mRNA biogenesis

Previous data from Campbell *et al* (2002) identified a purine-rich region lying approximately 100nt downstream of the 3'-end cleavage site of the *HTB1* gene. This region was shown to contribute to cell-cycle regulation of the upstream gene and it lies in the region of transcription termination. The question arose as to whether the DDE plays a role in 3'-end processing of yeast histone mRNAs. To test this hypothesis, the WT (W303), *rna14-3, Δrrp6* and *rna14-3/Δrrp6* strains were transformed with the *neo-HTB1* WT or with the DDE mutant genes (*Figure 3.1*). Northern blot analysis was performed on total RNA extracted from strains grown after 1 hr shift at 22°C and 37°C. Northern blots were probed with the *neo*-specific and *ACT1*-specific probes (Chapter 2, *Table 2.2*). Previous data indicates that *neo-HTB1* mRNAs expressed from the pSAC20 plasmid appeared to be less stable than WT *neo-HTB1* mRNA, while *neo-HTB1* RNAs expressed from the pSAC21 plasmid showed an altered pattern of cell-cycle accumulation (Campbell *et al*, 2002). The pSAC15 plasmid was not used in this previous study.

At the permissive temperature, mature mRNA levels harbouring the WT DDE or mutant DDE in the W303 background were low and appear to be unstable under these experimental conditions (*Figure 3.4(iii)*, 22°C, Lanes 1, 2, 3 and 4). A large amount of the hybridisation signal was found at the bottom of the gel (*Figure 3.4(iii)*, 22°C, See arrow) and represents degraded mRNAs, indicating that the *neo-HTB1* mRNAs are rather unstable in the W303 background compared to their expression in the S150-2B strain (*Figure 3.3*). The *neo-HTB1* WT, pSAC15, pSAC20 and pSAC21 transcripts appear to be stabilised in the *rna14-3* backgrounds (*Figure 3.4(iii)*, 22°C, Lanes 5, 6, 7 and 8). Using rRNA as an indicator for RNA loading variabilities, the relative levels of *neo-HTB1* mRNAs were calculated by dividing the optical density value for the *neo-HTB1* mRNA in each lane by the corresponding optical density value for the rRNA (Chapter 2, Section 2.9.5). The relative *neo-HTB1* mRNA levels in the *rna14-3* strain containing the PLJ31, pSAC15,

pSAC20 and pSAC21 plasmids are 1.53, 0.69, 0.89 and 1.13 respectively, suggesting that the pSAC15 and pSAC20 mutant *neo-HTB1* mRNAs are more susceptible to degradation than the WT or pSAC21 neo-*HTB1* mRNAs in this genetic background. There was an increase in the *neo-HTB1* mRNA levels in the double mutant, *rna14-3/Δrrp6* (*Figure 3.4(iii)*, 22°C, Lanes 9, 10, 11 and 12). The single mutant *Δrrp6* demonstrated that there was a slight increase of the mRNA levels compared to the WT (*Figure 3.4(iii)*, 22°C, Lanes 1, 2, 3 and 4 compared to Lanes 13, 14, 15 and 16). Lane 13 is slightly underloaded as judged by the rRNA and ACT 1 mRNA levels (*Figure 3.3(ii)*, 22°C, Lane 13). To make further conclusions, the rRNA and *neo-HTB1* mRNAs were quantified in the *Δrrp6* background, as discussed above. The relative *neo-HTB1* mRNA levels in the *Δrrp6* background containing the PLJ31, pSAC15, pSAC20 and pSAC21 plasmids are 0.54, 0.63, 1.42 and 1.6 respectively and 0.29, 0.33, 0.52 and 0.47 respectively in the W303 background.

At 37°C, cleavage is impaired in the WT and mutant DDE *neo-HTB1* mRNAs in the *rna14-3* background (*Figure 3.4(iii)*, 37°C, Lanes 21-24 compared to Lanes 17-20). Again, the pSAC15 and pSAC20 DDE mutant *neo-HTB1* mRNAs were more unstable than the PLJ31 and pSAC21 mRNAs. From quantification analysis, the relative *neo-HTB1* mRNA levels for PLJ31 and pSAC21 transcripts are 0.86 and 0.61 respectively, whereas the levels for pSAC15 and pSAC20 transcripts are 0.36 and 0.28 respectively. The instability of the DDE mutants in the *rna14-3* background suggests that the mutants appear to be better substrates for the exosome, particularly the pSAC15 and pSAC20 mutants. In the *rna14-3/Δrrp6* background, the *neo-HTB1* mRNAs are stabilised compared to the WT strain (*Figure 3.4(iii)*, 37°C, Lanes 25-28 compared to lanes 17-20). From quantification analysis, the relative *neo-HTB1* mRNA levels in the *Δrrp6* background harbouring the PLJ31, pSAC15, pSAC20 and pSAC21 plasmids are 0.38, 0.96, 1.56 and 1.77 respectively (*Figure 3.4(iii)*, 37°C, Lanes 29-32). Taken together, the data suggest that the mutations

in the DDE increase the susceptibility of the *neo-HTB1* mRNAs to degradation when 3'-end processing is inhibited. The increased relative stability of the DDE-mutant *neo-HTB1* mRNAs in the *Δrrp6* background suggestive that these transcripts might represent preferred substrates for the nuclear exosome.

Figure 3.4: Northern blot analysis of *neo-HTB1* mRNA in CFIA and exosome mutants. Total RNA, 60µg, was isolated from the following yeast strains, Lanes 1 and 17; W303B containing the PLJ31 plasmid, Lanes 2 and 18; W303B containing the pSAC15 plasmid, Lanes 3 and 19; W303B containing the pSAC20 plasmid, Lanes 4 and 20; W303B containing the pSAC21 plasmid, Lanes 5 and 21; *rna14-3* containing the PLJ31 plasmid, Lanes 6 and 22; *rna14-3* containing the pSAC15 plasmid, Lanes 7 and 23; *rna14-3* containing the pSAC20 plasmid, Lanes 8 and 24; *rna14-3* containing the pSAC21 plasmid, Lanes 9 and 25; *rna14-3/Δrrp6* containing the PLJ31 plasmid, Lanes 10 and 26; *rna14-3/Δrrp6* containing the pSAC15 plasmid, Lanes 11 and 27; *rna14-3/Δrrp6* containing the pSAC20 plasmid, Lanes 12 and 28; *rna14-3/Δrrp6* containing the pSAC21 plasmid, Lanes 13 and 29; *Δrrp6* containing the PLJ31 plasmid, Lanes 14 and 30; *Δrrp6* containing the pSAC15 plasmid, Lanes 15 and 31; *Δrrp6* containing the pSAC20 plasmid, Lanes 16 and 32; *Δrrp6* containing the pSAC21 plasmid, at the permissive temperature, 22°C (Lanes 1-16), or following incubation of the mutants for 1 hr at the non-permissive temperature, 37°C (Lanes 17-32). **(i)** Ethidium bromide stained gel showing the ribosomal RNAs. rRNA was used as a control of equal loadings on the gel. **(ii)** The blot was hybridised with the *ACT1* probe. **(iii)** The blot was hybridised with the neo-specific probe. **(iv)** The relative neo-*HTB1* mRNA levels are shown below the gels. The northern blot autoradiograph was spliced together from the same gel in order to clarify the results.

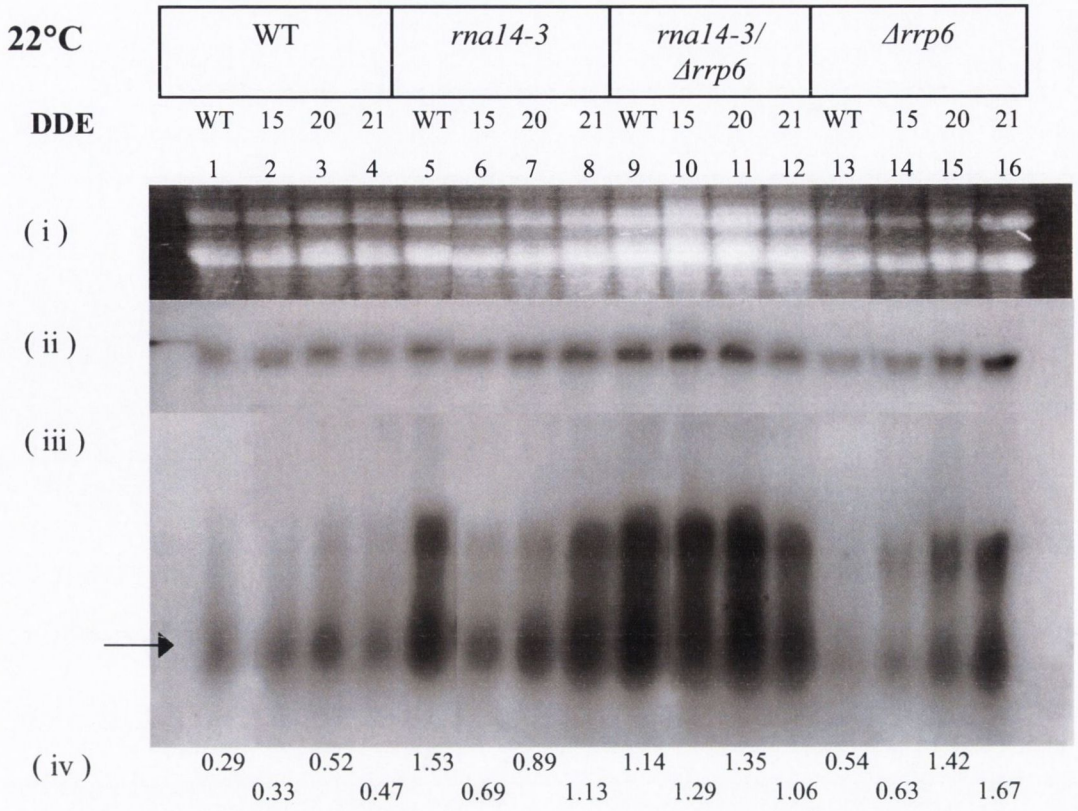
22°C
WT
rna14-3
rna14-3/ Δrrp6
Δrrp6
DDE
WT 15 20 21 WT 15 20 21 WT 15 20 21 WT 15 20 21
1 2 3 4 5 6 7 8 9 10 11 12 13 14 15 16
(i)
(ii)
(iii)
(iv)
0.29 0.52 1.53 0.89 1.14 1.35 0.54 1.42
0.33 0.47 0.69 1.13 1.29 1.06 0.63 1.67

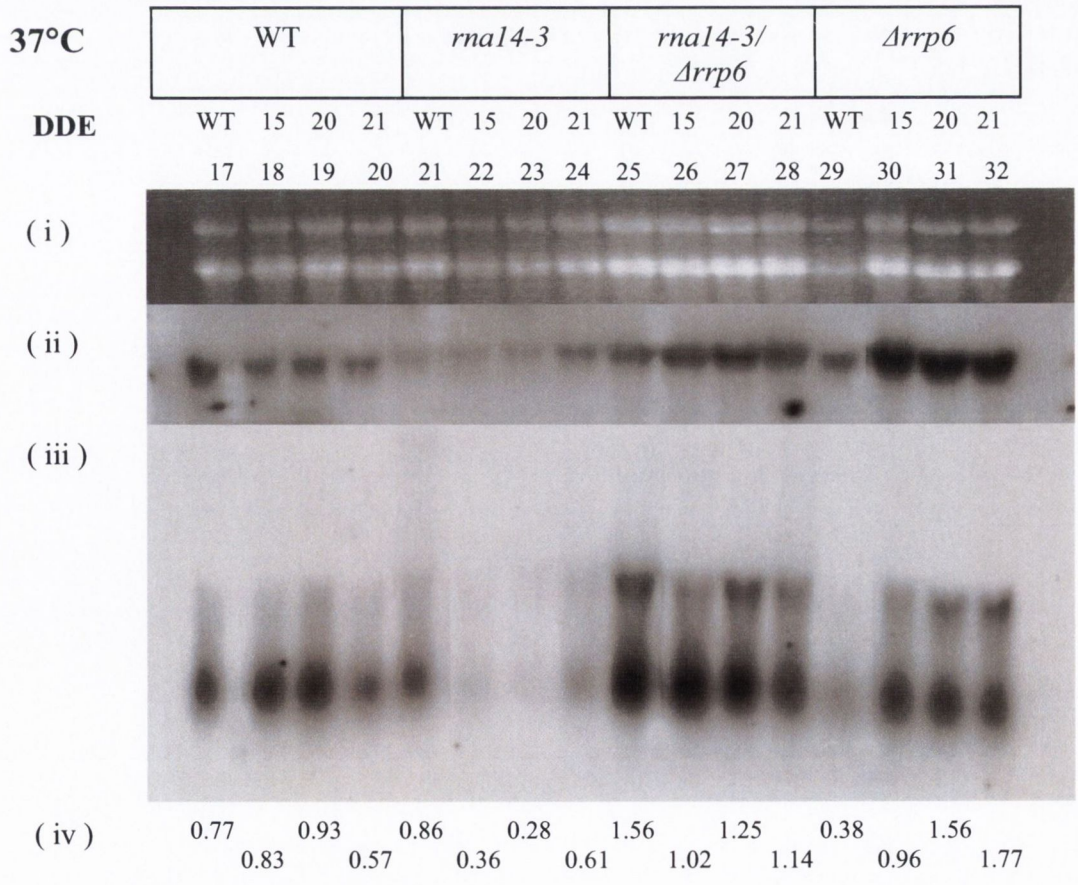
37°C
WT
rna14-3
rna14-3/ Δrrp6
Δrrp6
DDE
WT 15 20 21 WT 15 20 21 WT 15 20 21 WT 15 20 21
17 18 19 20 21 22 23 24 25 26 27 28 29 30 31 32
(i)
(ii)
(iii)
(iv)
0.77 0.93 0.86 0.28 1.56 1.25 0.38 1.56
0.83 0.57 0.36 0.61 1.02 1.14 0.96 1.77

3.2.4 CFIA factors and the nuclear exosome component, Rrp6, play a role in *HTB1* mRNA processing

Endogenous *HTB1* mRNA was also investigated in the *rna14-3, Δrrp6* and *rna14-3/Δrrp6* strains transformed with the WT DDE and DDE mutant plasmids. This experiment was performed as described in Chapter 2 (Section 2.9), with the modification that the Northern blots were finally probed to detect the endogenous *HTB1* sequences. Actin mRNA was used as an indicator for RNA loading variabilities (Chapter 2, Section 2.9.5).

The endogenous *HTB1* mRNA levels in the W303 background were low and similar levels were observed in the *rna14-3* strain at 22°C (*Figure 3.5(iii)*, 22°C, Lanes 1, 2, 3 and 4 compared to Lanes 5, 6, 7 and 8). The relative *HTB1* mRNA levels in the *rna14-3* background containing the PLJ31, pSAC15, pSAC20 and pSAC21 plasmids are 1.00, 0.8, 0.74 and 0.83 respectively, indicating that the relative mRNA levels are similar in this background. The endogenous *HTB1* mRNA levels slightly increased in the double mutants, *rna14-3/Δrrp6* (*Figure 3.5(iii)*, 22°C, Lanes 9, 10, 11 and 12). This slight increase was also evident in the *Δrrp6* background alone (*Figure 3.5(iii)*, 22°C, Lanes 1, 2, 3 and 4 compared to lanes 13, 14, 15 and 16). Interestingly, the endogenous *HTB1* mRNA levels in the *Δrrp6* background containing the DDE mutant plasmid, pSAC21, appear to be greater than the *HTB1* mRNA levels in the *Δrrp6* background containing the PLJ31, pSAC15 and pSAC20 plasmids (*Figure 3.5(iii)*, 22°C, Lane 16 compared to lanes 13, 14 and 15). However, quantification analysis revealed that the relative endogenous *HTB1* mRNAs in PLJ31, pSAC15, pSAC20 and pSAC21 in the *Δrrp6* background are 0.97, 1.22, 1.22 and 1.2 respectively (*Figure 3.5(iii)*, 22°C, Lanes 13, 14, 15 and 16). Therefore, it appears that the presence of the DDE mutant plasmids in the *Δrrp6* background slightly stabilised the endogenous *HTB1* mRNAs. However, since only one data set is available, it is not clear if this increase is statistically significant.

At the non-permissive temperature, endogenous *HTB1* mRNAs in the *rna14-3* background

containing the PLJ31, pSAC15, pSAC20 and pSAC21 plasmids were notably reduced, which demonstrated that the cleavage factor, Rna14-3, is essential for correct cleavage of the *HTB1* transcripts (*Figure.3.5(iii)*, 37°C, Lanes 21, 22, 23 and 24). Mature endogenous *HTB1* mRNAs were observed in the double mutants, *rna14-3/Δrrp6*. The relative mRNA levels of *HTB1* in the WT background containing the PLJ31, pSAC15, pSAC20 and pSAC21 plasmids are 1.54, 1.31, 1.23 and 1.55 respectively and 1.01, 1.10, 0.92 and 0.76 respectively in the *rna14-3/Δrrp6* background (*Figure 3.5(iii)*, 37°C, Lanes 17-20 compared to Lanes 25-28). This 20-25% difference in *HTB1* mRNA levels in the same genetic background most likely reflects experimental error since the densitometry analysis is only semi-quantitative. The transcripts were stabilised in the *Δrrp6* background (*Figure 3.5(iii)*, 37°C, Lanes 29-32). While Lane 29 is underloaded, there is a slight apparent stabilisation of the endogenous *HTB1* transcripts in the *Δrrp6* strain containing pSAC15, pSAC20 and pSAC21 *neo-HTB1* transcripts (*Figure 3.5(ii)*, 37°C, Lanes 30-32 compared to Lane 29). Quantification analysis indicates that the relative endogenous *HTB1* mRNA levels are 0.46, 1.27, 0.92 and 1.40 in Lanes 29-32. The quantification data indicates that there is an apparent increase in the endogenous *HTB1* levels in the *Δrrp6* background with the DDE mutants compared with the WT DDE when the cells were grown at 37°C. The increase in the endogenous *HTB1* mRNA levels in the DDE-mutants shows that the mRNA transcripts may be possible substrates for the nuclear exosome. This needs to be further investigated as it is not clear if this is statistically significant.

Figure 3.5: Northern blot analysis of endogenous *HTB1* mRNA in CFIA and exosome mutants. Total RNA, 60µg, was isolated from the following yeast strains, Lanes 1 and 17; W303B containing the PLJ31 plasmid, Lanes 2 and 18; W303B containing the pSAC15 plasmid, Lanes 3 and 19; W303B containing the pSAC20 plasmid, Lanes 4 and 20; W303B containing the pSAC21 plasmid, Lanes 5 and 21; *rna14-3* containing the PLJ31 plasmid, Lanes 6 and 22; *rna14-3* containing the pSAC15 plasmid, Lanes 7 and 23; *rna14-3* containing the pSAC20 plasmid, Lanes 8 and 24; *rna14-3* containing the pSAC21 plasmid, Lanes 9 and 25; *rna14-3/Δrrp6* containing the PLJ31 plasmid, Lanes 10 and 26; *rna14-3/Δrrp6* containing the pSAC15 plasmid, Lanes 11 and 27; *rna14-3/Δrrp6* containing the pSAC20 plasmid, Lanes 12 and 28; *rna14-3/Δrrp6* containing the pSAC21 plasmid, Lanes 13 and 29; *Δrrp6* containing the PLJ31 plasmid, Lanes 14 and 30; *Δrrp6* containing the pSAC15 plasmid, Lanes 15 and 31; *Δrrp6* containing the pSAC20 plasmid, Lanes 16 and 32; *Δrrp6* containing the pSAC21 plasmid, at the permissive temperature, 22°C (Lanes 1-16), or following incubation of the mutants for 1 hr at the non-permissive temperature, 37°C (Lanes 17-32). **(i)** Ethidium bromide stained gel showing the ribosomal RNAs. rRNA was used as a control of equal loadings on the gel. **(ii)** The blot was hybridised with the *ACT1* probe. **(iii)** The blot was hybridised with the *HTB1*-specific probe. **(iv)** The relative endogenous *HTB1* mRNA levels are shown below the gels. The northern blot autoradiograph was spliced together from the same gel in order to clarify the results.

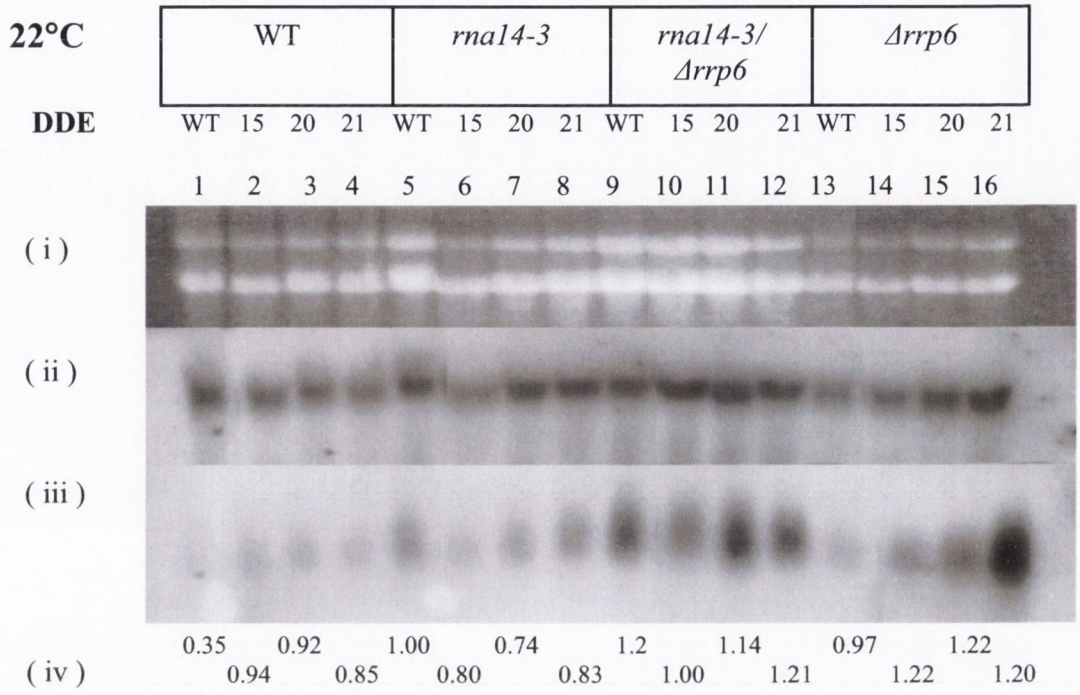
22°C
WT
rna14-3
rna14-3/ Δrrp6
Δrrp6
DDE
WT 15 20 21 WT 15 20 21 WT 15 20 21 WT 15 20 21
1 2 3 4 5 6 7 8 9 10 11 12 13 14 15 16
(i)
(ii)
(iii)
0.35 0.92 1.00 0.74 1.2 1.14 0.97 1.22
(iv)
0.94 0.85 0.80 0.83 1.00 1.21 1.22 1.20

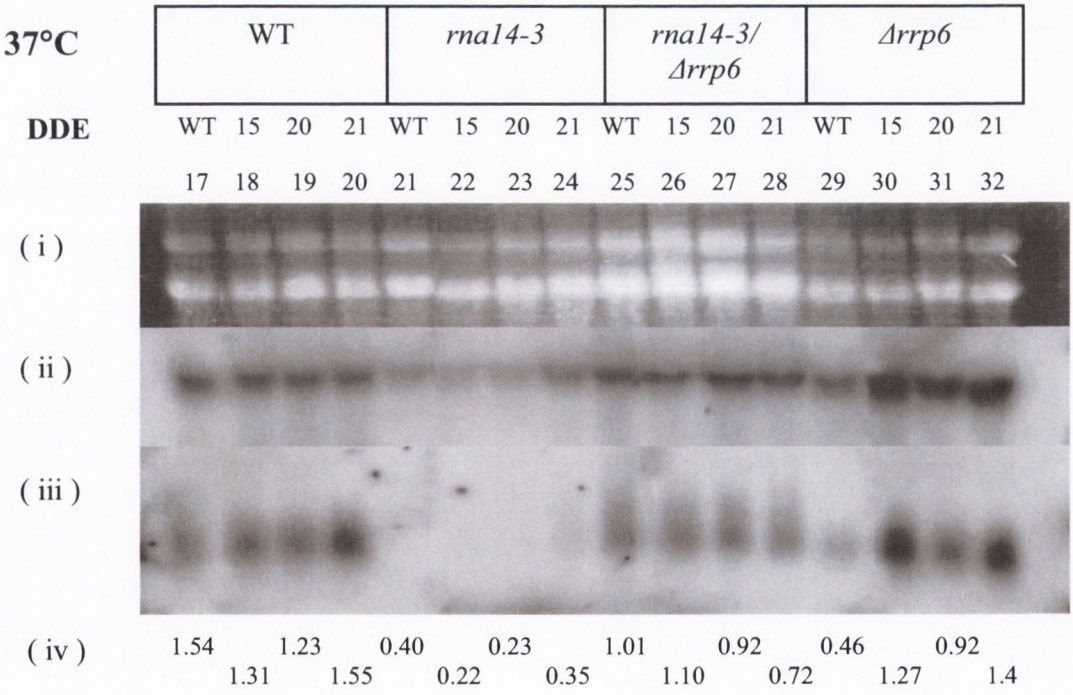
37°C
WT
rna14-3
rna14-3/ Δrrp6
Δrrp6
DDE
WT 15 20 21 WT 15 20 21 WT 15 20 21 WT 15 20 21
17 18 19 20 21 22 23 24 25 26 27 28 29 30 31 32
(i)
(ii)
(iii)
1.54 1.23 0.40 0.23 1.01 0.92 0.46 0.92
(iv)
1.31 1.55 0.22 0.35 1.10 0.72 1.27 1.4

3.2.5 The 5'→3' exosome, Rat1p, participates in *neo-HTB1* processing

The 5'→3' exonuclease, Rat1p, is a well-established termination factor, whose role in other processes, such as 3'-end processing, is currently being investigated (Luo *et al*, 2006). To examine the role of the 5'→3' exonuclease, Rat1, in the biogenesis of *neo-HTB1* mRNAs, the WT (RAT1) strain and the strain lacking Rat1 were transformed with the *neo-HTB1* PLJ31 (WT), pSAC15, pSAC20 and pSAC21 plasmids. Northern blot analysis was performed on total RNA extracted from the WT strain and the temperature-sensitive mutant, *rat1*, following 1 hr of incubation at the permissive (22°C) and non-permissive (37°C) temperatures (Chapter 2, Section 2.9). The membranes were probed with the neo-specific probe to detect the *neo-HTB1* sequences (Chapter 2, *Table 2.2*).

Mature *neo-HTB1* mRNA was produced from the PLJ31, pSAC15, pSAC20 and pSAC21 plasmids at the permissive temperature, in the RAT1 background (*Figure 3.6(iii)*, 22°C, Lanes 1-4), although the levels of pSAC20 *neo-HTB1* mRNA is lower as a result of underloading of this sample (*Figure 3.6(iii)*, 22°C, Lane 3). Mature mRNA levels were observed in the *rat1* background (*Figure 3.6(iii)*, 22°C, Lanes 5, 6, 7 and 8).

At 37°C, the steady state levels of the mature mRNA were slightly lower due to reduced transcription and/or increased turnover in the RAT1 background (*Figure 3.6*, 37°C, Lanes 9-12). Lane 12 is overloaded as observed by the rRNA and *ACT1* mRNA levels (*Figure 3.6(i), (ii)*, 37°C, Lane 12). The temperature-sensitive *rat1* strain at the non-permissive temperature exhibited a slight reduction of mature mRNA compared to the WT, RAT1, strain. Quantification analysis was conducted to confirm this observation. The relative *neo-HTB1* mRNA levels at 37°C for the PLJ31, pSAC15, pSAC20 and pSAC21 plasmids are 1.19, 1.04, 0.84 and 1.02 respectively in the WT background and are 0.89, 0.65, 0.58 and 0.6 respectively in the *rat1* background. This is consistent with a role for Rat1p in histone 3'-end processing (*Figure 3.6(iii)*, 37°C, Lanes 9-12 compared to Lanes 13-16). The DDE mutants, pSAC15, pSAC20 and pSAC21 behaved similarly to the WT DDE, indicating

that Rat1 activity does not require the DDE region of the *neo-HTB1* mRNAs. The *ACT1* mRNA levels were similar at 22°C and the steady state levels decreased slightly at 37°C in the Rat1 and *rat1* backgrounds (*Figure 3.6(ii)*, 37°C, Lanes 1-8 compared to Lanes 9-16). Again, the results indicate that *ACT1* mRNAs are more stable than the *neo-HTB1* mRNAs. Therefore, the mutant, *rat1*, which alters the processes involved in mRNA biogenesis, has little effect on the steady state levels of *ACT1* transcripts.

Figure 3.6: Northern blot analysis of *neo-HTB1* mRNA with the 5'→3' exonuclease, Rat1. Total RNA, 60μg, was isolated from the following yeast strains, Lanes 1 and 9; RAT1 containing the PLJ31 plasmid, Lanes 2 and 10; RAT1 containing the pSAC15 plasmid, Lanes 3 and 11; RAT1 containing the pSAC20 plasmid, Lanes 4 and 12; RAT1 containing the pSAC21 plasmid, Lanes 5 and 13; *rat1* containing the PLJ31 plasmid, Lanes 6 and 14; *rat1* containing the pSAC15 plasmid, Lanes 7 and 15; *rat1* containing the pSAC20 plasmid, Lanes 8 and 16; *rat1* containing the pSAC21 plasmid, at the permissive temperature, 22°C (Lanes 1-8), or following incubation of the mutants for 1 hr at the non-permissive temperature, 37°C (Lanes 9-16). **(i)** Ethidium bromide stained gel showing the ribosomal RNAs. rRNA was used as a control of equal loadings on the gel. **(ii)** The blot was hybridised with the *ACT1* probe. **(iii)** The blot was hybridised with the neo-specific probe. **(iv)** The relative *neo-HTB1* mRNA levels are shown below the gels. The northern blot autoradiograph was spliced together from the same gel in order to clarify the results.

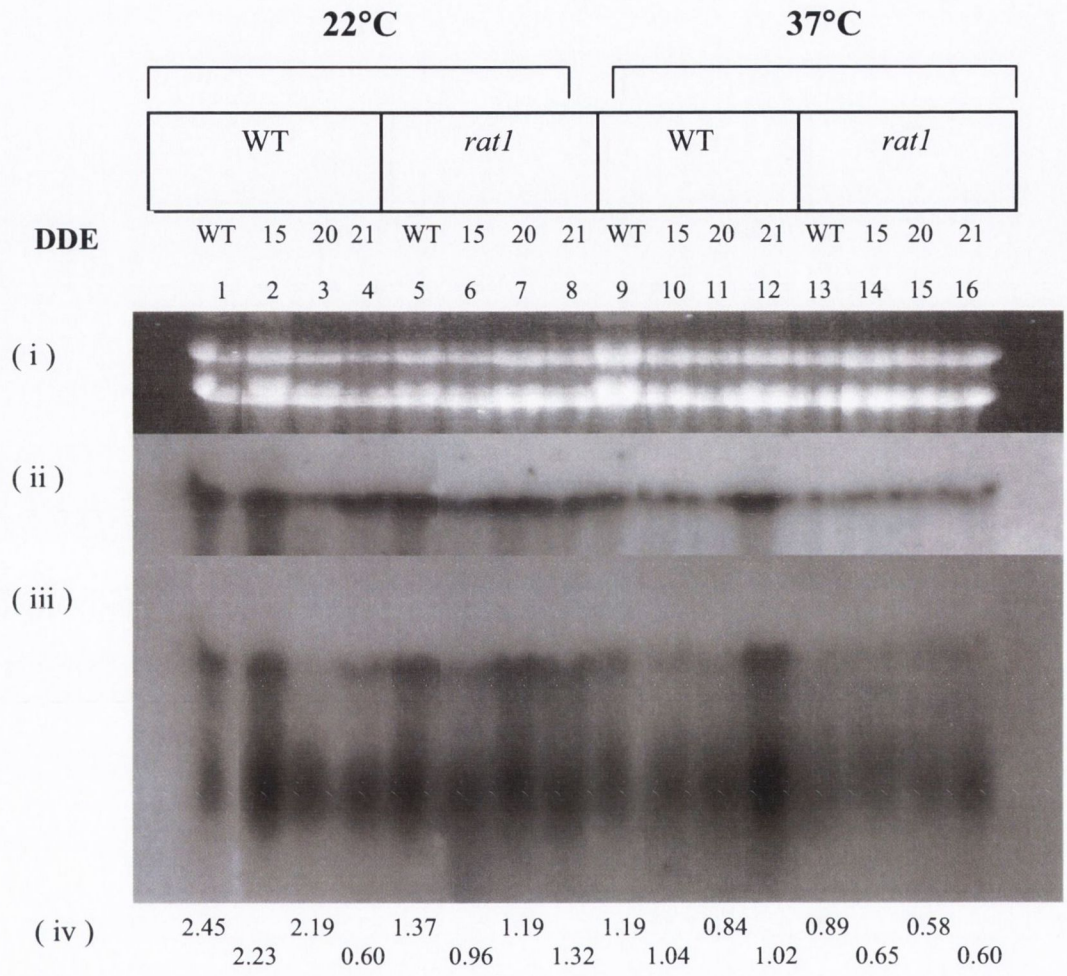
22°C
37°C
WT
rat1
WT
rat1
DDE
WT 15 20 21 WT 15 20 21 WT 15 20 21 WT 15 20 21
1 2 3 4 5 6 7 8 9 10 11 12 13 14 15 16
(i)
(ii)
(iii)
(iv)
2.45 2.19 1.37 1.19 1.19 0.84 0.89 0.58
2.23 0.60 0.96 1.32 1.04 1.02 0.65 0.60

3.2.6 The 5'→3' exosome, Rat1p, is involved in endogenous *HTB1* processing

The role of Rat1 in *HTB1* mRNA processing was also examined in the wild type (RAT1) and the mutant, *rat1*, transformed with the *neo-HTB1* PLJ31, pSAC15, pSAC20 and pSAC21 plasmids. Northern blot analysis was performed, as described in Chapter 2 (Section 2.9). Northern blots were probed with the endogenous *HTB1* sequences (*Table 2.2*).

Mature endogenous *HTB1* levels were observed at 22°C in the WT and *rat1* strains (*Figure 3.7(iii)*, 22°C). The loading variabilities were taken into account and the relative endogenous *HTB1* mRNA levels are unaffected by the presence of the pSAC15, pSAC20 and pSAC21 *HTB1* mRNAs in the *rat1* strain at 22°C (*Figure 3.7(iii)*, 22°C, Lanes 4-8). At the non-permissive temperature, *ACT1* mRNA levels were not notably reduced compared to the levels at the permissive temperature (*Figure 3.7(i)*, 37°C, Lanes 1-8 compared to Lanes 9-16). The endogenous *HTB1* transcripts were not extensively reduced in the RAT1 strain at 37°C compared to the levels at the permissive temperature (*Figure 3.7(iii)*, 37°C, Lanes 1-4 compared to Lanes 9-12). In the *rat1* background, endogenous *HTB1* transcripts were found to be slightly reduced compared to the RAT1 background at the non-permissive temperature (*Figure 3.7(iii)*, 37°C, Lanes 9-12 compared to Lanes 13-16). Quantification analysis indicates that the relative endogenous *HTB1* levels were 1.21, 1.37, 1.5 and 1.17 in the RAT1 background containing PLJ31, pSAC15, pSAC20 and pSAC21 plasmids respectively at 37°C, whereas the relative *HTB1* levels were 0.78, 0.58, 0.41 and 0.48 in the *rat1* background containing PLJ31, pSAC15, pSAC20 and pSAC21 plasmids respectively at 37°C. This indicates that Rat1 contributes to the biogenesis of the endogenous *HTB1* sequences. The presence of *neo-HTB1* mRNA containing WT DDE or DDE mutants did not alter the steady state levels of the endogenous *HTB1* mRNA in the WT or *rat1* backgrounds.

Figure 3.7: Northern blot analysis of the endogenous *HTB1* mRNA in the 5'→3' exonuclease, Rat1. Total RNA, 60μg, was isolated from the following yeast strains, Lanes 1 and 9; RAT1 containing the PLJ31 plasmid, Lanes 2 and 10; RAT1 containing the pSAC15 plasmid, Lanes 3 and 11; RAT1 containing the pSAC20 plasmid, Lanes 4 and 12; RAT1 containing the pSAC21 plasmid, Lanes 5 and 13; *rat1* containing the PLJ31 plasmid, Lanes 6 and 14; *rat1* containing the pSAC15 plasmid, Lanes 7 and 15; *rat1* containing the pSAC20 plasmid, Lanes 8 and 16; *rat1* containing the pSAC21 plasmid, at the permissive temperature, 22°C (Lanes 1-8), or following incubation of the mutants for 1 hr at the non-permissive temperature, 37°C (Lanes 9-16). **(i)** Ethidium bromide stained gel showing the ribosomal RNAs. rRNA was used as a control of equal loadings on the gel. **(ii)** The blot was hybridised with the *ACT1* probe. **(iii)** The blot was hybridised with the *HTB1*-specific probe. The northern blot autoradiograph was spliced together from the same gel in order to clarify the results. **(iv)** The relative endogenous *HTB1* mRNA levels are shown below the gels.

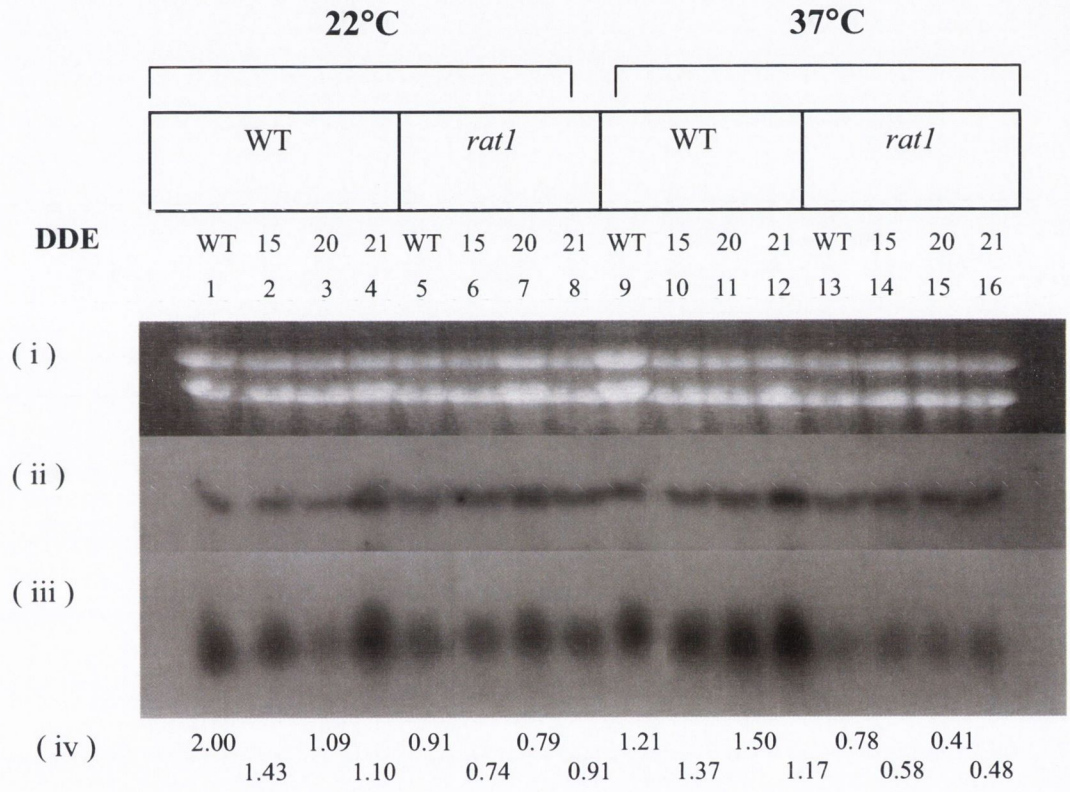
22°C
37°C
WT
rat1
WT
rat1
DDE
WT 15 20 21 WT 15 20 21 WT 15 20 21 WT 15 20 21
1 2 3 4 5 6 7 8 9 10 11 12 13 14 15 16
(i)
(ii)
(iii)
(iv)
2.00 1.09 0.91 0.79 1.21 1.50 0.78 0.41
1.43 1.10 0.74 0.91 1.37 1.17 0.58 0.48

3.3 Discussion

In this chapter, the role of the CFIA factors in the biogenesis of *HTB1* mRNAs was investigated. Data reveals that the CFIA mutants give rise to normal cleavage of *neo-HTB1* transcripts containing the PLJ31 plasmid at the permissive temperature, but the biogenesis of mature *neo-HTB1* mRNA is severely restricted at the non-permissive temperature. The lack of sustained levels of mature *neo-HTB1* mRNA at the non-permissive temperature in the *rna14*, *rna15* and *pcf11* backgrounds likely results from a decrease in 3'-end cleavage and the subsequent degradation of cleaved and uncleaved pre-mRNAs. Additionally, a very low level of read-through transcripts of the WT *neo-HTB1* mRNAs was apparent in the *rna14*, *rna15* and *pcf11* backgrounds, which possibly reflects an impairment of transcription termination at this temperature. The rapid degradation of the WT *neo-HTB1* mRNA in the *rna14*, *rna15* and *pcf11* strains suggests that these mRNAs were targeted to the exosome. These results are consistent with earlier data from Birse *et al* (1998), who demonstrated that the *rna14*, *rna15* and *pcf11* mutants impaired both 3'-end mRNA processing and transcription termination as observed from transcription run-on analysis, indicating a clear link between 3'-end processing and transcription termination (Birse *et al*, 1998).

The nuclear exosome has previously been shown to play a role in degrading unprocessed and aberrant pre-mRNAs. In addition to a role in the control of gene expression, the exosome is involved in processing of the 7S pre-rRNA to 5.8S rRNA, which forms a component of the 60S of the rRNA complex (Butler *et al*, 2002). The role of the nuclear exosome in the rapid turnover of WT *neo-HTB1* mRNAs in cells defective in 3'-end processing, *rna14-3/Δrrp6* and *rna15-2/Δrrp6* mutant strains, was investigated. Production of mature cleaved mRNA was partially restored for the WT *neo-HTB1* transcripts in the double mutant backgrounds at 37°C. Under these conditions, mature WT *neo-HTB1*

mRNAs were stabilised and, furthermore, the 3'-end cleavage defects were evident in the appearance of read-through transcripts.

Campbell *et al* (2002) have previously shown that the DDE lies in the region where transcription termination occurs (Campbell *et al*, 2002). This posed another question as to whether the exosome component, Rrp6p, interacts with the DDE mutants to play a role in *neo-HTB1* processing. The WT *neo-HTB1* transcripts were compared to pSAC15, pSAC20 and pSAC21 *neo-HTB1* transcripts, which contain mutations in the DDE, in the cleavage and exosome mutant backgrounds. In the *rna14-3* and *rna14-3/Δrrp6* strains, stable WT, pSAC15, pSAC20 and pSAC21 *neo-HTB1* mRNAs were observed; in fact, the transcripts appeared to be stabilised when compared to the levels in the WT, W303, strain (*Figure 3.4*). However, there was an apparent increase in RNA turnover in all three *neo-HTB1* mutants in the *rna14-3* background compared to the WT *neo-HTB1* transcripts, at both the permissive and non-permissive temperatures. This increase in turnover may indicate that the *neo-HTB1* mRNAs containing mutant DDEs are somehow better substrates for the exosome in the *rna14-3* genetic background, particularly pSAC15 and pSAC20 at 22°C. The other possibility is that the mutants, pSAC15 and pSAC20, may be very unstable when the RNA was prepared in this background. Campbell *et al* (2002) have previously shown that *neo-HTB1* mRNAs expressed from the pSAC20 plasmid are less stable than transcripts containing the WT DDE (Campbell *et al*, 2002). Conversely, the mutant DDE *neo-HTB1* mRNAs were more stabilised than the WT *neo-HTB1* mRNAs at both 22°C and 37°C in the *Δrrp6* mutant background, again suggesting that the DDE mutants are preferred substrates for the nuclear exosome. To confirm these observations, semi-quantitative analysis of the levels of *neo-HTB1* mRNAs were carried out. The data indicates that only a 1.16-2.9 fold stabilisation of the DDE mutant *neo-HTB1 TB1* mRNAs is apparent at 22°C. A 2.52-4.47 fold stabilisation of these mutant RNAs is found when the *Δrrp6* mutant cells were incubated at 37°C.

The substrate preference of the exosome for the DDE mutants is currently unclear, although since the DDE lies in the region of transcription termination, this may be a recognition site for the exosome. Currently, there is little information on how the exosome recognises its substrates. The steady state levels of *neo-HTB1* mRNAs were observed to be higher at both the permissive and non-permissive temperatures in the double mutants, *rna14-3/Δrrp6,* compared to the levels observed in the *rna14-3* mutant alone. The deletion of the exosome, as well as the cleavage factor, restored the levels of the WT, pSAC15, pSAC20 and pSAC21 *neo-HTB1* transcripts at 37°C, indicating a possible role for the exosome in the normal biogenesis of the *neo-HTB1* mRNAs. This also indicates that competition exists between the cleavage factor and exosome component for the DDE region.

The 3'-end processing of the endogenous *HTB1* mRNA levels was also explored in this chapter, using the cleavage factors and exosome mutants. At the restrictive temperature, *rna14-3* mutants demonstrated a reduction in the endogenous *HTB1* mRNA levels and levels were restored when Rrp6p was deleted in this background. Surprisingly, the DDE mutants appear to stabilise the endogenous *HTB1* mRNAs in the *Δrrp6* background at 37°C. Again, semi-quantitative densitometry analysis indicates a 2.0-3.0 fold stabilisation of *HTB1* mRNA levels in the pSAC15, 20 and 21 mutants relative to the levels observed with the *neo-HTB1* containing the WT DDE. This is similar to the stabilisation observed with the *neo-HTB1* mRNAs containing mutations in the DDE (*see above*). From the semi-quantitative analysis, it appears that variations in RNA levels of 1.23-1.25 fold can be accounted for from experimental error (*see variations in HTB1 mRNA levels in the WT background described above*). Therefore, the 2.0-3.0 fold stabilisation of *HTB1* mRNA in cells expressing DDE mutant forms of *neo-HTB1* appears to be significant. The reason for this apparent stabilisation of *HTB1* mRNAs is currently unclear. One possibility is that the mutant DDEs may titrate out some factor that is required for the turnover of *neo-HTB1* and

HTB1 mRNAs. This apparent stabilisation of *HTB1* mRNAs is similar to the stabilisation of DDE-mutant *neo-HTB1* mRNA at 37°C.

Working with elongation mutants, *Δhpr1* and *Δmft,* cleavage mutants, *rna14-3* and *rna15-2*, and the nuclear exosome mutants, Libri *et al* (2002) demonstrated that HSP104 transcripts are retained near the transcription site in the *Δhpr1, Δmft1, rna14-3* and *rna15-2* mutants, whereas *Δhpr1/Δrrp6, Δmft1/Δrrp6, rna14-3/Δrrp6* and *rna15-2/Δrrp6* mutants exhibited no retention of the HSP104 transcripts. These findings indicate that Rrp6p was involved in transcription site retention in the *Δhpr1, Δmft1, rna14-3* and *rna15* strains. Additional findings from Libri *et al* (2002) demonstrated that the 3'-ends of the RNA in the *Δhpr1* and *Δmft1* backgrounds were significantly reduced. In the double mutants, *Δhpr1/Δrrp6* and *Δmft1/Δrrp6*, complete restoration of the 3'-end levels similar to the WT was observed. This again led to the conclusion that Rrp6p degrades a significant amount of transcripts in *Δhpr1* and *Δmft1* transcripts (Libri *et al*, 2002).

Torchet *et al* (2002) have proposed a model to explain the role of the exosome component, Rrp6p, in pre-mRNA processing (Torchet *et al*, 2002). In this model, the wild type strain undergoes correct cleavage and polyadenylation, as shown in Figure 3.8. In the *rna14.1* and *rna15.2* backgrounds, correct cleavage does not occur and read-through transcripts are observed. The unprotected and unprocessed 3'-end is recognised by the exosome, Rrp6p, and by its partner, Dob1p, which degrades the 3'-end. The read-through transcripts in the *rna14.1/Δrrp6* background are stabilised and appear to undergo subsequent cleavage and polyadenylation. In combining these results with Libri *et al* (2002), it is possible to propose a model in which, under conditions when mRNA degradation is inhibited (*Δrrp6*), the stabilised pre-mRNAs can slowly be processed by the sub-optimal 3'-end processing machinery (*rna14* or *rna15*). This mechanism implies that there is a level of competition between the 3'-end processing machinery and the nuclear exosome for binding to the pre-mRNA. This suggests that the nuclear exosome may play a role in the normal biogenesis of

mRNAs. When the cleavage factors Rna14p and Rna15p are deleted, the unprocessed transcripts were degraded by the exosome. When the exosome Rrp6p was also deleted, stabilisation of the transcripts was observed, indicating that the cleavage factor processed the transcripts. Even in the double mutants, cleavage factors, *rna14* or *rna15*, with the exosome, *Δrrp6*, was found to lead to stabilisation of the transcripts. These findings show that the cleavage factors, Rna14p and Rna15p, compete with the nuclear exosome, Rrp6p, for the RNA. The results in this chapter favour such a competition model.

To date, only the Nrd1p and TRAMP complexes are known to recruit the exosome, Rrp6p. Nrd1p is a 3'-end RNA-binding protein and associates with the RNA-binding protein, Nab3, the putative RNA helicase, Sen1, and the cap-binding complex, Cbp80 and Cbp20 (Steinmetz *et al*, 2001). Interestingly, *nrd1* and the exosome mutants demonstrated termination defects in mRNAs and sn/snoRNAs, which indicate that the Nrd1 complex recruits the exosome, Rrp6p, to the RNA. Once the exosome, Rrp6p, binds to the RNA, it starts either 3'-end processing or degradation (Vasiljeva and Buratowski, 2006). The manner in which the exosome chooses between 3'-end processing and degradation remains unclear. In the degradation process, the Nrd1 complex recruits the exosome to the RNA and begins degradation of improper processed transcripts. In snoRNA processing, the exosome is recruited to the RNA and trims back the sn/snoRNAs until it is blocked at the Nrd1/Nab3 binding site. The purified Nrd1 complex was found to interact with the Trf4 and its partner Air2, which are members of the TRAMP complex. The TRAMP complex consists of a putative ATP-dependent RNA helicase, Mtr4p/Dob1p, Poly (A) polymerase, Trf4p, and Zinc knuckle binding protein, Air2p. It facilitates Rrp6p-mediated degradation of the RNA substrate *in vitro* without ATP being present. This result indicates that polyadenylation is important for degradation of unprocessed RNAs. Tf4p poly (A) polymerase and its partner Air2p polyadenylate RNA, which is then targeted to the exosome for degradation (LaCava *et al*, 2005). Further research work is required to fully

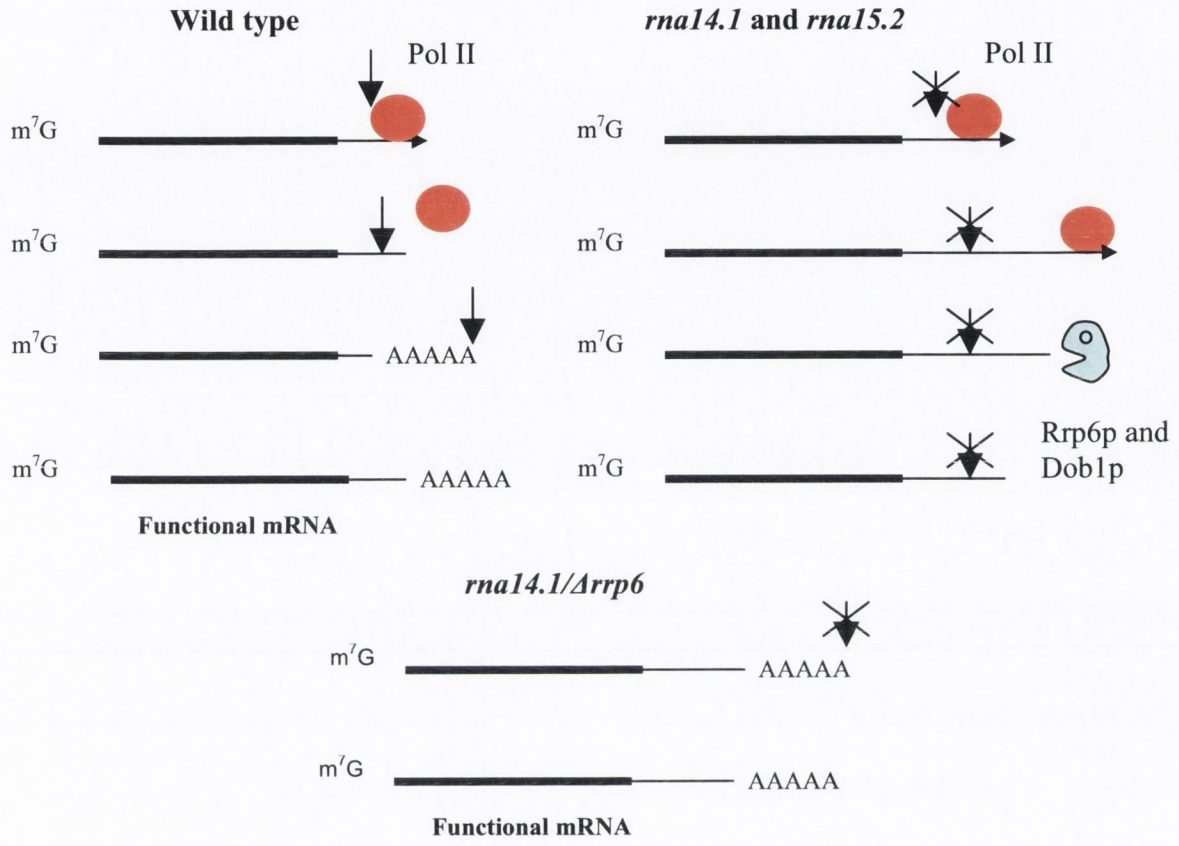

Figure 3.8: Model of the degradation and processing reactions with *rna14.1* and *rna15.2* and *rna14.1/Δrrp6* mutant strains. The RNA transcript is transcribed by RNA Polymerase II (red ball) and undergoes correct cleavage (arrows) in the wild type. In the *rna14.1* and *rna15.2* strains, the RNA is not cut (crossed arrow) and the Polymerase continues to transcribe. The Rrp6p and Dob1p rapidly degrade the unprocessed transcripts. In the double mutant, the transcripts are stabilised and produce functional mRNA.

understand how the exosome recognises the poly (A) tail for degradation. Recently, in late December 2006, Reis and Campbell worked with the components of the TRAMP complex and investigated if the exosome, Rrp6p, plays a role in histone mRNA up-regulation with the TRAMP complex. They discovered that Rrp6 plays a role in histone mRNA regulation of the HHF2 transcripts (Reis and Campbell, 2006).

Rat1p is a well-established termination factor, whereas its role in other functions such as 3'-end processing are currently being researched. Rat1 and its partner Rai1 were shown to be defective in transcription termination via CHIP analysis by Kim *et al* (2004). Since investigations were performed with the 3'→5' exonuclease, Rrp6, we proceeded to investigate the role of the 5'→3' exonuclease, Rat1. The analysis of the steady state levels of mature *neo-HTB1* and *HTB1* mRNAs were reduced in the *rat1* background at the non-permissive temperature compared to the wild type, RAT1. The DDE mutants in the *rat1* background showed no effect on the *neo-HTB1* and endogenous *HTB1* mRNAs compared to the WT DDE. Importantly, the results indicate that Rat1 plays a small role in 3'-end processing in the *neo-HTB1* and endogenous *HTB1* mRNAs.

Recently, Luo *et al* (2006) demonstrated a coupling of 3'-end processing to transcription termination with Rat1. Using anti-pol II chromatin immunoprecipitation (CHIP) techniques, the authors demonstrated that there were termination defects with the mutant *rat1*. For the first time, researchers investigated whether 3'-end processing factors interact with the termination factor Rat1. Cross-linking the two proteins, Pcf11 and Rna15, at the ADH4 3'-end, in the *rat1* background was used to determine whether 3'-end processing factors are recruited independent of Rat1. The deleted Rat1 strain showed strong inhibition of the recruitment of Pcf11 and Rna15 to the 3'-end. The wild type, Rat1, restored both termination and cleavage of Pcf11 and Rna15. This demonstrated that Rat1 is also essential for recruitment of 3'-end processing factors. In addition, Luo *et al* (2006) proposed a unification of allosteric and torpedo models behaving at the same time (Chapter 1, *Figure*

1.3). They deduced from their results that cleavage occurs at the poly (A) site, degradation of the cleaved 3'-end, followed by an allosteric change that causes the RNA Polymerase II to be released from the template (Luo *et al*, 2006).

In this chapter, we hypothesise that the CFIA and exosome compete for the processing step in the *neo-HTB1* mRNA. We demonstrate that CFIA, Rna14, Rna15 and Pcf11, and the 3'→5' exonuclease, Rrp6, play a role in *neo-HTB1* mRNA and the endogenous *HTB1* mRNA processing. The 5'→3' exonuclease, Rat1, was also shown to play a small role in processing of *neo-HTB1* mRNA and endogenous *HTB1* mRNAs. Additionally, the results suggest that the mRNAs containing mutations in the DDE increase the stability of the *neo-HTB1* mRNAs and the endogenous *HTB1* mRNAs in a *Δrrp6* mutant background.

Chapter 4

The nuclear exosome factor plays a role in *HTB1* biogenesis and cell-cycle regulation

4.1 Introduction

Replication-dependent histone mRNA synthesis is tightly regulated during the S-phase of the cell cycle in the yeast, *Saccharomyces cerevisiae* (Lycan *et al*, 1987). The tight regulation occurs as a result of transcriptional and post-transcriptional controls. The majority of research to date into the cell cycle has been carried out in mammalian histones. Mammalian histone mRNAs are non-polyadenylated and have a stem-loop structure. The stem-loop binding protein (SLBP) has been shown to be essential during the cell cycle. Using synchronised HeLa cells, Whitfield *et al* (2000) demonstrated that the levels of the SLBP increased at the G_1/S-phase border. The SLBP and histone mRNA accumulates as it enters the S-phase. At the end of the S-phase/G_2-border, the synthesis of histones decreases and the SLBP is degraded as the cell gets prepared for the next cell cycle (Whitfield *et al*, 2000). The SLBP interacts with the hZFP100 protein. Recently, hZFP100 protein was found to be important for cell-cycle regulation since it regulates the cells entering the S-phase (Wagner and Marzluff, 2006).

Yeast histone mRNAs do not have a stem-loop structure and are polyadenylated. Furthermore, no genes corresponding to the SLBP or U7 snRNP have been identified in yeast. Experiments have been carried out on the coding and non-coding sequences in the histone H2B mRNA to determine their role in cell-cycle regulation. Lycan *et al* (1987) first demonstrated that the H2B-lacZ gene containing 80 amino acids of the H2B 5' coding region showed no cell-cycle accumulation, indicating that the 5'-end of the histone gene was not involved in the cell cycle and that the 3'-end may play a role (Lycan *et al*, 1987). Xu *et al* (1990) created a model of the *HTB1* gene containing 17 amino acids and the 3'-end untranslated region, which was fused to a bacterial neomycin phosphotransferase gene under the GAL1 promoter. Deletion of 66 bases in the 3'UTR and the 17 amino acids of the *HTB1* ORF sequence caused cell-cycle defects of the *neo-HTB1* gene, whereas the wild type *HTB1* sequences participates in cell-cycle regulation on the neomycin fusion

gene (Xu *et al*, 1990). Further research was carried out on the fused *HTB1* gene. Campbell *et al* (2002) discovered a sequence named the distal downstream element (DDE), lying approximately 100nts downstream of the 3'-end cleavage sites, that contributes to cell-cycle regulation of the *neo-HTB1* transcripts (Campbell *et al*, 2002). The DDE mutants, pSAC14 and pSAC21, exhibited an S-phase accumulation, but there was a lack of turnover of the mRNA as cells entered the G_2-phase. Since the DDE sequences do not form part of the mature mRNA, it was postulated that either 3'-end processing and/or transcription termination of the mRNA are influenced by the DDE and that these events contribute to cell-cycle regulation of the *neo-HTB1* mRNA. Campbell *et al* (2002) showed that the DDE was located in the region where transcription termination occurred.

Recently, one of the cleavage factors in *Saccharomyces pombe*, Pfs2 (a member of PFI), was established to contribute to cell-cycle regulation. Wild type, $pfs2^+$, and mutant, *pfs2-11*, were initially nitrogen-starved to arrest the cells in the G_1-phase. After the block and re-feeding of the cells with nitrogen, flow cytometry data showed that the wild type (WT) enters the S-phase within 2 hrs, whereas the *pfs2-11* mutant remains in the G_1-phase (Wang *et al*, 2005).

Interestingly, to date no research has shown if any other 3'-end processing, degradation or export factors play a role in cell-cycle regulation of mRNA levels. Therefore, in this chapter, experiments were carried out to investigate if 3'→5' exonuclease, Rrp6, contributes to endogenous *HTB1* mRNA biogenesis and cell-cycle regulation. Further cell cycles were performed in the *rna14-3/Δrrp6* strains to evaluate the role of 3'-end processing factor in histone mRNA regulation during the cell cycle and to investigate a possible link between termination, 3'-end processing and cell-cycle regulation of histone mRNAs.

4.2 Results

4.2.1 The nuclear exosome contributes to the turnover of *HTB1* mRNA in the G_2-phase of the cell cycle

The component of the nuclear exosome, Rrp6p, acts as a surveillance mechanism to prevent unprocessed mRNAs from being exported from the nucleus. In Chapter 3, the exosome mutant, *Δrrp6*, was found to be accumulate mRNAs from both *neo-HTB1* and endogenous *HTB1* consistent with a role in mRNA degradation. To determine whether the nuclear exosome plays a role in the turnover process during the cell cycle, cell-cycle experiments were performed to examine the accumulation pattern of the endogenous *HTB1* mRNA in the W303 (WT) and *Δrrp6* mutant strains during the cell cycle.

First, a growth curve assessment was carried out to confirm whether the *Δrrp6* mutant strain differed from the W303A strain. The results indicate that both strains have similar growth rates at 30°C. This indicates that the doubling times of the two strains are similar and therefore a similar cell-cycle pattern is expected (*Data not shown*).

The W303 and *Δrrp6* cells were arrested in the G_1-phase with the α_1-mating factor. When the cells were released from cell-cycle arrest, samples were collected every 10 mins. RNA was extracted and Northern blots were hybridised with a DNA probe specific to the coding region of the endogenous *HTB1* and to the *ACT1* sequences, as described in Chapter 2 (Section 2.9, *Table 2.2*). The levels of the RNA at each time point were quantified, as described in Chapter 2 (Sections 2.9.4 and 2.9.5).

From Northern blot and quantification data, the endogenous *HTB1* levels were observed to accumulate in the W303 cells, reaching a peak at 70 mins (*Figure 4.1(A), (B)*). This was followed by decreases in steady state endogenous *HTB1* mRNA transcripts between 80 to 100 mins. The *ACT1* mRNA levels were constant throughout the cell cycle (*Figure 4.1(A)*). The *ACT1* DNA probe has been established to be non-cell-cycle regulated. The experiment was performed four times (*Figure 4.1(B)*, See error bars).

Further quantification work was performed by real-time PCR. Total RNA isolated from the cells was DNase I treated, followed by reverse transcription of the RNA to obtain a cDNA sequence. The cDNA product was amplified by real-time PCR and quantified, as described in Chapter 2 (Sections 2.10.4 and 2.10.5). The C_T values were used to calculate the normalised *HTB1* mRNA levels, as described in Chapter 2 (Section 2.10.5). In addition to the C_T value calculations, the melting temperature was calculated by the real-time program, Rotor-Gene 6 (Chapter 2, Section 2.10.5). The melt curves determined the melting point (T_m) of the amplified product; they provide an indication of potential contamination of the cDNA in the PCR reaction. The melting point for the amplified endogenous *HTB1* sequences in the W303 strain was 83°C, whereas the lower peak represented the negative control, T_m of 80.3°C (*Figure 4.1(C)*). The T_m of the negative control is much lower than the actual product of interest and only detects primer-dimers. The *ACT1* DNA amplified from W303 had a melting temperature of 85°C and the negative control was at 76.5°C (*Figure 4.1(D)*). The amplification plot showed the accumulation of the amplified PCR product over the number of PCR cycles. The red line represents the threshold value from which the C_T values were obtained. The data for the endogenous *HTB1* and *ACT1* mRNA levels were compiled and viewed using the real-time program Rotor-Gene 6, as described in Chapter 2 (Section 2.10.5). Finally, the relative endogenous *HTB1* mRNA levels were calculated and plotted on graphs, as described in Chapter 2 (Section 2.10.5). Endogenous *HTB1* mRNA levels from W303 cells peaked at 70 mins (*Figure 4.1(E)*). This was followed by a rapid decrease of mRNA transcripts between 80-90 mins. The semi-quantification data by densitometry of the Northern blots is confirmed by the real-time data. Real time PCR was conducted four times in the W303 background. RNA samples were extracted from *Δrrp6* cells following the release from the α_1-mating factor. Northern blots were hybridised with an endogenous *HTB1* probe. The RNA was observed to accumulate up to 70 mins in the WT strain. However, unlike the WT strain, the

endogenous *HTB1* transcripts continued to accumulate up to 50 to 60 mins with no apparent decrease in the mRNA levels for the mutant strain (*Figure 4.1(B)* compared to *Figure 4.2(A), (B)*).

To confirm this data, real-time RT-PCR was performed on the RNA samples from the *Δrrp6* cells. The T_m from the melt curve demonstrated that amplified endogenous *HTB1* DNA from *Δrrp6* was 84°C and the primer-dimers were detected in the negative control at 80°C (*Figure 4.2(C)*). The T_m for the *ACT1* in the *Δrrp6* strain was the same as observed for the *ACT1* in the W303 strain (*Figure 4.1(C)* compared to *Figure 4.2(C)*). From the amplification plots, the C_T values were calculated and the *Δrrp6* mRNA levels were then plotted on a graph, as described in Chapter 2, Section 2.10.5 (*Figure 4.2(E)*). The results confirmed that the endogenous *HTB1* mRNA levels accumulated with no apparent decrease in mRNA levels in the mutant strain, *Δrrp6* (*Figure 4.2(E)*). Again, as observed with the Northern blots, the endogenous *HTB1* accumulates up to 50 to 60 mins, followed by a small amount of decrease in mRNA in comparison to the wild type strain. The experiment was conducted six times for the mutant *Δrrp6*.

The relative levels of endogenous *HTB1*, as determined from quantification of the Northern blots and by real-time PCR, were compiled and the results are shown in Figure 4.3. The error bars demonstrate a general agreement between the two methods. The final analysis showed that the endogenous *HTB1* mRNA gradually accumulates, reaching a peak representing the S-phase at 70 mins (*Figure 4.3*). This was followed by a rapid decrease in mRNA from 80 mins onwards. The exosome mutant accumulates the endogenous *HTB1* up to 50-60 mins; however, the decrease of the mRNA afterwards is much diminished (*Figure 4.3*). *HTB1* mRNAs appear to accumulate at a similar level in the WT and mutants strains (Ratio for *HTB1*, 30 mins: 60 mins = 2.2 in the WT strain. Ratio for *HTB1*, 30 mins: 60 mins = 1.9 in the mutant strain). However, there is a reduced level of *HTB1* mRNA as cells enter the G_2-phase in the mutant strain, *Δrrp6* (Ratio for *HTB1*, 70 mins:

120 mins = 3.5 in the WT strain. Ratio for *HTB1*, 70 mins: 120 mins = 1.3 in the mutant strain). This demonstrates that mutation in the exosome has a major impact on progression in the cell-cycle accumulation pattern of *HTB1* mRNA and suggests that the nuclear exosome contributes to the turnover of endogenous *HTB1* mRNA in the G_2-phase of the cell cycle.

Figure 4.1: Cell-cycle regulation of the endogenous *HTB1* transcripts in the W303A strain.

The cells were synchronised to the G_1-phase of the cell cycle by the supplementation of the α_1-mating factor in YEPD medium. Samples were collected every 10 mins after the α_1-factor arrest was released. Total RNA, 30µg, was prepared for Northern blot analysis and 1µg of RNA was prepared for real-time analysis. **(A)** The mRNA levels were probed with the endogenous *HTB1* and *ACT1* probes. **(B)** The mRNA levels were quantified and scanned by densitometry. The endogenous *HTB1* levels were normalised using the levels of the *ACT1* mRNA and plotted on a graph. **(C)** The melt curve. Each melt curve is plotted versus the temperature (on top left). The arrow shown is the negative control. The amplification plot (on top right) is the fluorescence signal of each PCR reaction versus the cycle number. The W303A endogenous *HTB1* mRNA samples from 0 to 120 mins and negative control symbols are shown below. **(D)** The melt curve. Each melt curve is plotted versus the temperature (on top left). The arrow shown is the negative control. The amplification plot (on top right) is the fluorescence signal of each PCR reaction versus the cycle number. The W303A *ACT1* mRNA samples from 0 to 120 mins and negative control symbols are shown below. **(E)** The Northern blot and real-time data were compiled together for the relative endogenous *HTB1* mRNA levels from the W303A background.

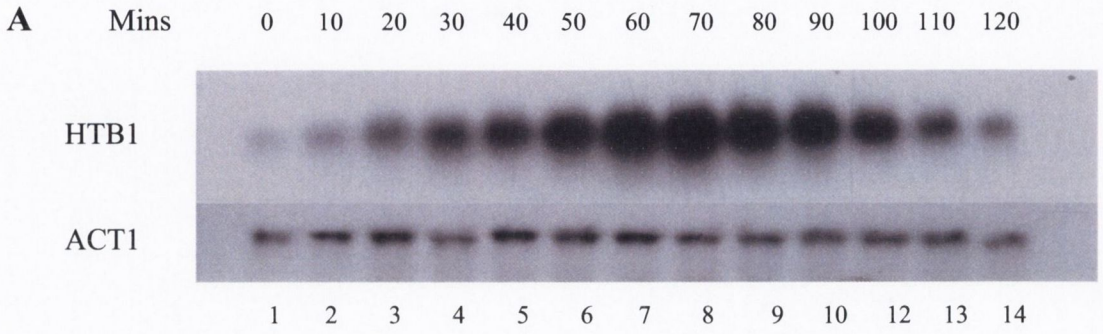
A
Mins
0 10 20 30 40 50 60 70 80 90 100 110 120
HTB1
ACT1
1 2 3 4 5 6 7 8 9 10 12 13 14

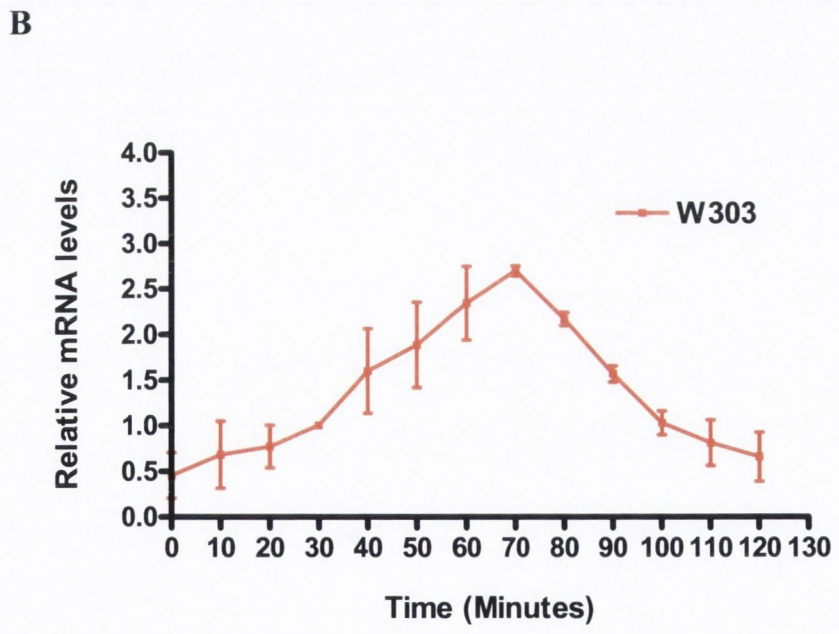
B
Relative mRNA levels
4.0
3.5
3.0
2.5
2.0
1.5
1.0
0.5
0.0
W303
0 10 20 30 40 50 60 70 80 90 100 110 120 130
Time (Minutes)

C. Endogenous HTB1 W303 transcripts

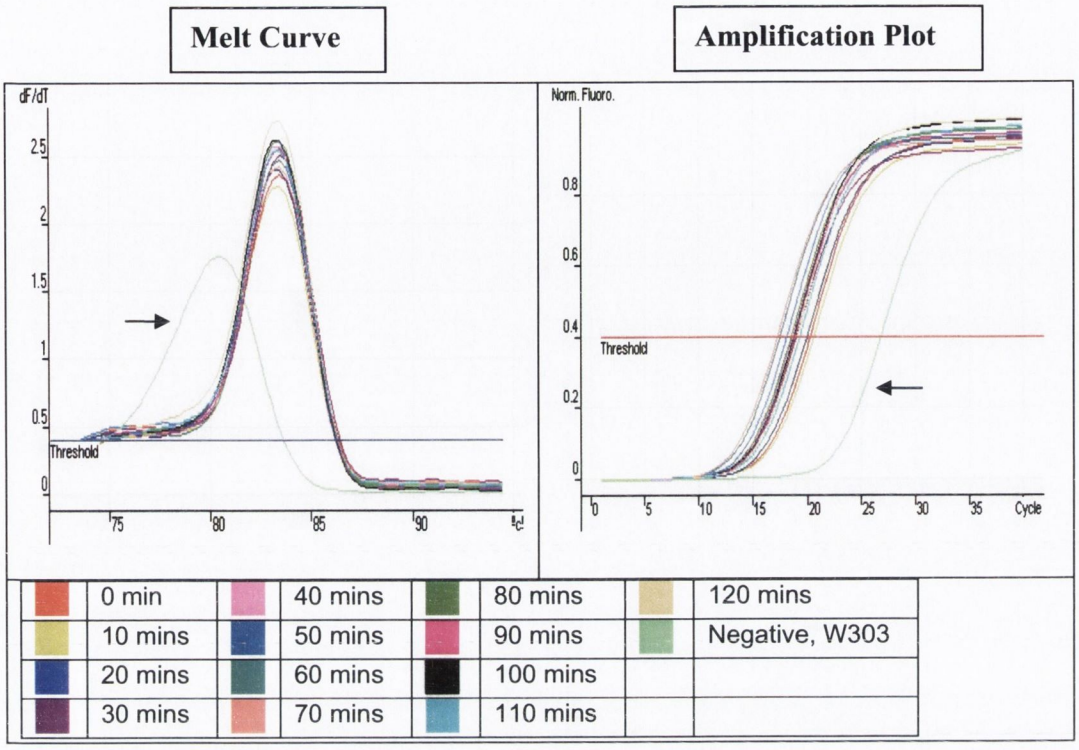

D. ACT1 W303 transcripts

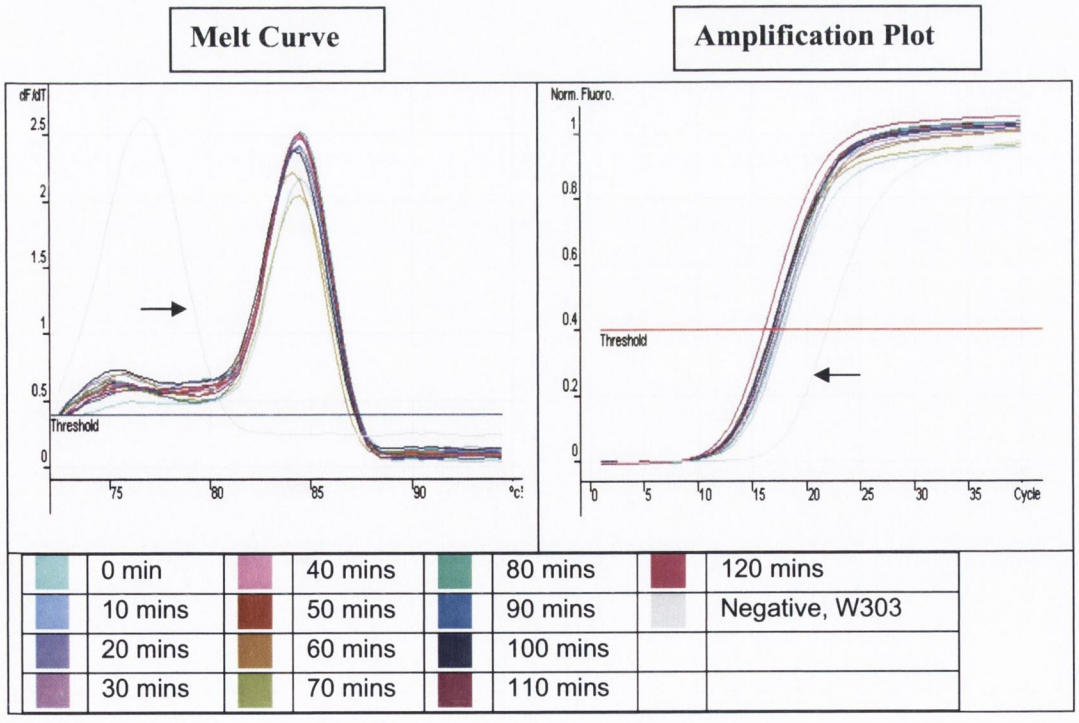

E

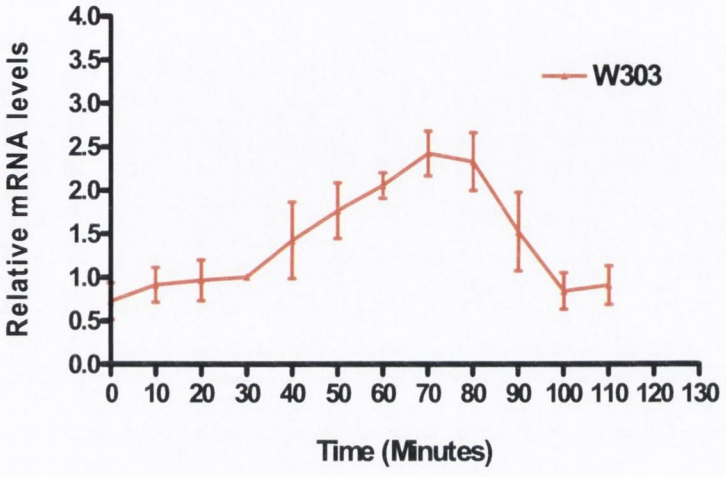
Relative mRNA levels
4.0
3.5
3.0
2.5
2.0
1.5
1.0
0.5
0.0
W303
0 10 20 30 40 50 60 70 80 90 100 110 120 130
Time (Minutes)

Figure 4.2: Cell-cycle regulation of the endogenous *HTB1* transcripts in the *Δrrp6* strain. The cells were synchronised to the G_1-phase of the cell cycle by the supplementation of the α_1-mating factor in YEPD medium. Samples were collected every 10 mins after the α_1-factor arrest was released. Total RNA, 30μg, was prepared for Northern blot analysis and 1μg of RNA was prepared for real-time analysis. **(A)** The mRNA levels were probed with the endogenous *HTB1* and *ACT1* probes. **(B)** The mRNA levels were quantified and scanned by densitometry. The endogenous *HTB1* levels were normalised using the levels of the *ACT1* mRNA and plotted on a graph. **(C)** The melt curve. Each melt curve is plotted versus the temperature (on top left). The arrow shown is the negative control. The amplification plot (on top right) is the fluorescence signal of each PCR reaction versus the cycle number. The *Δrrp6* endogenous *HTB1* mRNA samples from 0 to 120 mins and negative control symbols are shown below. **(D)** The melt curve. Each melt curve is plotted versus the temperature (on top left). The arrow shown is the negative control. The amplification plot (on top right) is the fluorescence signal of each PCR reaction versus the cycle number. The *Δrrp6 ACT1* mRNA samples from 0 to 120 mins and negative control symbols are shown below. **(E)** The Northern blot and real-time data were compiled together for the relative endogenous *HTB1* mRNA levels from the *Δrrp6* background.

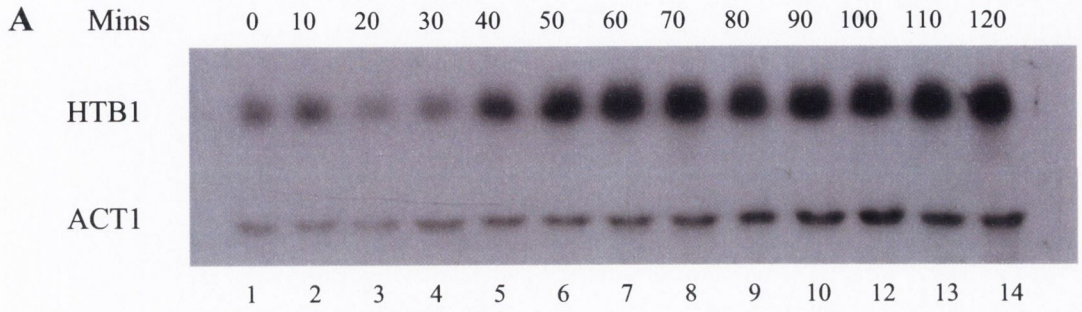
A
Mins
0 10 20 30 40 50 60 70 80 90 100 110 120
HTB1
ACT1
1 2 3 4 5 6 7 8 9 10 12 13 14

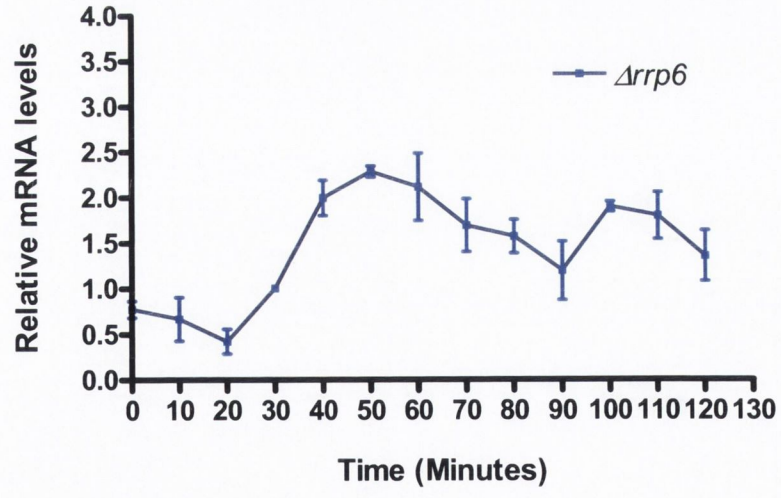
B
Relative mRNA levels
4.0
3.5
3.0
2.5
2.0
1.5
1.0
0.5
0.0
Δrrp6
0 10 20 30 40 50 60 70 80 90 100 110 120 130
Time (Minutes)

C. Endogenous HTB1 *Δrrp6* transcripts

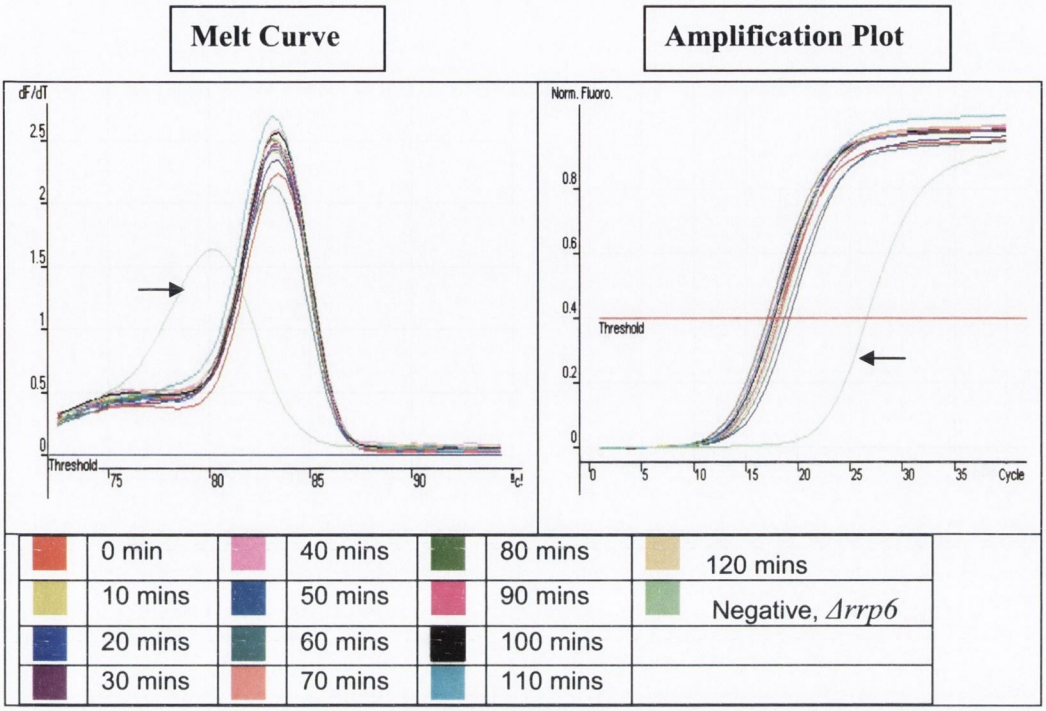

D. ACT1 *Δrrp6* transcripts

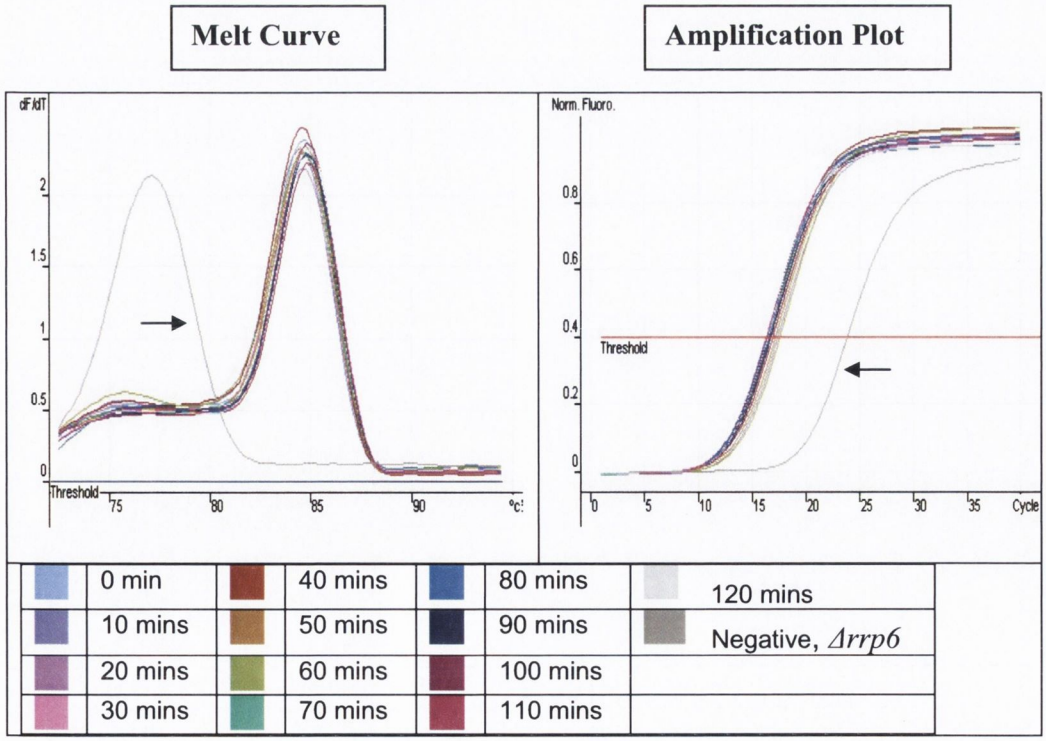

E

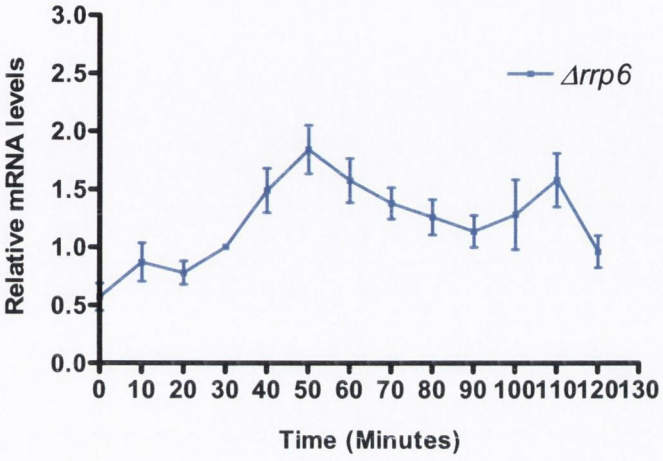
3.0
2.5
2.0
1.5
1.0
0.5
0.0
Relative mRNA levels
Δrrp6
0 10 20 30 40 50 60 70 80 90 100110120130
Time (Minutes)

Figure 4.3: Cell-cycle regulation of the endogenous *HTB1* transcripts in the W303A and *Δrrp6* strains. The data were collected and evaluated for the Northern blots and real-time PCRs. The endogenous *HTB1* mRNA levels were normalised and the errors bars are shown.

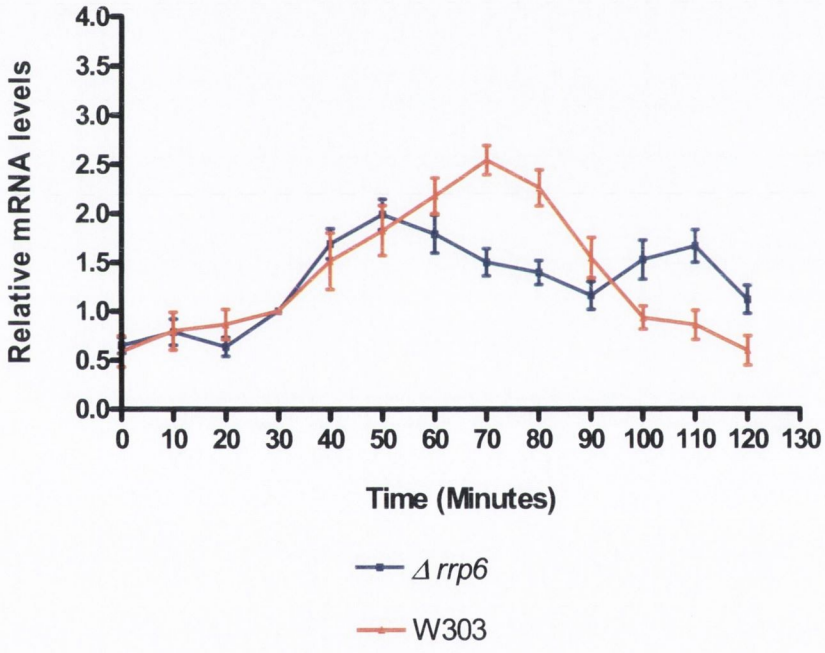

4.3 Characterisation of the role of the nuclear exosome in the regulation of *HTB1* mRNAs during the cell cycle

In Section 4.2.1 above, Northern blot and real-time PCR indicated that the nuclear exosome contributes to the turnover of the endogenous *HTB1* mRNA in the G_2-phase of the cell cycle. This posed the question as to whether the potential role of the exosome in *HTB1* mRNA turnover is related to its known role in degrading unprocessed and/or unterminated transcripts. It is possible that 3'-end processing of histone mRNAs is differentially regulated during the cell cycle, leading to an accumulation of unprocessed transcripts in the G_2-phase, which would be substrates for the nuclear exosome. Alternatively, the nuclear exosome may play a role in degrading *HTB1* mRNAs independently of its role in 3'-end processing. The alternative hypotheses were tested by examining the endogenous *HTB1* mRNA levels during the cell cycle in the *rna14-3/Δrrp6* mutant and the accumulation of read-through transcripts during the cell cycle was examined by RT-PCR (Chapter 2, Section 2.10.2).

4.3.1 *rna14-3/Δrrp6* mutant strains display 3'-end processing and termination defects in *HTB1* biogenesis

Firstly, experimental conditions were established to allow detection of read-through uncleaved transcripts of the endogenous *HTB1* mRNA in the *rna14-3/Δrrp6* background. RNA was isolated at 22°C and 37°C, extracted and purified, as described in Chapter 2 (Sections 2.10.2 and 2.10.3). A series of reverse primers were designed to complement the region immediately upstream and downstream of the 3'-end of the endogenous *HTB1* gene and a forward primer was anchored in the coding region of the *HTB1* gene (*Table 2.2*; *Figure 4.4*). RT-PCR was performed, as described in Chapter 2 (Sections 2.9.1 and 2.10.1), to detect the termination sites of the endogenous *HTB1* transcripts in the *rna14-3/Δrrp6* background.

At 22°C in the *rna14-3/Δrrp6* background, strong bands of 146nt, 230nt and a faint band of 303nt long were observed, suggesting that the majority of the transcripts terminate in the region where the DDE lies (*Figure 4.4*, 22°C, See stars, Lanes 1, 2 and 3). Bands of the expected sizes were not observed in the other lanes (*Figure 4.5*, 22°C, Lanes 4-6). At 37°C, RT-PCR products of the expected sizes of 146nt, 230nt, 303nt, 458nt, 553nt and 646nt were observed in the *rna14-3/Δrrp6* background (*Figure 4.4*, 37°C, Lanes 1-6). This indicates that 3'-end processing and transcription termination is impaired at this temperature, leading to the accumulation of read-through transcripts. Some artefacts which were not the correct sizes were observed (*Figure 4.5*, 37°C, Lanes 1, 3 and 4).

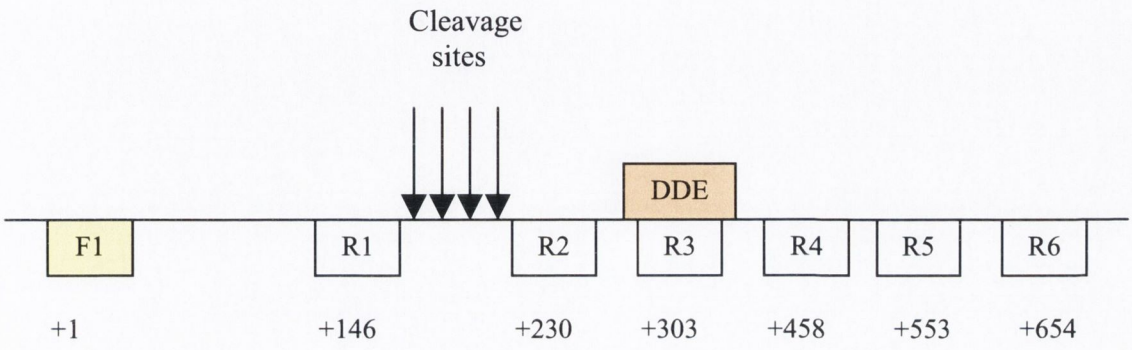

Figure 4.4: A systematic representation illustrating the primers used in RT-PCR to detect the endogenous *HTB1* sequences. The yellow box indicates the forward primer [HTB1For1 (F1)] and the clear boxes indicate the reverse primers [HTB1Rev1 (R1), HTB1Rev2 (R2), HTB1Rev3 (R3), HTB1Rev4 (R4), HTB1Rev5 (R5) and HTB1Rev6 (R6)]. The numbers below indicate the expected sizes of the RT-PCR products relative to the forward primer (F1). The locations of the primers in the endogenous *HTB1* sequence are indicated in Table 2.2. The orange box is the DDE and the arrows represent the cleavage sites.

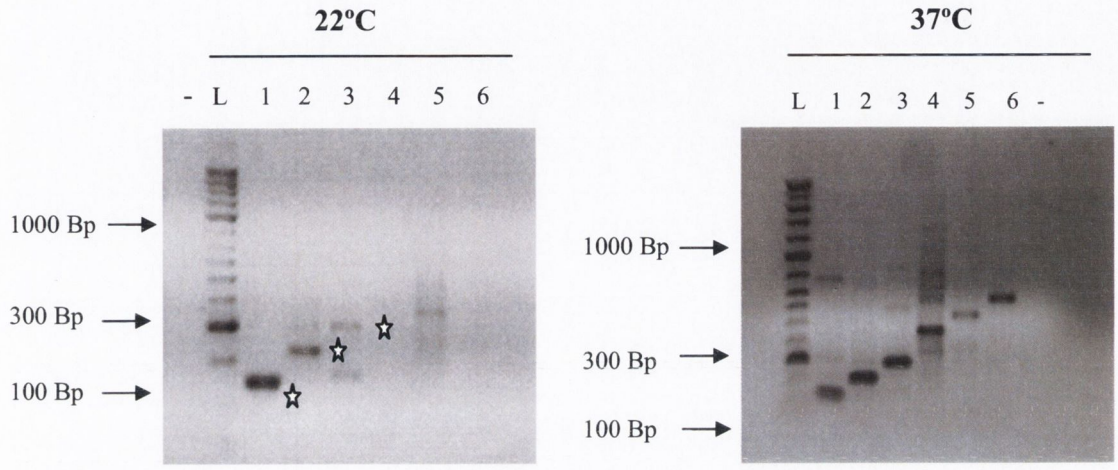

Figure 4.5: Analysis of *HTB1* transcripts in the *rna14-3/Δrrp6* strain at 22°C and 37°C.

RNA, 2µg, was extracted from *rna14-3/Δrrp6* strains, following incubation at 22°C or 37°C for 1 hr. The RNA was reverse-transcribed using the reverse primers shown in Figure 4.5 and PCR-amplified using the same reverse primers and the forward primer (F1). The PCR products were electrophoresed on a 1% agarose 1x TBE gel. Lane 1 (R1), R2 (Lane 2), R3 (Lane 3), R4 (Lane 4), R5 (Lane 5), R6 (Lane 6), (-) denotes the negative control. L denotes molecular weight ladder and the sizes of some of the bands are shown on the right-hand side of the gel.

4.3.2 Endogenous *HTB1* transcripts in the *rna14-3/Δrrp6* background are not cell-cycle regulated

Subsequent cell-cycle experiments were carried out using the *rna14-3/Δrrp6* mutant strains. Due to the temperature-sensitive phenotype of the *rna14-3* mutation, experiments were conducted in two ways to optimise the results and gain further information.

Firstly, yeast strains, W303 and *rna14-3/Δrrp6*, were grown in YEPD medium at 22°C. Cells were synchronised at the G_1-border of the cell cycle overnight by using the α_1-mating factor, as described in Chapter 2 (Section 2.7). Following alpha factor removal, the cells were incubated at 22°C or 37°C, and samples were collected every hr. The membranes were probed with the endogenous *HTB1* and *ACT1* sequences (*Table 2.2*).

Endogenous *HTB1* mRNA transcript levels for the W303 cells increased and accumulated up to 2 hrs, followed by a decrease from 3 hrs onwards at the permissive temperature (*Figure 4.6*, 22°C, Lanes 1-9). Levels of endogenous *HTB1* transcripts for the *rna14-3/Δrrp6* mutant strain demonstrated no significant decreases over 8 hrs (*Figure 4.6*, 22°C, Lanes 10-18). It should be noted that total RNA was overloaded in Lane 10 in the *rna14-3/Δrrp6* background (*Figure 4.6*, 22°C, rRNA, Lane 10). These results confirm previous findings that endogenous *HTB1* mRNAs continue to accumulate in the *Δrrp6* background.

To examine the role of RNA14 in the pattern of cell-cycle accumulation of endogenous *HTB1* mRNAs, cells were incubated continuously at 37°C to inactivate RNA14. At the non-permissive temperature, endogenous *HTB1* mRNA levels were lower compared to the levels at the permissive temperature with the W303 strain (*Figure 4.6*, 22°C, Lanes 1-9 compared to 37°C, Lanes 1-9). Despite this, accumulation of the endogenous *HTB1* mRNA was observed up to 1 to 2 hrs, followed by a decrease of the endogenous *HTB1* mRNA after 2 hrs. The *ACT1* mRNA levels were low in both W303 and *rna14-3/Δrrp6* strains, which is likely due to increased turnover or decreased transcription at 37°C. In the

rna14-3/Δrrp6 background, the endogenous *HTB1* mRNA levels were extremely low and unprocessed transcripts were apparent throughout the cell cycle (*Figure 4.6*, 37°C, smeared RNA, See arrows, Lanes 10-18). There was no continuous accumulation of the *HTB1* mRNA similar to the accumulation observed at 22°C in the *rna14-3/Δrrp6* background. However, some stable mature transcripts were apparent in the *rna14-3/Δrrp6* background at 37°C (*Figure 4.6*, 37°C, See arrows on right-hand side, Lanes 3, 6 and 7).

Figure 4.6: Northern blot of the endogenous *HTB1* transcripts of the W303A and *rna14-3/Δrrp6* strains at the permissive and non-permissive temperatures. The cells W303A and *rna14-3/Δrrp6* were synchronised to the G_1-phase of the cell cycle by the addition of the α_1-mating factor. **(22°C)** The samples were collected from 22°C every hr after the α_1-factor arrest was released. **(37°C)** Cells were incubated at 37°C and samples were collected every hr. Total RNA, 60µg, from each time point was loaded onto a formaldehyde gel. The RNA was transferred to nylon membranes and was probed with the endogenous *HTB1* and *ACT1* sequences. The 0 hr time point is immediately after the alpha factor removal.

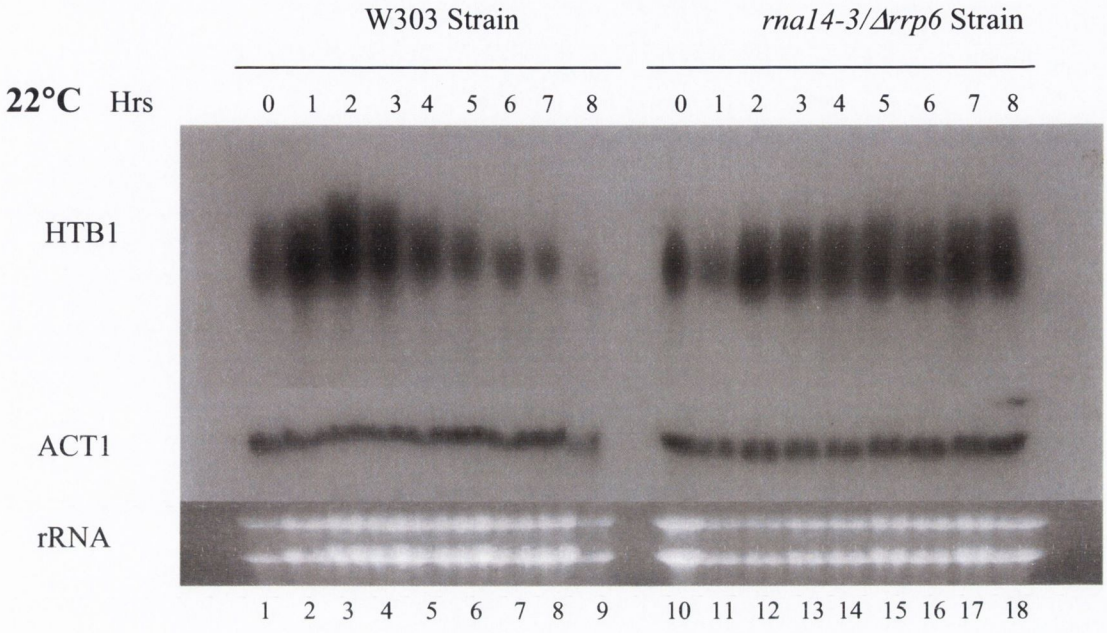
W303 Strain
rna14-3/Δrrp6 Strain
22°C Hrs
0 1 2 3 4 5 6 7 8
0 1 2 3 4 5 6 7 8
HTB1
ACT1
rRNA
1 2 3 4 5 6 7 8 9
10 11 12 13 14 15 16 17 18

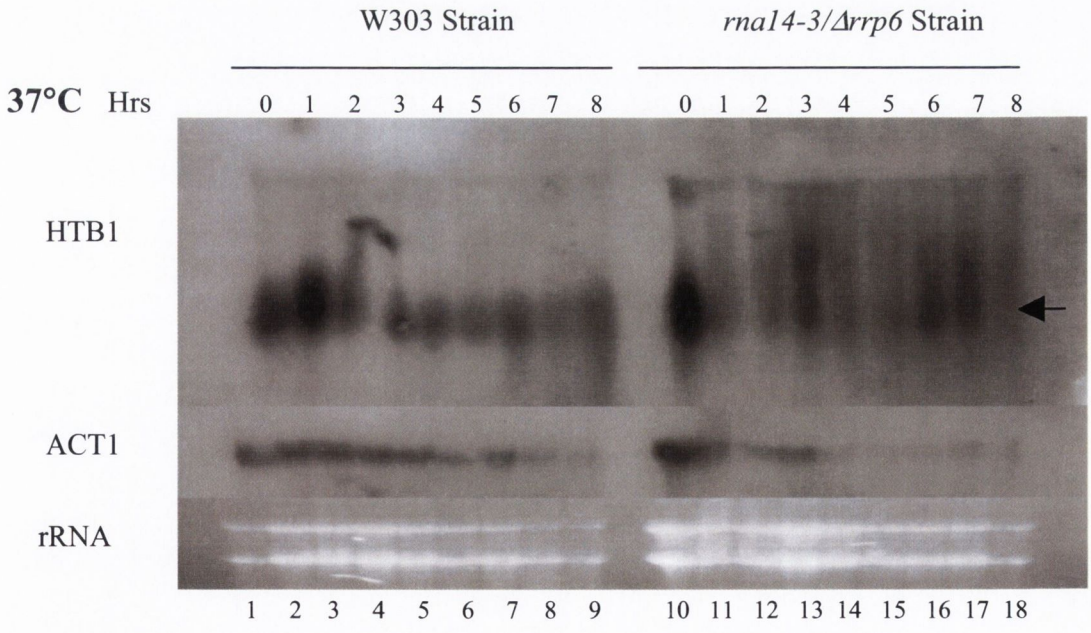
W303 Strain
rna14-3/Δrrp6 Strain
37°C Hrs
0 1 2 3 4 5 6 7 8
0 1 2 3 4 5 6 7 8
HTB1
ACT1
rRNA
1 2 3 4 5 6 7 8 9
10 11 12 13 14 15 16 17 18

4.3.2.1 Termination occurs downstream of the endogenous HTB1 sequences in the rna14-3/Δrrp6 mutant strain

The results obtained in Section 4.3.2 above indicate that the levels of mature *HTB1* mRNAs were severely reduced at the non-permissive temperature in the *rna14-3/Δrrp6* strain and cell-cycle accumulation was disrupted. Mature *HTB1* mRNA transcripts were apparent throughout the cell cycle, although the levels were greatly reduced. These transcripts most likely represent read-through unprocessed pre-mRNAs that have been chased into mature transcripts, as was previously observed in Chapter 3 (*Figure 3.3*). To determine if there is any differential 3'-end processing of these transcripts during the cell cycle, RT-PCR was carried out using the forward and reverse primers described in Figure 4.5 and as described in Chapter 2 (Sections 2.10.2 and 2.10.3). The RNA samples were taken from 2 hrs and 6 hrs from the cells used in the Northern blots in Figure 4.7. These time points represent the S-phase and the late G_2-phase of the cell cycle as determined by the levels of *HTB1* mRNAs in the WT, W303, cells.

The majority of the transcripts correspond to correctly cleaved mature mRNA (R1, 146nt and R2, 231nt), were detected in the 2 hr sample in the W303 background at 22°C (*Figure 4.7(A)*, see arrows, Lanes 3 and 4). The first transcript of the endogenous *HTB1*, 146nt, was detected in the 6 hr sample at 22°C (*Figure 4.7(A)*, See arrows, Lane 9). Only non-specific RT-PCR products were observed with the primers R3 and R5 (*Figure 4.7(A)*, Lanes 5, 6, 11 and 12). The lack of the R2 product (231nt) in the 6 hr sample most likely reflects the reduced levels of *HTB1* mRNA at this time point. At 37°C, the first endogenous *HTB1* transcript of 146nt was detected in both the 2 hr and the 6 hr samples (*Figure 4.7(B)*, Lanes 3 and 9). There was no specific read-through products detected by RT-PCR in the W303 background, although some non-specific products were apparent. These results indicate that endogenous *HTB1* mRNAs are correctly processed at all stages of the cell cycle in the W303 background.

At the permissive temperature in the *rna14-3/Δrrp6* background, the first two endogenous *HTB1* transcripts (146nt and 230nt) were observed in the 2 hr sample and no additional specific longer transcripts were apparent (*Figure 4.7(C)*, see arrows, Lanes 3 and 4). In the 6 hr sample, only the 146nt product was amplified, although there may be a small amount of the 230nt product (*Figure 4.7(C)*, see arrows, Lanes 9 and 10). In the other lanes, non-specific bands were observed (*Figure 4.7(C)*, Lanes 10, 11 and 12). At 37°C in the *rna14-3/Δrrp6* background, transcripts of 146nt, 230nt and 303nt were detected in the 2 hr and the 6 hr samples (*Figure 4.7(D)*, See arrows, Lanes 3, 4, 5, 9, 10 and 11). The 553nt long transcript was detected weakly in 2hr and 6 hrs, indicating that 3'-end processing and transcription had been inhibited under these conditions (*Figure 4.7(D)*, see arrows, Lanes 6 and 12). It is most likely that the longer transcript represents the small pool of terminated, but unprocessed, pre-mRNAs in the cell.

Figure 4.7: Detection of unprocessed transcripts in the W303A and *rna14-3/Δrrp6* strains at the permissive and non-permissive temperatures. RNA, 2µg, was reverse-transcribed and amplified. The PCR products were amplified using the forward primer, F1 (HTB1For1) and reverse primers R1 (HTB1Rev1), R2 (HTB1Rev2), R3 (HTB1Rev3) and R5 (HTB1Rev5). **(A)** and **(B)** amplification of RNA from 2 hr and 6 hr time points from the W303A background at 22°C and 37°C respectively. **(C)** and **(D)** amplification of RNA from the 2 hr and 6 hr time points from the *rna14-3/Δrrp6* background at 22°C and 37°C respectively. The L symbol denotes the ladder and the – sign denotes the negative control.

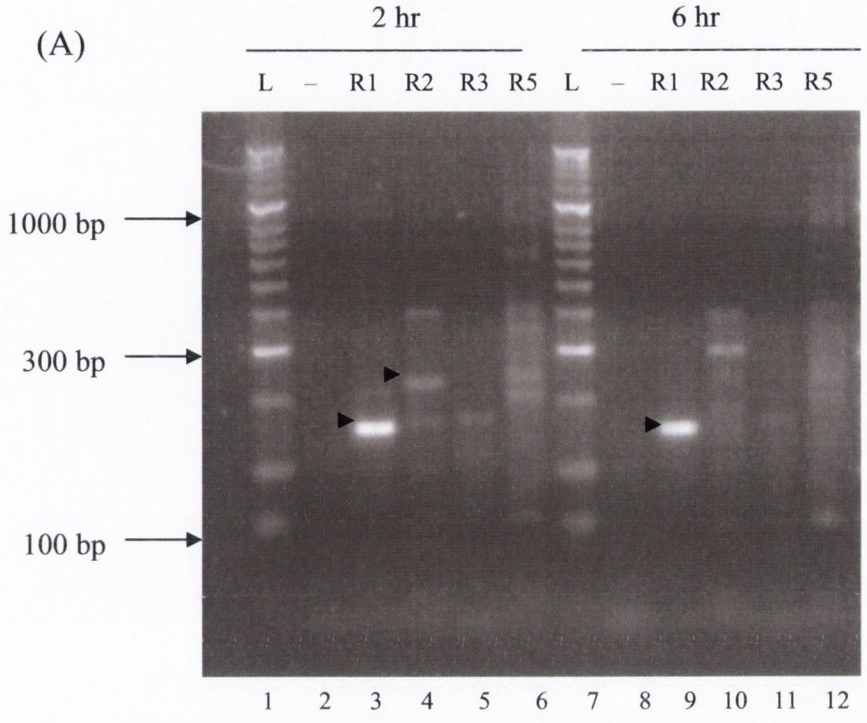
(A)
2 hr
6 hr
L – R1 R2 R3 R5 L – R1 R2 R3 R5
1000 bp
300 bp
100 bp
1 2 3 4 5 6 7 8 9 10 11 12

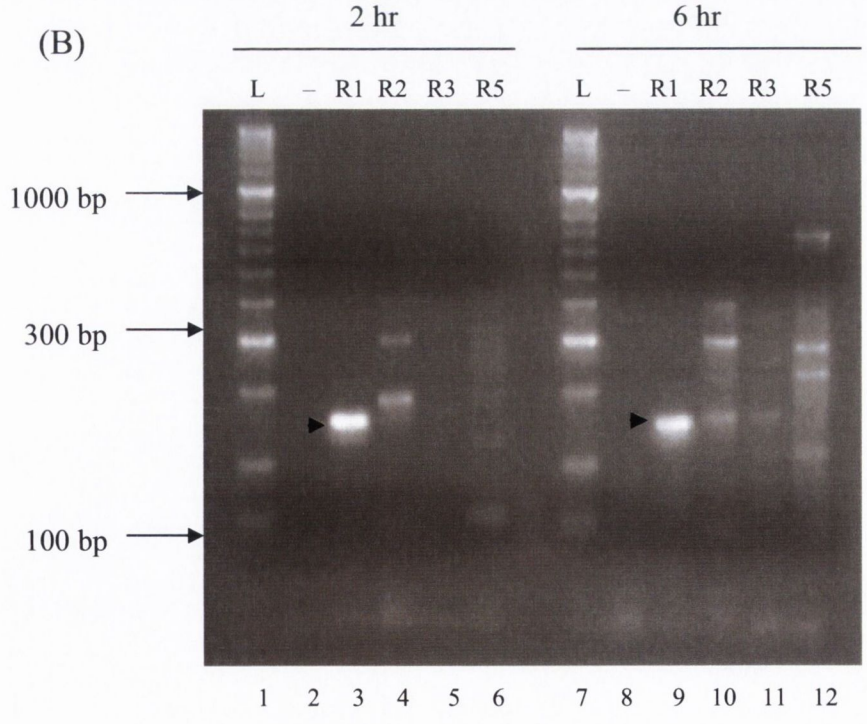
(B)
2 hr
6 hr
L – R1 R2 R3 R5 L – R1 R2 R3 R5
1000 bp
300 bp
100 bp
1 2 3 4 5 6 7 8 9 10 11 12

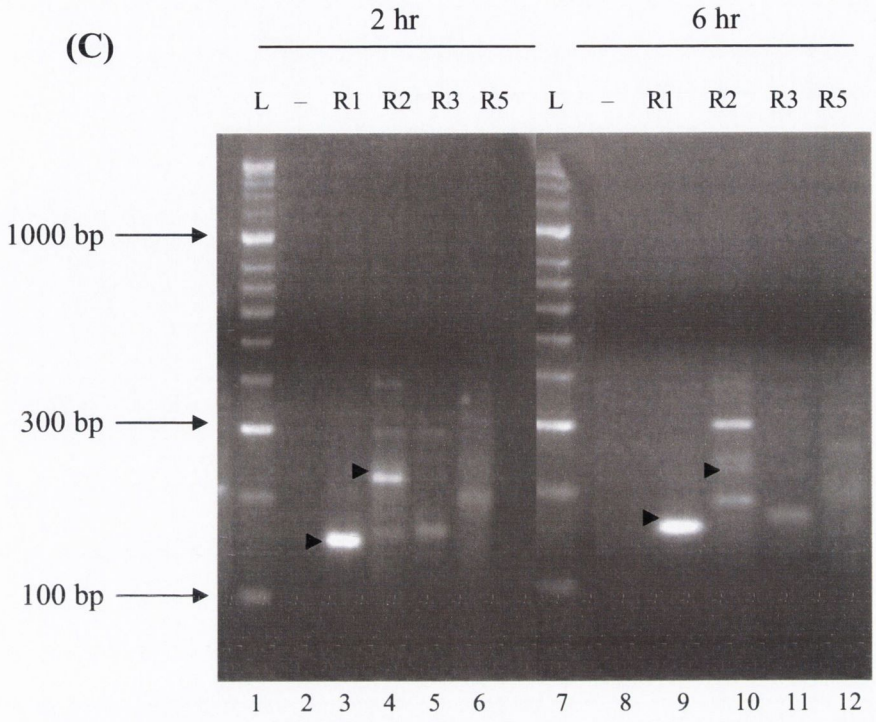
(C)
2 hr
6 hr
L – R1 R2 R3 R5 L – R1 R2 R3 R5
1000 bp
300 bp
100 bp
1 2 3 4 5 6 7 8 9 10 11 12

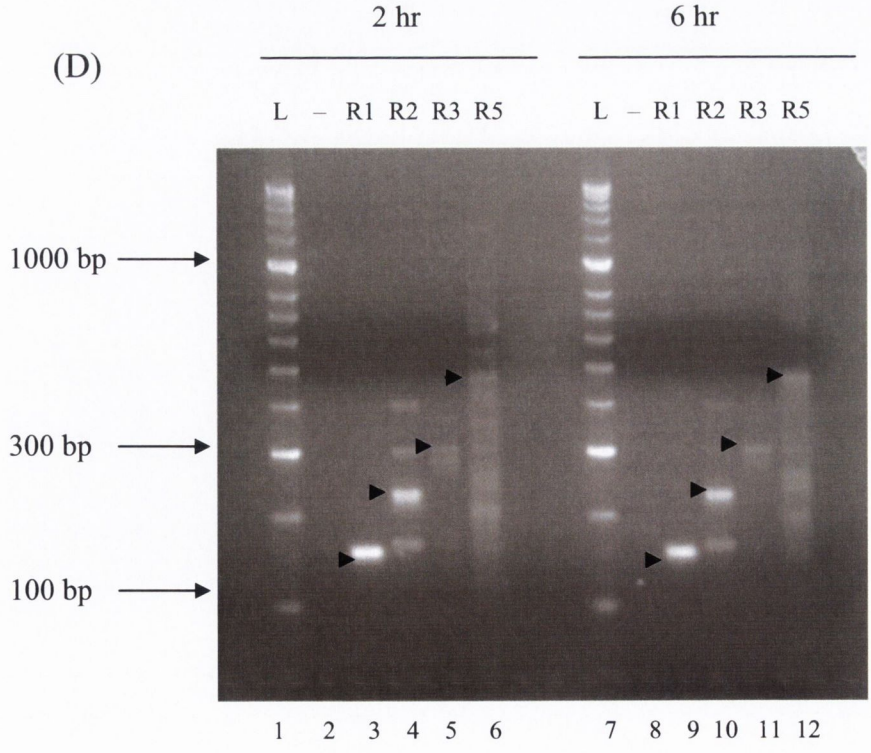
(D)
2 hr
6 hr
L – R1 R2 R3 R5 L – R1 R2 R3 R5
1000 bp
300 bp
100 bp
1 2 3 4 5 6 7 8 9 10 11 12

4.3.3 Endogenous *HTB1* mRNA transcripts gradually turnover in the G_2-phase in the *rna14-3/Δrrp6* cells

The previous cell-cycle experiments were carried out by maintaining the cells at 37°C to ensure that Rna14p remained inactive throughout the cell cycle. These conditions greatly reduced the amount of endogenous *HTB1* mRNAs in the cell. The experiments were repeated under different conditions, in which Rna14p was inactivated for only 1 hr following removal of the alpha factor. The W303 and *rna14-3/Δrrp6* strains were grown in YEPD medium at 22°C. The cells were synchronised at the G_1-border of the cell cycle overnight by using the α_1-mating factor. Cell pellets were washed and placed in pre-warmed YEPD medium and incubated for 1 hr at 22°C and 37°C. After 1 hr, the cells were washed and placed in 22°C pre-warmed YEPD medium and samples were collected every hr. The membranes were probed with the endogenous *HTB1* and *ACT1* sequences.

The endogenous *HTB1* mRNA transcripts in the W303 background increased and accumulated in the first 2 hrs and subsequently decreased at 22°C, as previously observed (*Figure 4.8*, 22°C, Lanes 1-9). The endogenous *HTB1* transcripts for the *rna14-3/Δrrp6* mutant strain increased and demonstrated no decrease up to 4 hrs (*Figure 4.8*, 22°C, Lanes 10-18). The *ACT1* levels were similar for the *rna14-3/Δrrp6* strain at this temperature (*Figure 4.8*, 22°C, *ACT1*).

At 37°C, the endogenous *HTB1* mRNA levels in the W303 strain demonstrated a similar pattern of the cell cycle at 22°C, but the endogenous *HTB1* mRNA levels were lower (*Figure 4.9*, 37°C, Lanes 1-9 compared to *Figure 4.8*, 22°C, Lanes 1-9). The endogenous *HTB1* mRNA transcripts peaked at 1 hr, followed by a decrease from 2 hrs onwards in the W303 background (*Figure 4.8*, 37°C, Lanes 1-9). However, the *ACT1* and rRNA levels are slightly underloaded in the later time points (*Figure 4.8*, 37°C, Lanes 7-9). The *rna14-3/Δrrp6* mRNA transcripts levels were high following the release of the α_1-factor at 0 hr and slowly decreased over 8 hrs (*Figure 4.8*, 22°C, Lanes 10-18). The *ACT1* mRNA in the

rna14/Δrrp6 background is low at the 7 hr and 8 hr time points (*Figure 4.8*, 37°C, Lanes 17-18). This data suggests that the slow decrease of the endogenous *HTB1* mRNA in the *rna14-3/Δrrp6* background resulted from the disabled Rna14 protein, combined with the deletion of the RRP6 gene, and this phenotype persists for the entire time of the experiment. The slower decrease in the endogenous *HTB1* mRNAs in the *rna14-3/rrp6* cells, compared to the rate in the *Δrrp6* cell alone, suggests that 3'-end processing may contribute to the cell-cycle accumulation patterns of the endogenous *HTB1* transcripts.

Figure 4.8: Northern blot of the endogenous *HTB1* transcripts of the W303A and *rna14-3/Δrrp6* strains at 22°C and 37°C. The cells, W303A and *rna14-3/Δrrp6*, were synchronised to the G_1-phase of the cell cycle by the addition of α_1-mating factor. **(22°C)** After α_1-factor removal, cells were incubated at 22°C for 1 hr and then collected every hr thereafter. **(37°C)** After α_1-factor removal, the cells were incubated at 37°C for 1 hr and then returned at 22°C. Samples were collected every hr thereafter. Total RNA, 60µg, from 22°C and 37°C were probed with the endogenous *HTB1* and *ACT1* sequences. The 0 hr time point is immediately after the alpha factor removal.

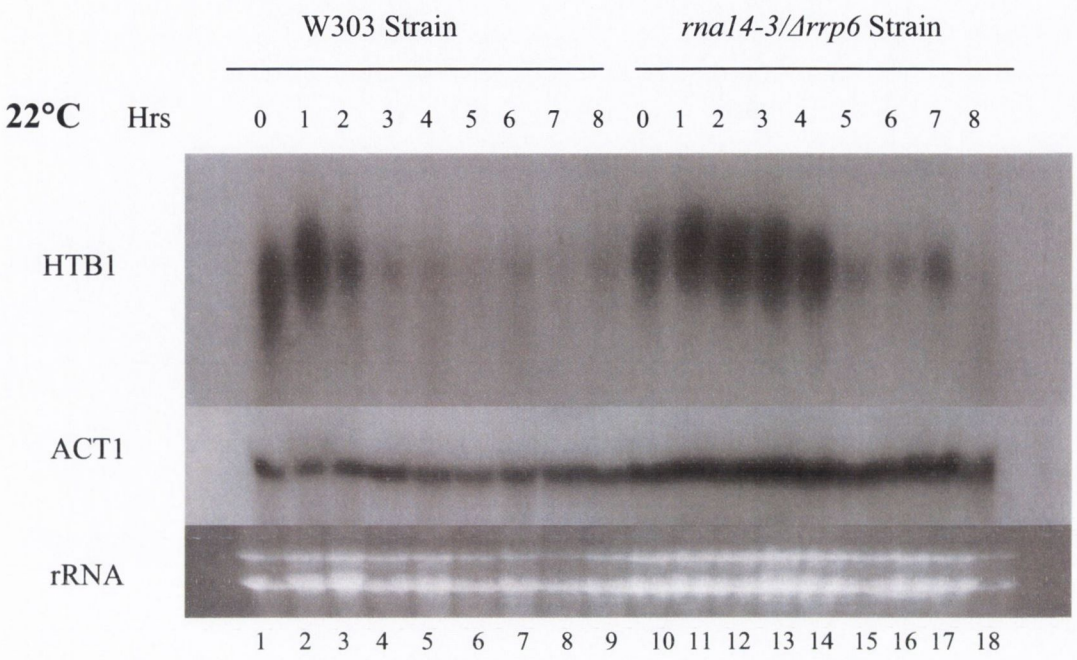
W303 Strain
rna14-3/Δrrp6 Strain
22°C
Hrs
0 1 2 3 4 5 6 7 8 0 1 2 3 4 5 6 7 8
HTB1
ACT1
rRNA
1 2 3 4 5 6 7 8 9 10 11 12 13 14 15 16 17 18

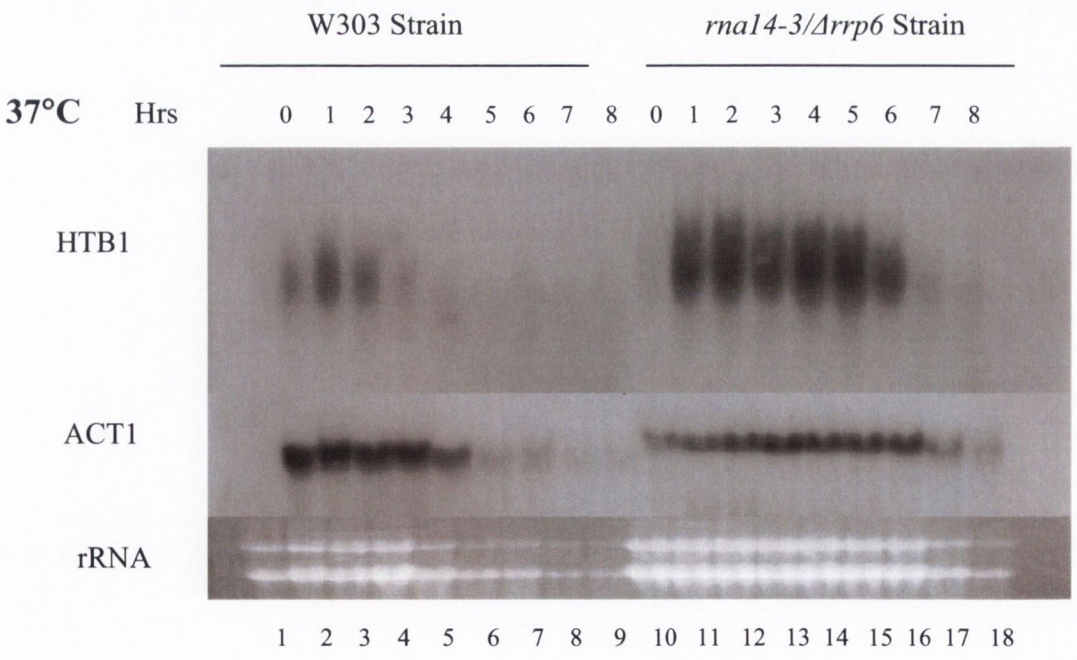
W303 Strain
rna14-3/Δrrp6 Strain
37°C
Hrs
0 1 2 3 4 5 6 7 8 0 1 2 3 4 5 6 7 8
HTB1
ACT1
rRNA
1 2 3 4 5 6 7 8 9 10 11 12 13 14 15 16 17 18

4.3.3.1 Termination defects in the rna14-3/Δrrp6 background during the cell cycle

The RNA samples from the 1 hr and 6 hr time points were reverse-transcribed, as described in Chapter 2 (Section 2.10.2), to detect the read-through transcripts in the W303 and *rna14-3/Δrrp6* backgrounds. The samples were obtained from the Northern blots, as presented in Figure 4.8.

At 22°C in the W303 background, there was a strong band of 146nt long in both the 1 hr and 6 hr samples (*Figure 4.9(A)*, See arrows, Lanes 3 and 9). There was a second endogenous *HTB1* transcript detected at 230nt long in the 1hr sample, although this band was noticeably weaker (*Figure 4.9(A)*, Lane 4). At 37°C, the first two transcripts, 146nt and 230nt, were detected strongly in both samples (*Figure 4.9(B)*, Lanes 3, 4, 9 and 10). This may represent a slight reduced level of 3'-end processing at 37°C. The other bands seen on the gel are artefacts.

In the *rna14-3/Δrrp6* strain, only the first two endogenous *HTB1* transcripts were detected (146nt and 230nt) in both the 1 hr and 6 hr samples at the permissive temperature (*Figure 4.9(C)*, Lanes 3, 4, 9 and 10). Endogenous *HTB1* transcripts of 146nt, 230nt, 303nt and 553nt were strongly detected downstream at 37°C in the 1 hr sample and similarly in the 6 hr sample (*Figure 4.9(D)*, Lanes 3, 4, 5, 6, 7, 8, 9, 10, 11 and 12). No PCR products were evident in Lane 11 due to no RNA being present during RT-PCR (*Figure 4.9(D)*, Lane 11). This data shows that 3'-end processing and transcription termination were inhibited under these conditions.

Figure 4.9: Detection of read-through endogenous *HTB1* transcripts during the cell cycle in W303A and *rna14-3/Δrrp6* strains. RNA, 2µg, from 1 hr and 6 hr time points were reverse-transcribed and amplified. The PCR products were amplified using the forward primer, F1 (HTB1For1) and reverse primers R1 (HTB1Rev1), R2 (HTB1Rev2), R3 (HTB1Rev3) and R5 (HTB1Rev5). **(A)** and **(B)** amplification of RNA from the 1 hr and 6 hr samples from the W303A background from cells incubated at 22°C and 37°C for 1 hr after the alpha factor removal. **(C)** and **(D)** amplification of RNA from the 1 hr and 6 hr samples from the *rna14-3/Δrrp6* background from cells incubated at 22°C and 37°C after the alpha factor removal.

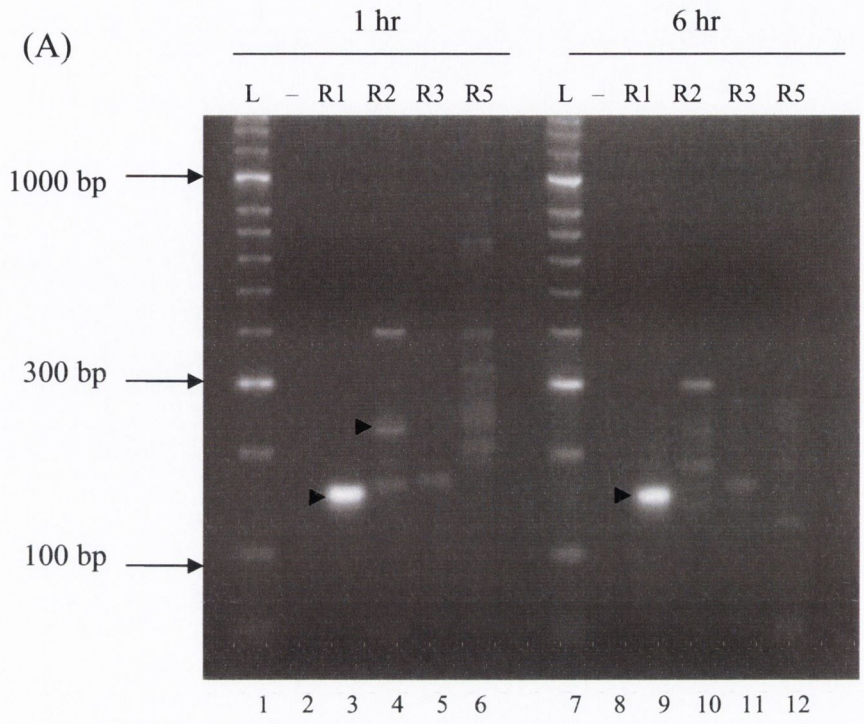
(A)
1 hr
6 hr
L – R1 R2 R3 R5
L – R1 R2 R3 R5
1000 bp
300 bp
100 bp
1 2 3 4 5 6 7 8 9 10 11 12

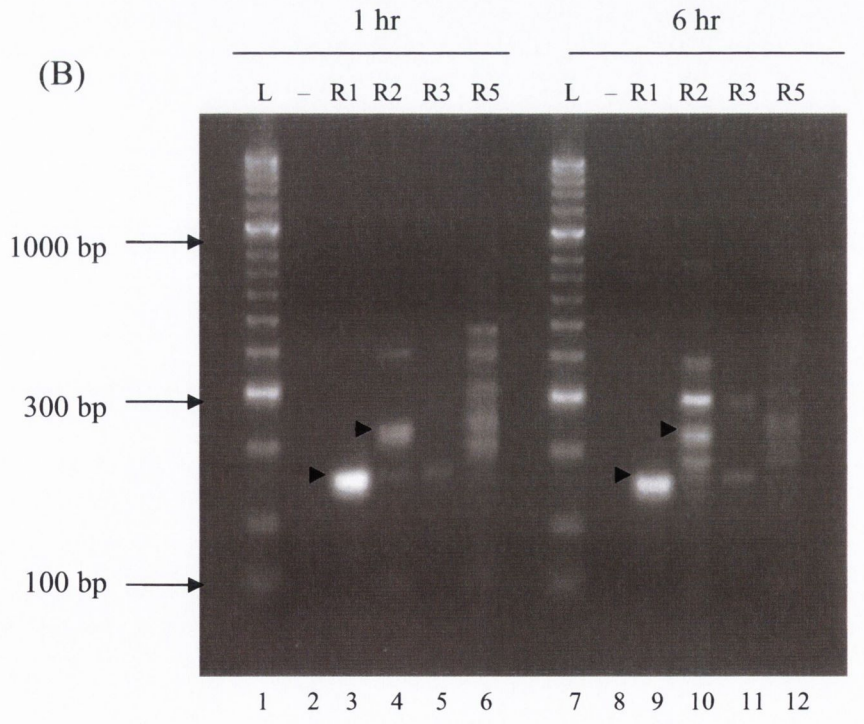
(B)
1 hr
6 hr
L – R1 R2 R3 R5
L – R1 R2 R3 R5
1000 bp
300 bp
100 bp
1 2 3 4 5 6 7 8 9 10 11 12

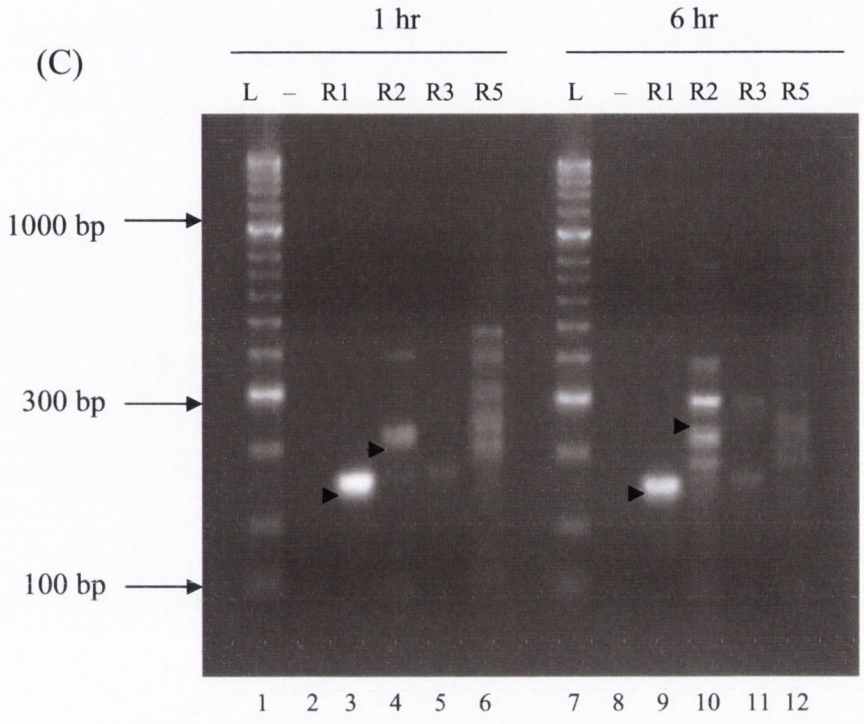
(C)
1 hr
6 hr
L – R1 R2 R3 R5
L – R1 R2 R3 R5
1000 bp
300 bp
100 bp
1 2 3 4 5 6 7 8 9 10 11 12

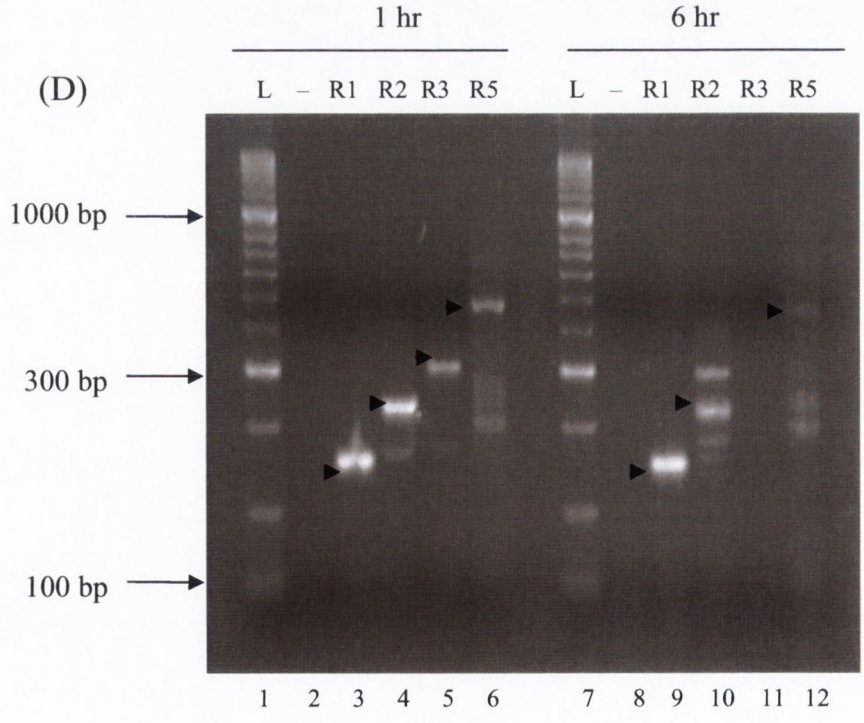
(D)
1 hr
6 hr
L – R1 R2 R3 R5
L – R1 R2 R3 R5
1000 bp
300 bp
100 bp
1 2 3 4 5 6 7 8 9 10 11 12

4.4 Discussion

A new model was recently proposed to explain histone 3'-end processing in mammalian cells (*see Figure 1.8* in Kolev and Steitz, 2005). The stem-loop binding protein (SLBP) was shown to be involved in histone processing during the cell cycle. The SLBP is critical since without it no accumulation of histone mRNAs is observed in the S-phase of the cell cycle. Another histone trans-acting factor in the mammalian cell, U7 snRNP, is not required for histone cell-cycle regulation, as the U7 snRNP was not altered by the cell cycle (Whitfield *et al*, 2000). In the yeast, *Saccharomyces pombe*, pfs2 was discovered to be critical in cell-cycle regulation prior to the S-phase. Pfs2 is a cleavage and polyadenylation factor, and was the first yeast 3'-end processing factor to be linked with cell-cycle regulation (Wang *et al*, 2005). Further research into mammalian and yeast histones is warranted in order to establish further links with 3'-end processing factors and cell-cycle regulation.

The well-known nuclear exosome component, Rrp6p, contributes to RNA quality control and degrades aberrant pre-mRNAs (Libri *et al*, 2002). Previous results, given in Chapter 3, suggested the involvement of the nuclear exosome, Rrp6p, in nuclear degradation of the *neo-HTB1* and endogenous *HTB1* mRNAs in non-cell-cycle regulated cells. This led to an interesting question of whether the nuclear exosome contributes to the cyclic accumulation of histone mRNAs during the cell cycle. Northern blotting and real-time PCR were utilised to investigate the cyclic accumulation pattern in the W303 and exosome mutant, *Δrrp6,* backgrounds. The results show that the endogenous *HTB1* mRNA peaked at 70 mins, representing the S-phase, followed by a rapid decrease into the G_2-phase in WT, W303, cells. In *Δrrp6* cells, the endogenous *HTB1* mRNA accumulated with similar kinetics as that observed in the WT cells. However, little decrease in the level of this accumulated RNA was observed as cells entered the G_2-phase. This data suggests that Rrp6p contributes to the turnover process of the endogenous *HTB1* transcripts in the G_2-phase of the cell

cycle and highlights a potential role for the nuclear exosome in cell-cycle regulation of histone mRNAs. Interestingly, in late December 2006, Reis and Campbell (2006) worked with the Trf4 component of the TRAMP complex, which recruits Rrp6p and initiates degradation of the associated RNA. The RNA-binding subunits of TRAMP, Air2 and Air1, were shown to be similar to the WT HHF2 mRNAs suggesting that these components play no role in the regulation of the HHF2 mRNA. In the *Δrrp6* cells, an increased accumulation of the HHF2 mRNAs in the S-phase and a slower cell cycle were observed. These findings indicate that the exosome plays a role in the S-phase of the HHF2 transcripts (Reis and Campbell, 2006).

Campbell *et al* (2002) identified the distal downstream element (DDE) which was situated approximately 100nt downstream of the 3'-end cleavage site of the *HTB1* gene. The DDE was shown to assist cell-cycle regulation and transcription termination (Campbell *et al*, 2002). Specifically, mutation in the DDE led to a lack of turnover of the neo-*HTB1* mRNAs as the cells entered the G_2-phase. Taken together, the data indicates that events downstream of the 3'-end of the RNA appear to be important for turnover of histone mRNAs in the G_2-phase of the cell cycle.

Having uncovered a potential role for the nuclear exosome in the degradation process in the G_2-phase of the cell cycle, the question arose as to how the exosome might recognise its substrates for degradation and, specifically, how it might preferentially target histone mRNAs for degradation in the G_2-phase. Recent experiments by Vasiljeva and Buratowski (2006) have shed some light on the possible mechanism of substrate recognition by the exosome (Vasiljeva and Buratowski, 2006). Using tandem affinity purification procedures, the authors showed that purified exosome complex is associated with the RNA-binding protein, Nrd1, which has previously been shown to play a role in transcription termination of sn/snoRNAs (Steinmetz and Brow, 1998). Furthermore, incubation of the purified exosome complex with the RNA substrates led to the chewing-back of the transcripts to a

specific defined region. This region was found to contain an Nrd1p binding site (CUUGUAAACGGU). Removal of the Nrd1p site led to complete degradation of the RNA substrate. From these results, Vasiljeva and Buratowski (2006) have proposed a model for the substrate recognition by the exosome, in which Nrd1 recruits the exosome to substrates to promote degradation. In some RNAs where additional Nrd1 recognition sites are available, Nrd1 prevents complete degradation by blocking the progress of the exosome. Torchet and Tollervey (2002) have shown that read-through unprocessed transcripts in the *rna14.1/Δrrp6* background result from lack of 3'-end processing, can be chewed back by the core exosome complex to a position close to the normal poly (A) site of the mRNA (Torchet *et al.*, 2002). These transcripts are subsequently polyadenylated and produce functional mRNAs. It is likely that this chewing back to a specific location reflects the presence of Nrd1-binding sites that prevent further degradation by the exosome. In the presence of Rrp6, complete degradation of the transcripts is observed, suggesting that Rrp6 may add processivity to the core exosome or prevent binding of Nrd1 to the transcript. Nrd1 recognition sites are found approximately 100-106nts downstream of the Gal7 gene, which was used in the study outlined above. Previously, the DDE site was shown to contribute to the accumulation of the *neo-HTB1* mRNA in the G_2-phase also lies approximately 100nts downstream of the cleavage sites of the *HTB1* mRNA (Campbell *et al*, 2002). Furthermore, analysis of the sequences in the DDE region reveals that a putative Nrd1 site can be identified (CUCAGAAAAGUUUCC). Like the Nrd1-binding site, the DDE contains a pyrimide stretch, followed by a purine-rich stretch. The DDE had originally been identified based on its similarity to the U7 snRNP interaction site in mammalian histone mRNAs, which contains a loosely conserved consensus sequence CUCAGAAAA. Thus, it is possible that Nrd1 may be specifically recruited to the DDE in the G_2-phase to allow recruitment of the exosome. Alternatively, the DDE site may bind a specific S-phase protein that prevents interaction of Nrd1 with the region.

Since the nuclear exosome is known to degrade read-through unprocessed pre-mRNAs, another possible mechanism of exosome recruitment might be that pre-mRNA 3'-end formation may be differentially regulated during the cell cycle, resulting in the accumulation of unprocessed pre-mRNAs in the G_2-phase, which would be substrates for the exosome. To test this hypothesis, cell-cycle experiments were performed to determine if differential 3'-end processing occurred in the S- and G_2-phases of the cell cycle in the *rna14-3/Δrrp6* background. Firstly, cell-cycle experiments were carried out at 37°C to ensure that RNA14 protein remained inactive throughout the cell cycle at the non-permissive temperature. At 22°C, the W303 strain exhibited cyclic accumulation of the endogenous *HTB1* mRNAs in 2 hrs, followed by rapid decrease into the G_2-phase in both the permissive and non-permissive temperatures. At the non-permissive temperature, the mRNA levels were slightly reduced due to increased turnover or reduced transcription of the mRNA. From RT-PCR, it is apparent that the majority of the transcripts were correctly cleaved and were detected at the permissive and non-permissive temperatures in the W303 background. Interestingly, at 22°C, the *rna14-3/Δrrp6* mutant showed a cell-cycle accumulation of the endogenous *HTB1* mRNA up to the S-phase, but there was no decrease of this RNA as cells progressed into the G_2-phase. The data is similar to that demonstrated with the *Δrrp6* mutant, where the endogenous *HTB1* transcripts increased and accumulated over time during the cell cycle. This suggests that the nuclear exosome could play a major role in degrading the transcripts in the *rna14-3/Δrrp6* mutant at the permissive temperature. However, at the non-permissive temperature, the endogenous *HTB1* mRNA in the *rna14-3/Δrrp6* mutant showed decreased abundance and was unprocessed. However, some stabilised and mature transcripts were also observed at 37°C. RT-PCR revealed that read-though transcripts were detected at the non-permissive temperature, indicating that 3'-end processing and termination were impaired in the

rna14-3/Δrrp6 mutant. From these sets of experimental conditions, it was difficult to determine whether the exosome was acting in concert with the 3'-end processing machinery.

Therefore, the cell-cycle experiment was repeated, but this time the Rna14p was inactivated by incubation for only one hour at the non-permissive temperature. Again, the W303 cells demonstrated a cyclic accumulation and decrease of *HTB1* at both 22°C and 37°C. In the *rna14-3/Δrrp6* mutant, the endogenous *HTB1* mRNA persisted up to 4 hrs at the permissive temperature. At the non-permissive temperature, the endogenous *HTB1* mRNA in the *rna14-3/Δrrp6* background increased at the beginning of the cell cycle and persisted up to 6 hours. This delayed decrease in the *rna14-3/Δrrp6* cells suggest that 3'-end processing is contributing to the cyclic accumulation of endogenous *HTB1* mRNAs. The presence of longer read-through at 6 hours following inactivation of Rna14p indicates that 3'-end processing remained inactive throughout the time course of the experiment. Therefore, mature *HTB1* mRNA most likely results from the action of the core exosome on the unprocessed and read-through transcripts. These longer transcripts may be hyper-adenylated and stabilised, as postulated by Torchet *et al* (2002) and Libri *et al* (2002).

In conclusion, the nuclear exosome bearing the Rrp6p subunit appears to play a role in the cell cycle by carrying out a turnover process in the G_2-phase of endogenous *HTB1* mRNAs. Also, the cleavage factor plays a role in the cell cycle with the nuclear exosome. In this chapter, cell cycle experiments showed a link between transcription termination, 3'-end processing (CFIA) and the nuclear exosome.

Chapter 5

Analysis of *HTB1* mRNAs export from the nucleus

5.1 Introduction

Nuclear pore complexes (NPCs) are highly conserved structures situated in the nuclear envelope and provide a channel for the transport of RNA and proteins between the nucleus and the cytoplasm (Allen *et al*, 2000). NPCs consist mainly of approximately 50 nucleoporins that function in docking and translocation of mRNP to the cytoplasm. The well-characterised components of the NPCs are the nucleoporins Nup159p/Rat7p and Nup42p/Rip1p. Rat7p encodes for ribonucleic acid trafficking proteins and Rip1p encodes for Rev-interacting proteins.

The nucleoporin Nup159p/Rat7p is essential in mRNA export. Gorsch *et al* (1995) demonstrated that at the non-permissive temperature in the temperature-sensitive mutant strain, *rat7*, bulk poly $(A)^+$ RNA accumulates in the nucleus (Gorsch *et al*, 1995). Field emission scanning electron microscopy revealed that Nup159p/Rat7p associates with the cytoplasmic ring on the cytoplasmic face of the NPC (Kiseleva *et al*, 2004).

Nup159p/Rat7p interacts with the NPC-associated export factor Gle1p, Rat8p/Dbp5p, an ATP-driven RNA helicase, and the nucleoporins, Nup82p and Nsp1p (*See Figure 1.4* in Belgareh *et al*, 1998). Rat8p/Dbp5p is a shuttling transport factor that interacts with the 3'-end of newly emerging mRNAs and associates with Rat7p through its N-terminal domains (Hodge *et al*, 1999). Interestingly, Gle1p interacts with IP_6, one of many small molecules of phosphoinositides found in cells. Recent evidence indicates that IP_6 regulates Rat8p/Dbp5p activity in remodeling the proteins associated with the mRNPs as they leave the nucleus through the NPC (Cole and Scarcelli, 2006).

Another nucleoporin called Nup42p/Rip1p was discovered by two-hybrid analysis to interact with the nuclear export signal of the HIV-1 Rev protein. Saavedra *et al* (1997) found that Rip1p is not required for export of mRNAs under normal growth conditions, but is required for export of heat-shock mRNAs under stressful conditions. Severe inhibition of export of the bulk poly $(A)^+$ RNA was observed during heat stress (Saavedra *et al*,

1997). Strahm *et al* (1999) demonstrated the over-expression of Rip1 rescued the mutant phenotype in gle1 cells. This indicates that Rip1p plays a role in non-heat-shock mRNA export through its interaction with Gle1p (Strahm *et al*, 1999). Gle1p/Rss1p interacts directly with Rip1p and Rat8p, which is essential for mRNA export under heat-shock conditions. Rat8p associates with Gle1p, but does not interact with Rip1p. Under stress conditions, it is assumed that Gle1p and Rat8p dissociate from the RNA, causing a reduction in mRNA export, and that Rip1p is required to stabilise this interaction. Heat-shock mRNAs are exported under stressful conditions and this type of selective export remains unexplained (Bond, 2006; Rollenhagen *et al*, 2004).

Investigations into identifying nuclear export factors have led to an understanding of the mechanism of export of mRNAs from the nucleus to the cytoplasm. Using two-hybrid analyses, Burkard and Butler (2000) demonstrated that the nuclear exosome, Rrp6p, interacts with the nucleo-cytoplasmic export shuttling protein, Npl3p. As the Npl3p exists as a complex with Rrp6p, it was suggested that both proteins monitor the integrity of pre-mRNAs before nuclear export to the cytoplasm (Burkard and Butler, 2000; Vasiljeva and Buratowski, 2006). While it is known that correct 3'-end processing of polyadenylated mRNAs is required for efficient export of the transcripts, the mechanism of communication between the 3'-end processing factors, various transcripts and export factors with the NPC remains unclear.

The export of *HTB1* mRNAs from the nucleus is explored in this chapter. To understand the histone mRNA levels in the nuclear export mutants, the role of the NPC components, Rat7 and Rip1, is examined. In addition, the fate of histone mRNAs in the *rat7-1/Δrrp6* background is examined. Mutations in the DDE are investigated to determine whether the DDE plays a role in histone mRNA levels.

5.2 Results

5.2.1 The export factor Rat7 contributes to endogenous *HTB1* mRNA levels

Current knowledge of the nuclear export of histone mRNA in yeast is limited. In this chapter, experiments using the export mutant strains, *rat7-1* and *rat7-1/Δrrp6*, were carried out to investigate their impact on histone mRNA levels. Also, the role of the DDE mutants in the export of the endogenous *HTB1* mRNAs was investigated. The strains, RAT7, *rat7-1* and *rat7-1/Δrrp6*, containing the plasmids, PLJ31, pSAC15, pSAC20 and pSAC21, were grown in YEPGal medium at 22°C to approximately 1–1.6 OD_{660}. When the cells reached a desirable OD_{660}, they were then centrifuged. Pellets were suspended in pre-warmed medium (YEPGal) of 22°C and 37°C for 1 hr. Northern blots were finally hybridised with a DIG-labelled DNA probe, complementary to the coding section of the endogenous *HTB1* gene, as described in Chapter 2 (Section 2.9).

A few loading variabilities from the rRNA and *ACT1* mRNAs at 22°C were taken into account, particularly in the *rat7-1/Δrrp6* sample containing the PLJ31 plasmid (*Figure 5.1(ii), (iii)*, 22°C, Lane 9). The endogenous *HTB1* mRNA levels were observed to be slightly higher in the wild type (RAT7) strain than in the *rat7-1* strain (*Figure 5.1(i), (ii), (iii)*, 22°C, Lanes 1-4 compared to Lanes 5-8). Quantification of the blots indicated that there was a slight reduction in the *HTB1* mRNA levels in the *rat7-1* and *rat7-1/Δrrp6* backgrounds, regardless of the DDE mutants. It appears that the endogenous *HTB1* and *ACT1* transcripts are more stabilised in the *rat7-1/Δrrp6* background, but from quantification analysis, the relative endogenous *HTB1* mRNAs are similar in the *rat7-1* and *rat7-1/Δrrp6* backgrounds. The relative endogenous *HTB1* mRNA levels for PLJ31, pSAC15, pSAC20 and pSAC21 plasmids in the *rat7-1* background are 0.91, 0.74, 1.06 and 0.90 respectively, while the relative mRNA levels for PLJ31, pSAC15, pSAC20 and pSAC21 plasmids in the *rat7-1/Δrrp6* background are 0.63, 1.02, 0.96 and 0.92 respectively (*Figure 5.1(iii)*, 22°C, Lanes 5-8 compared to Lanes 9-12).

At 37°C, the endogenous *HTB1* transcripts were observed to be slightly reduced in the *rat7-1* background compared to the RAT7 background (*Figure 5.1(iii)*, 37°C, Lanes 5, 6, 7 and 8). This suggests that Rat7p may play a role in the export of *HTB1* mRNAs. The double mutant exhibited higher endogenous *HTB1* transcript levels than the RAT7 and *rat7-1* strains (*Figure 5.1(iii)*, 37°C, Lanes 9-12 and 1-4 compared to Lanes 5-8). The increase in the endogenous *HTB1* transcript levels in the double mutant is consistent with previous findings in which the transcripts are retained in the nucleus as a consequence of *rat7-1* defects and that they are substrates for the nuclear exosome (Hilleren and Parker, 2001). To take the loading variabilities of the RNA into account, quantification was conducted with data suggesting that the mutant DDE, pSAC15, pSAC20 and pSAC21 levels were similar to the WT DDE (PLJ31). This indicates that the presence of the *neo-HTB1* mutant mRNAs had no effect on the endogenous *HTB1* mRNA levels in this mutant background.

Figure 5.1: Northern blot analysis of the endogenous *HTB1* mRNA in the export mutants. Total RNA, 60µg, was isolated from the following yeast strains, Lane 1; RAT7 containing the PLJ31 plasmid, Lane 2; RAT7 containing the pSAC15 plasmid, Lane 3; RAT7 containing the pSAC20 plasmid, Lane 4; RAT7 containing the pSAC21 plasmid, Lane 5; *rat7-1* containing the PLJ31 plasmid, Lane 6; *rat7-1* containing the pSAC15 plasmid, Lane 7; *rat7-1* containing the pSAC20 plasmid, Lane 8; *rat7-1* containing the pSAC21 plasmid, Lane 9; *rat7-1/Δrrp6* containing the PLJ31 plasmid, Lane 10; *rat7-1/Δrrp6* with pSAC15 plasmid, Lane 11; *rat7-1/Δrrp6* containing the pSAC20 plasmid, Lane 12; *rat7-1/Δrrp6* containing the pSAC21 plasmid, at the permissive temperature, 22°C, or following incubation of the mutants for 1 hr at the non-permissive temperature, 37°C. **(i)** Ethidium bromide stained gel showing the ribosomal RNAs. **(ii)** The blot was hybridised with the *ACT1* probe. **(iii)** The blot was hybridised with the endogenous *HTB1*-specific probe. **(iv)** The relative endogensous *HTB1* mRNA levels are shown below the gels.

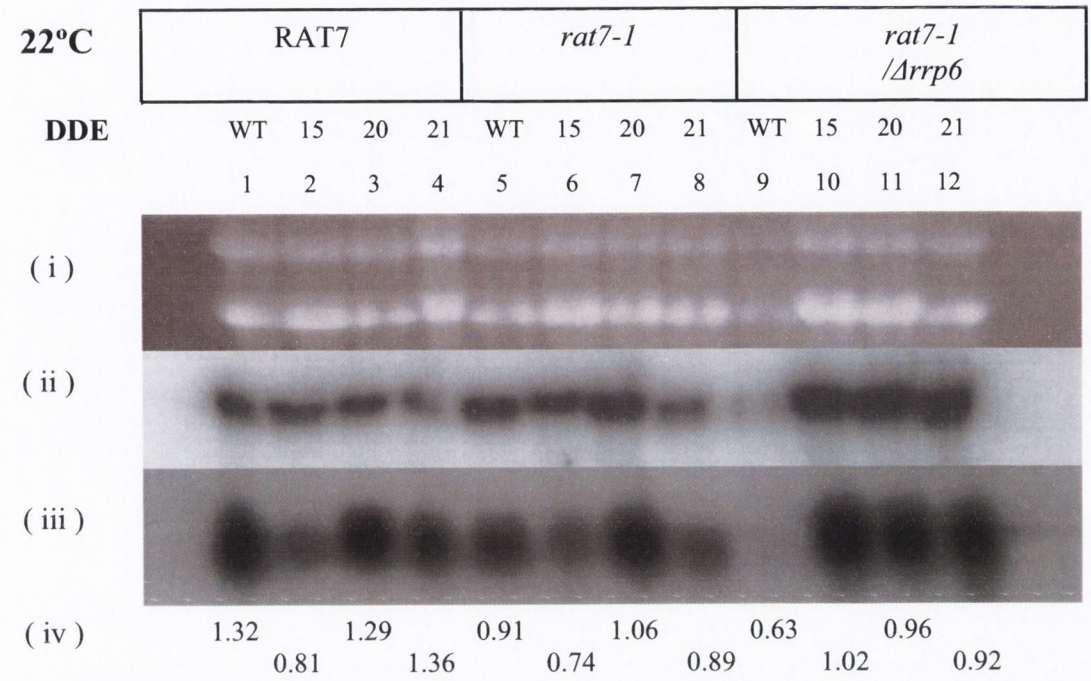
22°C
RAT7
rat7-1
rat7-1 /Δrrp6
DDE
WT 15 20 21 WT 15 20 21 WT 15 20 21
1 2 3 4 5 6 7 8 9 10 11 12
(i)
(ii)
(iii)
(iv)
1.32 1.29 0.91 1.06 0.63 0.96
0.81 1.36 0.74 0.89 1.02 0.92

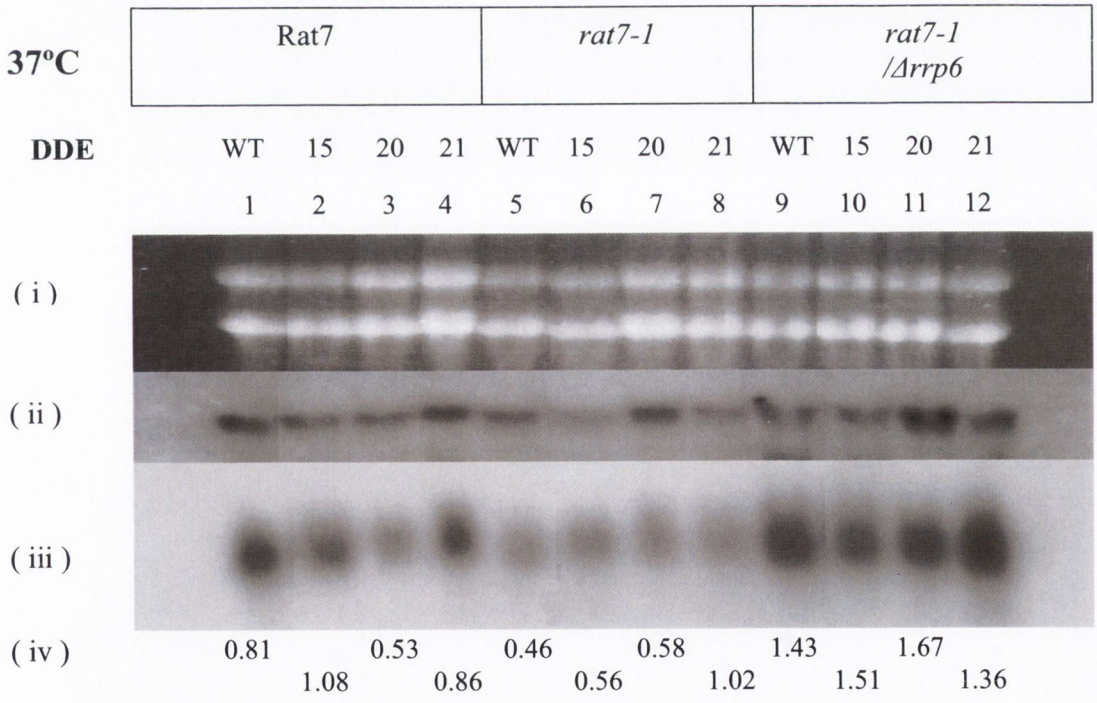
37°C
Rat7
rat7-1
rat7-1 /Δrrp6
DDE
WT 15 20 21 WT 15 20 21 WT 15 20 21
1 2 3 4 5 6 7 8 9 10 11 12
(i)
(ii)
(iii)
(iv)
0.81 0.53 0.46 0.58 1.43 1.67
1.08 0.86 0.56 1.02 1.51 1.36

5.2.2 The nuclear export factor, Rat7, plays a role in *neo-HTB1* mRNA levels

The fate of the *neo-HTB1* mRNA in the strains, RAT7, *rat7-1* and *rat7-1/Δrrp6*, containing the plasmids, PLJ31, pSAC15, pSAC20 and pSAC21, were examined, as described in Section 5.2.1. Membranes were finally hybridised with a DIG-labelled DNA probe, complementary to the neo section of the *neo-HTB1* gene (*Table 2.1*).

Mature *neo-HTB1* mRNAs were observed in the wild type, RAT7, at the permissive temperature (*Figure 5.2(iii)*, 22°C, Lanes 1-4). The lower band in all the lanes appears to represent a degradation product of the *neo-HTB1* transcript (Campbell *et al*, 2002; personal communications; *see also* Figure 3.4). Taking loading variabilities and quantification analysis into account, less *neo-HTB1* mRNA was observed in the *rat7-1* strain with the mutant DDE, pSAC15 and pSAC21, compared to the wild type (*Figure 5.2(iii)*, 22°C, Lanes 6 and 8 compared to Lane 5). The relative *neo-HTB1* mRNAs in the WT and pSAC20 are 0.97 and 0.92 respectively, while the relative *neo-HTB1* mRNA levels for pSAC15 and pSAC21 are 0.48 and 0.37 respectively in the *rat7-1* background. The reduction in the pSAC15 and pSAC21 mutants in the *rat7-1* background requires further investigation. The WT DDE in the *rat7-1/Δrrp6* background was underloaded as observed by the rRNA and *ACT1* mRNA (*Figure 5.2(i), (ii)*, 22°C, Lane 9). The relative *neo-HTB1* mRNA levels in the *rat7-1/Δrrp6* background for the WT DDE are low compared to the DDE mutants (Data not shown). The quality of the RNA may be poor as a result from poor RNA extractions from the *rat7-1/Δrrp6* strain containing the PLJ31 plasmid (*Figure 5.2(iii)*, 22°C, Lane 9). However, the levels of the pSAC15, 20 and 21 *neo-HTB1* mRNAs were similar in the *rat7-1/Δrrp6* background (*Figure 5.2(iii)*, 22°C, Lanes 10-12).

At the non-permissive temperature, mature *neo-HTB1* mRNA transcripts were observed for the RAT7 strain (*Figure 5.2(iii)*, 37°C, Lanes 1-4). In the *rat7-1* strain, *neo-HTB1* mRNA levels were reduced compared to the WT strain (*Figure 5.2(iii)*, 37°C, Lanes 5-8).

In the double mutants, the *neo-HTB1* transcript levels were similar to those observed in the *rat7-1* background (*Figure 5.2(iii)*, 37°C, Lanes 9-12 compared to Lanes 5-8). Instead of the *neo-HTB1* transcripts being restored in the *rat7-1/Δrrp6* background, the *neo-HTB1* transcripts are similar to the *rat7-1* background, which indicates that if these mRNAs are accumulating in the nucleus, then they are most likely degraded independently of RRP6 at the non-permissive temperature.

Figure 5.2: Northern blot analysis of the *neo-HTB1* mRNA in the export mutants.

Total RNA, 60µg, was isolated from the following yeast strains, Lane 1; RAT7 containing the PLJ31 plasmid, Lanes 2; RAT7 containing the pSAC15 plasmid, Lane 3; RAT7 containing the pSAC20 plasmid, Lane 4; RAT7 containing the pSAC21 plasmid, Lane 5; *rat7-1* containing the PLJ31 plasmid, Lane 6; *rat7-1* containing the pSAC15 plasmid, Lane 7; *rat7-1* containing the pSAC20 plasmid, Lane 8; *rat7-1* containing the pSAC21 plasmid, Lane 9; *rat7-1/Δrrp6* containing the PLJ31 plasmid, Lane 10; *rat7-1/Δrrp6* containing the pSAC15 plasmid, Lane 11; *rat7-1/Δrrp6* containing the pSAC20 plasmid, Lane 12; *rat7-1/Δrrp6* containing the pSAC21 plasmid, at the permissive temperature, 22°C, or following incubation of the mutants for 1 hr at the non-permissive temperature, 37°C. **(i)** Ethidium bromide stained gel showing the ribosomal RNAs. **(ii)** The blot was hybridised with the *ACT1* probe. **(iii)** The blot was hybridised with the neo-specific probe. **(iv)** The relative *neo-HTB1* mRNA levels are shown below the gels.

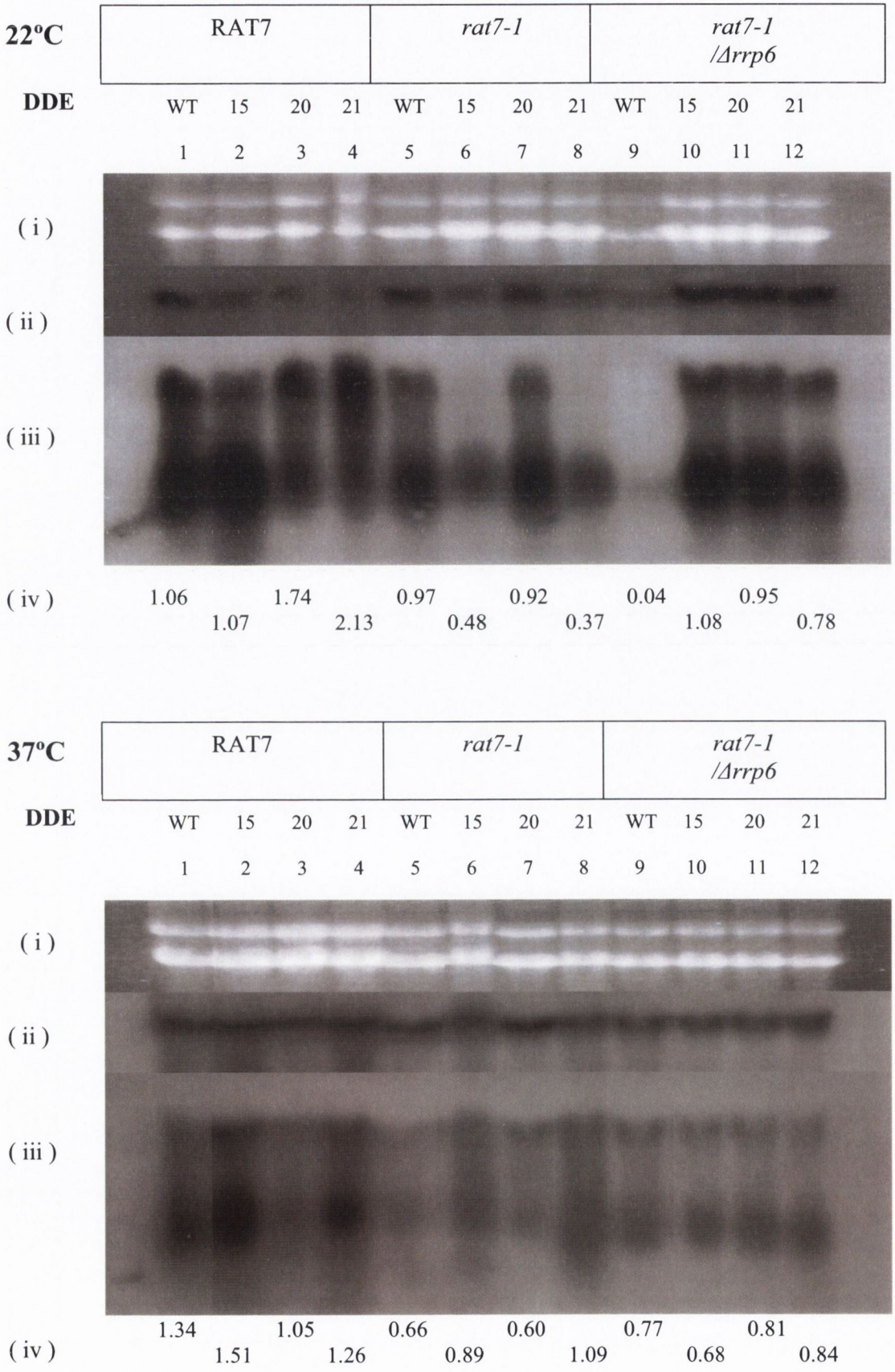
22°C
RAT7
rat7-1
rat7-1 /Δrrp6
DDE
WT 15 20 21 WT 15 20 21 WT 15 20 21
1 2 3 4 5 6 7 8 9 10 11 12
(i)
(ii)
(iii)
(iv)
1.06 1.74 0.97 0.92 0.04 0.95
1.07 2.13 0.48 0.37 1.08 0.78
37°C
RAT7
rat7-1
rat7-1 /Δrrp6
DDE
WT 15 20 21 WT 15 20 21 WT 15 20 21
1 2 3 4 5 6 7 8 9 10 11 12
(i)
(ii)
(iii)
(iv)
1.34 1.05 0.66 0.60 0.77 0.81
1.51 1.26 0.89 1.09 0.68 0.84

5.2.3 *Neo-HTB1* mRNA levels is influenced by both Rat7p and temperature

Experiments were carried out to determine whether any functional *neo-HTB1* mRNAs are exported in the RAT7, *rat7-1* and *rat7-1/Δrrp6* backgrounds. The levels of neomycin phosphotransferase was determined by using the resistance antibiotic geneticin, G418, as an indicator of functional protein as the neomycin gene encodes for neomycin phosphotransferase II, which detoxifies the antibiotic. Protein expression was investigated here, to investigate if mutations in the DDE affected the export of the *neo-HTB1* mRNAs. The wild type strain, RAT7, and the thermosensitive mutants, *rat7-1* and *rat7-1/Δrrp6*, were transformed with the plasmids, PLJ31, pSAC15, pSAC20 and pSAC21. The cells were grown to an OD_{660} of 1.6 and then diluted to $1x10^7$ cell/ml and $1x10^6$ cell/ml. The dilutions were spotted onto YEPGal plates with 0μg/ml and 300μg/ml of G418 antibiotic. In the wild type RAT7 background, functional neomycin protein was produced at 22°C in the presence of G418 (300μg/ml) (*Figure 5.3(A)*). At 37°C, the RAT7 strain expressing *neo-HTB1* from the PLJ31 plasmid showed a low level of G418 resistance in 300μg/ml of G418, while the mutants, pSAC15, pSAC20 and pSAC21, showed no resistance (*Figure 5.3(B)*). This is consistent with a model where the *neo-HTB1* mRNAs are not exported to the cytoplasm at 37°C in the RAT7 background.

The *rat7-1* mutant harbouring the PLJ31, pSAC15, pSAC20 and pSAC21 plasmids showed a low resistance to G418 (300μg/ml) at 22°C, possibly as a result of a small amount of *neo-HTB1* mRNA export (*Figure 5.3(C)*). No growth was observed at 37°C in the presence or absence of G418 in the *rat7-1* background (*Figure 5.3(D)*). At 22°C, growth was observed in the double mutants, *rat7-1/Δrrp6*, in the presence and absence of G418, consistent with a model where the lack of nuclear degradation of mRNAs by the exosome restores mRNA export under conditions when it is impaired (*Figure 5.3(E)*). No growth in the presence and absence of G418, consistent with a model where lack of the

rat7-1/Δrrp6 strain containing the plasmids, PLJ31, pSAC15, pSAC20 and pSAC21, at the non-permissive temperature (*Figure 5.3(F)*).

Figure 5.3: Expression levels of the *neo-HTB1* WT and DDE-mutant transcripts in the export mutants. RAT7, *rat7-1* and *rat7-1/Δrrp6* cells containing the WT plasmid and mutant plasmids were grown in YEPGal medium at 22°C to approximately 1–1.6OD_{660} and were diluted to $1x10^6$ and $1x10^5$ cell/ml. Dilutions were spotted onto YEPGal medium agar plates, consisting of 0μg/ml and 300μg/ml of G418 antibiotic. The plates were incubated at 22°C and 37°C for 7 days. (A) RAT7 strain at 22°C. (B) RAT7 strain at 37°C. (C) *rat7-1* strain at 22°C. (D) *rat7-1* strain at 37°C. (E) *rat7-1/Δrrp6* strain at 22°C. (F) *rat7-1/Δrrp6* strain at 37°C.

[A] **22°C**

RAT7 0 µg/ml G418 RAT7 300 µg/ml G418

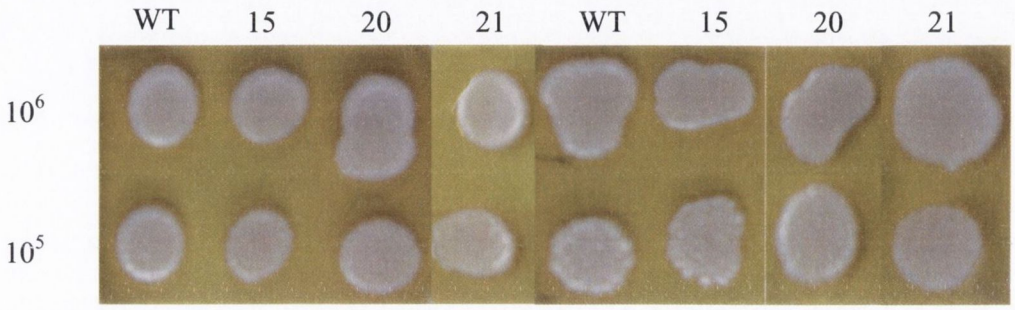

[B] **37°C**

RAT7 0 µg/ml G418 RAT7 300 µg/ml G418

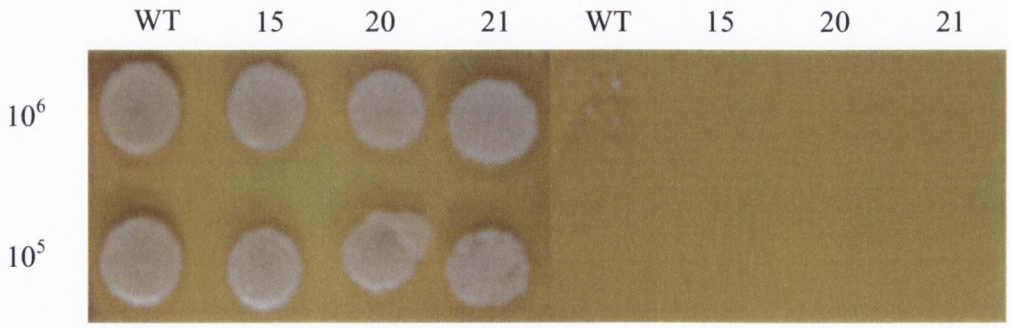

[C] **22°C**

rat7 0 μg/ml G418 *rat7* 300 μg/ml G418

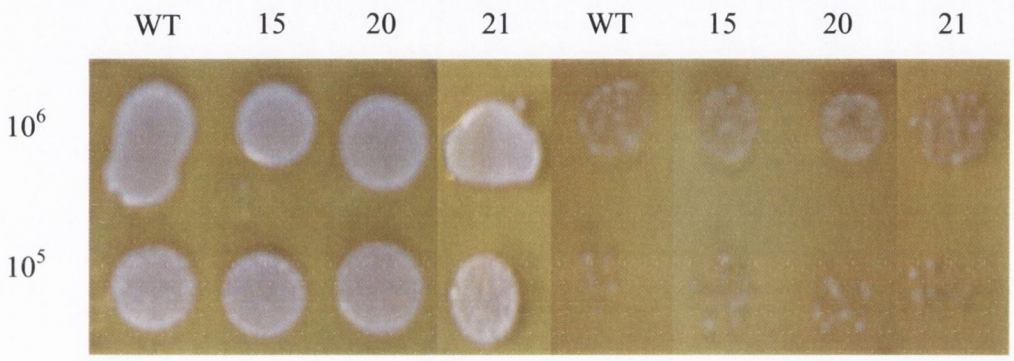

[D] **37°C**

rat7 0 μg/ml G418 *rat7* 300 μg/ml G418

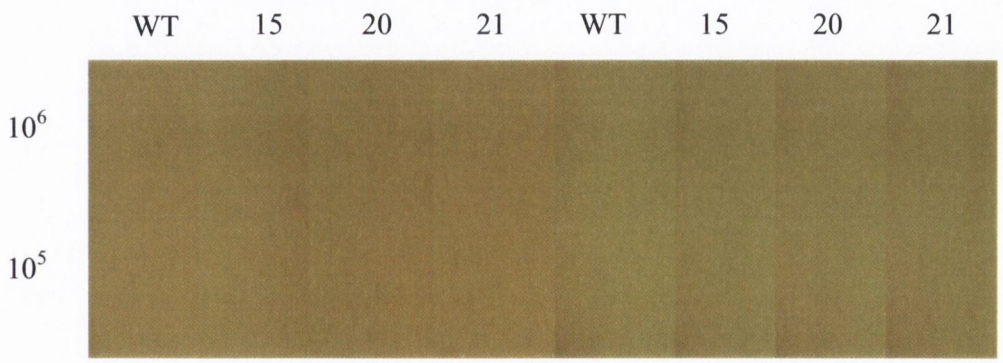

[E]

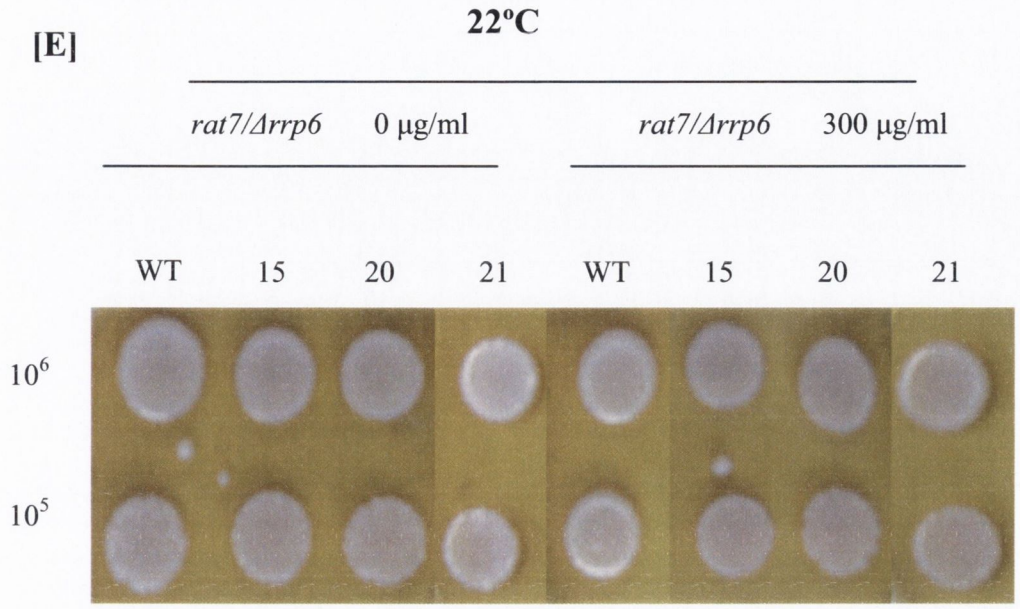
22°C
rat7/Δrrp6 0 μg/ml
rat7/Δrrp6 300 μg/ml
WT 15 20 21 WT 15 20 21
10^6
10^5

[F]

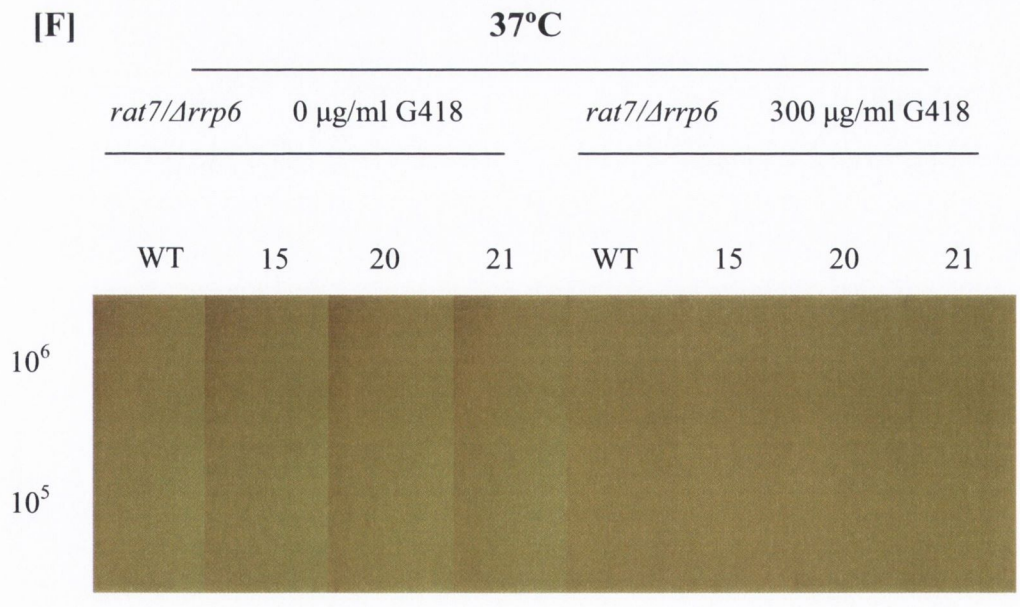
37°C
rat7/Δrrp6 0 μg/ml G418
rat7/Δrrp6 300 μg/ml G418
WT 15 20 21 WT 15 20 21
10^6
10^5

5.2.4 The nuclear export factor, Rip1, is not essential for histone mRNA levels

Nup42/Rip1 nucleoporin forms a complex with a group of other nucleoporins, which include Dbp5/Rat8, Nup100, Nsp1, Nup82, Gle1 and Nup159/Rat7, situated in the cytoplasmic filaments of the NPC (Vinciguerra and Stutz, 2004). Nup42/Rip1 is known to be required for export of heat-shock mRNAs under stressful conditions and is also required for general mRNA export under normal conditions. Experiments were performed to determine whether the nucleoporin, Nup42/Rip1, may possibly contribute to histone mRNA export.

The wild type, W303, and heat-sensitive mutant, *rip1-1*, were grown in YEPD medium. The cultures were introduced into 22°C and 37°C for 1 hr. RNA extractions and Northern blotting were carried out, as described in Chapter 2 (Section 2.9). Membranes were finally probed with the endogenous *HTB1* and *ACT1* sequences (*Table 2.2*).

At 22°C, the endogenous *HTB1* transcript levels in the WT and *rip1-1* mutant backgrounds were similar (*Figure 5.4(iii)*, Lanes 1 and 2). The *ACT1* mRNA levels were slightly increased at the non-permissive temperature compared to the permissive temperature for both WT and *rip1-1* mutant (*Figure 5.4(ii)*, Lanes 3 and 4 compared to Lanes 1 and 2). To investigate further, the *ACT1* and endogenous *HTB1* mRNA levels were quantified at both temperatures to take account of any loading differences. The relative endogenous *HTB1* mRNA levels for W303 and *rip1-1* at 22°C are 0.71 and 0.98 respectively, and at 37°C are 1.13 and 1.14 respectively. This data indicates that the endogenous *HTB1* mRNAs are not altered in the *rip1-1* mutant background. Hence, Rip1 nucleoporin is unlikely to be required for histone export.

Figure 5.4: Northern blot analysis of the endogenous *HTB1* mRNA in the mutant, *rip1-1*. Total RNA, 60µg, was isolated from the following yeast strains, Lane 1; W303, Lane 2; *rip1-1* mutant, at the permissive temperature, 22°C, or following incubation of the mutants for 1 hr at the non-permissive temperature, 37°C. **(i)** Ethidium bromide stained gel showing the ribosomal RNAs. rRNA was used as a control for equal loading on the gel. **(ii)** The blot was hybridised with the *ACT1* probe. **(iii)** The blot was hybridised with the endogenous *HTB1*-specific probe.

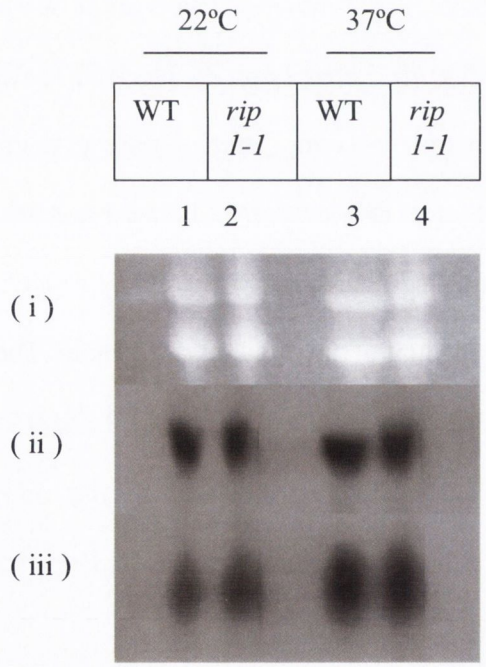

5.3 Discussion

In this chapter, the events surrounding the endogenous *HTB1* mRNA export from the nucleus to the cytoplasm were investigated in the mutants, *rat7-1* and *rat7-1/Δrrp6*, and their WT counterpart, RAT7. The data indicates that the mature endogenous *HTB1* mRNA levels are present in the WT strain at 22°C. There was a slight reduction in the endogenous *HTB1* mRNA levels in the *rat7-1* and *rat7-1/Δrrp6* backgrounds at the permissive temperature and the steady state levels of the *HTB1* mRNA were similar in the *rat7-1* and *rat7-1/Δrrp6* strains. At the non-permissive temperature, a slight reduction of the *HTB1* mRNA levels was observed in the *rat7-1* background, indicating that Rat7p likely plays a role in the export of *HTB1* mRNAs. Deletion of *Δrrp6* in the *rat7-1* background restored the steady state levels of the endogenous *HTB1* mRNA at the non-permissive temperature. The presence of the *neo-HTB1* WT or DDE mutant strains did not significantly alter the endogenous *HTB1* mRNA profiles in any of the strains. Taken together, the results indicate that deletion of the RRP6 in the *rat7-1* background restores the endogenous *HTB1* mRNA levels and the endogenous *HTB1* mRNA levels are sensitive to mutations in the *rat7-1* background at 37°C. The results are consistent with the current model of mRNA export from the nucleus.

Hilleren and Parker (2001) showed that PGK1pG transcripts in the *rat7-1* background are hyper-adenylated and export of the transcripts was inhibited (Hilleren and Parker, 2001). The transcripts were retained as a result of defects in export and 3'-end processing followed by degradation by the 3'-5' exonuclease machinery, the exosome. Other experiments involving the exosome by Hilleren *et al* (2001) and Thomsen *et al* (2003) have shown that the retention of the transcripts are dependent on the nuclear exosome, particularly Rrp6 (Hilleren *et al*, 2001; Thomsen *et al*, 2003). These findings have led to the hypothesis that the mRNA surveillance mechanism exists within the nucleus.

An interesting discovery was made with the *neo-HTB1* transcripts in the *rat7-1* and *rat7-1/Δrrp6* mutants in this chapter. At 22°C, the DDE mutants, pSAC15 and pSAC21, were unstable in the *rat7-1* background. From quantification analysis, the levels of pSAC15 and pSAC21 were approximately 2-fold less than the WT or pSAC20 transcripts. The underlying reason for the reduced pSAC15 and pSAC21 *neo-HTB1* levels in the *rat7-1* background is currently unclear. Since it is known that the half-life of the *neo-HTB1* mRNAs is less than one minute, these reduced levels may reflect small changes in growth conditions in these cultures or the quality of the RNA during RNA extractions. A similar differential stability of the DDE mutant *neo-HTB1* mRNAs was evident in the *rna14-3* background at the permissive temperature (*Figure 3.4*), while enhanced stability of these transcripts was observed in the *Δrrp6* mutant. It was actually pSAC15 and pSAC20 plasmids in the *rna14-3* background, as shown in Figure 3.4. Taken together, the data suggests that *neo-HTB1* mRNAs containing mutations in the DDE region may have altered substrate specificity for the nuclear exosome in the *rat7-1* background. Further research is required to draw firm conclusions on the role of the DDE in RNA export.

A second interesting observation was that the *neo-HTB1* mRNA levels were slightly reduced in the *rat7-1* background at 37°C, indicating that the transcript levels are similar to the endogenous *HTB1* mRNAs. However, unlike the *HTB1* mRNAs, neither the WT *neo-HTB1* or the DDE mutant mRNA levels were restored in the double mutant *rat7-1/Δrrp6* at the non-permissive temperature. This suggests that the *neo-HTB1* mRNAs may be degraded by a mechanism independent of the nuclear exosome under certain conditions. Analysis of the G418 resistance of strains harbouring the *neo-HTB1* WT and DDE mutant genes reveals that the export of these transcripts may be possibly affected by the growth conditions and genetic background of the cells. A very interesting observation was made at the non-permissive temperature with the WT DDE and mutant DDE in the RAT7 background. Yeast growth of the *neo-HTB1* transcripts was not inhibited at 37°C since cell

growth was observed in the absence of G418. At this temperature, a low level of G418 resistance was observed for cells containing the WT *neo-HTB1* gene and no resistance was observed in cells containing the mutant DDE gene in the RAT7 background. This data indicates that there may be a specific inhibition of the export of *neo-HTB1* mRNAs at 37°C and somehow the DDE mutants exacerbate this defect. It is possible that Rat7p dissociates from the NPC at 37°C, similarly to proteins such as Gle1p and Rat8p, which reduces the efficiency of mRNA export under stress conditions. Rip1p appears to stabilise the association of these proteins with the NPC (Bond, 2006; Hilleren and Parker, 2001). However, since export of bulk mRNAs is not inhibited, the defect most likely results from the dissociation of specific export factors from *neo-HTB1* mRNAs at the high temperature. One candidate might be the protein Nrd1p, which is known to associate with the 3'-end of mRNAs and to be involved in the recruitment of the nuclear exosome. From Northern blot analysis, the *neo-HTB1* mRNA levels were reduced after 1 hr incubation at 37°C, indicating that the transcripts are unstable at high temperatures.

A low level of G418 resistance was observed in *rat7-1* cells at 22°C, suggesting that yeast growth is inhibited even under the permissive temperature conditions. Deletion of RRP6 in the *rat7-1* background resulted in the *neo-HTB1* transcripts being stabilised and eventually exported from the nucleus under the permissive conditions. However, the deletion of RRP6 did not restore the transcripts at 37°C. This is consistent with the Northern blot data since the *neo-HTB1* mRNAs were observed to be unstable in the *rat7-1/Δrrp6* background at 37°C. This supports the view that *neo-HTB1* mRNA instability at 37°C is independent of RRP6.

Previous studies have indicated that export of mRNAs is inhibited in cells exposed to heat-shock temperatures of 42°C. The export of mRNA is inhibited in the yeast strain S288C at 42°C, but not at 37°C (Cole Charles, Dartmouth University, personal communications).

The strain, W303, experiences heat stress at 37°C and induces heat-shock proteins at this temperature, however mRNA export in this genetic background at 37°C has not been examined. The strain FY23 is a derivative of S288C and therefore should not be heat stressed at 37°C (Cole, C., Dartmouth University, personal communications). Previous data from Hilleren *et al* (2001) has indicated that deletion of RRP6 in a *rat7-1* background can partially restore mRNA export since functional mRNA translation was observed in the double mutant background (Hilleren *et al*, 2001). Other studies have indicated that the export defect in *rat7-1* is a kinetic defect, in so far as mRNA export is slowed down, but not completely inhibited. Taken together, it appears that the *neo-HTB1* transcripts are inherently unstable at 37°C, either due to reduced transcription or increased mRNA degradation, and therefore export is severely affected at 37°C, even in a WT background. Another nucleoporin involved in export, Nup42/Rip1, was investigated with the endogenous *HTB1* mRNA. The results from Northern blots and quantification data indicated that the steady state levels of the endogenous *HTB1* and *ACT1* mRNAs were not altered in the mutant background, *rip1-1*, at 37°C. The result that Rip1p was not playing a role in the export of endogenous *HTB1* mRNAs under non-stressed conditions was not unexpected since previous studies had established that Rip1p mainly functions in the export of mRNAs under stress conditions. Under stress conditions, the export of bulk mRNAs is inhibited, whereas mRNAs encoding heat-shock proteins are preferentially exported (Bond, 2006). It may be possible that Rip1p preserves the structure of the nuclear pore complex by allowing the partial export under stress conditions. Due to the genetic background of the *rip1-1* strain, it was not possible to introduce the plasmids containing the *neo-HTB1* constructs into this strain. Further work is necessary to characterise the lack of export of *neo-HTB1* mRNAs under stress conditions.

New research is presented in this chapter on the histone mRNA levels with the export mutants. The RAT7 gene was found to be important for histone mRNA transport of both

endogenous *HTB1* and *neo-HTB1* transcripts. The other export factor, Nup42/Rip1, was not observed to play a role. The results with the export mutants increased our understanding of histone biogenesis within the cell.

Chapter 6

Investigating the role of RNase MRP/RNase P complex in *HTB1* mRNA processing

6.1 Introduction

In eukaryotes, mitochondrial RNA processing (RNase MRP) and Ribonuclease processing (RNase P) complexes, both of which are ribonucleoprotein enzymes, are responsible for processing of the 5'-end of rRNAs and 5'-end of tRNAs. The RNase MRP complex cleaves a specific site, A3, in the internal transcribed spacer 1 region of precursor rRNA, leading to the release of the mature 5'-end of 5.8S rRNA (Li *et al*, 2004b). The RNase P complex is involved in endonucleolytic cleavage of the 5'-leader of precursor tRNAs to a mature 5' termini.

The RNase MRP/RNase P complex consists of 8 essential core proteins, Pop1, Pop3, Pop4, Pop5, Pop6, Pop7, Pop8 and Rpp1. In addition, RNase MRP contains one unique protein, Snm1p, and an RNA subunit, NME1 (nuclear mitochondrial endonuclease 1). RNase P contains the same core proteins, as well as an additional unique protein, Rrp2p, and an RNA subunit, RPR1 (Xiao and Engelke, 2005). The two complexes are evolutionary and structurally conserved (Eenennaam *et al*, 2001a). Within *Saccharomyces cerevisiae*, both complexes reside in the nucleus and mitochondria (Lindahl *et al*, 2000).

Tollervey *et al* (1994) discovered Pop1 protein through analysis of temperature-sensitive lethal yeast strains, which exhibited altered $5.8S_S$:$5.8S_L$ ratio. The mature 5.8S exists in two forms: the long form ($5.8S_L$) is 7 nucleotides longer at the 5'-end than the short form ($5.8S_S$). The short form, $5.8S_S$, was found to be under-accumulated in the Pop1 protein, indicating that this protein is required for 5.8S processing (Tollervey *et al*, 1994). Mutations in Pop1-1 also reduced the RNase MRP and RNase P RNA levels at the non-permissive temperatures, thus revealing that Pop1p is a component of these complexes.

The function of RNase MRP and RNase P complexes in rRNA processing has been well characterised. Recent evidence has uncovered a role for RNase MRP in mRNA biogenesis. Gill *et al* (2004) uncovered a role of RNase MRP complex in degrading the CLB2 mRNA, leading to cell-cycle progression. The degradation products were found to be substrates for

the 5'→3' exonuclease Xrn1, but not 3'→5' exonuclease Rrp6, which is a component of the exosome (Gill *et al*, 2004).

Recently in our laboratory, three-hybrid analysis was performed to identify proteins that bind to the distal downstream element (DDE) of the *neo-HTB1* mRNA (Beglan, unpublished data). Pop4p was identified as one of the DDE-binding proteins. Based on previous findings on the role of RNase MRP complex in the regulation of CLB2 mRNA during the cell cycle, an investigation was carried out with *pop1-1* mutant to determine if the RNase MRP and/or RNase P complexes play a role in the biogenesis of the *neo-HTB1* and endogenous *HTB1* mRNAs. The mutant *pop1-1* was presented to the laboratory as a gift from David Tollervey, Edinburgh University.

6.2 Results

6.2.1 POP1 plays a role in *HTB1* processing

The role of the RNase MRP/RNase P complex in *HTB1* mRNA biogenesis was investigated using the temperature-sensitive mutation, *pop1-1*. W303 and the thermosensitive mutant, *pop1-1*, were grown in YEPD medium at 22°C to an OD_{660} of 1.6 (*Table 2.1*). Cells were collected and the pellets were suspended in 22°C and 37°C pre-warmed medium (YEPD). Cells were retrieved following 1 hr of incubation. Total RNA was extracted, electrophoresed and Northern blotted, as described in Chapter 2 (Section 2.9). Membranes containing RNA were hybridised with a DIG-labelled DNA probe, complementary to the endogenous *HTB1* gene (*Table 2.2*).

In the W303 strain, *ACT1* mRNA levels were similar at the permissive and non-permissive temperatures, as were the endogenous *HTB1* mRNA levels (*Figure 6.1(ii), (iii)*, Lane 1 compared to lane 3). Both endogenous *HTB1* mRNA and *ACT1* mRNA levels were reduced in the *pop1-1* background at both at 22°C and 37°C (*Figure 6.1(ii), (iii)*, Lanes 2 and 4). While equal amounts of RNA, as determined by OD_{260}/OD_{280} readings, were loaded onto each lane, the total RNA pool appears to be lower in the *pop1-1* strain at both temperatures (*Figure 6.1(i), (ii), (iii)*, Lanes 2 and 4). The rRNA levels are understandably low in the *pop1-1* background given that the *pop1-1* cells are defective in correct rRNA synthesis. Quantification analysis indicates that only a 1.2-fold difference was observed between the W303 and *pop1-1 ACT1* transcripts at 22°C while only a 1.1-fold difference was observed for the W303 and *pop1-1 ACT1* transcripts at 37°C. This data indicates that the *ACT1* mRNA levels for the W303 and *pop1-1 ACT1* strains are similar. At 22°C, there was a 2-fold decrease in endogenous *HTB1* mRNA levels in the *pop1-1* mutant compared with the wild type, whilst a 3-fold decrease was observed at 37°C. Despite the reduced total RNA pool in the *pop1-1* strain, quantification of the Northern blot suggests that the

endogenous *HTB1* mRNA is more sensitive to mutations in *pop1-1* than the *ACT1* mRNA (*Figure 6.1(ii), (iii)*, Lanes 2 and 4).

Figure 6.1: Northern blot analysis of the endogenous *HTB1* mRNA in the mutant, *pop1-1*. Total RNA, 60μg, was isolated from the following yeast strains, Lanes 1 and 3; W303A, Lanes 2 and 4; *pop1-1*, at the permissive temperature, 22°C (Lanes 1 and 2), or following incubation of the mutants for 1 hr at the non-permissive temperature, 37°C (Lanes 3 and 4). **(i)** Ethidium bromide stained gel showing the ribosomal RNAs. **(ii)** The blot was hybridised with the *ACT1* probe. **(iii)** The blot was hybridised with the endogenous *HTB1* probe.

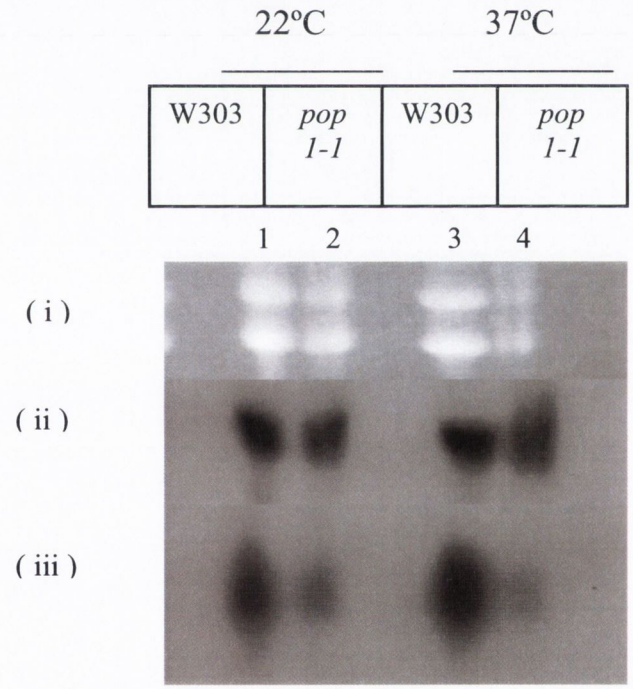

6.2.2 Mutations in POP1 affects *neo-HTB1* mRNA production

In order to investigate whether the *neo-HTB1* mRNA levels were sensitive to mutations in *pop1-1*, the W303 and *pop1-1* strains were transformed with the plasmids, PLJ31, pSAC15, pSAC20 and pSAC21. Cell cultures were grown in YEPGal medium at 22°C to an optical density of 1-1.6 OD_{660} and then collected. Following centrifugation, the pellets were suspended in pre-warmed medium (YEPGal) of 22°C and 37°C for 1 hr. The isolated RNA was probed with the *neo-HTB1* probe (Chapter 2, Section 2.9).

At the permissive temperature, mature *neo-HTB1* and *ACT1* mRNAs were observed with the PLJ31, pSAC15, pSAC20 and pSAC21 plasmids in the W303 background (*Figure 6.2(ii), (iii),* Lanes 1-4). Levels of mature *neo-HTB1* transcripts were weak in the W303 background under the experimental conditions used. This has been consistently observed (*See figures 3.4 and 6.1*). Despite loading equal amounts of total RNA as judged by OD_{260}/OD_{280} ratios, the overall total RNA pool and, in particular, the levels of rRNA were greatly lowered in the *pop1-1* strains at both the permissive and non-permissive temperatures (*Figure 6.2(i)*, Lanes 5-8 and lanes 13-16). The reduced levels of rRNAs in the *pop1-1* background probably reflect defective rRNA processing caused by the mutation in the strain (*Figure 6.2(i)*, Lanes 5-8 and lanes 13-16). In the *pop1-1* background, levels of the WT DDE and DDE mutants in the *neo-HTB1* and *ACT1* mRNAs were reduced compared to the W303 strain at 22°C (*Figure 6.2(ii), (iii)*, Lanes 5-8 compared to lanes 1-4).

At the non-permissive temperature, some mature *neo-HTB1* mRNA was observed in the W303 background, but the levels in the *pop1-1* background were particularly reduced (*Figure 6.2(iii)*, Lanes 9, 10, 11 and 12 compared to lanes 13, 14, 15 and 16). The rRNA levels were also reduced at 37°C in the *pop1-1* background (*Figure 6.2(i)*, Lanes 13-16). This data indicates that Pop1-1 deletion caused defective rRNA processing and decreased levels of *neo-HTB1* and *ACT1* mRNA levels.

Figure 6.2: Northern blot analysis of the *neo-HTB1* mRNA in the mutant, *pop1-1*.

Total RNA, 60μg, was isolated from the following yeast strains, Lanes 1 and 9; W303A containing the PLJ31 plasmid, Lanes 2 and 10; W303A containing the pSAC15 plasmid, Lanes 3 and 11; W303A containing the pSAC20 plasmid, Lanes 4 and 12; W303A containing the pSAC21 plasmid, Lanes 5 and 13; *pop1-1* containing the PLJ31 plasmid, Lanes 6 and 14; *pop1-1* containing the pSAC15 plasmid, Lanes 7 and 15; *pop1-1* containing the pSAC20 plasmid, Lanes 8 and 16; *pop1-1* containing the pSAC21 plasmid, at the permissive temperature, 22°C (Lanes 1-8), or following incubation of the mutants for 1 hr at the non-permissive temperature, 37°C (Lanes 9-16). **(i)** Ethidium bromide stained gel showing the ribosomal RNAs. **(ii)** The blot was hybridised with the *ACT1* probe. **(iii)** The blot was hybridised with the neo-specific probe.

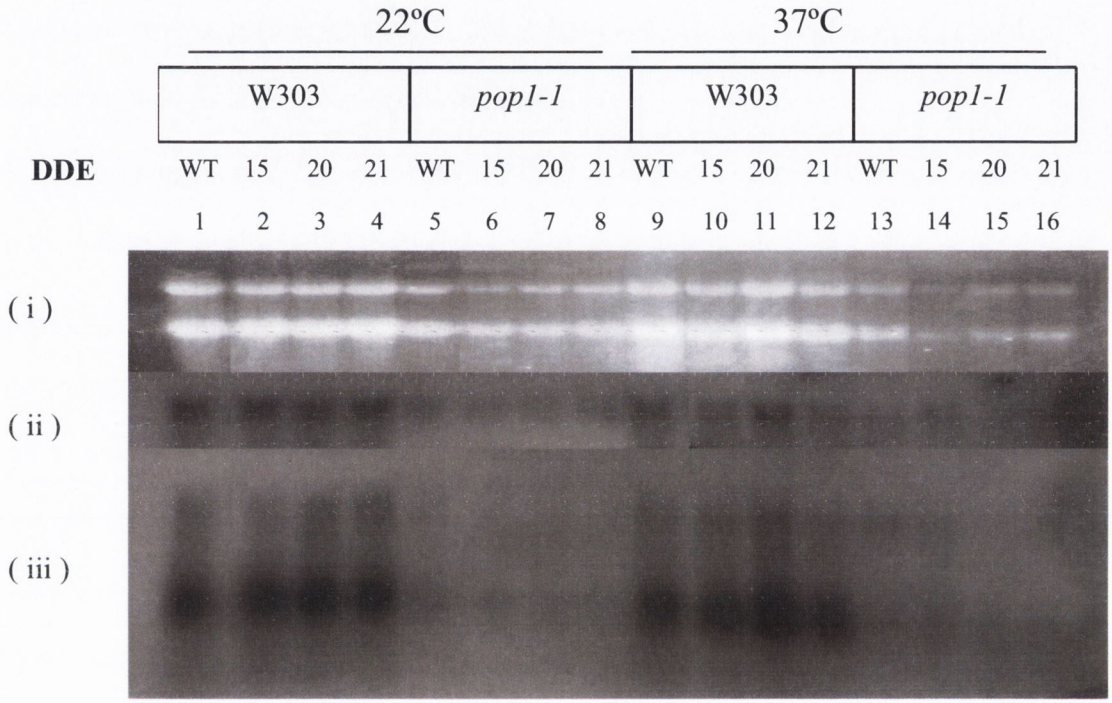
22°C
37°C
W303
pop1-1
W303
pop1-1
DDE
WT 15 20 21 WT 15 20 21 WT 15 20 21 WT 15 20 21
1 2 3 4 5 6 7 8 9 10 11 12 13 14 15 16
(i)
(ii)
(iii)

6.2.3 POP1 mutations affect mRNA processing of the endogenous *HTB1* transcripts

Experiments were performed to determine whether the presence of the WT or mutant DDE in the cell can influence the total endogenous *HTB1* mRNA levels in the *pop1-1* background. With this in mind, endogenous *HTB1* mRNAs were examined in the W303 and *pop1-1* strains containing the plasmids PLJ31, pSAC15, pSAC20 and pSAC21. Experiments were performed as described in Section 6.2.1. Membranes were probed to detect the endogenous *HTB1* sequences (*Table 2.1*).

At 22°C, endogenous *HTB1* and *ACT1* mRNA levels were lower in the *pop1-1* strain than in the wild type strain, W303, confirming previous results in Figure 6.1 (*Figure 6.3(ii),(iii)*, Lanes 1-4 compared to lanes 5-8). Again, rRNA levels were lower in the *pop1-1* strain, indicating that Pop1 is essential for normal rRNA processing (*Figure 6.3(i)*, Lanes 1, 2, 3 and 4 compared to lanes 5, 6, 7 and 8).

Endogenous *HTB1* mRNA levels in the W303 background were slightly reduced at the non-permissive temperature (*Figure 6.3(iii)*, Lanes 9-12). Reduced rRNA and endogenous *HTB1* mRNA levels were observed in the *pop1-1* background (*Figure 6.3(i), (iii)*, Lanes 13-16). The presence of the PLJ31, pSAC15, pSAC20 and pSAC21 *neo-HTB1* transcripts in the *pop1-1* background did not significantly alter the endogenous *HTB1* mRNA levels at the permissive and non-permissive temperatures (*Figure 6.3(iii)*, Lanes 5-8 and 13-16). Also, the *ACT1* mRNA levels were low in the *pop1-1* background at 22°C and 37°C (*Figure 6.3(ii)*, Lanes 5-8 and 13-16). Taken together, this data suggests that the RNase MRP/RNase P complexes are essential for successful rRNA synthesis and may also play a role in mRNA biogenesis.

Figure 6.3: Northern blot analysis of the endogenous *HTB1* mRNA in the mutant, *pop1-1*. Total RNA, 60µg, was isolated from the following yeast strains, Lanes 1 and 9; W303A containing the PLJ31 plasmid, Lanes 2 and 10; W303A containing the pSAC15 plasmid, Lanes 3 and 11; W303A containing the pSAC20 plasmid, Lanes 4 and 12; W303A containing the pSAC21 plasmid, Lanes 5 and 13; *pop1-1* containing the PLJ31 plasmid, Lanes 6 and 14; *pop1-1* containing the pSAC15 plasmid, Lanes 7 and 15; *pop1-1* containing the pSAC20 plasmid, Lanes 8 and 16; *pop1-1* containing the pSAC21 plasmid, at the permissive temperature, 22°C (Lanes 1-8), or following incubation of the mutants for 1 hr at the non-permissive temperature, 37°C (Lanes 9-16). **(i)** Ethidium bromide stained gel showing the ribosomal RNAs. **(ii)** The blot was hybridised with the *ACT1* probe. **(iii)** The blot was hybridised with the endogenous *HTB1*-specific probe.

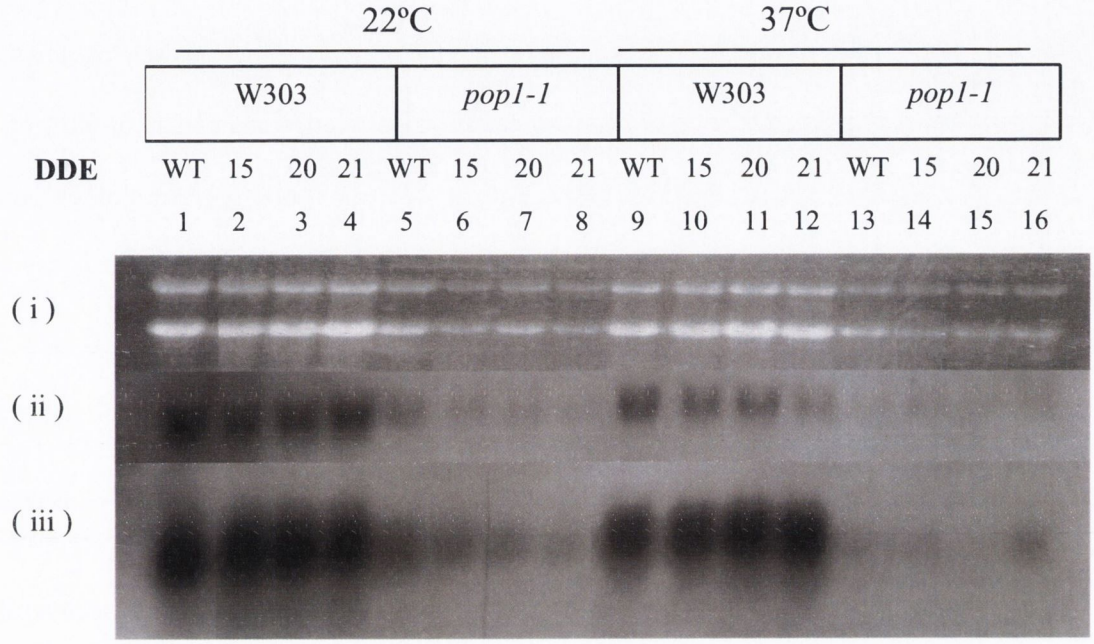
22°C
37°C
W303
pop1-1
W303
pop1-1
DDE
WT 15 20 21 WT 15 20 21 WT 15 20 21 WT 15 20 21
1 2 3 4 5 6 7 8 9 10 11 12 13 14 15 16
(i)
(ii)
(iii)

6.3 Discussion

Recent research in our laboratory has uncovered a number of proteins that bind to the distal downstream element in our histone model. One of the proteins uncovered was POP4, a protein subunit that is part of the RNase MRP/RNase P complex. The RNase MRP complex consists of an RNA subunit, NME1, and 9 proteins (Pop1, Pop3, Pop4, Pop5, Pop6, Pop7, Pop8, Rpp1 and SNM1). The holoenzyme functions in cleaving the internal transcribed spacer 1 region, generating the maturation of the 5'-end of the 5.8S rRNA (Li *et al,* 2004b). With this in mind, this chapter focused on Pop1p, another protein member of the RNase MRP/RNase P complex, which was presented to the laboratory by David Tollervey, Edinburgh University.

Research concerning RNase MRP and RNase P complexes has focused on the subunit compositions, binding of the protein subunits, catalysis and substrate recognition to the hairpin sequences in the complexes. Tollervey *et al* (1994) first discovered *pop1-1* mutant (Tollervey *et al*, 1994). Up until 2004, most research using *pop1-1* mutant focused on its role in the biogenesis of Pol III-transcribed RNAs. The *pop1-1* mutant showed low levels of RNase MRP and P RNAs compared to the wild type at 37°C. Tollervey and his colleagues concluded that Pop1p was required to stabilise and maintain the steady state levels of the RNase MRP and P RNAs. In further experiments, Pop1p was found to have a direct role in altering the structure of RNase MRP and P RNAs.

Recently, Gill *et al* (2004) discovered that the RNase MRP complex functions in RNA degradation and cell-cycle regulation in *Saccharomyces cerevisiae* (Gill *et al*, 2004). This was the first report indicating that these complexes may play a role in mRNA biogenesis. The Clb2p, β-type cyclin, is important for initiation and completion of mitosis. The wild type demonstrated a normal cell-cycle pattern, but the *nme1* mutant caused a delay in the CLB2 mRNA degradation and no cell-cycle pattern was observed as the cycle progressed. Further experiments demonstrated that the delay was due to the accumulation of the steady

state levels of the CLB2 mRNA. Crucially, these experiments demonstrated that the RNase MRP complex plays a role in mRNA degradation. Since we observed a reduction in the *HTB1* and *ACT1* mRNA levels, we put forward a theory that the *pop1-1* mutant causes mRNA degradation, in addition to defective rRNA synthesis. Therefore, to understand the role of the RNase MRP/RNase P complex, *Pop1-1*, in histone processing at the molecular level, we looked at the *neo-HTB1* and endogenous *HTB1* mRNAs in the *pop1-1* background.

A number of technical problems hampered the analysis of the *HTB1* mRNA in the *pop1-1* strain. Firstly, despite loading equal amounts of the total RNA (60μg) in each lane, the levels of rRNA were notably reduced in the *pop1-1* strain at both the permissive and non-permissive temperatures. The reduced pool of total RNA may reflect a higher level of overall RNA degradation in this mutant background. The reduction in the total RNA pool in the *pop1-1* strain led to reduced levels of mRNA present on the agarose gels. Thus, *ACT1*, endogenous *HTB1* and *neo-HTB1* mRNAs were extensively reduced in the *pop1-1* strain at both the permissive and non-permissive temperatures. Despite the reduced levels, this data suggests that both *HTB1* and *neo-HTB1* mRNAs are differentially sensitive to mutations in *pop1-1* since the levels of these RNAs were notably reduced compared to the *ACT1* mRNA levels. This reduction may reflect the shorter half-life of these mRNAs compared to the half-life of *ACT1* mRNA. It is likely that the RNase MRP complex has degraded the mRNA, which is consistent with the findings of Gill *et al* (2004). Since Pop1 is not known to play a role in transcription initiation or elongation, the reduced levels of endogenous *HTB1* and *neo-HTB1* in the *pop1-1* background points to an increased turnover/degradation rate of these mRNAs in this strain. Also, our experiments show that the DDE mutants did not extensively alter the endogenous *HTB1* and *neo-HTB1* levels in comparison to the WT DDE, suggesting that this section of the pre-mRNA transcript does not recognise Pop1p.

We hypothesise in our model, that the mutant RNase MRP increases the *neo-HTB1* and endogenous *HTB1* transcripts and end up being degraded by the cell cyclins when the cell-cycle is delayed. This theory of the mRNA degradation process is supported by Gill *et al* (2004). The RNase MRP complex also generates mature 5.8S rRNA. This is important, as the ribosomal complex brings the tRNA and mature mRNA together for translation initiation (Woodhams *et al*, 2007). Should be defective, the rRNA will not attach to the mRNA and tRNA during translation initiation. This may trigger the mRNA to be degraded. It is possible that the RNase MRP/RNase P complex may have further functions in the RNA-processing systems. This requires further investigation and further experiments are required to confirm the role of the RNase MRP/RNase P complexes in histone mRNA biogenesis.

Chapter 7

Conclusion

7.1 In Summary

In eukaryotes, pre-mRNAs engage in a number of tightly co-ordinated processes to progress into functional mRNAs. This includes transcription, 3'-end formation, termination, nuclear degradation and processing by ribonucleases (Libri *et al*, 2002; Vasiljeva and Buratowski, 2006; Zhao *et al*, 1999; Tollervey, 2005). Mature mRNAs are finally exported from the nucleus as messenger ribonucleoprotein complexes (mRNP). Cis-acting sequences are the binding sites for trans-acting factors that organise DNA for transcription and regulate gene expression. The trans-acting factors required for mRNA biogenesis in yeast have many mammalian counterparts. One apparent exception to this conservation of trans-acting factors are those involved in histone mRNA biogenesis in yeast and mammals. While mammalian cells require a set of unique factors such as the SLBP, the ZFP100 and the U7 snRNP, these factors are not present in the yeast cell. Furthermore, the cis-acting sequences defining the 3'-end cleavage site of histone mRNAs are not conserved in yeast. This divergence in the mechanism of histone mRNA 3'-end formation requires further investigation.

Early studies using crude cell extracts showed that efficient 3'-end processing of a precursor H2B2 mRNA occurs *in vitro* (Butler *et al*, 1990), suggesting that the general mRNA 3'-end processing machinery is involved in histone biogenesis. However, this area has remained unexplored. This project, therefore, has set out to investigate the trans-acting factors responsible for histone biogenesis in *Saccharomyces cerevisiae*. Importantly, histone production is tightly linked to DNA synthesis in the S-phase of the cell cycle. For that reason, cell-cycle regulation of histones was investigated, along with the roles of 3'-end processing and termination, to expand our knowledge of the processes within the cell cycle.

The 3'-end of *HTB1* mRNAs are generated by the general cleavage and polyadenylation factors

The role of the 3'-end processing factors, RNA14, RNA15 and PCF11, in *HTB1* mRNA biogenesis was investigated. The 3'-end processing of the *neo-HTB1* mRNA was examined in the temperature-sensitive mutants *rna14-1*, *rna15-2* and *pcf11-2*. The results indicate that 3'-end cleavage was impaired in these mutant backgrounds. Since very little unprocessed read-through pre-mRNAs was observed at the non-permissive temperature, this suggested that the unprocessed pre-mRNAs were rapidly degraded in these mutant strains by the nuclear exosome.

To confirm whether the nuclear exosome contributed to mRNA histone biogenesis, *neo-HTB1* mRNA levels were examined in the *rna14-3/Δrrp6* and *rna15-2/Δrrp6* mutant strains. The data revealed that the double mutant *neo-HTB1* transcripts were partially restored to the levels observed in the WT strain. This suggested that under conditions where 3'-end processing is impaired, mature transcripts can be generated by an alternative mechanism. Torchet *et al* (2002) have previously shown a similar production of mature mRNAs in *rna14-3/Δrrp6* cells.

The next question addressed is whether the cleavage factor and exosome component, Rrp6, might interact with the DDE region of the *HTB1* gene. Previously, Campbell *et al* (2002) showed that the DDE lay in the region where transcription termination occurred (Campbell *et al*, 2002). Differential stability of *neo-HTB1* mRNAs bearing mutations in the DDE were observed in the *rna14-3* background at both the permissive and non-permissive temperatures, suggesting that the DDE mutants may be better substrates for the nuclear exosome in this background. Similarly, the DDE mutants were more stable than the WT in the *Δrrp6* cells when incubated at 37°C, again suggesting that the DDE mutants were better substrates for the nuclear exosome. The preference of the exosome for the DDE mutants is currently unclear. However, since the DDE lies in the region of transcription termination,

the DDE region may be a recognition site for the nuclear exosome under certain genetic and environmental conditions. These results also suggest that there is competition for the pre-mRNA substrate between the cleavage factors and exosome component.

A model was put forward by Torchet *et al* (2002) to explain how the exosome component, Rrp6p, plays a role in pre-mRNA processing (Torchet *et al*, 2002). When the cleavage factors Rna14-1 and Rna15-2 were deleted, 3'-end processing was inhibited and termination defects were observed (Chapter 3, Figure 3.8). The unprocessed 3'-ends were degraded by the exosome, Rrp6p, and its partner, Dob1p. In the double mutants, *rna14-3/Δrrp6* and *rna15-2/Δrrp6*, the pre-mRNAs were stabilised. Even when the exosome was knocked out along with the cleavage factors, mature transcripts were still generated, perhaps by the action of the core exosome. This proposed model is supported by results presented in this study. Recently, Vasiljeva and Buratowski's group have proposed a model whereby the nuclear exosome, independent of Rrp6, can chew back pre-mRNAs in a 3' to 5' direction until an Nrd1 site is encountered. It is predicted that the presence of Rrp6 would relieve this block, allowing continued complete degradation of the pre-mRNA substrate. An alternative hypothesis might be that stabilisation of pre-mRNAs in *rna14/Δrrp6* cells allows 3'-end cleavage by a sub-optimal 3'-end processing machinery.

The biogenesis of the endogenous *HTB1* transcripts was also explored in the cleavage and exosome mutants. Quantification analysis from Northern blots suggested that Rna14p was required for endogenous *HTB1* processing. One surprising observation was that the presence of *neo-HTB1* mRNAs containing mutations in the DDE seemed to stabilise the endogenous *HTB1* in cells incubated at 37°C. Why the endogenous *HTB1* mRNAs should be stabilised by the presence of DDE-mutant forms of *neo-HTB1* in *Δrrp6* mutants remains unanswered, but one might speculate that the DDE mutant transcripts may sequester factors that are required for the normal turnover of *HTB1* mRNAs.

The 5'→3' exonuclease, Rat1, contributes to *HTB1* mRNA biogenesis

Investigations in this project with the 3'→5' exonuclease, Rrp6, led to an interest in the role of the 5'→3' exonuclease, Rat1, in histone mRNA biogenesis. The results generated in Chapter 3 indicate that Rat1 plays a small role in processing of the *neo-HTB1* and endogenous *HTB1* mRNAs since they were slightly reduced in the temperature-sensitive strain, *rat1*, at the non-permissive temperature. The neo-*HTB1* mRNA levels containing the mutations in the DDE were similar to the WT *neo-HTB1* mRNA in the *rat1* background, indicating that the DDE region is not required for Rat1p activity. Rat1p is a well-known termination factor (Kim *et al*, 2004). Recent research has shown that the 3'-end processing factors, Pcf11 and Rna15, are recruited to the pre-mRNA by Rat1 to enhance termination (Luo *et al*, 2006). This data supports the torpedo model theory.

Rrp6 plays a role in cell-cycle regulation of endogenous *HTB1* mRNAs

Yeast histones are tightly co-ordinated with DNA synthesis during the cell cycle. Previously, Campbell *et al* (2002) have shown that the DDE region in the histone model played a role in the cell cycle. The DDE mutants, pSAC14 and pSAC21, disrupted the cell-cycle accumulation pattern (Campbell *et al*, 2002). Interestingly, as discussed in Chapter 3, the nuclear exosome, Rrp6, contributes to nuclear degradation of the *neo-HTB1* and endogenous *HTB1* mRNAs. Furthermore, *neo-HTB1* mRNAs containing mutations in the DDE are differentially stabilised in the *Δrrp6* cells. These observations led us to question whether the nuclear exosome participated in the cell cycle. The data revealed that in the *Δrrp6* background, while endogenous *HTB1* mRNAs accumulated in a manner similar to the WT cells, there was a marked reduction in the level of these mRNAs in the G_2-phase. Therefore, we hypothesised that the nuclear exosome contributes to the turnover process of endogenous *HTB1* mRNAs in the G_2-phase of the cell cycle.

Since the nuclear exosome appears to contribute to the turnover of the endogenous *HTB1* mRNA in the G_2-phase, a question arises as to how the exosome might distinguish between *HTB1* mRNA pools in the S-phase and G_2-phase. One possibility is that differential 3'-end processing is occurring during the cell cycle, leading to the production of unprocessed and unterminated transcripts, which are normal substrates for the exosome, in G_2-phase.

To test this hypothesis, cell-cycle experiments were carried out using the *rna14-3/Δrrp6* mutant strain. The results indicated that at the permissive temperature, the *rna14-3/Δrrp6* mutant exhibited cyclic accumulation of the *HTB1* mRNAs, but the subsequent degradation of the mRNAs was greatly reduced. This reduced turnover of the *HTB1* mRNAs was similar to that observed in the *Δrrp6* mutant alone, confirming the earlier findings that the nuclear exosome is contributing to degrading the transcripts. Under conditions where Rna14p was inactivated, the endogenous *HTB1* transcripts accumulated and subsequently slowly decreased over the course of the cell cycle at both the permissive and non-permissive temperatures in the *rna14-3/Δrrp6* background. The turnover of the *HTB1* transcripts was greatly reduced at both temperatures, but was observed to be longer in the non-permissive temperature. This indicates that Rna14p contributes to the delayed turnover of the *HTB1* mRNAs and plays a role in the cell cycle. RT-PCR revealed that 3'-end processing and termination were impaired at all stages of the cell cycle in the *rna14-3/Δrrp6* background at 37°C, suggesting that there is no specific accumulation of read-through pre-mRNAs. In Chapter 4, the data established a potential communication link between transcription termination, 3'-end processing and the nuclear exosome during the cell cycle.

The export of *HTB1* levels likely requires Rat7p, but is independent of Rip1p

As seen in Chapters 3 and 4, the results revealed that the cleavage factor (CFIA) and the nuclear exosome are important for histone mRNA biogenesis. Additionally, it has been acknowledged that correct 3'-end processing of mRNAs and appropriate degradation of aberrant mRNAs are required for efficient transport of the transcripts from nucleus to the cytoplasm (Vinciguerra and Stutz, 2004). It was of interest to examine the export mechanism of histone mRNAs from the nucleus, which is the concluding step in histone mRNA biogenesis before entering the cytoplasm for translation. The nuclear pore complex (NPC) is the only channel between the nucleus and cytoplasm that allows the mRNA to enter the cytoplasm. Therefore, in Chapter 5, the two nucleoporins, Rat7 and Rip1, which are components of the NPC, were investigated to increase our knowledge of the possible export of histone mRNAs.

The Northern blot analysis demonstrated that the endogenous *HTB1* transcripts in the *rat7-1* background were reduced compared to RAT7, suggesting that RAT7 played a role in the endogenous *HTB1* mRNA levels. As expected, the endogenous *HTB1* transcripts were restored in the *rat7-1/Δrrp6* mutant. The restored transcripts indicated that the deletion in the RAT7 gene caused the transcripts to be retained, while the deletion of the RRP6 gene caused no degradation of its substrates at the non-permissive temperature. The presence of the WT DDE and DDE mutant *neo-HTB1* mRNAs did not alter the endogenous *HTB1* profile.

To clarify whether the DDE contributed to *neo-HTB1* mRNA levels, the export mutant strains expressing the *neo-HTB1* DDE mutants were probed with the neo-*HTB1* specific probe. At the permissive temperature, little *neo-HTB1* mRNAs were observed with the DDE mutants, pSAC15 and pSAC21, in the *rat7-1* background. Evidence from quantification analysis revealed that the WT DDE and DDE mutant, pSAC20, were more

stable than pSAC15 and pSAC21. The fundamental reason for pSAC15 and pSAC21 *neo-HTB1* mRNAs being unstable in the *rat7-1* background is unclear. Similar analysis was observed with the DDE mutants in the *rna14-3* background. The reduced levels may be caused by alterations in the half-life of the RNA or possibly the quality of the RNA during the RNA extractions. This role of the DDE in mRNA export requires further research to allow definite conclusions to be drawn. At the non-permissive temperature in the *rat7-1* background, the *neo-HTB1* mRNA levels were reduced, signifying that Rat7 is likely to be important for *neo-HTB1* mRNA export. The increase in stabilisation of the *neo-HTB1* mRNAs in the double mutant, *rna14-3/Δrrp6*, was not observed as being similar to the endogenous *HTB1* mRNAs, suggesting that the *neo-HTB1* mRNA may be degraded by a mechanism independent of the nuclear exosome in the *rat7* background.

Having established that RAT7 contributed to the steady state levels of *neo-HTB1* mRNAs, we next examined the protein levels in the export strains harbouring the WT DDE and DDE mutants, using G418 resistance as a marker for functional protein production. Unexpectedly, the RAT7 cells containing the WT DDE showed a low level of resistance, whereas the DDE mutants demonstrated no resistance when incubated at 37°C. Since growth of cells containing the WT DDE and DDE mutants at 37°C were not impaired in the absence of G418, this indicated that there may possibly be specific inhibition of the export and/or translation of the *neo-HTB1* mRNAs at 37°C in the RAT7 background. It is accepted that Gle1p and Rat8p dissociates from the mRNA under stress conditions (Rollenhagen *et al*, 2004). Therefore, it may be possible that Rat7p dissociates from the NPC at the non-permissive temperature. A low level of G418 resistance was observed at 22°C in the *rat7-1* background, which was consistent with the Northern blots, since reduced *neo-HTB1* mRNAs were observed in the *rat7-1* background. No G418 resistance was observed in *rat7-1* cells at 37°C. Clearly, the data indicates that the export of

neo-HTB1 mRNAs is inhibited, which is consistent with Hilleren *et al* (2001) as they showed that the export of the PGK1pG transcripts were inhibited in the *rat7-1* background (Hilleran and Parker, 2001). There was no increase in the steady state levels of the *neo-HTB1* transcripts in the double mutant background, *rat7-1/Δrrp6*, at 37°C. This was consistent with the previous Northern blots since no stabilisation of the *neo-HTB1* mRNAs was observed at 37°C. Taken together, the data indicates that the *neo-HTB1* mRNA levels in the WT and export mutants is unstable at 37°C and defends the theory that the instability of the *neo-HTB1* mRNA is independent of RRP6 at 37°C.

The export factor, Nup42/Rip1p, was examined to determine its involvement in the steady state levels of the *neo-HTB1* mRNAs. Quantification analysis suggested that the endogenous *HTB1* and *ACT1* mRNAs were not altered in the mutant background, *rip1-1*, under non-stressed conditions. Hence, the results indicated that Nup42/Rip1 was a non-essential factor in *HTB1* processing. Previous studies have shown that Rip1p performs under stress conditions and only allows mRNAs encoding heat-shock proteins being exported (Bond, 2006). Supplementary work is necessary to establish if Rip1p plays a role with endogenous *HTB1* mRNAs under stress conditions.

Endogenous *HTB1* messenger RNA levels are reduced in the pop1 strains

Yeast three-hybrid analyses have established that Pop4, an RNase P/RNase MRP component, interacts directly with the distal downstream element (DDE) of the yeast histone model (Beglan and Bond, unpublished data). This prompted us to investigate the assumption that Pop1p, which is another member of the RNase P/RNase MRP complex, may recognise the DDE sequences by surveying the *neo-HTB1* and endogenous *HTB1* mRNAs in the *pop1-1* background. Examination of the RNase P/RNase MRP mutant, *pop1-1*, revealed that the rRNA levels were low at the non-permissive temperature. The

low rRNA levels were consistent with data from Tollervey *et al* (1994), signifying that rRNA synthesis was defective (Tollervey *et al*, 1994). The interesting facet was that the *neo-HTB1* and endogenous *HTB1* mRNAs were also reduced at both temperatures, 22°C and 37°C, in the *pop1-1* mutant. Quantification analysis indicated that the *ACT1* mRNA levels between the W303 and *pop1-1* strains are similar. Therefore, when mRNAs from the the *pop1-1* mutant were compared to wild type, a greater difference in abundance was noted for the *neo-HTB1* and endogenous *HTB1* mRNAs compared to the *ACT1* mRNA. The rationalisation for the mRNA reduction was that there was a high level of turnover/degradation in the *pop1-1* background. This hypothesis is supported by Gill *et al* (2004), who demonstrated that the RNase MRP complex functions in RNA degradation and cell-cycle regulation with the CLB2 mRNA in *Saccharomyces cerevisiae* (Gill *et al*, 2004). Furthermore, the DDE mutants, pSAC15, pSAC20 and pSAC21, did not differ from the WT DDE, indicating that the Pop1 protein does not recognise the DDE region. Advance study is required to confirm the role of RNase MRP/RNase P complexes in histone mRNA biogenesis.

This thesis presents new research by investigating 3'-end processing, nuclear degradation, termination, ribonucleases and export in histone mRNA biogenesis. Initially, before this research was conducted, the mechanisms in yeast histone biogenesis were unclear. This is the first time that an investigation into the nuclear exosome, cleavage, ribonucleases and export factors where shown to be required for histone processing. This project uncovers the communications and mechanisms required for the efficient production of yeast histones. In addition, cell-cycle experiments reveal that the nuclear exosome plays a role in the degradation of *HTB1* mRNAs as the cells enter the G_2-phase and that 3'-end cleavage may also contribute to this process. Defects in 3'-end processing, degradation and export mechanisms in humans can alter cell viability and normal development. Defects in 3'-end

processing by depletion of CstF-64 causes cell-cycle arrest and apoptosis. Loss of cleavage activity in mammals also causes thrombosis, or development of blood clots (Zoller *et al*, 1999). Defects in Poly (A) polymerase (PAP) and poly (A)-binding protein II (PAB II) have been implicated in apoptosis, lymphocytic leukaemia, breast cancer and oculopharyngeal muscular dystrophy (Scorilas, 2002). Further understanding of yeast histone mRNA biogenesis will lead to an increase in understanding of the mammalian cell. This may also assist in resolving some mammalian diseases.

Chapter 8

References

Ahn, S.H., Buratowski, S. and Kim, M. (2004) Phosphorylation of serine 2 within the RNA polymerase II C-terminal domain couples transcription and 3'-end processing, *Mol Cell*, Vol. 13, pp. 67-76.

Alberts, B., Johnson, A. and Lewis, J. (2002) *Molecular Biology of the cell*. New York: Garland.

Allen, T., Cronshaw, J., Bagley S., Kiseleva E. and Goldberg, M. (2000) The nuclear pore complex: Mediator of translocation between nucleus and cytoplasm, *J Cell Sci*, No. 113, pp. 1651-59.

Allmang, C., Mann, M., Petfalski E., Podtelejnikov A., Tollervey D. and Mitchell, P. (1999) The yeast exosome and human PM-Scl related complexes of 3'→5' exonucleases, *Genes Dev*, Vol. 13, pp. 2148-58.

Altheim, B. and Schultz, M. (1999) Histone modification governs the cell-cycle regulation of a replication-independent chromatin assembly pathway in *Saccharomyces cerevisiae*, *PNAS*, Vol. 96, pp. 1345-50.

Amrani, N., Wyers, F. and Lacroute, F. (1997) PCF11 encodes a third protein component of yeast cleavage and polyadenylation factor I, *Mol Cell Biol*, Vol. 17, pp. 1102-09.

Ansari, A. and Hampsey, M. (2005) A role for the CPF 3'-end processing machinery in RNAP II-dependent gene looping, *Genes Dev*, Vol. 19, pp. 2969-78.

Arigo, J., Carroll, K., Ames, J. and Corden, J. (2006) Regulation of yeast NRD1 expression by premature transcription termination, *Mol Cell*, Vol. 21, pp. 641-51.

Bailer, S., Balduf, C., Katahira J., Podtelejnikov A., Rollenhagen C., Mann M., Pante N. and Hurt, E. (2000) Nup116p associates with the Nup82p-Nsp1p-Nup159p nucleoporin complex, *J Biol Chem*, Vol. 275, pp. 23540-48.

Barabino, S., Jenny, A., Minvielle-Sebastia L., Hubner W. and Keller, W. (1997) The 30-kD subunit of mammalian cleavage and polyadenylation specificity factors and its yeast homolog are RNA-binding zinc finger proteins, *Genes Dev*, Vol. 11, pp. 1703-16.

Barilla, D., Lee, B. and Proudfoot, N. (2001) Cleavage/polyadenylation factor IA associates with the carboxyl-terminal domain of RNA polymerase II in *Saccharomyces cerevisiae*, *PNAS*, Vol. 98, pp. 445-50.

Battle, D. and Doudna, J. (2001) The stem-loop binding protein forms a highly stable and specific complex with the 3' stem-loop of histone mRNAs, *RNA*, No. 7, pp. 123-32.

Baxevanis, A. and Landsman, D. (1997) Histone and histone fold sequence and structures: A database, *Nuc Acids Res*, Vol. 25, pp. 272-73.

Baxevanis, A. and Landsman, D. (1998) Histone sequence database: New histone fold family members, *Nuc Acids Res*, Vol. 27, pp. 372-75.

Belgareh, N., Snay-Hodge, C., Pasteau, F., Cole, C. and Doye, V. (1998) Functional characterisation of a Nup159p-containing nuclear pore complex, *Mol Cell Biol*, Vol. 9, pp. 3475-92.

Benoit, B., Juge, F., Iral, F., Audibert, A. Simonelig, M. (2002) Chimeric human CstF-77/*Drosophila* suppressor of forked proteins rescue suppressor of forked mutant lethality and mRNA 3'-end processing in *Drosophila*, *PNAS*, Vol. 99, pp. 10593-98.

Birse, C., Proudfoot, N., Lee B., Keller W. and Minvielle-Sebastia, L. (1998) Coupling termination to transcription to messenger RNA maturation in yeast, *Science*, Vol. 280, pp. 298-301.

Bond, U. (2006) Stressed out! Effects of environmental stress on mRNA metabolism, *FEMS Yeast Res*, Vol. 6, pp. 160-70.

Bond, U. and Yario, T. (1994) The steady state levels and structure of the U7 snRNP are constant during the human cell cycle: Lack of cell-cycle regulation of histone mRNA 3'-end formation, *Cell Mol Biol Res*, Vol. 40, pp. 27-34.

Bond, U., Yario, T. and Steitz, J. (1991) Multiple processing-defective mutations in a mammalian histone pre-mRNA are suppressed by compensatory changes in U7 RNA both in vivo and in vitro, *Genes Dev*, No. 5, pp. 1709-22.

Brodsky, A. and Silver, P. (2000) Pre-mRNA processing factors are required for nuclear export, *RNA*, Vol. 6, pp. 1737-49.

Brouwer, R., Pruijn, G.J. and Venrooij, J.V. (2001) The human exosome: An autoantigenic complex of exoribonucleases in myositis and scleroderma, *Arthritis Res*, No. 3, pp. 102-06.

Burkard, K. and Butler, S. (2000) A nuclear 3′-5′ exonuclease involved in mRNA degradation interacts with poly (A) polymerase and the hnRNA protein Npl3p, *Mol Cell Biol*, Vol. 20, pp. 604-16.

Butler, S. (2002) The yin and yang of the exosome, *Trends in Cell Biol*, Vol. 12, pp. 90-96.

Butler, S., Sadhale, P. and Platt, T. (1990) RNA processing in vitro produces mature 3'-ends of a variety of *Saccharomyces cerevisiae* mRNAs, *Mol Cell Biol*, Vol. 6, pp. 2599-2605.

Cai, T., Aulds, J., Gill T., Cerio M., and Schmitt, M. (2002) The *Saccharomyces cerevisiae* RNase mitochondrial RNA processing is critical for cell cycle progression at the end of mitosis, *Genetics*, Vol. 161, pp. 1029-42.

Calvo, O. and Manley, J. (2001) Evolutionary conserved interaction between CstF-64 and PC4 links transcription, polyadenylation and termination, *Mol Cell*, Vol. 7, pp. 1013-23.

Calvo, O. and Manley, J. (2005) The transcriptional coactivator PC4/Sub1 has multiple functions in RNA polymerase II transcription, *EMBO J*, Vol. 24, pp. 1009-20.

Campbell, S., Bond, U., Olmo, M. li del, and Beglan, P. (2002) A sequence element downstream of the yeast *HTB1* gene contributes to mRNA 3'-end processing and cell-cycle regulation, *Mol Cell Biol*, Vol. 22, pp. 8415-25.

Canadillas, P., Manuel, J. and Varani, G. (2003) Recognition of GU-rich polyadenylation regulatory elements by human CstF-64 protein, *EMBO J*, Vol. 22, pp. 2821-30.

Cho, D., Scharl, E. and Steitz, J. (1995) Decreasing the distance between the two conserved sequence elements of histone pre-messenger RNA interferes with 3'-end processing in vitro, *RNA*, Vol. 1, pp. 905-14.

Cole, C., Dartmouth University, personal communications.

Cole, C. and Scarcelli, J. (2006) Transport of messenger RNA from the nucleus to the cytoplasm, *Curr Opin Cell Biol*, Vol. 18, pp. 299-306.

Colgan, D. and Manley, J. (1997) Mechanism and regulation of mRNA polyadenylation, *Genes Dev*, No. 11, pp. 2755-66.

Dantonel, J-C. and Laszlo, T. (1997) Transcription factor TFIID recruits factor CPSF for formation of 3'-end of mRNA, *Nature*, Vol. 398, pp. 399-402.

Darnell, J. (2000) *Molecular Cell Biology*. New York: WH Freeman.

Dejong, E., Marzluff, W. and Nikonowicz, E. (2002) NMR structure and dynamics of the RNA-binding sire for the histone mRNA stem-loop binding protein, *RNA*, Vol. 8, pp. 83-96.

Dheur, S. and Minivielle-Sebastia, L. (2003) Pti1p and Ref2p found in association with the mRNA 3'-end formation complex direct snoRNA maturation, *EMBO J*, Vol. 22, pp. 2831-40.

Dheur, S. and Minivielle-Sebastia, L. (2005) Yeast mRNA poly (A) tail length control can be reconstituted in vitro in the absence of pab1p-dependent poly (A) nuclease activity, *J Biol Chem*, Vol. 280, No.26, pp. 24532-8.

Dichtl, B., Blank, D. and Keller, W. (2002a) A role for SSU72 in balancing RNA polymerase II transcription elongation and termination, *Mol Cell*, Vol. 10, pp. 1139-50.

Dichtl, B., Blank, D., Sadowski M., Hubner W., Weiser S. and Keller, W. (2002b) Yhh1p/Cft1p directly links poly (A) site recognition and RNA polymerase II transcription termination, *EMBO J*, Vol. 21, pp. 4125-35.

Dichtl, B. and Tollervey, D. (1997) Pop3p is essential for the activity of the RNase MRP and RNase P ribonucleoproteins in vivo, *EMBO J*, Vol. 16, pp. 417-29.

Dominski, Z., Erkmann, J., Yang X., Sanchez R. and Marzluff, W. (2002) A novel zinc finger protein is associated with U7 snRNP and interacts with the stem-loop binding protein in the histone pre-mRNP to stimulate 3'-end processing, *Genes Dev*, Vol. 16, pp. 58-71.

Dominski, Z. and Marzluff, W. (1999) Formation of the 3'-end of histone mRNA, *Gene*, Vol. 239, pp. 1-14.

Dominski, Z., Yang, XC., Kaygun H., Dadlez M. and Marzluff, W. (2003) A 3' exonuclease that specifically interacts with the 3'-end of histone mRNA, *Mol Cell*, Vol. 12, pp. 295-305.

Dominski, Z., Yang, X-c. and Marzluff, W. (2005) The polyadenylation factor CPSF-73 is involved in histone pre-mRNA processing, *Cell*, Vol. 123, pp. 37-48.

Dunn, E., Hammell, C., Hodge, C. and Cole, C. (2005) Yeast poly (A) binding protein, Pab1, and PAN, a poly (A) nuclease complex recruited by pab1, connect mRNA biogenesis to export, *Genes Dev*, Vol. 19, pp. 90-103.

Eenennaam, H.V., Heijden, A. van der, and Pruijn, G. (2001a) Basic domains target protein subunits of the RNase MRP complex to the nucleolus independently of complex association, *Mol Cell Biol*, Vol. 12, pp. 3680-89.

Eenennaam, H.V., Lugtenberg, D., Vogelzangs J., van Venrooij W., and Pruijn, G. (2001b) hPop5, a protein subunit of the human RNase MRP and RNase P endoribonucleases, *Jour Biol Chem*, Vol. 276, pp. 31635-641.

Ericksson, P., Mendiratta, G. and Clark, D. (2005) Global regulation by the yeast Spt10 protein is mediated through chromatin structure and the histone upstream activating sequence elements, *Mol Cell Biol*, Vol. 25, pp. 9127-37.

Fahrner, K., Yarger, J. and Hereford, L. (1980) Yeast histone mRNA is polyadenylated, *Nucleic Acids Res*, Vol. 8, pp. 5725-37.

Gavin, A-c., Krause, R. and Superti-Furga, G. (2002) Functional organisation of the yeast proteome by systematic analysis of protein complexes, *Nature*, Vol. 415, pp. 141-47.

Gilbert, W. and Guthrie, C. (2004) The Glc7p nuclear phosphatase promotes mRNA export by facilitating association of Mex67p with mRNA, *Mol Cell*, Vol. 13, pp. 201-12.

Gill, T., Aulds, J. and Schmitt, M. (2006) A specialised processing body that is temporally and asymmetrically regulated during the cell cycle in *Saccharomyces cerevisiae*, *J Cell Biol*, Vol. 173, pp. 35-45.

Gill, T., Cai, T., Aulds, J., Wierzbicki, S. and Schmitt, M. (2004) RNase MRP cleaves the CLB2 mRNA to promote cell cycle progression: Novel method of mRNA degradation, *Mol Cell Biol*, Vol. 24, pp. 945-53.

Gorsch, L., Dockendorff, T. and Cole, C. (1995) A conditional allele of the novel repeat-containing yeast nucleoporin RAT7/NUP159 causes both rapid cessation of mRNA export and reversible clustering of nuclear pore complexes, *Jour Cell Biol*, Vol. 129, pp. 939-55.

Gromak, N., West, S. and Proudfoot, N. (2006) Pause site promotes transcriptional termination of mammalian RNA polymerase II, *Mol Cell Biol*, Vol. 26, pp. 3986-96.

Gross, S. and Moore, C. (2001a) Five subunits are required for reconstitution of the cleavage and polyadenylation activities of *Saccharomyces cerevisiae* cleavage factor I, *PNAS*, Vol. 98, pp. 6080-85.

Gross, S. and Moore, C. (2001b) An RNA15 interaction with the A-rich yeast polyadenylation signal is an essential step in mRNA 3'-end formation, *Mol Cell Biol*, Vol. 21, pp. 8045-55.

Grunstein, M. and Mann, R. (1992) *Histones: Regulators of transcription in yeast*. Cold Spring Harbour Press, pp. 1295-1316.

Guisbert Karen, Li Hao and Gutherie Christine. (2006) *Saccharomyces cerevisiae* is modulated by Nab4/Hrp1 *in vivo*. PLos Biol, Vol.5, No.1.

Hagiwara, M. and Nojima, T. (2007) Cross-talks between transcription and post-transcriptional events within a 'mRNA factory', *J Biochem*.

Hana, K. and Lee, Y. (2001) Interaction of poly (A) polymerase with the 25-kDa subunit of cleavage factor I, *Biochem Biophys Res Commun*, Vol. 289, pp. 513-18.

Harris, Bohni R., Schneiderman M., Ramamurthy L., Schumperli D and Marzluff., W. (1991) Regulation of histone mRNA in the unperturbed cell cycle: Evidence suggesting control at two post-transcriptional steps, *Mol Cell Biol*, Vol. 11, pp. 2416-24.

He, X., Cheng, H., Pappas D., Hampsey M. and Moore, C. (2003) Functional interactions between the transcription and mRNA 3'-end processing machineries mediated by Ssu72 and Sub1, *Genes Dev*, Vol. 17, pp. 1030-42.

He, X. and Moore, C. (2005) Regulation of yeast mRNA 3'-end processing by phosphorylation, *Cell*, Vol. 19, pp. 619-29.

Hector, R., Wilson, S. and Swanson, M. (2002) Dual requirement for yeast hnRNP Nab2p in mRNA poly (A) tail length control and nuclear export, *EMBO J*, Vol. 21, pp. 1800-10.

Heintz, N. (1991) The regulation of histone gene expression during the cell cycle, *Biochimica et Biophysica Acta*, No. 1088, pp. 327-39.

Helden, J.V., Olmo, M. and Perez-Ortin, J. (2000) Statistical analysis of yeast genomic downstream sequences reveals putative polyadenylation signals, *Nucleic Acids Res*, Vol. 28, pp. 1000-10.

Helmling, S., Zhelkovsky, A. and Moore, C. (2001) Fip1 regulates the activity of poly (A) polymerase through multiple interactions, *Mol Cell Biol*, Vol. 21, pp. 2026-37.

Hereford, L. and Osley, M. (1981) Cell-cycle regulation of yeast histone mRNA, *Cell*, Vol. 24, pp. 367-75.

Hilleren, P. and Parker, R. (2001) Defects in the mRNA factors Rat7p, Gle1p, Mex67p and Rat8p cause hyperadenylation during 3'-end formation of nascent transcripts, *RNA*, Vol. 7, pp. 753-64.

Hilleren, P., Rosbash, M., Parker, R. and Jensen, T.H. (2001) Quality control of mRNA 3'-end processing is linked to the nuclear exosome, *Nature*, Vol. 413, pp. 538-42.

Hirose, Y. and Manley, J. (1998) RNA polymerase II is an essential mRNA polyadenylation factor, *Nature*, Vol. 395, pp. 93-96.

Hodge, C., Colot, H., Stafford, P. and Cole, C. (1999) Rat8p/Dbp5p is a shuttling transport factor that interacts with Rat7p/Nup159p and Gle1p and suppresses the mRNA export defect of xpo1-1 cells, *EMBO J*, Vol. 18, pp. 5778-88.

Hoffman, I. and Birnstiel, M. (1990) Cell cycle-dependent regulation of histone precursor mRNA processing by modulation of U7 snRNA accessibility, *Nature*, Vol. 346, pp. 665-68.

Hoof, A.V., Lennertz, P. and Parker, R. (2000) Yeast exosome mutant accumulate 3'-extended polyadenylated forms of U4 small nuclear RNA and small nucleolar RNAs, *Mol Cell Biol*, Vol. 20, pp. 441-52.

Houser-Scott, F., Xiao, S., Millikin C., Zengel J., Lindahl L. and Engelke, D. (2002) Interactions among the protein and RNA subunits of *Saccharomyces cerevisiae* nuclear RNase P, *PNAS*, Vol. 99, pp. 2684-89.

Howe, J.K. (2002) RNA polymerase II conducts a symphony of pre-mRNA processing activities, *Biochimica et Biophysica Acta*, Vol. 1577, pp. 308-24.

Ito, H., Fukuda, Y., Murata, K. and Kimura, A. (1983) Transformation of intact yeast cells treated with alkali cations, *J Bacteriol*, Vol. 153, pp. 163-68.

Jaeger, S., Barends, S., Giege R., Eriani G. and Martin, F. (2005) Expression of metazoan replication-dependent histone genes, *Biochimie*, No. 87, pp. 827-34.

Jenny, A., Hauri, H-P. and Walter, K. (1994) Characterisation of cleavage and polyadenylation specificity factor and cloning of its 100-kilodalton subunit, *Mol Cell Biol*, Vol. 14, pp. 8183-90.

Jenny, A. and Keller, W. (1996) Sequence similarity between the 73-kilodalton protein of mammalian CPSF and a subunit of yeast polyadenylation factor I, *Science*, No. 274, pp. 1514-17.

Jensen, T.H., Dower, K., Libri, D. and Rosbash, M. (2003) Early formation of mRNP: License for export or quality control?, *Mol Cell*, Vol. 11, pp. 1129-38.

Jimeno, S., Rondon, A., Luna, R. and Aguilera, A. (2002) The yeast THO complex and mRNA export factors link metabolism with transcription and genome instability, *EMBO J*, Vol. 21, pp. 3526-35.

Kaufmann, I., Martin, G., Friedlein A., Langen H. and Keller, W. (2004) Human Fip1 is a subunit of CPSF that binds to U-rich RNA elements and stimulates poly (A) polymerase, *EMBO J*, Vol. 23, pp. 616-26.

Kerwitz, Y., Kühn, U., Lilie, H., Knoth, A., Scheuermann, T. and Wahle, E. (2003) Stimulation of poly (A) polymerase through a direct interaction with the nuclear poly (A) binding protein allosterically regulated by RNA, *EMBO J*, Vol. 22, pp. 3705-14.

Kessler, M., Gross, S., Henry M., Shen E., Zhao J., Silver P. and Moore, C. (1997) Hrp1, a sequence-specific RNA-binding protein that shuttles between the nucleus and the cytoplasm, is required for mRNA 3'-end formation in yeast, *Genes Dev*, No. 11, pp. 2545-56.

Kim, M., Vasiljeva, L., Rando O., Zhelkovskey, A. and Buratowski, S. (2006) Distinct pathway for snoRNA and mRNA termination. *Mol Cell*, Vol. 24, No.5, pp. 723-34.

Kim, M., Buratowski, S., Rando O., Nedea E., Greenblatt J., Krogan N., and Vasiljeva, L. (2004) The yeast Rat1 exonuclease promotes transcription termination by RNA polymerase II, *Nature*, Vol. 432, pp. 517-22.

Kiseleva, E., Allen, T., Rutherford, S. and Goldberg, M. (2004) Yeast nuclear pore complexes have a cytoplasmic ring and internal filaments, *J Struc Biol*, No. 145, pp. 272-88.

Kolev, N. and Steitz, J. (2005) Symplekin and multiple other polyadenylation factors participate in 3'-end maturation of histone mRNAs, *Genes Dev*, Vol. 19, pp. 2583-92.

Komarnitsky, P., Cho, E-J. and Buratowski, S. (2000) Different phosphorylated forms of RNA polymerase II and associated mRNA processing factors during transcription, *Genes Dev*, No. 14, pp. 2452-60.

Krieg, P. (1996) A laboratory guide to RNA: Isolation, analysis and synthesis. New York: John Wiley, pp. 44-45.

Kyburz, A., Sadowski, M., Dichtl, B. and Keller, W. (2003) The role of the yeast cleavage and polyadenylation factor subunit Ydh1p/Cft2p in pre-mRNA 3'-end formation, *Nucleic Acids Res*, Vol. 31, pp. 3936-45.

LaCava, J., Houseley, J., Saveanu, C., Petfalski E., Thompson E., Jacquier A. and Tollervey, D. (2005) RNA degradation by the exosome is promoted by a nuclear polyadenylation complex, *Cell*, Vol. 121, pp. 713-24.

Lang, W., Platt, T. and Reeder, R. (1998) *Escherichia coli* rho factor induces release of yeast RNA polymerase II, but not polymerase I or III, *PNAS*, Vol. 95, pp. 4900-05.

Lee, J-Y. and Engelke, D. (1989) Partial characterisation of an RNA component that co-purifies with *Saccharomyces cerevisiae* RNase P, *Mol Cell Biol*, Vol. 9, pp. 2536-43.

Li, X., Sephorah, Z. and Lindahl, L. (2004) Identification of a functional core in the RNA component of RNase MRP of budding yeasts, *Nucleic Acids Res*, Vol. 32, pp. 3703-11.

Libri, D., Boulay J., Thomsen R., Rosbash M. Dower, K. and Jensen, H. (2002) Interactions between mRNA export commitment, 3'-end quality control and nuclear degradation, *Mol Cell Biol*, Vol. 22, pp. 8254-66.

Licatalosi, D., Geiger G., Minet M., Schroeder S., Cilli K., McNeil JB.,and Bentley, D. (2002) Functional interaction of yeast pre-mRNA 3'-end processing factors with RNA polymerase II, *Mol Cell*, Vol. 9, pp. 1101-11.

Lindahl, L., Fretz, S., Epps, N. and Zengel, J. (2000) Functional equivalence of hairpins in the RNA subunits of RNase MRP and RNase P in *Saccharomyces cerevisiae*, *RNA*, No. 6, pp. 653-58.

Lund, M. and Guthrie, C. (2005) The DEAD-Box protein Dbp5p is required to dissociate Mex67p from exported mRNPs at the nuclear rim, *Mol Cell*, Vol. 20, pp. 645-51.

Luo, W., Johnson, A. and Bentley, D. (2006) The role of Rat1 in coupling mRNA 3'-end processing to transcription termination: Implications for a unified allosteric-torpedo model, *Genes Dev*, No. 20, pp. 1050-56.

Luscher, B. and Schumperli, D. (1987) RNA 3' processing regulates histone mRNA levels in a mammalian cell cycle mutant. A processing factor becomes limiting in G1-arrested cells, *EMBO J*, Vol. 6, pp. 1721-26.

Lycan, D., Osley, M.A. and Hereford, L. (1987) Role of transcriptional and post-transcriptional regulation in expression of histone genes in *Saccharomyces cerevisiae*, *Mol Cell Biol*, Vol. 7, pp. 614-21.

Mandart, E. and Parker, R. (1995) Effects of mutations in the *Saccharomyces cerevisiae* RNA14, RNA15 and PAP1 genes on polyadenylation in vivo, *Mol Cell Biol*, Vol. 15, pp. 6979-86.

Mangus, D., Evans, M. and Jacobson, A. (2003) Poly (A) binding proteins: Multifunctional scaffolds for the post-transcriptional control of gene expression, *Genome Biol*, No. 4, p. 223.

Mangus, D., Evans, M. and Jacobson, A. (2004a) Positive and negative regulation of poly (A) nuclease, *Mol Cell Biol*, Vol. 24, pp. 5521-33.

Mangus, D., Smith, M. and Jacobson, A. (2004b) Identification of factors regulating poly (A) tail synthesis and maturation, *Mol Cell Biol*, Vol. 24, pp. 4196-4206.

Manley, J. and Takagaki, Y. (1996) The end of the message — Another link between yeasts and mammals, *Science*, Vol. 274, pp. 1481-82.

Martin, F., Schaller, A., Eglite, S., Schumperli, D. and Muller, B. (1997) The gene for histone RNA hairpin binding protein is located on human chromosome 4 and encodes a novel type of RNA binding protein, *EMBO J*, Vol. 16, No. 4, pp. 769-78.

Marzluff, W. (2005) Metazoan replication-dependent histone mRNAs: A distinct set of RNA polymerase II transcripts, *Curr Opin Cell Biol*, Vol. 17, pp. 274-80.

McCracken, S., Fong, N., Yankulov, K. and Bentley, D. (1997) The C-terminal domain of RNA polymerase II couples mRNA processing to transcription, *Nature*, Vol. 385, pp. 357-61.

Milligan, L., Tollervey, D., Allmang C., Shipman T. and Torchet, C. (2005) A nuclear surveillance pathway for mRNAs with defective polyadenylation, *Mol Cell Biol*, Vol. 25, pp. 9996-10004.

Murthy, K. and Manley, J. (1995) The 160-kD subunit of human cleavage-polyadenylation specificity factor co-ordinates pre-mRNA 3'-end formation, *Genes Dev*, Vol. 9, pp. 2672-83.

Nadea, E., Moore, C. and Greenblatt, J. (2003) Organisation and function of APT, a subcomplex of the yeast cleavage and polyadenylation factor involved in the formation of mRNA and small nucleolar RNA 3'-ends, *J Biol Chem*, Vol. 278, pp. 33000-10.

Noble, C., Beuth, B. and Taylor I. (2007) Structure of nucleotide-bound Clp1-Pcf11 polyadenylation factor, *Nucleic Acids Res*, Vol. 35, No.1, pp. 87-99.

Noble, C., Hollingworth, D., Martin S., Ennis-Adeniran V., Smerdon S., Kelly G., Taylor I. and Ramos, A. (2005) Key features of the interaction between Pcf11 CID and RNA polymerase II CTD, *Nat Struc Mol Biol*, Vol. 12, pp. 144-51.

Noble, C., Walker, P., Calder, I. and Taylor, I. (2004) Rna14-Rna15 assembly mediates the RNA-binding capability of *Saccharomyces cerevisiae* cleavage factor IA, *Nucleic Acids Res*, Vol. 32, pp. 3364-75.

Ohnacker, M., Preker, P. and Keller, W. (2000) The WD-repeat protein Pfs2p bridges two essential factors within the yeast pre-mRNA 3'-end processing complex, *EMBO J*, Vol. 19, pp. 37-47.

Osley, M. and Lycan, D. (1987) Trans-acting regulatory mutations that alter transcription of *Saccharomyces cerevisiae* histone genes, *Mol Cell Biol*, Vol. 7, pp. 4204-10.

Pandey, N., Bond, U., Williams A., Sun J., Brown V. and Marzluff, W. (1994) Point mutations in the stem-loop at the 3'-end of mouse histone mRNA reduce expression by reducing the efficiency of 3'-end formation, *Mol Cell Biol*, Vol. 14, pp. 1709-20.

Pappas, D. and Hampsey, M. (2000) Functional interaction between Ssu72 and the Rpb2 subunit of RNA polymerase II in *Saccharomyces cerevisiae*, *Mol Cell Biol*, Vol. 20, pp. 8343-51.

Park, N., Martinson, H. and Tsao, D. (2004) The two steps of poly (A)-dependent termination, pausing and release, can be uncoupled by truncation of the RNA polymerase II carboxyl-terminal repeat domain, *Mol Cell Biol*, Vol. 24, pp. 4092-4103.

Preker, P., Lingner, J., Minivielle-Sebastia, L. and Keller, W. (1995) The FIP1 gene encodes a component of a yeast pre-mRNA polyadenylation factor that directly interacts with poly (A) polymerase, *Cell*, Vol. 81, pp. 379-89.

Proudfoot, N. (1998) How RNA polymerase II terminates transcription in higher eukaryotes, *Trends Biochem Sci*, Vol. 14, pp. 105-10.

Proudfoot, N. (2004) New perspectives on connecting messenger RNA 3'-end formation to transcription, *Curr Opin Cell Biol*, Vol. 16, pp. 272-80.

Proudfoot, N. and O'Sullivan, J. (2002) Polyadenylation: A tail of two complexes, *Curr Biol*, Vol. 12, pp. 855-57.

Reed, R. (2003) Coupling transcription, splicing and mRNA export, *Curr Opin Cell Biol*, Vol. 15, pp. 326-31.

Rigo, F. and Martinson, H. (2005) The RNA tether from the poly (A) signal to the polymerase mediates coupling of transcription to cleavage and polyadenylation, *Mol Cell*, Vol. 20, pp. 733-45.

Rollenhagen, C., Hodge, C. and Cole, C. (2004) The nuclear pore complex and the DEAD box protein Rat8p/Dbp5p have non-essential features which appear to facilitate mRNA export following heat shock, *Mol Cell Biol*, Vol. 24, pp. 4869-79.

Rosonina, E. and Blencowe, B. (2004) Analysis of the requirement for RNA polymerase II CTD heptapeptide repeats in pre-mRNA splicing and 3'-end cleavage, *RNA*, Vol. 10, pp. 581-89.

Rüegsegger, U., Beyer, K. and Keller, W. (1996) Purification and characterisation of human cleavage factor Im involved in the 3'-end processing of messenger RNA precursors, *J Biol Chem*, Vol. 271, pp. 6107-13.

Ryan, K., Calvo, O. and Manley, J. (2004) Evidence that polyadenylation factor CPSF-73 is the mRNA 3' processing endonuclease, *RNA*, No. 10, pp. 565-73.

Saavedra, C., Hammel, C., Heath, C. and Cole, C. (1997) Yeast heat shock mRNAs are exported through a distinct pathway defined by Rip1p, *Genes Dev*, Vol. 11, pp. 2845-56.

Salinas, C., Sinclair, D., O'Hare, K. and Brock, H. (1998) Characterisation of a *Drosophilia* homologue of the 160-kDa subunit of the cleavage and polyadenylation specificity factor CPSF, *Mol Gen Genet*, Vol. 157, pp. 672-80.

Salinas, K., Wierzbicki, S., Zhou, L. and Schmitt, M. (2005) Characterisation and purification of *Saccharomyces cerevisiae* RNase MRP reveals a new unique protein component, *J Biol Chem*, Vol. 280, pp. 11352-60.

Scharl, E. and Steitz, J. (1996) Length suppression in histone messenger RNA 3'-end maturation: Processing defects of insertion mutant premessenger RNAs can be compensated by insertions into the U7 small nuclear RNA, *PNAS*, Vol. 93, pp. 14659-64.

Sive, H., Heintz, N. and Roeder, R. (1986) Multiple sequence elements are required for maximal in vitro transcription of a human histone H2B gene, *Mol Cell Biol*, Vol. 6, pp. 3329-40.

Spector, M., Raff, A., DeSilva, H., Lee, K. and Osley, M. A. (1997) Hir1p and Hir2p functional as transcriptional corepressors to regulate histone gene transcription in the *Saccharomyces cerevisiae* cell cycle, *Mol Cell Biol*, Vol. 17, pp. 545-52.

Steinmetz, E. and Brow, D. (1998) Control of pre-mRNA accumulation by the essential yeast protein Nrd1 requires high-affinity transcript binding and a domain implicated in RNA polymerase II association, *PNAS*, Vol. 95, pp. 6699-6704.

Steinmetz, E. and Brow, D. (2003) Ssu72 protein mediates both poly (A)-coupled and poly (A)-independent termination of RNA polymerase II transcription, *Mol Cell Biol*, Vol. 23, pp. 6339-49.

Steinmetz, E., Conrad, N., Brow, D. and Corden, J. (2001) RNA-binding protein Nrd1 directs poly (A)-independent 3'-end formation of RNA polymerase II transcripts, *Nature*, Vol. 413, pp. 327-31.

Straber, K., Babler, J. and Hurt, E. (2000) Binding of the Mex67p/Mtr2p heterodimer to FXFG, GLFG and FG repeat nucleoporins is essential for nuclear mRNA export, *J Cell Biol*, Vol. 150, pp. 695-706.

Strahm, Y., Rosbash, M., Fahrenkrog B., Zenklusen D., Rychner E., Kantor J and Stutz, F. (1999) The RNA export factor Gle1p is located on the cytoplasmic fibrils of the NPC and physically interacts with the FG-nucleoporin Rip1p, the DEAD-box protein Rat8p/Dbp5p and a new protein Ymr255p, *EMBO J*, Vol. 18, pp. 5761-77.

Sutton, A., Bucaria, J., Osley, M. and Sternglanz, R. (2001) Yeast ASF1 protein is required for cell-cycle regulation of histone gene transcription, *Genetics*, No. 158, pp. 587-96.

Tacahashi, Y., Helmling, S. and Moore, C. (2003) Functional dissection of the zinc finger and flanking domains of the Yth1 cleavage/polyadenylation factor, *Nucleic Acids Res*, Vol. 31, pp. 1744-52.

Takagaki, Y. and Manley, J. (2000) Complex protein interactions within the human polyadenylation machinery identify a novel component, *Mol Cell Biol*, Vol. 20, pp. 1515-25.

Teixeira, A., West, S. and Thomas, B. (2004) Autocatalytic RNA cleavage in the human β-globin pre-mRNA promotes transcription termination, *Nature*, Vol. 432, pp. 526-30.

Thomsen, R., Libri, D., Boulay J., Rosbash M., and Jensen, T. (2003) Localisation of nuclear retained mRNAs in *Saccharomyces cerevisiae*, *RNA*, Vol. 9, pp. 1049-57.

Tollervey, D., Lygerou, Z., Mitchell, P., Petfalski, E. and Seraphin, B. (1994) The POP1 gene encodes a protein component common to the RNase MRP and RNase P ribonucleoprotein, *Genes Dev*, Vol. 8, pp. 1423-33.

Torchet, C., Bousquet-Antonelli, C., Milligan, L., Thompson E., Kufel J. and Tollervey, D. (2002) Processing of 3'-extended read-through transcripts by the exosome can generate functional mRNAs, *Mol Cell*, Vol. 9, pp. 1285-96.

Uetz, P., Giot, L., Cagney, G. and Rothberg, J. (2000) A comprehensive analysis of protein-protein interactions in *Saccharomyces cerevisiae*, *Nature*, Vol. 403, pp. 623-27.

Vasiljeva, L. and Buratowski, S. (2006) Nrd1 interacts with the nuclear exosome for 3' processing of RNA polymerase II transcripts, *Mol Cell*, Vol. 21, pp. 239-48.

Vinciguerra, P. and Stutz, F. (2004) mRNA export: An assembly line from genes to nuclear pores, *Curr Opin Cell Biol*, Vol. 16, pp. 285-92.

Vries, H. de, Ruegsegger, U., Hubner, W., Friedlein, A., Langen, H. and Keller, W. (2000) Human pre-mRNA cleavage factor IIm contains homologs of yeast proteins and bridges two other cleavage factors, *EMBO J*, Vol. 19, pp. 5895-5904.

Wagner, E. and Marzluff, W. (2006) ZFP100, a component of the active U7 snRNP limiting for histone pre-mRNA processing, is required for entry into S phase, *Mol Cell Biol*, Vol. 26, pp. 6702-12.

Wallace, R., Shaffer, J., Murphy, R., Bonner, J., Hirose, T. and Itakura, K. (1979) Hybridisation of synthetic oligodeoxyribonucleotides to phi chi 174 DNA: The effect of single base pair mismatch, *Nucleic Acids Res*, Vol. 6, pp. 3543-57.

Wang, S-W., Kazuhide, A., Win, T., Toda, T. and Norbury, C. (2005) Inactivation of the pre-mRNA cleavage and polyadenylation factor Pfs2 in fission yeast causes lethal cell cycle defects, *Mol Cell Biol*, Vol. 25, pp. 2288-96.

Welting, T. and Pruijn, G. (2004) Mutual interactions between subunits of the human RNase MRP ribonucleoprotein complex, *Nucleic Acids Res*, Vol. 32, pp. 2138-46.

West, S., Gromak, N. and Proudfoot, N. (2004) Human 5'→3' exonuclease Xrn2 promotes transcriptional termination at co-transcriptional cleavage sites, *Nature*, Vol. 432, pp. 522-25.

Whitfield, M., Zheng, L-X., Baldwin A., Ohta T., Hurt M. and Marzluff, W. (2000) Stem-loop binding protein, the protein that binds the 3'-end of histone mRNA, is cell-cycle regulated by both translational and post-translational mechanisms, *Mol Cell Biol*, Vol. 20, pp. 4188-98.

Woodhams, M. Stadler, P. Penny, D. and Collins, L. (2007) RNase MRP and the RNA processing cascade in the eukaryotic ancestor, *BMC Evolut Biol*, Vol. 7.

Williams, A. and Marzluff, W. (1995) The sequences of the stem and flanking sequences at the 3'-end of histone mRNA are critical determinants for the binding of the stem-loop binding protein, *Nucleic Acids Res*, Vol. 23, pp. 654-62.

Wu, R. and Bonner, W. (1981) Separation of basal histone synthesis from s-phase histone synthesis in dividing cells, *Cell*, Vol. 27, pp. 321-30.

Xiao, S. and Engelke, D. (2005) Characterisation of conserved sequences elements in eukaryotic RNase P RNA reveals roles in holoenzyme assembly and tRNA processing, *RNA*, Vol. 11, pp. 885-96.

Xiao, S., Engelke, D., Scott, F. and Fierke, C. (2002) Eukaryotic ribonuclease P: A plurality of ribonucleoprotein enzymes, *Annu Rev Biochem*, No. 71, pp. 165-89.

Xu, H., Johnson, L. and Grunstein, M. (1990) Coding and non-coding sequences at the 3'-end of yeast histone H2B mRNA confer cell-cycle regulation, *Mol Cell Biol*, Vol. 10, pp. 2687-94.

Yang, X., Purdy, M., Marzluff, W. and Dominski, Z. (2006) Characterization of 3'hExo, a 3' exonuclease specifically interacting with the 3' end of histone mRNA. *J Biol Chem*, Vol.281, No.41, pp 30447-54.

Zarudnaya, M., Kolomiets, I. and Hovorun, D. (2002) What nuclease cleaves pre-mRNA in the process of polyadenylation?, *IUBMB Life*, Vol. 54, pp. 27-31.

Zenklusen, D. and Stutz, F. (2002) Stable mRNP formation and export require cotranscriptional recruitment of the mRNA export factors Yra1p and Sub2p by Hpr1p, *Mol Cell Biol*, Vol. 22, pp. 8241-53.

Zhang, Z., Fu, J. and Gilmour, D. (2005) CTD-dependent dismantling of the RNA polymerase II elongation complex by the pre-mRNA 3'-end processing factor, Pcf11, *Genes Dev*, No. 19, pp. 1572-80.

Zhang, Z. and Gilmour, D. (2006) Pcf11 is a termination factor in *Drosophilia* that dismantles the elongation complex by bridging the CTD of RNA polymerase II to the nascent transcript, *Mol Cell*, Vol. 21, pp. 65-74.

Zhao, J., Hyman, L. and Moore, C. (1999) Formation of mRNA 3'-ends in eukaryotes: Mechanism, regulation and interrelationships with other steps in mRNA synthesis, *Microbiol Mol Biol Rev*, Vol. 63, pp. 405-45.

Zhao, J., Kessler, M. and Moore, C. (1997) Cleavage factor II of *Saccharomyces cerevisiae* contains homologues to subunits of the mammalian cleavage/polyadenylation specificity factor and exhibits sequence-specific, ATP-dependent interaction with precursor RNA, *J Biol Chem*, Vol. 272, pp. 10831-38.

Zhao, J. and Moore, C. (1999) Pta 1, a component of yeast CF II, is required for both cleavage and poly (A) addition of mRNA precursor, *Mol Cell Biol*, Vol. 19, pp. 7733-40.

Zheng, L., Dominski, Z., Elms, P., Xiao-Cui Y., Christy R., Christoph B. and Marzluff, W. (2003) Phosphorylation of stem-loop binding protein (SLBP) on threonines triggers degradation of SLBP, the sole cell-cycle regulated factor required for regulation of histone mRNA processing, at the end of S phase, *Mol Cell Biol*, Vol. 23, pp. 1590-1601.

Zorio, D. and Bentley, D. (2004) The link between mRNA processing and transcription: Communication works both ways, *Exp Cell Res*, Vol. 296, pp. 91-97.